Stratigraphy and Conodont Biostratigraphy of the Uppermost Carboniferous and Lower Permian from the North American Midcontinent

Darwin R. Boardman II
Oklahoma State University
Stillwater, Oklahoma 74078–3031

Bruce R. Wardlaw
U.S. Geological Survey
Reston, Virginia 20192–0002

Merlynd K. Nestell
University of Texas at Arlington
Arlington, Texas 76019–0408

PART A—General Sequence Stratigraphy and Conodont Biostratigraphy (including new species) of the Uppermost Carboniferous (upper Gzhelian) to Lower Permian (lower Artinskian) from the North American Midcontinent

Bruce R. Wardlaw, Darwin R. Boardman II, and Merlynd K. Nestell

PART B—Conodont Distribution, Systematics, Biostratigraphy, and Sequence Stratigraphy of the Uppermost Carboniferous and Lower Permian (uppermost Wabaunsee, Admire, Council Grove, and lower Chase Groups) from the North American Midcontinent

Darwin R. Boardman II, Merlynd K. Nestell, and Bruce R. Wardlaw

Contents

Part A

Figures

Plate

Part B (on cd-rom in back pocket)

Figures

Plates

Authors' Preface

This study was initiated in 1991, and originally was planned to be a summary of the sequence stratigraphy and naming of the new conodont species document that would be printed; the sometimes more detailed discourse about stratigraphic philosophy and observation to accompany the more detailed discussion and illustration of the conodont biostratigraphy was to be a digital supporting document. The research greatly evolved in scope in order to adequately deal with taxonomic, stratigraphic, and sequence stratigraphic issues.

Part A is largely a summary of the most essential elements of the conodont taxonomy, biostratigraphy, and sequence stratigraphy and is a printed document. Part B contains detailed conodont biostratigraphy, including an in-depth analysis of the problems of stratigraphic misplacement of species, clarification of types, and more complete discussion of the sequence stratigraphic concepts and is included on a cd-rom in the back envelope of this volume. Some redundancy exists between Part A and Part B, but we felt the basic concepts are better served in this format.

—Darwin R. Boardman II
Bruce R. Wardlaw
Merlynd K. Nestell

This entire Bulletin also is available on the Kansas Geological Survey web site at http://www.kgs.ku.edu/Publications/Bulletins/255/index.html.

Part B—Conodont Distribution, Systematics, Biostratigraphy, and Sequence Stratigraphy of the Uppermost Carboniferous and Lower Permian (Admire, Council Grove, and lower Chase Groups) from the North American Midcontinent

Darwin R. Boardman II
Boone Pickens School of Geology
Oklahoma State University
Stillwater, Oklahoma 74078–3031

Merlynd K. Nestell
Department of Mathematics
University of Texas at Arlington
Arlington, Texas 76019–0408

Bruce R. Wardlaw
U. S. Geological Survey
MS 926A National Center
Reston, Virginia 20192–0002

Abstract

Maximum-marine flooding levels and marine-condensed sections from uppermost Carboniferous and Lower Permian fourth-order (0.1–1m.y.) depositional sequences of the North American midcontinent reveal a rich stratigraphic succession of species of *Streptognathodus* and *Sweetognathus* conodonts that permits high-precision correlation of the Carboniferous–Permian boundary as well as the Asselian–Sakmarian and Sakmarian–Artinskian boundaries. Eleven new species of *Streptognathodus* are described: *Streptognathodus binodosus, S. denticulatus*, *S. elongianus*, *S. florensis*, *S. lineatus*, *S. nevaensis*, *S. postconstrictus*, *S. postelongatus*, *S. robustus*, *S. translinearis*, and *S. trimilus*. Seventeen species are redescribed and clarified and include *Streptognathodus alius*, *S. barskovi*, *S. bellus*, *S. brownvillensis*, *S. conjunctus*, *S. constrictus, S. elongatus*, *S. farmeri*, *S. flexuosus*, *S. fuchengensis*, *S. fusus*, *S. invaginatus*, *S. isolatus*, *S. longissimus, S. minacutus, S. nodulinearis,* and *S. wabaunsensis*.

The correlated level of the Carboniferous–Permian boundary is recognized in the lower part of the Red Eagle Depositional Sequence based on the introduction of *Streptognathodus isolatus* Chernykh, Ritter, and Wardlaw; *Streptognathodus minacutus* Barskov and Reimers; *Streptognathodus invaginatus* Reshetkova and Chernykh; *Streptognathodus fuchengensis* Zhao; and *Streptognathodus nodulinearis* Reshetkova and Chernykh. The correlated Carboniferous–Permian boundary occurs in the depositional sequence that represents the maximum-marine highstand of the Council Grove Composite Third Order Sequence. This level represents a significant marine-flooding event that should be correlatable in numerous shelfal sections throughout the world.

Although the Asselian–Sakmarian boundary has not been rigorously defined, *Sweetognathus merrilli* has been informally utilized as a Sakmarian indicator. Due to the ecologically controlled distribution of species of *Sweetognathus,* we prefer to use a species of *Streptognathodus* as a defining species. We propose that *Streptognathodus barskovi* (Kozur) Reshetkova be considered as a potentially defining or ancillary defining species for the Sakmarian Stage. In the North American midcontinent, *Streptognathodus barskovi* appears in the same depositional sequence with *Sweetognathus merrilli* in the Eiss (Lower Bader) Depositional Sequence. Historically, *Sweetognathus whitei* has been used to mark the Sakmarian–Artinskian boundary. In our succession *Sweetognathus whitei* and *Streptognathodus florensis* appear in the basal part of the Barneston Depositional Sequence. We suggest that *Streptognathodus florensis* be further investigated as a possible defining or ancillary defining taxon for the base of the Artinskian Stage. This depositional sequence also forms the maximum-marine highstand of the Chase Third-Order Composite Depositional Sequence suggesting that this level is a significant marine-flooding event that should be widely traceable in numerous shelfal sections.

Introduction

This report is an outgrowth of our long-standing research programs that include high-resolution multitaxial biostratigraphic, chronostratigraphic, and sequence stratigraphic analysis of Carboniferous and Permian strata. Much of the conodont-range data presented in this paper were generated as a direct result of conodont-biofacies analysis used for delineating late Carboniferous–Early Permian depositional sequences and generating sea-level-fluctuation curves (Boardman and Nestell, 1993). Open-marine shelfal late Carboniferous and Early Permian strata contain abundant representatives of the evolutionary clades of the conodont *Streptognathodus*. Recently, a number of conodont workers (Akhmetshina, 1990; Akhmetshina et al., 1984; Barrick and Boardman, 1989; Barskov and Alekseev, 1975; Barskov et al., 1981; Barskov et al., 1987; Chernykh and Chuvashov, 1986; Chernykh and Reshetkova, 1987; Chernykh and Ritter, 1997; Chuvashov et al., 1993; Kozur and Mostler, 1976; Movschovitsch et al., 1979; Reshetkova and Chernykh, 1986; Ritter, 1994, 1995; Wang, 1991; Wardlaw, 1990; Zhao, 1982) have demonstrated the potential for using late Carboniferous and Permian species of *Streptognathodus* for biostratigraphic and chronostratigraphic analysis. Apparently, many species of *Streptognathodus* are cosmopolitan in distribution, thus making them reliable fossils for global correlation. Additionally, species of *Sweetognathus* have also been employed for correlating Lower Permian strata throughout the world. *Sweetognathus expansus* has been proposed as a basal Permian indicator (Kozur, 1994), *Sw. merrilli* a basal Sakmarian index (Chuvashov et al., 2002a), and *Sw. whitei* as a basal Artinskian taxon (Chuvashov et al., 2002b).

Due to the paucity of ammonoids in Carboniferous–Permian boundary strata outside of the Soviet Union (Boardman et al., 1994) and endemism of fusulinaceans (Ross, 1979), conodonts appear to hold the most promise for accurate correlation for Carboniferous–Permian boundary strata. However, a number of problems still need to be resolved before conodonts can be fully utilized.

The first problem is the paucity of well-documented conodont successions from regions outside of the southern Urals. To fully understand the range of intraspecific variation within one horizon as well as to document the phylogenetic relationships (species morphoclines) in time, bed-by-bed sampling as well as numerous illustrations of conodonts from each significant horizon are imperative. Although the North American midcontinent has one of the best stratigraphic successions of latest Carboniferous and earliest Permian conodonts, only a scant number of *Streptognathodus* specimens have been illustrated. Furthermore, few of these specimens are tied to detailed measured stratigraphic sections.

A second problem is the overwhelming lack of consistent usage of species names. The literature contains poorly illustrated types, vaguely diagnosed and described species, and incomplete or inaccurate stratigraphic data, all of which have resulted in inconsistent application of names as well as contradictory range data (Chuvashov et al., 1993). Finally, although many species of *Streptognathodus* and *Sweetognathus* may be cosmopolitan in distribution, there is no evidence that all species are. Detailed collection and illustration of conodonts from a number of stratigraphic horizons representing many geographic regions, is necessary to test the cosmopolitan distribution of these conodonts. Besides documenting the geographic extent of each species, the timing of migration from one region to another needs to be carefully examined. By correlating the appearances of individual species of *Streptognathodus* and *Sweetognathus* to global sea-level transgressive-regressive events, the migration of species from the basin of origin outward can be independently tested.

Worldwide upper Carboniferous to Lower Permian strata are marked by cyclothems that apparently resulted from numerous episodes of sea-level advances and retreats associated with waxing and waning of continental glaciers in Gondwanaland (Boardman et al., 1984; Boardman and Heckel, 1989; Boardman, 1999; Crowell, 1978; Crowell and Frakes, 1975; Crowley and Baum, 1991; Heckel, 1977, 1986; Schenk, 1967; Veevers and Powell, 1987; Wanless and Shepard, 1936; Yang, 1996). Magnitudes of sea-level rise and fall associated with glaciation and deglaciation apparently fall within the similar ranges (50–100 m) commonly associated with Pleistocene glacial episodes (Aldis et al., 1988; Crowley and Baum, 1991). Periodic major sea-level drops of about 50–100 m would likely have isolated many of the intracratonic basins, thereby creating the potential for the evolution of new species through allopatric speciation. New species evolving as peripheral isolates during lowstand could then migrate to other basins during the next major sea-level rise that would have reconnected many of the basins. Major sea-level rises should be associated with the introduction of new species, without a plethora of intermediates, on a global basis if this theoretical pattern is correct. Likewise in the basin of new species origin, transitional forms might be present. Sea-level curves that document the relative rises and falls of sea level could give an independent test of the migration of new species from one region or province into another.

Based on sequence stratigraphic analysis, sea-level fluctuation curves have been generated for the midcontinent North America late Carboniferous (Heckel, 1986; Boardman and Heckel, 1989; Boardman, 1999) and for the latest Carboniferous and earliest Permian (Boardman and Nestell, 1993; Boardman et al., 1995). Data presented by Boardman and Heckel (1989), Heckel and Weibel (1991), Connolly and Stanton (1992), Soreghan (1994), and Raatz (1996) suggest that the pattern of sea-level rises and falls can itself be correlated in different basins, especially when matching the sequential magnitudes of sea-level rises coupled with major drops in sea level. Boardman and Heckel (1989) demonstrated that the first and last occurrences of numerous Middle and Upper Pennsylvanian (Upper Desmoinesian, Missourian through middle Virgilian) species of ammonoids, fusulinaceans, and conodonts are strongly correlated to the inferred pattern of sea-level fluctuations in the North American midcontinent and north-central Texas. Heckel and Weibel (1991) biostratigraphically correlated the Late Pennsylvanian sea-level curve from the Illinois basin with that of the North American midcontinent using the succession of conodonts. Connolly and Stanton (1992) correlated cyclothems

from the Pedregosa basin of Arizona to those of the midcontinent using the patterns of cyclicity and fusulinaceans. Raatz (1996) correlated upper Desmoinesian through the lower Virgilian depositional sequences of the Sacramento Mountains in New Mexico to those of the North American midcontinent based on a pattern of sea-level fluctuations coupled with high-resolution biostratigraphy.

In this report we establish an outcrop-based sequence stratigraphic framework for the latest Carboniferous and Lower Permian strata of the midcontinent. The sea-level curve derived from this analysis is biostratigraphically calibrated using the introduction and extinctions of conodont, fusulinacean, and ammonoid species. The resulting biostratigraphically calibrated sea-level curve is constructed to facilitate high-resolution interbasinal correlation.

This study focuses on upper Carboniferous and Lower Permian (Brownville Limestone Member through Fort Riley Limestone Member, upper Wabaunsee Group to middle Chase Group) strata that crop out in the North American midcontinent region from southern Nebraska through northern Oklahoma (figs. 1–2). Conodont distribution and range data presented are based on over 1,000 in situ samples from 57 measured sections (Locality Register–Appendix II). The sequence stratigraphic framework is presented herein for the uppermost Wabaunsee, Admire, Council Grove, and lower Chase Groups. Sections from northern and southern outcrop regions are utilized in order to test for the possible effects of different lithofacies on the distribution of conodont species. Marine uppermost Wabaunsee, Admire, Council Grove, and Chase strata from southern Kansas and northernmost Oklahoma are generally more carbonate-rich as compared to coeval strata from northern Kansas and Nebraska that have a much higher percentage of open-marine as well as marginal-marine siliciclastics.

Scope and Methodology of Study

The main purposes of this report are as follows:

1) Provide an outcrop-based sequence stratigraphic framework for the uppermost Wabaunsee Group, Admire Group, Council Grove Group, and lower Chase Group.
2) Provide North American reference sections for the correlated positions of the Gzhelian/Asselian, Asselian/Sakmarian, and Sakmarian/Artinskian boundaries.
3) Resolve stratigraphic problems concerning the provenance of previously reported species of *Streptognathodus and Sweetognathus*.
4) Provide a standard terminology for morphological features of *Streptognathodus* and present a systematic discussion and revision of *Streptognathodus* species.
5) Describe new species and provide English translations of most previously described species of *Streptognathodus* (circa 2000).
6) Relate the introduction of *Streptognathodus* and *Sweetognathus* species to the Carboniferous–Permian sea-level curve (modified from Boardman and Nestell, 1993; Boardman et al., 1995).
7) Present a range chart showing distribution of species of *Streptognathodus* in Carboniferous–Permian boundary strata. Provide a range chart of species of *Streptognathodus* from Aidaralash Creek and the Usolka section in the Ural Mountains of Kazakhstan and Russia, respectively.
8) Provide a diagram illustrating the inferred phylogenetic relationships between significant morphoclines of *Streptognathodus* and for *Sweetognathus*.
9) Discuss problems of provincialism within species of *Streptognathodus* and *Sweetognathus*.

Regional Geology and General Stratigraphic Overview

Uppermost Carboniferous and lowermost Permian (uppermost Wabaunsee, Admire, Council Grove, Chase) cyclothemic strata of this study crop out on a broad northern shelf region of the Anadarko basin (fig. 20). Outcrops in Nebraska, northern Kansas, and central Kansas straddle the Nemaha Ridge and the western edge of the Forest City basin and the easternmost terminus of the Salina basin. Outcrops in southern Kansas are located on the eastern edge of the Sedgwick basin, whereas outcrops in northern Oklahoma are on the Cherokee platform. Because of the inferred paleogeographic location of the land-sea interface, a north-south transect from Kansas through northern Oklahoma represents a dip section that demonstrates the successive pinchouts of marine into nonmarine red-bed deposits (figs. 21, 22).

A number of paleotopographic features, including structurally positive and negative features as well as faults, are present in the broad shelf area from Oklahoma to Nebraska. They had considerable effect on the thicknesses and lithologic nature of each of the depositional sequences (Mazzullo et al., 1997). Additionally, changes in the rates of subsidence of the Anadarko basin had a dramatic effect on the nature of the depositional sequences from the Pennsylvanian to the Permian

time interval. Maximum areal extent of the starved-basinal facies of the Anadarko basin as well as maximum subsidence rates occurred during Missourian time (Rascoe, 1962). A gradual trend of reduced subsidence rates and concomitant restriction of the Anadarko basin through sediment infilling occurred from Virgilian through Wolfcampian time (figs. 23–28). Admire and Council Grove basinal facies were restricted to six counties in the Panhandle areas of Texas and Oklahoma, whereas no basinal facies are present in the Chase Group (fig. 28).

Major changes in climate from the Virgilian to the Wolfcampian have been suggested based on changing lithofacies and mineralogy including an increase in dolomite and celestite along with evaporitic minerals gypsum, anhydrite, and halite. A number of late-highstand peritidal carbonates of the Council Grove Group contain abundant celestite and dolomite, as well as anhydrite molds. Additionally, gypsum-, halite-, and chert-replaced anhydrite nodules occur in some of the siliciclastic intervals. The increase in evaporitic minerals probably represents a major climatic change from a wetter to generally drier climate (Miller and West, 1993). This change probably represents the movement of the midcontinent region into drier latitudes during the Early Permian time interval (Scotese, 1986).
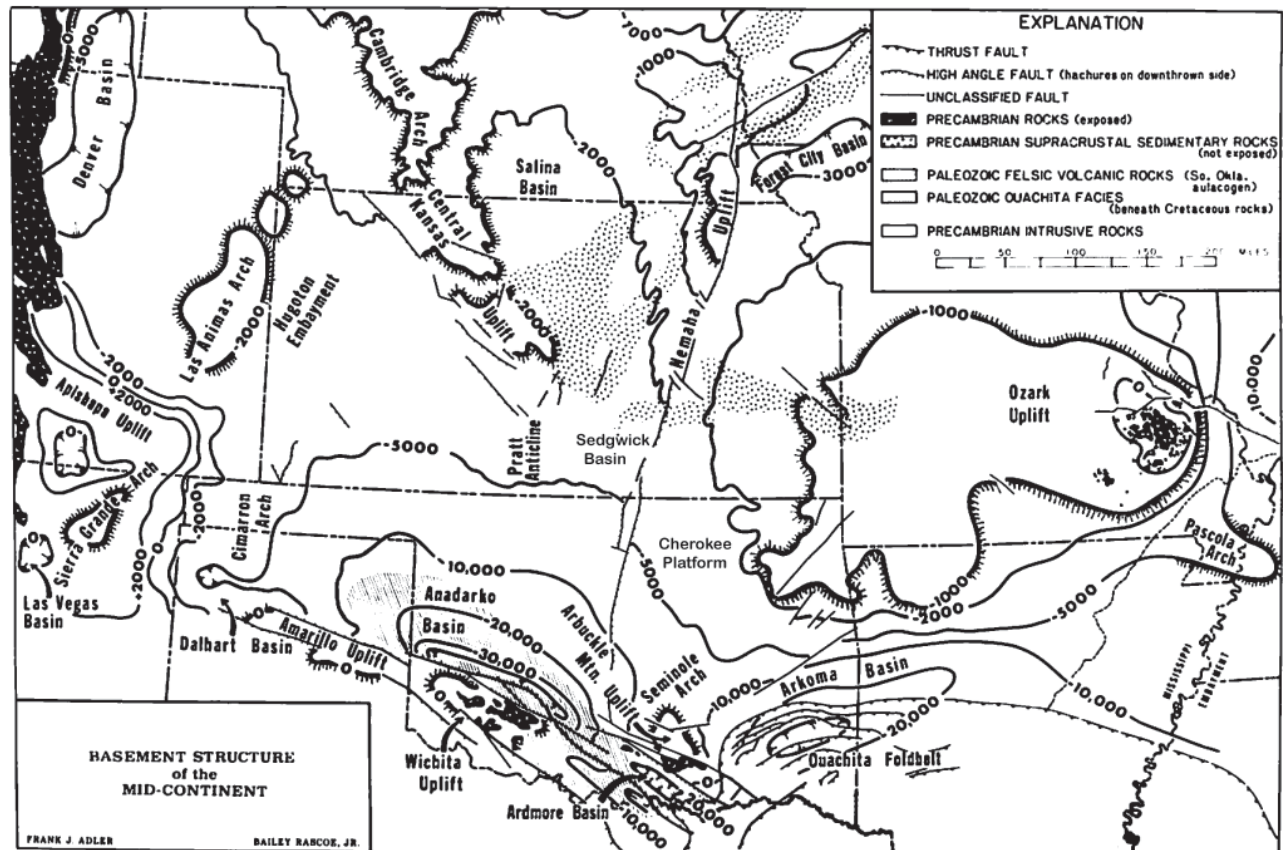
FIGURE 20—Basement structure of the midcontinent (modified from Adler, 1971).
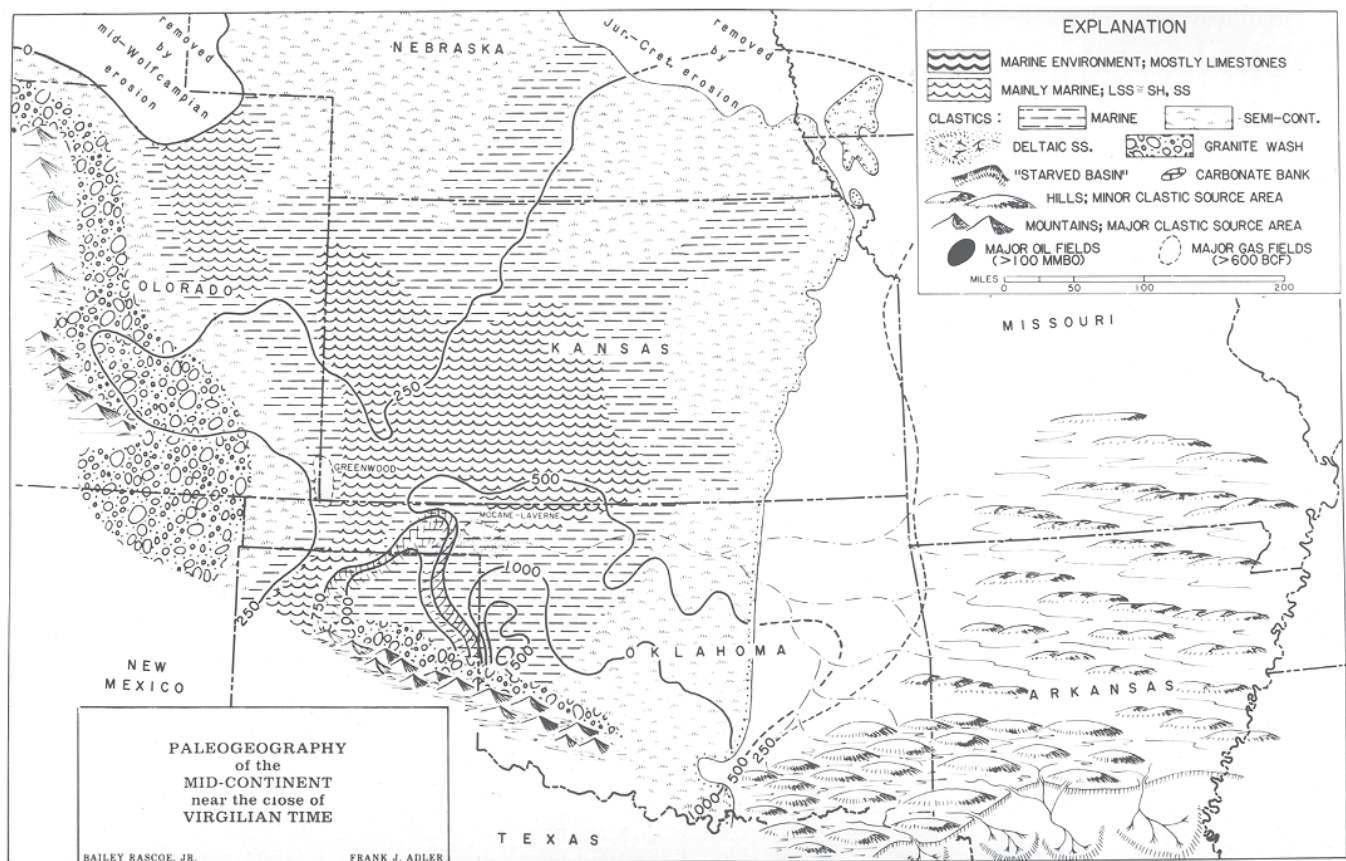
FIGURE 21—Lithofacies and paleogeography of the late Virgilian in the midcontinent (modified from Rascoe and Adler, 1983).
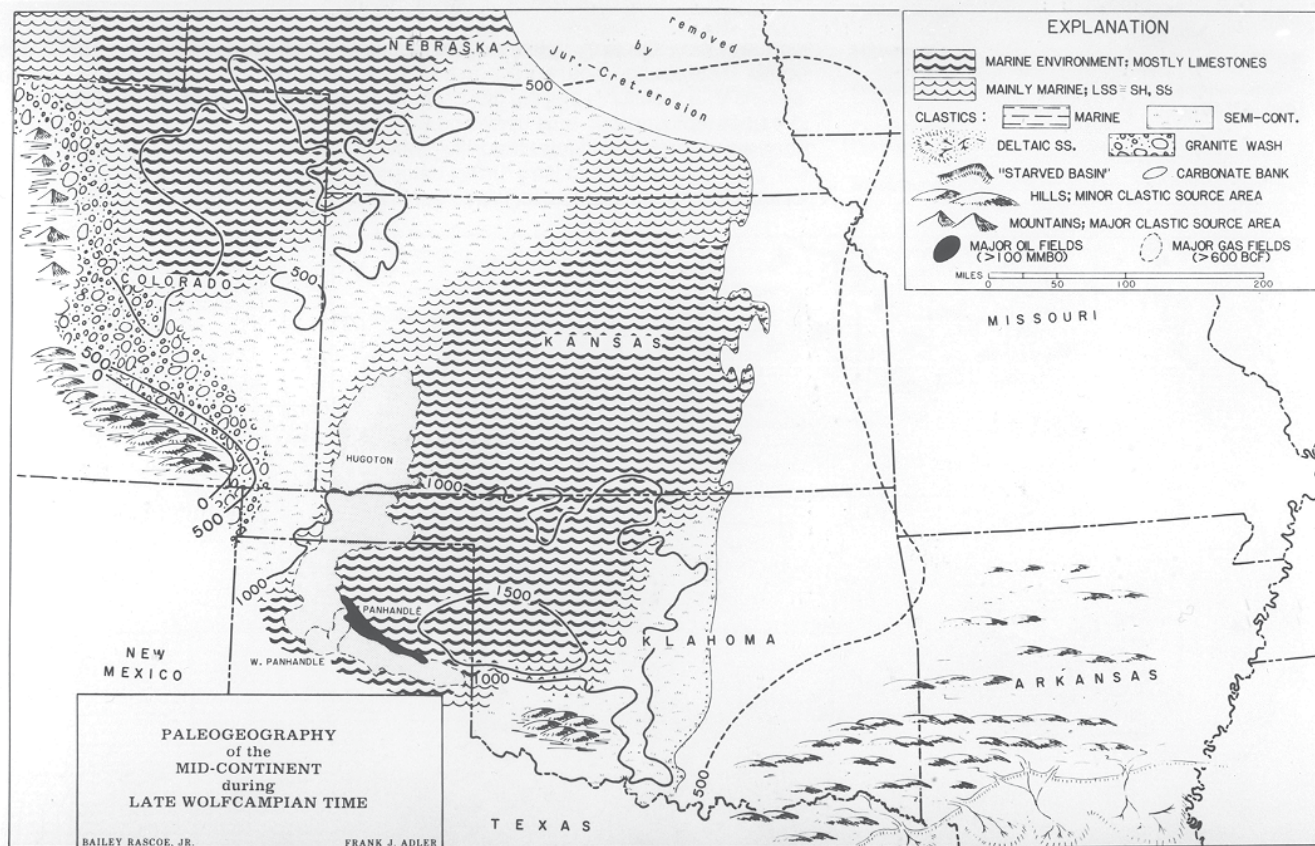
FIGURE 22—Lithofacies and paleogeography of the Late Wolfcampian in the midcontinent (modified from Rascoe and Adler, 1983).

Uppermost Wabaunsee, Admire, Council Grove, and Chase strata are characterized by a complex shelfwide mixed siliciclastic-carbonate system that records a hierarchy of stratigraphic forcing similar to that described by Goldhammer et al. (1991) for the carbonate-dominated Desmoinesian cyclothemic strata of the Paradox basin. Cyclothemic-scale depositional sequences from the Wabaunsee and Admire Groups consist of thick marginal-marine and nonmarine clastics separated by thin carbonate-dominated highstand deposits. In contrast, cyclothemic-scale depositional sequences from the Council Grove and Chase Groups are composed of a two-component (hemicycle) system, one being carbonate-dominated and the other siliciclastic-dominated. The carbonate-dominated hemicycle of the depositional sequences generally is thick (1–25 m) and generally represents more dominantly marine conditions. Facies within the carbonate hemicycle for the Council Grove Group are delineated by Puckette et al. (1995). Additionally, Mazzullo et al. (1995, 1997) discuss lithofacies comprising the carbonate hemicycles of the Chase Group. For purposes of this report we follow Puckette et al. (1995) and Mazzullo et al. (1995, 1997) for interpretations of the carbonate-dominated part of each depositional sequence. The thick carbonates are overlain by a relatively thick (5–15-m) red and green caliche-bearing blocky silty mudstones and siltstones hemicycle that commonly contains well-defined pedogenic features (Miller and West, 1993; Miller et al., 1996; Olszewski and Patzkowsky, 2003). These red and green deposits are generally thought to have formed during late stages of sea-level fall, lowstand, and perhaps earliest transgression. Close examination of both the dominantly marine-carbonate

hemicycle as well as the dominantly nonmarine-siliciclastic hemicycle reveal a much more complicated scenario for their origin. The thick (5–15-m) red and green mudstone hemicycles are also highly complex. Within these intervals, extensive evidence of pedogenesis is present including columnar peds, blocky peds, pseudoanticlines, root traces, boxwork carbonates, desiccation cracks, carbonate nodules, and rhizocretions (Joeckel 1991; Miller and West, 1993; Miller, 1994; Miller et al., 1996). Siliciclastics that comprise the paleosol parts of these intervals are thought to have been eolian-derived in central Kansas through Nebraska (Joeckel 1989), whereas in southernmost Kansas and Oklahoma fluvially derived siliciclastics are clearly also present. In stark contrast to Virgilian depositional sequences that have well-developed incised-valley fills (Archer and Feldman, 1995), incised-valley fills are rare to absent in the Council Grove outcrop belt from northernmost Oklahoma to Nebraska. The origin of the accommodation space necessary for deposition of this part of the hemicycle remains enigmatic. Two scenarios for the origin of the siliciclastics seem the most viable. The first model invokes eolian-derived siliciclastics and the vertical aggradation of the paleosols. The second scenario proposed by Miller et al. (1996) is significantly more complex and evokes the idea that at least part of the vertical thickness observed in this hemicycle is the result of siliciclastic infilling of accommodation space during sea-level fall, then modification of these sediments via pedogenesis during lowstand or lowstands. Evidence for the first model includes the abundance of silt in this hemicycle coupled with the well-defined stacked paleosols (Miller and West, 1993). However, the general absence of fluvial systems in the Kansas and Nebraska outcrop
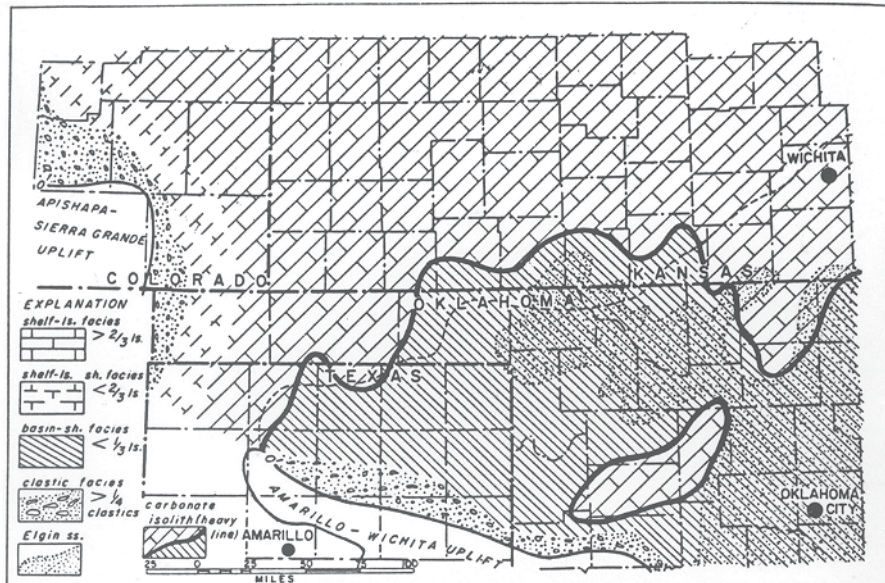
FIGURE 23—Lithofacies map of the Shawnee Group (modified from Rascoe, 1962).
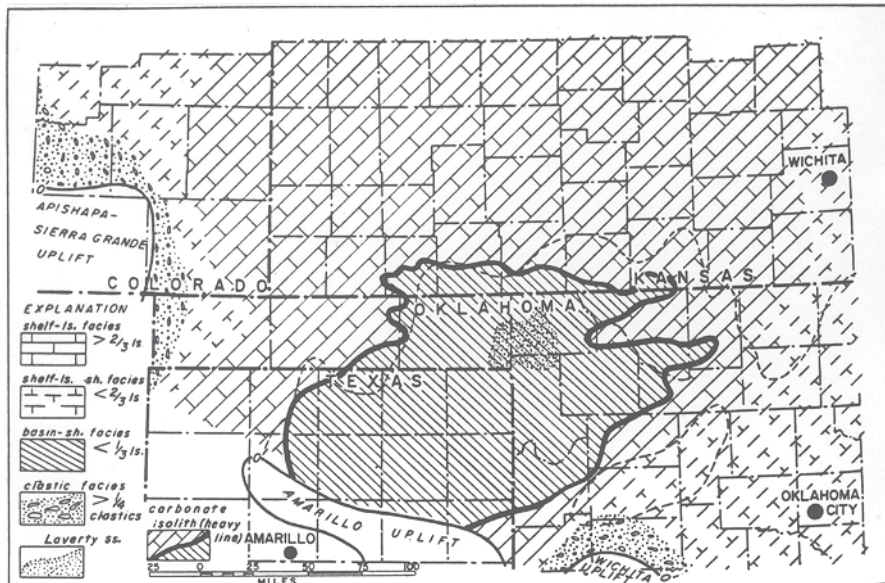
FIGURE 24—Lithofacies map of the Sacfox Subgroup of the Wabaunsee Group (modified from Rascoe, 1962).

belt coupled with the presence of clay in these intervals argues against this idea. The second model is supported in a number of ways:

1) The top of the carbonate hemicycle of many Wabaunsee–Chase sequences lacks direct evidence of subaerial exposure.

2) Marginal-marine fossils are present in several of these siliciclastic hemicycles including the Johnson Shale, Roca Shale, Eskridge Shale, Stearns Shale, Hooser Shale Member, and Speiser Shale.

3) The presence of both silt-sized particles and clay-sized particles suggests that eolian sedimentation cannot alone account for the distribution of grain sizes.

These thick siliciclastic intervals are commonly punctuated by thin (<1 m) carbonates and mudstones that indicate marine-influenced deposition (Miller and West, 1993). The thin marine or marginal-marine deposits commonly contain a low-diversity foraminifer and ostracode microfaunal assemblage

along with a low-diversity molluscan-dominated or rarely brachiopod macrofossil assemblage. Typically, these siliciclastic intervals contain up to two of these minor marine bands. Each of these marine bands is separated by red to green blocky to crumbly mudstones that demonstrate clear evidence of pedogenic features.

Lithofacies

The following facies are currently recognized from the Wabaunsee, Admire, Council Grove, and Chase Groups.

Facies: Offshore

Siliclastic Offshore (>50 m Below Euphotic Zone)

1) **Black fissile to blocky, commonly silty, highly fossiliferous shales and mudstones with abundant *Streptognathodus***
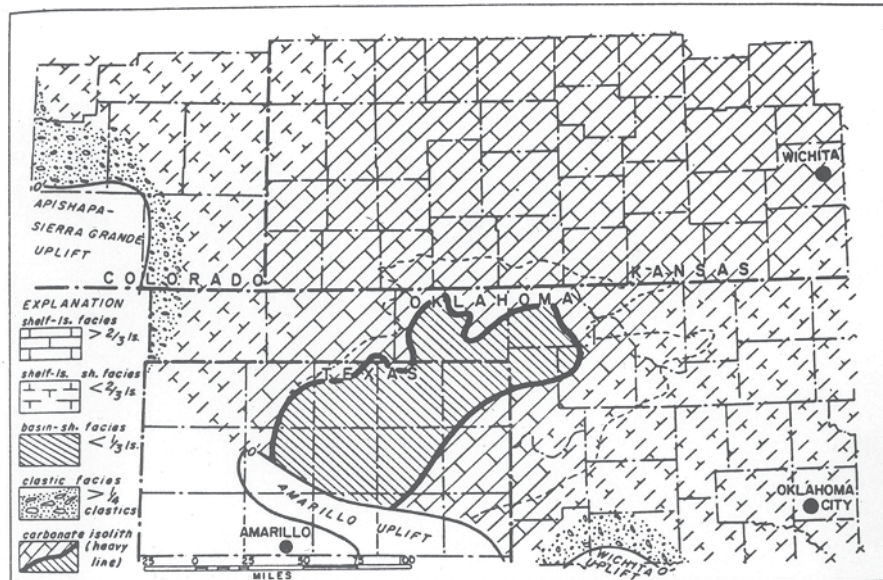
FIGURE 25—Lithofacies map of the Nemaha Subgroup of the Wabaunsee Group (modified from Rascoe, 1962).
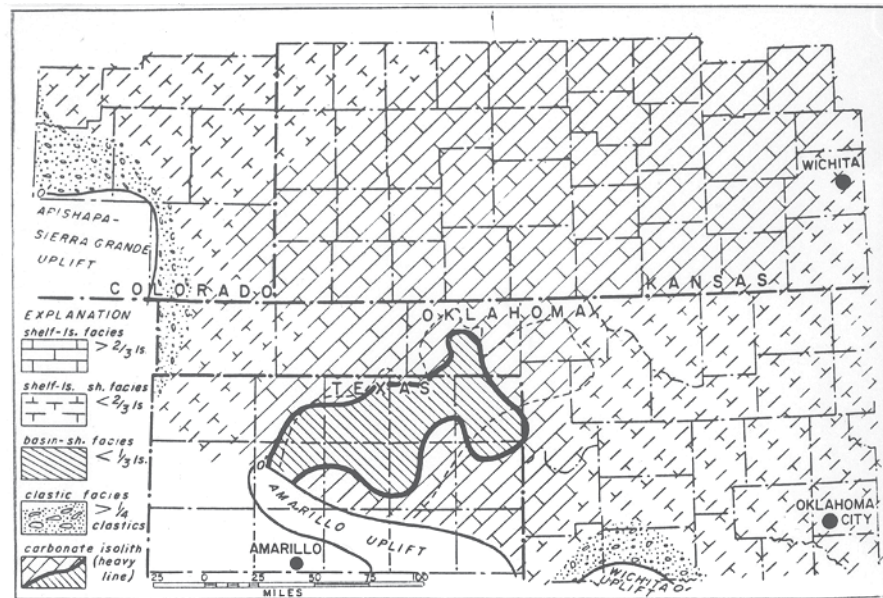
FIGURE 26—Lithofacies map of the Richardson Subgroup of the Wabaunsee Group (modified from Rascoe, 1962).

conodonts, *Ammodiscus* foraminifers, inarticulate brachiopods, abundant fish debris, and ammonoids.

This facies is restricted to the lower Council Grove Group including the upper part of theAmericus Limestone Member, middle part of the Hughes Creek Shale Member, upper part of the Hughes Creek Shale Member, Bennett Shale Member, and in a shale parting within the lower part of the Neva Limestone Member. These black shales are best developed in northern Kansas and Nebraska, but have been documented in the Hugoton embayment (Puckette et al., 1995; Amador, 2000). This facies contains the conodont *Streptognathodus* biofacies and *Ammodiscus* foraminifer biofacies, along with locally abundant ammonoids and inarticulate brachiopods. Furthermore, this facies shows evidence of condensed sedimentation as evidenced by high conodont abundance (100–1,000 platform conodonts/

kilogram). The lower Council Grove marine condensed sections differ from those of the Desmoinesian-middle Virgilian strata in lacking nonskeletal radiolarian-bearing phosphate nodules. The phosphate nodules likely formed in response to a regional thermocline augmented by upwelling of nutrient-rich waters from the starved intracratonic basin across the broad shelf during or near maximum transgression (Schenk, 1967; Heckel, 1977). Progressive restriction of the Anadarko basin from infilling and the concomitant reduced subsidence during the late Carboniferous through the Lower Permian interval served to shut off upwelling of cool nutrient waters onto the shelf.

2) Gray fissile to blocky, commonly silty, highly fossiliferous shales and mudstones with abundant *Streptognathodus* conodonts, diverse foraminifers, abundant brachiopods with *Rhipidomella* and marginiferids, crinoids, bryozoans.
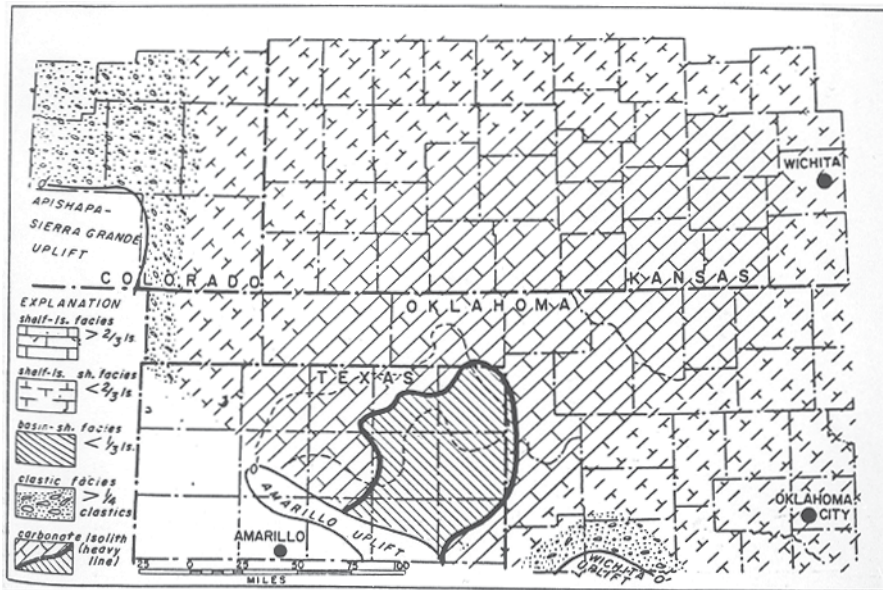
FIGURE 27—Lithofacies map of the Admire and Council Grove Groups (modified from Rascoe, 1962).
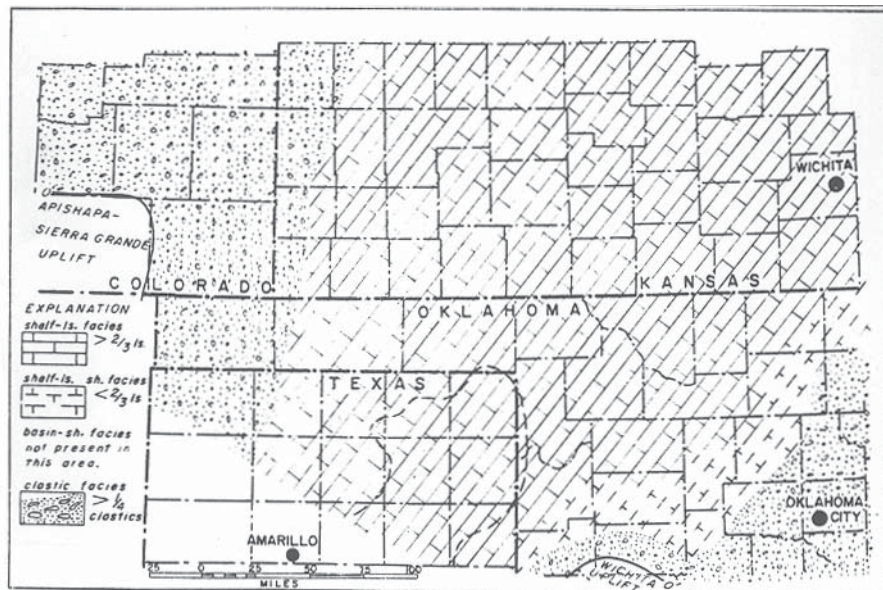
FIGURE 28—Lithofacies map of the Chase Group (modified from Rascoe, 1962).

This facies is restricted to the lower Council Grove Group including the upper part of the Americus Limestone Member, middle part of the Hughes Creek Shale Member, upper part of the Hughes Creek Shale Member, Bennett Shale Member, and in a shale parting within the lower part of the Neva Limestone Member. It is usually associated with the black-shale facies (1) and immediately overlies or underlies it.

 3) **Gray fissile to blocky highly fossiliferous calcareous and commonly siliceous shales and mudstones with abundant *Streptognathodus* conodonts, diverse foraminifers, abundant brachiopods with *Rhipidomella* and other brachiopods, crinoids, bryozoans, and abundant siliceous sponge spicules.**

This facies is common in the lower Chase Group and represents the maximum transgressive facies in the Florence Limestone Member, Threemile Limestone Member, and the Schroyer Limestone Member.

Carbonate Offshore (at or slightly above Euphotic Zone, 40–50 m)

4) **Highly fossiliferous shaly, glauconitic wackestone with *Streptognathodus* conodonts, abundant and diverse foraminifers, brachiopods, bryozoans, crinoids, and locally ammonoids with evidence of condensed sedimentation along with phosphatized mollusks.**

This facies is very common in lower Council Grove strata cropping out in southern Kansas and northern Oklahoma. It is characterized by highly fossiliferous, shaly, glauconitic wackestones with the *Streptognathodus* conodont biofacies and phosphatized mollusks. It is deposited in slightly shallower water than the black and gray offshore shales at or near the euphotic zone and is common when the offshore black and gray shales change facies over inferred paleotopographic highs.

Facies: Normal-Marine Shelf Within the Euphotic Zone

Carbonates

5) Highly fossiliferous wackestones to packstones with *Streptognathodus* conodonts, abundant and diverse foraminifers with locally abundant fusulinaceans, brachiopods, bryozoans, corals, and crinoids.

This facies is abundant throughout the Wabaunsee, Admire, and Council Grove Groups and represents normal-marine subtidal carbonates deposited below fair-weather wave base.

6) Highly fossiliferous wackestones to packstones with mixed conodont fauna of *Streptognathodus–Adetognathus* (*Sweetognathus* above Red Eagle Limestone) foraminifers with mixed fauna of mollusks, brachiopods, bryozoans, corals, and crinoids.

This facies is a shoaling facies represented by a mixture of offshore and nearshore conodonts.

7) Highly fossiliferous packstones to grainstones with rare conodonts, abundant fusulinaceans.

This facies is abundant throughout the lower Council Grove Group and represents normal-marine subtidal carbonates deposited in moderate to high energy within wave base.

8) Crossbedded ooid grainstones with rare abraded fossil fragments.

This facies is rare in Wabaunsee-lower Chase Groups that crop out but is locally common in the subsurface Council Grove Group strata of the Hugoton embayment. It represents very shallow marine high-wave-energy environments.

9) Grapestone packstone to grainstone.

This facies is common only in the subsurface Council Grove Group of the Hugoton embayment and was inferred to occur in a shoaling environment that had alternations of quiescence and turbulence. Additionally, the cement for this facies is anhydrite suggesting the rock was saturated with sulfate-enriched brines.

10) Molluscan packstones to grainstones.

This facies occurs in shallow moderate-wave-energy environments and contains abundant gastropods and bivalves with little evidence of stenohaline taxa. The upper part of the Eiss Limestone Member of central Kansas that contains *Sweetognathus merrilli* is an excellent example. The Hamlin Shale in northern Oklahoma near Foraker contains a molluscan coquina that is made up completely of *Myalina* shells. This monotaxial shell heap probably represents very nearshore deposition.

11) Phylloid-algal boundstones.

This facies is restricted to the lower Council Grove Group on outcrop, especially the Red Eagle Limestone of northern Oklahoma and the Neva Limestone Member of northern and central Kansas.

Siliciclastic

12) Gray shales to silty mudstones with normal-marine faunas.

This facies is surprisingly rare within the study interval and is locally abundant in northern Kansas and southern Nebraska within lower Council Grove Group strata (especially Foraker). The rarity of this facies is attributed to a lack of high-stand deltaic sedimentation. The common silt content within this facies suggests possible eolian derivation from the northern midcontinent source. This facies contains brachiopods, bryozoans, and locally abundant fusulinaceans.

Facies: Marginal Marine, Nearshore

Carbonates

13) Stromatolitic boundstones.

This facies is rare but occurs in the Houchen Creek limestone bed of the Admire Group, basal Americus Limestone Member, and the top of the Howe Limestone Member, all of which are restricted to northern Kansas.

14) *Ottonosia* stromatolitic wackestones to packstones.

This facies is common within the Crouse Limestone of southern and central Kansas. Commonly, *Composita* brachiopods are the nucleus for the growth of the *Ottonosia* colonies. Generally, the brachiopods within this facies are silicified. It is interpreted to form in shallow, moderately high energy environments with moderately hypersaline waters.

15) Silty, locally dolomitic ostracode and bivalve mudstones to wackestones.

This facies is very common in the late regressive deposits of numerous Council Grove and Chase Group cycles and represents brackish to hypersaline lagoonal carbonates. It contains very little evidence of normal-marine salinities as evidenced by the virtual absence of stenohaline organisms. Locally, evaporitic minerals are abundantly present in this facies.

16) Thinly laminated carbonate mudstones with locally abundant mud cracks.

This facies is locally present in Council Grove Group late-regressive deposits such as in the Foraker Limestone and represents tidal-flat sedimentation.

Siliciclastics

17) Marginal-marine black-shale facies.

This facies occurs immediately above maximum-marine flooding levels in a number of minor-scale Council Grove Group depositional sequences including above the lower part of the Americus Limestone Member, upper part of the Johnson Shale, basal Legion Shale Member above the Sallyards Limestone Member, above the lower part of the Burr Limestone Member, above a limestone in the Salem Point Shale Member, above an unnamed limestone in the middle of the Stearns Shale, above the lower part of the Middleburg Limestone Member, above the lower part of the Crouse Limestone, above the lower part of the Funston Limestone, and in the upper part of the Fort Riley Limestone Member. These shales contain a limited ostracode and bivalve fauna with no conodonts. Additionally, evaporite minerals including gypsum and anhydrite (largely replaced by silica) are locally present in this lithofacies. This facies typically grades

laterally into poorly fossiliferous silty carbonates with shallow-water indicators such as low-diversity ostracode and bivalve assemblages. We view this facies as representing a marginal-marine perhaps lagoonal environment created by extremely rapid sea-level fall coupled with a dramatic increase in the influx of siliciclastic sediments immediately following maximum-marine flooding. This sea-level fall created localized low oxygen and perhaps variable salinity conditions on the proximal or high shelf. This facies was not distinguished by Olszewski and Patzkowsky (2003), who lumped it in with the offshore black-shale facies.

18) Marginal-marine light-gray, green, or tan, blocky to fissile, poorly fossiliferous silty mudstones and shales.

This facies occurs in numerous carbonate-dominated hemicycles within the Admire to Chase Groups interval. This lithofacies commonly overlies the previous lithofacies or may directly overlie and separate carbonates within the hemicycle. This lithofacies is poorly fossiliferous, usually containing a low-diversity ostracode and foraminifer assemblage, may contain silica-replaced evaporite nodules, and grades laterally into poorly fossiliferous shallow- to restricted-marine carbonates. This facies is interpreted to represent a marginal-marine condition created by rapid forced regression accompanied by an increase in siliciclastic sedimentation on the shelf. The facies commonly separates high-frequency fifth-order cycles within the overall thicker carbonate hemicycle.

Facies: Terrestrial

19) Green blocky silty mudstones to shaly siltstones.

This facies is also noted to contain abundant pedogenic features such as columnar peds, angular to subangular peds, slickensides, etc. This facies has been interpreted to represent paleosols.

20) Red blocky silty mudstones to shaly siltstones.

This facies is also noted to contain abundant pedogenic features such as columnar peds, angular to subangular peds, slickensides, etc. This facies has been interpreted to represent paleosols.

21) Coals.

This facies is restricted to the Wabaunsee and Admire Groups. A changeover from wetter to dry environments is thought to mark the end of coal formation at the base of the Council Grove Group.

22) Boxwork carbonates.

This facies is associated with well-developed paleosols and is thought to represent secondary calcification of shrinkage cracks. It is very common in the top of the Admire Group immediately below the Americus Limestone Member.

Identification of Depth Trends within Depositional Sequences

Paleowater depth-trend analysis used in this research is based on textural trends of carbonates and siliciclastic rocks combined with detailed paleoecologic analysis using both macro-invertebrates as well as microfossils. Paleoecological analysis used in this report for delineating paleodepth trends within

the depositional sequence, as well as for identifying flooding surfaces and maximum-marine flooding condensed sections, is based on the models presented by Elias (1937), Moore (1964), and Boardman et al. (1984) for macro-invertebrates and Boardman et al. (1995) for microfossil taxa. Distinctive microfaunal biofacies are present in Late Carboniferous and Early Permian strata of the North American midcontinent (fig. 29). Marginal-marine deposits are characterized by a very low diversity microfaunal assemblage consisting of *Geisina* ostracodes, *Thurammina* foraminifers, and no conodonts. These deposits usually occur in green, gray to black, clayey to silty mudstones. Nearshore shallow normal-marine deposits contain a low-diversity microfaunal assemblage consisting of the *Cavellina* ostracode biofacies, encrusting foraminifers with agglutinated foraminifers including *Ammodiscus* cf. *A. semiconstrictus* var. *regularis*, and the *Adetognathus–Sweetognathus* conodont biofacies. This biofacies occurs in carbonates as well as in siliciclastic-dominated facies. The moderate-depth open-shelf microfaunal assemblage consists of a high-diversity ostracode *Amphissites* biofacies, a high-diversity benthic foraminifer biofacies including *Tetrataxis, Globivalvulina, Climacammina, Deckerella, Endothyra, Endothyranella,* and *Ammobaculites*, as well as fusulinaceans, along with the *Streptognathodus* conodont biofacies. This facies is usually found in wackestones, but also occurs in shales that are in close stratigraphic proximity to the fossiliferous wackestones. Deeper-shelf marine deposits occur in the offshore black-shale facies and equivalent shaly, glauconitic, and fossiliferous wackestones. These deposits contain a reduced-diversity benthic assemblage including inarticulate brachiopods (e.g., *Orbiculoidea*) and the *Ammodiscus* foraminifer biofacies, along with a pelagic component consisting of rare ammonoids, fish debris, and the *Streptognathodus* conodont biofacies. This deep-shelf assemblage is well represented in maximum-marine flooding marine condensed sections of the offshore black-shale facies but is restricted to the lower Council Grove Group.

Sequence Stratigraphic Nomenclature, Identification of Fourth-order Sequence Boundaries, and Systems-tracts Delineation

Information presented in this report permits the application of traditional biostratigraphic techniques plus establishes the data base for correlation of marine-condensed sections within the cyclothemic-scale depositional sequences. Analogous methodology has been employed for correlating marine-condensed sections within Neogene depositional sequences of the North American Gulf Coast using foraminifers and nannoplankton. Characterization and biostratigraphic correlation of marine-condensed sections of glacially induced high-frequency depositional sequences has been well established for late Neogene strata of the Gulf Coast (Shaffer, 1990). Similar methodology permitted Boardman and Heckel (1989) to biostratigraphically correlate sea-level curves from late Carboniferous strata of the North American midcontinent and north-central Texas by using ammonoids and conodonts from the marine-condensed sections of the cyclothemic depositional sequences (fig. 30). Although late Carboniferous and Early
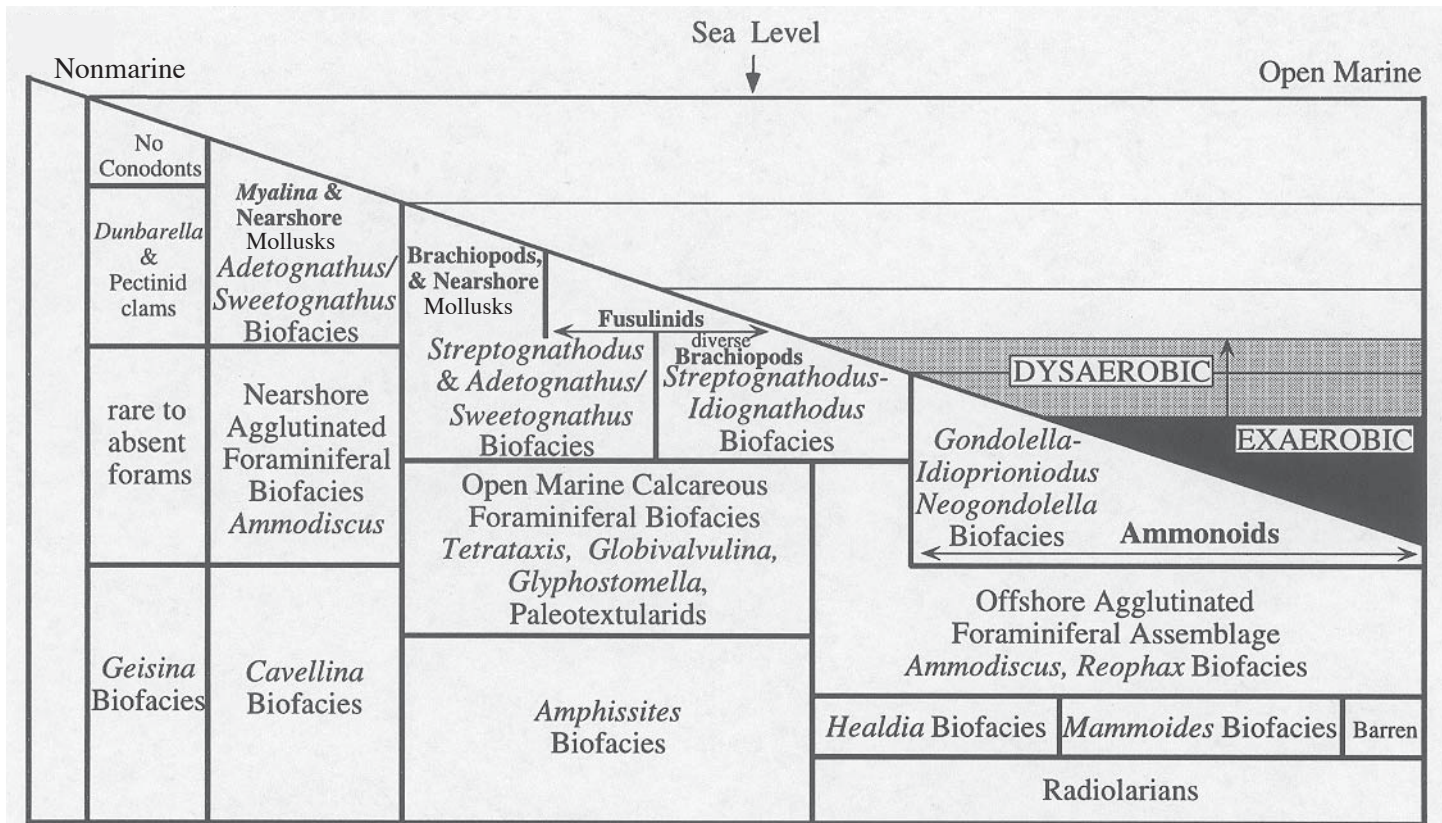
FIGURE 29—Onshore-offshore model for uppermost Carboniferous and Lower Permian depth and oxygen-related biofacies (modified from Boardman et al., 1984; Boardman and Nestell, 1993; and Boardman et al., 1995).

Permian shelfal cyclothemic strata of the North American midcontinent does not fit the classical criteria for establishment of a chronostratigraphic boundary stratotype, some authors, (e.g., Loutit et al., 1988) have argued that stage boundaries should be placed at sequence boundaries. Regardless of methodology used for defining the chronostratigraphic boundaries, it is possible to get frequent glimpses into the diversity of conodonts represented in this region at any one time, because there are numerous conodont-bearing cyclothems whose periodicity apparently falls within the Milankovitch band of 20,000–400,000 years (Heckel, 1986; Boardman and Nestell, 1993; Boardman et al., 1995) in the same geographical region (fig. 3). Documentation of the vertical succession of conodont faunas allows correlation of the shallow shelfal cycles of the midcontinent to slope or basinal cycles of the type-Permian region of the southern Urals (Aidaralash Creek in Kazakhstan or Usolka in Russia). Late Carboniferous and Early Permian fourth-order depositional sequences demonstrate a plexus of superimposed orders of cyclicity (frequency) as well as amplitudes. Similar hierarchies with superposed cycles have been described in carbonate Pennsylvanian strata of the Paradox basin (Goldhammer et al., 1991), carbonate Triassic strata of northern Italy (Goldhammer et al., 1987, 1990), and in Cenozoic siliciclastic strata of the Gulf Coast of Mexico (Mitchum and van Wagoner, 1991). Documentation for various orders of cyclicity within the midcontinent cyclothemic succession has been illustrated by Busch and West (1987), Miller et al. (1992), Miller and West (1993), Boardman and Nestell (1993), and Youle et al. (1994).

The fundamental unit for sequence stratigraphic analysis of late Carboniferous and Lower Permian strata of the midcontinent region is the cyclothemic-scale depositional sequence that has been referred to as fifth-order depositional sequences by some authors (e.g., Watney et al., 1989) or as fourth-order depositional sequences by others (e.g., Goldhammer et al., 1991; Youle et al., 1994). Little agreement exists on the hierarchical ordinal scheme of depositional sequences. Posamentier, Allen, and James (1992, p. 311) argue, "sequence stratigraphic principles are scale and time independent." Furthermore, Mitchum and van Wagoner (1991, p. 134) define "a sequence is a genetically related succession of strata with no apparent internal unconformities, composed of parasequences and parasequence sets arranged in systems tracts, and bounded by unconformities or their relative conformities. A stratal package conforming to this definition is properly called a sequence, no matter what its frequency." They further state that "a stratal package bounded by unconformities but internally composed of high-frequency sequences, cannot itself be properly called a sequence." They proposed the term composite sequence for a succession of genetically related sequences that stack into lowstand-, transgressive-, and highstand-sequence sets.

In contrast to the methodologically based definition of depositional sequence advocated by Mitchum and van Wagoner (1991) and Posamentier, Allen, and James (1992), Vail et al. (1991) argued that a depositional sequence is only formed during a third-order cycle that ranges from 0.5 to 3 million years in duration. This narrow definition as advocated by Vail et al. (1991)

FIGURE 30—Sea-level curve for the Upper Pennsylvanian (latest Desmoinesian-middle Virgilian) for the North American midcontinent with correlation to north-central Texas (modified from Heckel, 1986; Boardman and Heckel, 1989).

precludes application of the term of depositional sequences for unconformity-bounded stratal packages that form within the normal Milankovitch band periodicities (20,000, 40,000, 100,000, and 400,000 years). However, in strata that were deposited during major glacial episodes such as in the Pliocene–Pleistocene (Carter et al., 1991), Miocene (Moore et al., 1982), and in the Carboniferous–Permian (Heckel, 1986; Boardman and Heckel, 1989; Boardman and Nestell, 1993; Youle et al., 1994), third-order cyclicity is secondary and is derived from analysis of the stacking patterns of cyclothemic-scale (fourth-order) depositional sequences. The amplitudes of Pliocene–Pleistocene sea-level fluctuations (Carter et al., 1991) as well as late Carboniferous–Early Permian eustatic events (Heckel, 1986; Boardman and Heckel, 1989; Boardman and Nestell, 1993; Boardman et al., 1995) are of similar magnitude of third-order Mesozoic and early Cenozoic tectono-eustatic-induced transgressions and regressions (Mitchum and van Wagoner, 1991). Moreover, it is apparent that the order of cyclicity (frequency) may have

little bearing on the amplitude of the sea-level change during times of major glaciation. High-amplitude late Carboniferous sea-level changes are apparently related to the 400,000-year orbital eccentricity cycle (Heckel, 1986), whereas late Pleistocene high-amplitude sea-level changes are controlled by 100,000-year orbital eccentricity cycles (Denton and Hughes, 1983). Therefore, the figure demonstrating a reduction in amplitude of sea-level change with increasing order of eustatic cycle presented by Mitchum and van Wagoner (1991, fig. 7, p. 140) may not be applicable during times of earth history in which there were major glacial episodes. Because the accommodation space created by glacial-eustatic rises in sea level can be identical to that created by tectono-eustasy, it seems untenable to demand that only third-order sea-level changes produce true depositional sequences. Therefore, we view depositional sequences as being scale and time independent following Posamentier, Allen, and James (1992). For the purposes of this report, we follow the hierarchal sequence stratigraphic nomenclature as proposed by Goldhammer et al. (1991) and Youle et al. (1994).

Based on observed stacking patterns, fourth-order sequences can be objectively grouped into composite third-order depositional sequences following Mitchum and van Wagoner (1991). A similar methodology was utilized by Youle et al. (1994), who proposed composite third-order sequences for Middle Pennsylvanian strata of the Anadarko basin based on stacking patterns of fourth-order cyclothemic-scale depositional sequences. Watney et al. (1995) suggested that third-order genetic sets could be generated using gamma ray, thorium-uranium ratios, and Fouier harmonics. However, this method has not been attempted in Carboniferous–Permian boundary strata. In contrast to the derivation of third-order cyclicity based on stacking patterns, Ross and Ross (1985, 1987) presented charts demonstrating coastal-onlap curves and defining third-order depositional sequences for Carboniferous and Lower Permian strata of the North American midcontinent based largely on faunal criteria. For the purposes of this report, we follow the methodology of Youle et al. (1994). Depositional sequences from the upper Wabaunsee and Admire Groups comprise the late-highstand sequence sets in a third-order composite depositional sequence that includes most of the Virgilian strata. The Council Grove Group comprises one third-order sequence (Council Grove Third-Order Sequence) with the base of the Americus Limestone Member representing the transgressive surface. The Bennett Shale Member of the Red Eagle Limestone contains the most widespread maximum-marine flooding condensed section of the Council Grove Group, and thus corresponds also to maximum transgression of the composite third-order sequence. Additionally, the Red Eagle Limestone extends further paleo-landward into Oklahoma than any other unit of the Council Grove Group (Branson, 1964, p. 61). The Foraker and Red Eagle sequences form a retrogradational stacking pattern of sequences that comprise the transgressive-systems tract of the third-order sequence. The highstand-systems tract includes sequences that stack into aggradational (Lower and Upper Grenola Sequences) and progradational stacking pattern (Beattie through Funston Sequences) with a very major Type 1 unconformity being developed in the Speiser Shale at the top of the Council Grove Group. The Wreford and Barneston Sequences of the overlying Chase Group belong to the retrogradational transgressive-systems tract to the Chase Third-Order Sequence. The Barneston Limestone also has been demonstrated to extend further paleo-landward into Oklahoma (Branson, 1964, p. 61).

In addition to the cyclothemic-scale fourth-order sequences, many high-frequency fifth-order sequences are evident within the fourth-order packages. Within the dominantly marine part of many latest Carboniferous and Early Permian midcontinent cyclothemic depositional sequences (e.g., Foraker and Grenola sequences), widely correlatable, subsequence-scale divisions (higher-order sequences) on the order of 1–5 m in thickness are present. These higher-order sequences form the parasequences and parasequence sets that clearly stack into the systems tracts that subdivide the fourth-order depositional sequences. Clear evidence of a basinward shift in facies is present in cases where the fifth-order sequences are not terminated by subaerial exposure. In addition to the fifth-order cyclicity in the dominantly marine part of the fourth-order depositional sequence, the

minor transgressive-regressive marine bands with distinctive transgressive- and highstand-systems tracts that are commonly present within the thick siliciclastic-dominated intervals that overlie the thick carbonate-dominated part of the sequence (Miller and West, 1993) also represent high-frequency fifth-order depositional sequences. These higher-order sequences are referred to as fifth-order transgressive-regressive cycles following the terminology of Goldhammer et al. (1991). The fifth-order cycles that are terminated by subaerial exposure are referred to as exposure cycles, whereas fifth-order cycles that are terminated without subaerial exposure are referred to as subtidal cycles (Goldhammer et al., 1991).

Type 1 Depositional Sequences (as defined by van Wagoner et al., 1988), such as those in this study, have been subdivided into the lowstand-systems tract, transgressive-systems tract, highstand-systems tract, and the forced regressive-systems tract (Posamentier, Allen, James, et al., 1992; Hunt and Tucker, 1992, 1995; and the equivalent falling sea-level systems tract of Nummedal, 1992, and Nummedal and Molenaar, 1995). Historically, the lowstand-systems tract is composed of the basin-floor fans, slope fans, and prograding coastal wedges. Lowstand deposits on the shelf form the prograding wedge deposited during late sea-level fall or early sea-level rise. The shelfal expression of the prograding wedge consists largely of incised-valley-fill deposits formed during late sea-level fall or earliest eustatic rise. Incised-valley fills have thus far not been documented in Admire, Council Grove, and lower Chase strata of the midcontinent. During the time interval in which these rocks were deposited, progressively more arid conditions predominated, and sea-level fall resulted in subaerial exposure of the majority of the shelf resulting in meteoric diagenesis of the highstand/forced regressive carbonates. A small number of the tops of the highstand/forced regressive carbonates (Five Point Limestone, Long Creek Limestone, Howe Limestone, Eiss Limestone, Middleburg Limestone, Schroyer Limestone, and Kinney Limestone Members) demonstrate direct subaerial exposure as evidenced by red internal sediment infilling solution vugs and brecciation associated with regolith development, whereas the rest are evidently capped by nearshore- to marginal-marine siliciclastics. Therefore, sequence boundaries generally lie within the thick (5–15 m) red to green mudstone intervals in the siliciclastic deposits that separate the dominantly carbonate facies. Thick siliciclastic intervals contain zones that exhibit a plethora of pedogenic structures indicative of extensive paleosol development (Miller and West, 1993). The thick siliciclastic packages dramatically thicken to the south of Osage County, Oklahoma. The predominant percentage of the thick package is composed of fluvial depositional systems with fewer paleosols.

Because minor marine bands (higher-order cycles) punctuate the complex of paleosols, several unconformities are typically present within each thick siliciclastic section. This makes identification of the shelfal expression of the fourth-order master-depositional-sequence boundary difficult to identify. The following stratigraphic surfaces could be utilized as the master-sequence boundary:

    a) the stratigraphic position that corresponds to the surface above which the first sediments were deposited during a sea-level fall (Posamentier, Allen, James, et al., 1992),

b) the basal unconformity corresponding to the first evidence of a major basinward shift in facies and the first evidence of subaerial exposure (van Wagoner, 1990),

c) the top of the paleosol interval that is coincident with the easily identifiable transgressive surface (ravinement) (Watney et al., 1989; French and Watney, 1993),

d) the subaerial exposure surface that corresponds to maximum sea-level lowstand (Hunt and Tucker, 1995),

e) the maximum flooding surface (marine-condensed section) (Galloway 1989a, 1989b; Watney et al., 1995).

Placing the sequence boundary at the first indication of forced regression would result in the maximum-lowstand erosional surface lying above the sequence boundary. The basal unconformity surface also would yield a sequence boundary lying below the maximum sea-level lowstand, but would provide an easier surface to identify in the field as well as in the subsurface. Use of the top of the paleosol interval that is coincident with the transgressive surface would provide an easy surface to identify in the field as well as in the subsurface, but would likely represent a diachronous surface from the distal- to the proximal-shelf setting. It is for this reason that this level is not coincident with the true sequence boundary. Theoretically, the best option is to place the sequence boundary at the unconformity surface that corresponds to the maximum lowstand, following Hunt and Tucker (1995). However, this procedure also presents a serious challenge in identifying which part of the paleosol interval corresponds to maximum lowstand. The unconformity surface that extends furthermost basinward corresponds to this master-sequence boundary. In order to delineate master-sequence boundaries for these late Carboniferous–Early Permian depositional sequences, a number of dip cores would have to be analyzed from the proximal shelf to the distal shelf and into the Anadarko basin. Unfortunately, availability of cores from this stratigraphic interval is largely restricted to the proximal-shelf region and the Hugoton embayment. We, therefore, in the absence of this crucial data, recognize a master-sequence-boundary zone that includes the true master-sequence boundary. This sequence-boundary zone is bounded at the base by the first evidence of subaerial exposure and at the top by the highest subaerial exposure surface, which is also coincident with the transgressive surface of the succeeding depositional sequence. Based on the glacial-eustatic model for sea-level fluctuation, it is likely that the master-sequence boundary lies near the top of the paleosol interval. As a result of our utilization of a sequence-boundary zone, we do not recognize a lowstand-systems tract, but include the sequence-boundary zone within the forced-regressive-systems tract. If and when the precise position of the master-sequence boundary is picked, then a lowstand-systems tract including strata above the sequence boundary and below the transgressive-systems tract could be recognized. Because the initial surface of forced regression lies immediately above the marine-condensed section, and the marine-condensed section represents the latest transgressive-systems tract and the earliest highstand-systems tract, the stratigraphic thickness of the highstand-systems tract as utilized in this study is limited to the upper part of the marine-condensed section. The transgressive-systems tract includes strata from the base of the transgressive surface to the marine-condensed section (downlap surface).

These deposits form a retrogradational parasequence-set stacking pattern. The highstand-systems tract historically encompasses the upper part of the marine-condensed section along with the thick dominantly marine part of the depositional sequence that includes aggradational- to progradational-parasequence sets formed during late stages of sea-level rise, eustatic stillstand, and early sea-level fall (van Wagoner et al., 1988). Sinusoidal-shaped sea-level fluctuation curves such as presented by Jervey (1988) and Posamentier et al. (1988) have served as the paradigm for modeling depositional sequences. This model has been used to demonstrate that the majority of the highstand-systems tract is associated with aggradation and progradation occurring during maximum eustatic stillstand and early sea-level fall. The idealized symmetrical sinusoidal sea-level fluctuation curve is in stark contrast to actual observed highly asymmetric sea-level curves produced by glacial buildup and decay documented for the late Pleistocene, Holocene, and for the Pennsylvanian time intervals. Based on oxygen-isotope data from Imbrie et al. (1984), Collier et al. (1990) illustrated a late Pleistocene sea-level curve for the last 400,000 years and demonstrated exceptionally rapid sea-level rises associated with deglaciations, followed by episodic, generally gradual sea-level falls caused by slow glacial buildups. Additionally, they showed that the sea-level falls were punctuated by sea-level rises that represented episodic reversals in the trend towards glacial buildups. Maximum lowstands occurred immediately before the major sea-level rises associated with major deglaciations. In terms of specific rates, Broecker and von Donk (1970) documented that late Pleistocene glacial buildups were slow-lasting, as much as 90,000 years, whereas deglaciations are exceedingly rapid, taking place in no more than 10,000 years. Carter et al. (1986, p. 640) determined that glacial advances and retreats were episodic in addition to being asymmetrical, thereby resulting in rapid episodic transgressions associated with slow episodic regressions. The pattern of exceptionally rapid episodic transgressions with slow episodic regressions associated with glaciation and deglaciation of the Pleistocene is virtually identical with observations of Pennsylvanian and Early Permian depositional sequences by Heckel (1977, 1986), French and Watney (1993), and Boardman and Nestell (1993) as well as to the patterns we report (fig. 31). Although the overall time for ice-sheet build-up is much slower than sea-level melt resulting in rapid transgressions and slow regressions, minor drops in sea level as part of the episodic regressions may be rapid, resulting in a rapid basinward shift in shallow-marine facies. This is demonstrated as part of our research presented herein. The asymmetric sea-level rises resulted in an exceptionally limited maximum-marine stillstand in terms of duration and amount of sediment deposited contrasted to the symmetrical sinusoidal sea-level model. The asymmetrical model suggests that the thick aggradational to progradational sedimentary package that has been traditionally placed in the highstand-systems tract is deposited during times of falling sea-level. Evidence for falling sea level includes widespread subaerial exposure of subtidal carbonates documented by Watney et al. (1989), as well as in this report, along with evidence of rapid basinward shift in facies resulting in facies dislocation. This suggests that during times in earth history dominated by major glaciation, the forced-regressive-systems tract or

A.

meters
-150 -100 -50 0

Eustatic Highstands

I

V

VII

IX

XI

Age (ka)
100
200
300
400

B.

Shoreline   50m

Eustatic Highstands

Nolans Limestone

Winfield Limestone

Barneston Limestone

Wreford Limestone

Funston Limestone

Crouse Limestone

Middleburg Limestone Member

Eiss Limestone Member

Beattie Limestone

upper Grenola Limestone

lower Grenola Limestone

Red Eagle Limestone

Foraker Limestone

Five Point Limestone Member

Falls City Limestone
Aspinwall Limestone Member
Brownville Limestone Member

Chase Group

Council Grove Group

Admire Group

C.

EUSTACY

HIGH

TIME

LOW HIGH

HIGHSTAND-SYSTEMS TRACT 1

LOW HIGH

LOWSTAND-SYSTEMS TRACT -
LOWSTAND FAN

TIME

LOW HIGH

LOWSTAND-SYSTEMS TRACT -
LOWSTAND WEDGE

TIME

LOW HIGH

TRANSGRESSIVE-SYSTEMS TRACT

TIME

LOW HIGH

HIGHSTAND-SYSTEMS TRACT, II

TIME

LOW

FIGURE 31—A. Sea-level curve for the late Quaternary based on oxygen isotope data in Imbrie et al. (1984).

B. Sea-level curve for the uppermost Carboniferous to lower Permian (modified from Boardman and Nestell, 1993; Boardman et al., 1995).

C. Sinusoidal sea-level-curve model with superimposed systems tracts (modified from Jervey, 1988; Posamentier et al., 1988).

the equivalent falling-sea-level-systems tract, best describes the thick aggradational to progradational parasequence sets historically relegated to the highstand-systems tract. We follow the definition of the forced-regressive-systems tract by Hunt and Tucker (1995) who stated ". . . includes all sediments deposited during times of falling relative sea-level regardless of the depositional environment." The lower systems-tract boundary is placed at the horizon that shows evidence of forced regression and the top by the master-sequence boundary. Even though our forced-regressive-systems tract is very close to the usage of the traditional highstand-systems tract of the Exxon model, we suggest that ours is a better conceptual approach.

Maximum-flooding surfaces have also been proposed as sequence boundaries for genetic stratigraphic sequences (Galloway, 1989a, 1989b; Watney et al., 1995), a conceptual alternative to depositional sequences. The genetic stratigraphic sequences (GSUs) are supposedly easier to define and correlate because the sequence boundaries are placed at maximum-flooding surfaces (marine-condensed sections). This is ideal in cases where the marine-condensed sections are represented by highly radioactive shales (hot shales) that carry a distinctive high gamma-ray neutron response, or likewise where downlap surfaces that equate to the maximum-flooding surfaces are easily identified on seismic lines. These hot shales make three-dimensional sequence stratigraphic analysis easier in that the sequences are easier to correlate in the subsurface. This approach provides much easier definition and correlation in sequences where radioactive black fissile shales represent the marine-condensed sections. However, in this study radioactive black shales are restricted to the lower Council Grove Group (Puckette et al., 1995). Additionally, the black shales are discontinuous in both the subsurface as well as surface outcrops. These black-shale marine-condensed sections grade laterally into shaly, glauconitic, and phosphatic fossiliferous wackestones (carbonate marine-condensed sections) and typically lose the high distinctive gamma-ray signatures. Watney et al. (1989) demonstrated that marine-condensed sections that lack the phosphatic black fissile shales in Missourian depositional sequences (e.g., Quindaro and Hickory Creek Shale Members) also lack the high gamma-ray responses based on scintillation analysis of surface outcrops. Because of the scarcity of easily identifiable radioactive shales, three-dimensional sequence stratigraphic analysis including subsurface-well data must include thin-section as well as paleoecological analysis from cores in order to document maximum-flooding surfaces that define the GSUs. It is for this reason that we do not consider this approach to be superior to the traditional depositional sequences defined on the basis of widespread unconformities.

Because the late Carboniferous and Early Permian global chronostratigraphic framework is not formally established, we provisionally use the marine-cyclothem names as names for the fourth-order depositional sequences. Additionally, there is a paucity of reliable absolute dates for this time interval. Therefore, we recognize different orders of depositional sequences, but do not attempt to correlate a particular order to an absolute time duration, nor do we attempt to relate a particular Milankovitch frequency to an observed sequence.

Wabaunsee Group Sequences

Brownville Composite Fourth-Order Depositional Sequence

The stratigraphically lowest fourth-order depositional sequence in this study is the Brownville Composite Fourth-Order Sequence (figs. 3, 4, 32). This sequence includes approximately the upper meter of the Pony Creek Shale, Brownville Limestone, Towle Shale, Aspinwall Limestone, and the lower part of the Hawxby Shale Members. This fourth-order sequence is composed of two fifth-order sequences. The Pony Creek Shale Member, Brownville Limestone Member, and majority of the Towle Shale Member comprise the Brownville Fifth-Order Sequence, and the upper part of the Towle Shale, Aspinwall Limestone, and the lower part of the Hawxby Shale Members constitute the Aspinwall Fifth-Order Sequence.

Typically, the transgressive surface of the Brownville Fourth-Order Sequence is located within a meter below the top of the Pony Creek Shale Member. Above the transgressive surface, thin discontinuous limestones and fossiliferous gray shales are present and contain abundant *Myalina* clams, bryozoans, ostracodes, and rare *Adetognathus* conodonts. Throughout the study area, the lower part of the Brownville Limestone Member is represented by highly fossiliferous wackestones to packstones with an offshore open-marine fauna of brachiopods, crinoids, fusulinaceans, and *Streptognathodus* conodonts. Maximum-marine flooding of the Brownville Sequence occurs at or near the top of the Brownville Limestone Member in northern Oklahoma through central Kansas. Maximum flooding is characterized by marine cements, glauconite, phosphatized mollusks, and abundant *Streptognathodus* conodonts, as well as a diverse open-marine fauna of brachiopods, corals, bryozoans, crinoids, and fusulinaceans. In northern Kansas the top of the Brownville Limestone Member is a highly fossiliferous wackestone but with only minor evidence of condensation. In that region, a green highly fossiliferous shale at the base of the Towle Shale Member is interpreted to represent the maximum-flooding marine-condensed section. This shale contains phosphatized mollusks, along with crinoids, brachiopods, fusulinaceans, and abundant *Streptognathodus*.

The forced-regressive-systems tract of the Brownville Fifth-Order Sequence includes the lower two-thirds of the Towle Shale Member throughout the outcrop belt with the exception of the basal 0.3 m that represents the maximum-flooding marine-condensed section in northern Kansas. Throughout outcrops in Kansas, caliche-bearing red mudstones with local fluvial channels are present in the middle part of the Towle Shale Member (Mudge and Yochelson, 1963). In northernmost Oklahoma, the basal Towle is a black mudstone with abundant *Crurithyris* and *Neochonetes* brachiopods along with sparse *Adetognathus*, whereas the middle part of the Towle Shale Member is extremely silty with slightly fossiliferous carbonate concretions but lacks conodonts. At the top of the Towle (0.61 m below the Aspinwall Limestone Member) in northern Oklahoma, there is an oxidized zone that may indicate subaerial exposure. The top of the Towle Shale Member in that region is a gray highly fossiliferous mudstone with moderate numbers of *Adetognathus*. The fifth-order sequence boundary is placed at the contact of the

FIGURE 32—Lithostratigraphy of outcrop stratigraphic sections utilized to characterize the Brownville Composite Fourth-Order Sequence; localities 2, 3, 1, A20, and A26. Some stratigraphic data for this cross section were provided by Boyd (1999).

red mudstone and thin limestone in the upper part of the Towle Shale Member throughout Kansas, and at the contact between the red-stained silty mudstone and fossiliferous non-silty shale in northernmost Oklahoma.

The initial marine flooding of the Aspinwall Fifth-Order Sequence occurs in the upper part of the Towle Shale Member throughout the study area and coincides with abundant low-diversity ostracode and bivalve fauna in northern and central Kansas and by a low-diversity brachiopod (*Neochonetes*) assemblage in northern Oklahoma. Maximum flooding occurs in a thin crinoidal packstone in the upper part of the Aspinwall

Limestone Member in northern Kansas and in the basal Aspinwall Limestone Member in southern Kansas and northern Oklahoma. In northern Kansas maximum flooding is marked by moderate numbers of *Adetognathus* along with crinoids, whereas maximum flooding in southern Kansas and northern Oklahoma is marked by a more open-marine assemblage of bryozoans, crinoids, and brachiopods along with increased numbers of *Adetognathus*. In northern Kansas, the lower part of the Aspinwall Limestone Member is represented by a relatively thick bed of poorly fossiliferous hematic sand-infilled mudcracked limestone in the lower part followed by a crinoidal packstone and a poorly

fossiliferous carbonate in the upper part. In central Kansas the Aspinwall interval contains numerous thin fossiliferous limestones interbedded with fossiliferous silty shales, whereas in northern Oklahoma and southern Kansas, the Aspinwall consists of two highly fossiliferous limestones separated by a thin highly fossiliferous shale with an open-marine fauna. The Hawxby Shale Member in all regions contains red to green to gray, silty, blocky mudstones at or near the base that are interpreted as paleosols. The interval from the top of the Aspinwall Limestone Member through the lower part of the Hawxby Shale Member represents the highstand/forced-regressive-systems tract. The sequence boundary separating the Aspinwall Sequence from the Falls City Sequence lies near the base of the Hawxby Shale Member.

The Brownville Sequence contains a unique assemblage of *Streptognathodus* including *S. brownvillensis* Ritter, *S. bellus* Chernykh and Ritter, and *S. elongianus* Wardlaw, Boardman, and Nestell.

Falls City Composite Fourth-Order Depositional Sequence

The upper part of the Hawxby Shale Member, Falls City Limestone, and the West Branch Shale Member (figs. 3, 5, 33) comprise the Falls City Sequence. The Falls City Fourth-Order Sequence is composed of three fifth-order sequences. The upper part of the Hawxby and lower part of the Falls City Limestone constitute the Falls City Fifth-Order Sequence A, the upper part of the Falls City Limestone ledge and the majority of the West Branch Shale Member constitute the Falls City Fifth-Order Sequence B, and the upper part of the West Branch that contains fossiliferous carbonates and shales bounded above and below by paleosols comprises the Falls City Fifth-Order Sequence C.

The transgressive surface of the Falls City Sequence occurs in the upper part of the Hawxby Shale Member. The uppermost part of the Hawxby Shale Member is a gray, highly fossiliferous shale that contains bryozoans, crinoids, brachiopods, and *Adetognathus* conodonts. This unit is interpreted as representing the initial stages of marine flooding of the Falls City Sequence. In northern Kansas, maximum flooding in the Falls City Sequence corresponds with a thin *Crurithyris*-bearing wackestone mapped as a limestone lens in the uppermost part of the Hawxby Shale Member. In central and southern Kansas, maximum flooding corresponds to a highly fossiliferous wackestone near the middle of the Falls City Limestone. In northern Oklahoma, maximum flooding occurs in the basal member of the Falls City Limestone. A highly fossiliferous wackestone with a mixed megafauna of bryozoans, brachiopods, crinoids, and clams along with a mixed *Adetognathus–Streptognathodus* conodont assemblage characterizes maximum-marine flooding in all regions. The highstand/forced-regressive-systems tract includes the uppermost part of the Falls City Limestone and the West Branch Shale Member.

The Falls City Fifth-Order Sequence B occurs in all outcrop regions. It is composed of the upper ledge of the Falls City Limestone and the majority of the West Branch Shale Member. The maximum flooding of the Falls City Fifth-Order Sequence B occurs in the upper ledge of the Falls City Limestone and contains sparse *Adetognathus*, locally abundant mollusks, sparse brachiopods, and bryozoans.

The Falls City Fifth-Order Sequence C occurs in all outcrop regions in the upper part of the West Branch Shale Member. In northern Kansas, this fifth-order sequence is represented by a highly fossiliferous wackestone that carries a low-diversity mixed brachiopod, bryozoan, and molluscan assemblage that overlies a well-developed rooted green blocky mudstone. In northern Kansas, either a coaly mudstone or caliche-bearing green blocky mudstone overlies the carbonate. In central Kansas, this sequence is manifested by a fossiliferous limestone that overlies a blocky mudstone and boxwork limestone and is in turn overlain by a coal bed. In southern Kansas and in northernmost Oklahoma, this sequence is manifested by fossiliferous thin-bedded foraminiferal packstones and wackestones and interbedded shales containing a low-diversity productid brachiopod and bryozoan fauna at the maximum-flooding surface and by abundant *Myalina* clams in the initial transgressive deposits. This sequence is underlain by a well-developed coal bed and underclay (= paleosol) and overlain by a coaly shale and underclay (= paleosol). No conodonts have been recovered from this high-order sequence in the outcrop belt.

The Falls City Sequence contains *Streptognathodus alius* Akhmetshina and *S. bellus*. The co-occurrence of *S. alius* with *S. bellus* distinguishes the Falls City from the Brownville Sequence.

Five Point Composite Fourth-Order Depositional Sequence

The Five Point Limestone and the Hamlin Shale Members of the Janesville Shale comprise the Five Point Fourth-Order Depositional Sequence (figs. 3, 6, 34). The Five Point Sequence is composed of three fifth-order depositional sequences. The Five Point Fifth-Order Sequence A consists of the Five Point Limestone and the basal Hamlin Shale Members. The Five Point Fifth-Order Sequence B consists of a fossil-bearing carbonate or shale in the lower part and middle of the Hamlin Shale Member, and the Five Point Fifth-Order Sequence C includes the Houchen Creek limestone bed and the overlying Oaks shale.

The transgressive surface of the Five Point Sequence is also equivalent to the maximum-flooding surface and is recognized by a highly fossiliferous glauconitic wackestone that contains a fully open-marine fauna including brachiopods, bryozoans, corals, crinoids, fusulinaceans, as well as a *Streptognathodus*-dominated conodont assemblage. This depositional sequence contains the greatest diversity of marine fossils from any sequence within the Admire Group. Due to the fact that maximum flooding occurs at the base of the depositional sequence, virtually the entire Five Point Limestone Member and overlying Hamlin Shale Member comprise the highstand/forced-regressive-systems tract. The top of the Five Point Limestone Member in most regions in Kansas as well as Oklahoma consists of highly fossiliferous packstones and wackestones that were subaerially exposed as evidenced by red-clay internal-sediment infillings of vugs along with regolith development on top of the limestone. This indicates rapid sea-level lowering and is prima facie evidence for forced regression. The base of the Hamlin Shale Member where exposed consists of red blocky caliche-bearing mudstones indicative of paleosols. Two fifth-order depositional sequences are developed within the Hamlin Shale Member. The first of these developed in the lower part of the Hamlin Shale Member is represented by a foraminiferal-crinoidal packstone in northern
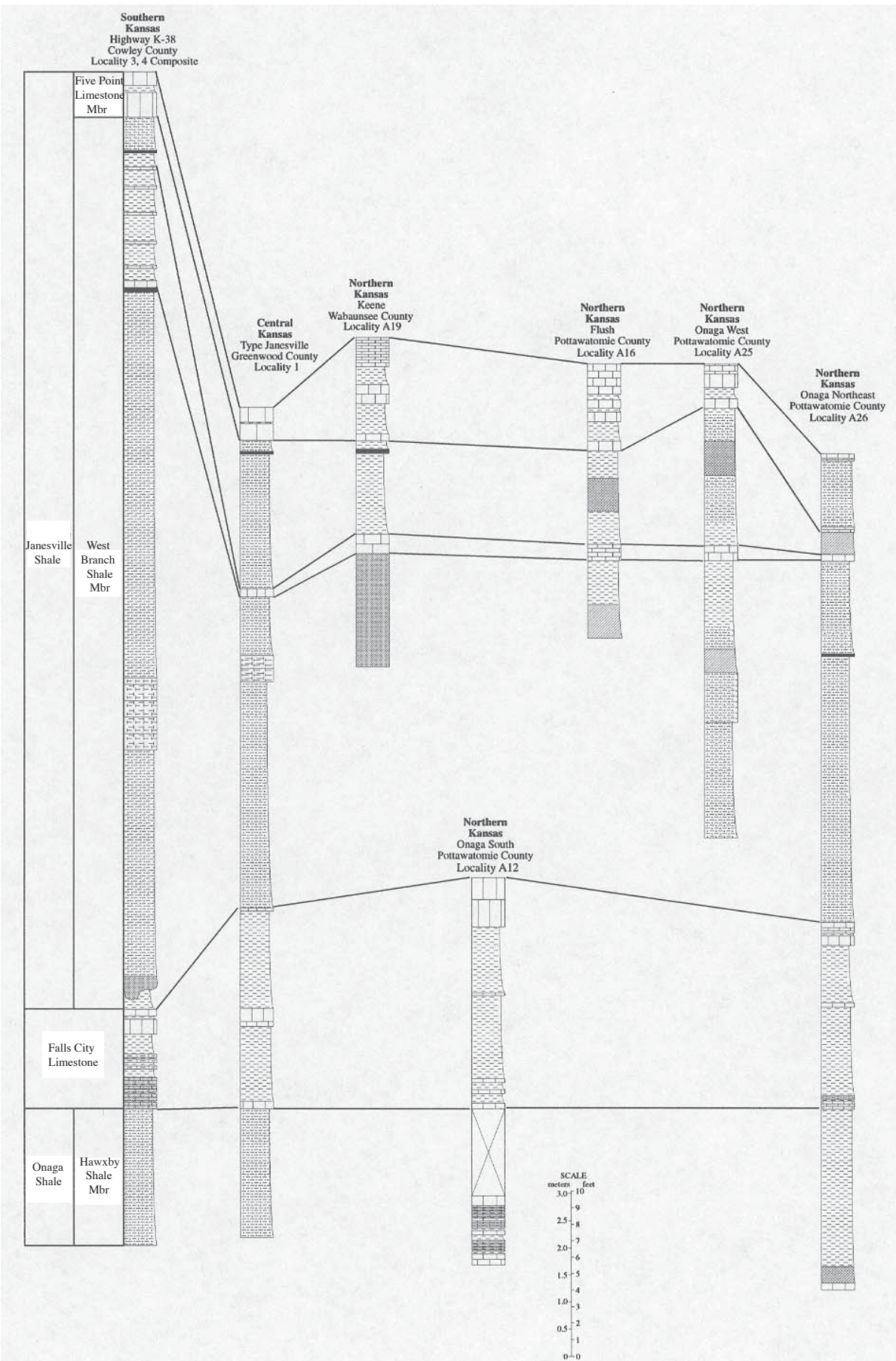
FIGURE 33—Lithostratigraphy of outcrop stratigraphic sections utilized to characterize the Falls City Composite Fourth-Order Sequence; localities 3–4 (composite), 1, A19, A12, A16, A25, and A26. Some stratigraphic data for this cross section were provided by Vann (1994).
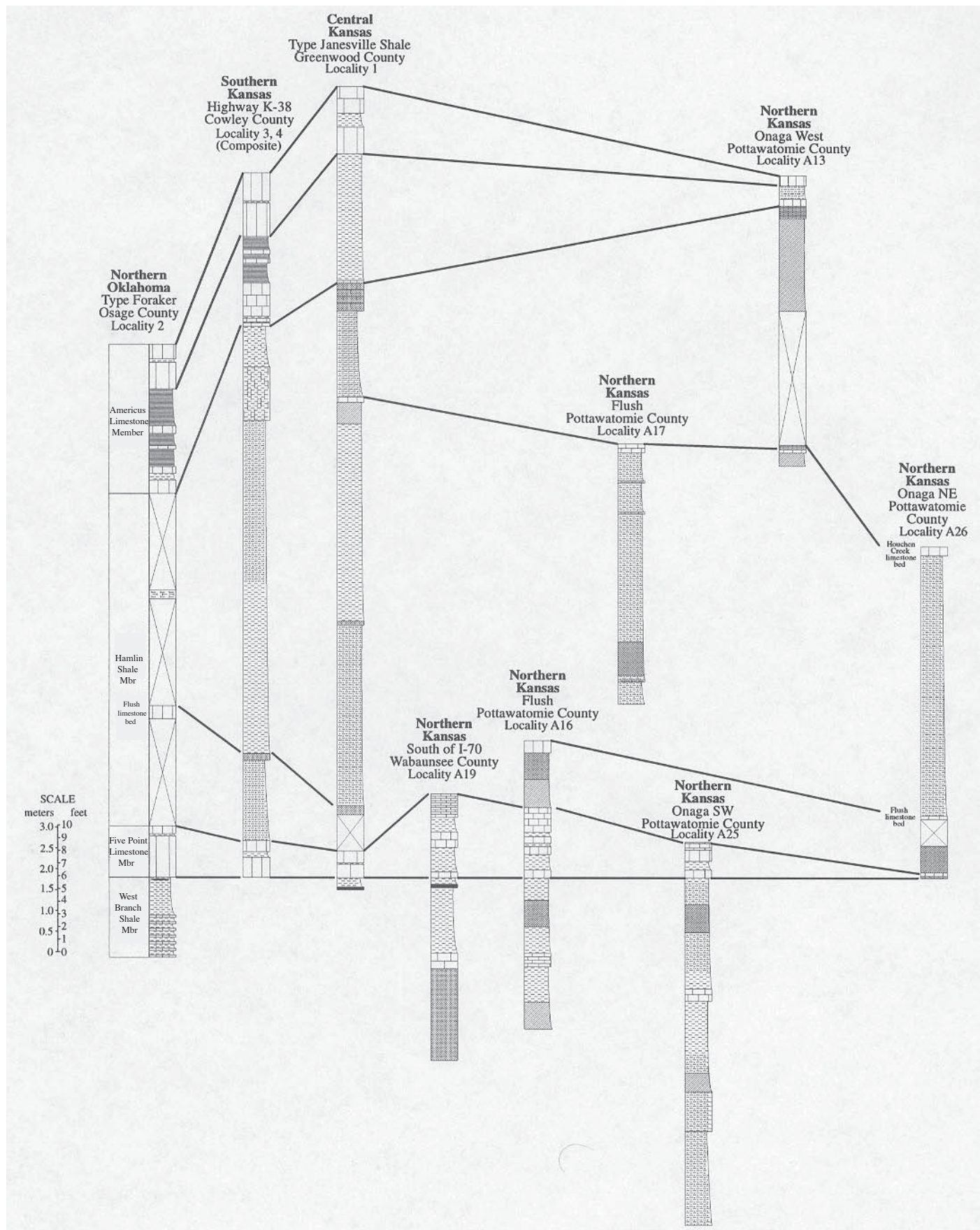
FIGURE 34—Lithostratigraphy of outcrop stratigraphic sections utilized to characterize the Five Point Composite Fourth-Order Sequence; localities 2, 3–4 (composite), 1, A19, A16, A25, A17, A13, and A26. Some stratigraphic data for this cross section were provided by Vann (1994).
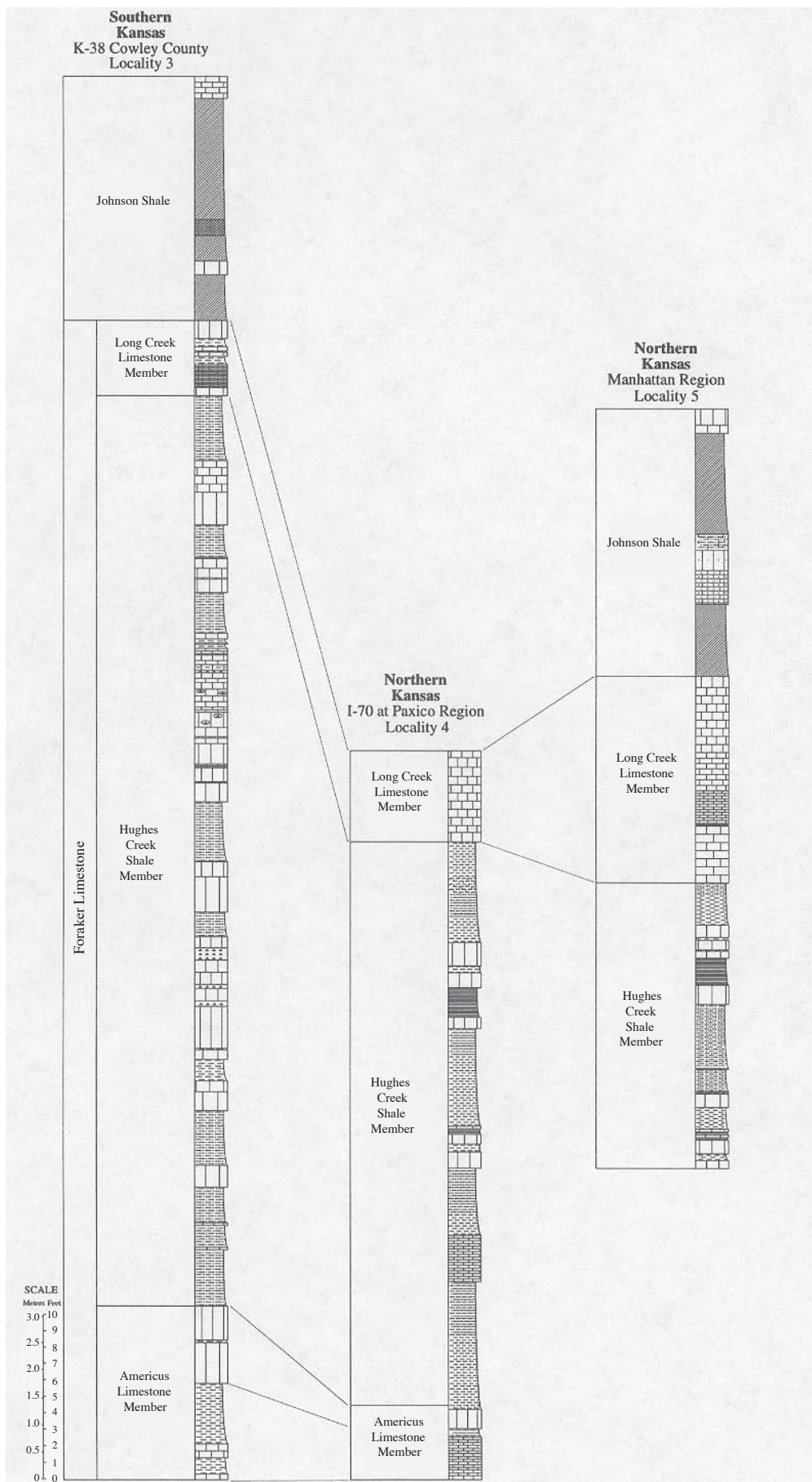
FIGURE 35—Lithostratigraphy of outcrop stratigraphic sections utilized to characterize the Foraker Composite Fourth-Order Sequence; localities 4, 5, and 6. Some stratigraphic data for this cross section were provided by Keairns (1995).

Kansas, a moderately fossiliferous shale in southern Kansas, and a *Myalina*-bearing packstone/grainstone in northern Oklahoma. The second of these occurs in the upper part of the Hamlin Shale Member. This sequence is manifested by a stromatolitic carbonate mapped as the Houchen Creek Limestone Member in Nebraska and Houchen Creek limestone bed in northern Kansas, and by an unnamed fossiliferous limestone in central and southern Kansas. This limestone is underlain and overlain by red and green blocky mudstones.

The Five Point Sequence contains *Streptognathodus flexuosus* Chernykh and Ritter along with S. *brownvillensis* Ritter.

Council Grove Group Sequences

Foraker Composite Fourth-Order Depositional Sequence

The Americus Limestone Member, Hughes Creek Shale Member, Long Creek Limestone Member, and the lower two-thirds of the Johnson Shale (figs. 3, 7, 35) comprise the Foraker Depositional Sequence. The Foraker Sequence is composed of eight fifth-order sequences that are correlatable across the entire outcrop area. The lower six fifth-order sequences are capped by nearshore marine to marginal-marine deposits consisting of poorly fossiliferous silty shales, whereas the upper two are capped by green to red blocky caliche-bearing mudstones indicative of paleosols. The fifth-order depositional sequences that are capped by marginal-marine deposits are analogous to the subtidal fifth-order cycles of Goldhammer et al. (1991) for the Desmoinesian of the Paradox basin, whereas those capped by subaerially exposure surfaces are similar to this exposure fifth-order cycles. The exposure cycles occur at the top of the Foraker Fourth-Order Sequence in a similar fashion to those of the Paradox basin. The base of each fifth-order sequence is defined by a major flooding surface characterized by a highly fossiliferous wackestone with ubiquitous horizontal boxworks of the trace fossil *Thalassinoides* and an abundant open-marine fauna including bryozoans, brachiopods, and fusulinaceans. Chaplin (1996) interpreted the occurrences of horizontal boxworks of *Thalassinoides* to represent transgressive surfaces in analogous Lower Permian Chase Group strata of the midcontinent. Maximum-marine flooding surfaces are represented by highly fossiliferous wackestones without evidence of condensed sedimentation in cases of minor to intermediate sea-level rises. Highly fossiliferous glauconitic and phosphatic wackestones or dark-gray to black shales with evidence of condensed sedimentation for more major sea-level rises are found. Three of the fifth-order sequences contain marine-condensed sections including the upper part of the Americus Limestone Member (Fifth-Order Sequence B), the middle part of the Hughes Creek Shale Member (Fifth-Order Sequence D), and the upper part of the Hughes Creek Shale Member (Fifth-Order Sequence E). These maximum-marine flooding-surface condensed sections contain an abundant *Streptognathodus*-dominated conodont fauna with major evidence of condensed sedimentation including abundant glauconite and phosphatized mollusks in addition to the conodonts that range from 100 to 1,000 platforms/kilogram. In northern Kansas and Nebraska, these marine-condensed sections have well-developed

black shales, whereas in central and southern Kansas they occur as shaly, glauconitic, and phosphatic wackestones. Maximum-marine flooding surfaces of the lower part of the Americus (Fifth-Order Sequence A, lowermost Hughes Creek (Fifth-Order Sequence C), top Hughes Creek–Long Creek (Fifth-Order Sequence F), Long Creek (Fifth-Order Sequence G), contain a mixed *Adetognathus–Streptognathodus* biofacies with no evidence of condensed sedimentation. Maximum-marine flooding of the lower Johnson (Fifth-Order Sequence H) contains only a sparse assemblage of ostracodes and encrusting foraminifers without conodonts.

The transgressive surface of the Foraker Sequence occurs at the base of the Americus Limestone Member and consists of a regionally extensive, transgressive lag-and-ravinement surface characterized by an ostracode-rich conglomeratic shale or carbonate. Maximum-marine flooding for the Foraker Fourth-Order Depositional Sequence is placed at the condensed section of the upper Hughes Creek Shale Member (Foraker Fifth-Order Sequence E) as it corresponds to the most widespread black-shale bed and greatest condensed interval in the sequence. Fifth-order sequences above this level demonstrate progressively shallower water facies developed at maximum-marine flooding coupled with the cycles being terminated by subaerial exposure. The transgressive-systems tract of the Foraker Fourth-Order Sequence encompasses the Americus Limestone Member and the lower two-thirds of the Hughes Creek Shale Member, whereas the forced-regressive-systems tract encompasses the top of the Hughes Creek Shale Member, the Long Creek Limestone Member, and the lower two-thirds of the Johnson Shale.

The Foraker Fourth-Order Sequence contains three distinctive conodont faunas that can be correlated across the entire outcrop area.

The Upper Americus Fifth-Order Sequence contains *Streptognathodus wabaunsensis* Gunnell, *S. elongatus* Gunnell, *S. farmeri* Gunnell, and *S. flexuosus* Chernykh and Ritter.

The Lower Hughes Creek Fifth-Order Sequence contains *Streptognathodus flexuosus* Chernykh and Ritter, *S. conjunctus* Barskov, Isakova, and Shchastlivceva, S. *wabaunsensis* Gunnell, *S. farmeri* Gunnell, and *S. elongatus* Gunnell. This conodont fauna can be distinguished from the upper Americus fauna by the addition of *S. conjunctus* to the Hughes Creek assemblage.

The Upper Hughes Creek Fifth-Order Sequence contains *Streptognathodus conjunctus* Barskov, Isakova, and Shchastlivceva, *S. binodosus* Wardlaw, Boardman, and Nestell, *S. binodosus* transitional to *nodulinearis-isolatus*, and *S. elongatus* Gunnell. This conodont assemblage is unique from the underlying upper Americus and lower Hughes Creek fauna in that *S. binodosus* and advanced *binodosus* are present in this fauna and *S. wabaunsensis* and *S. farmeri* are missing.

Red Eagle Composite Fourth-Order Depositional Sequence

The upper Johnson Shale, Glenrock Limestone Member, Bennett Shale Member, Howe Limestone Member, and Roca Shale (figs. 3, 8, 36) comprise the Red Eagle Depositional Sequence. Maximum-marine flooding of this sequence corresponds to the provisional correlated position of the base of the Permian in North America based on the appearance of
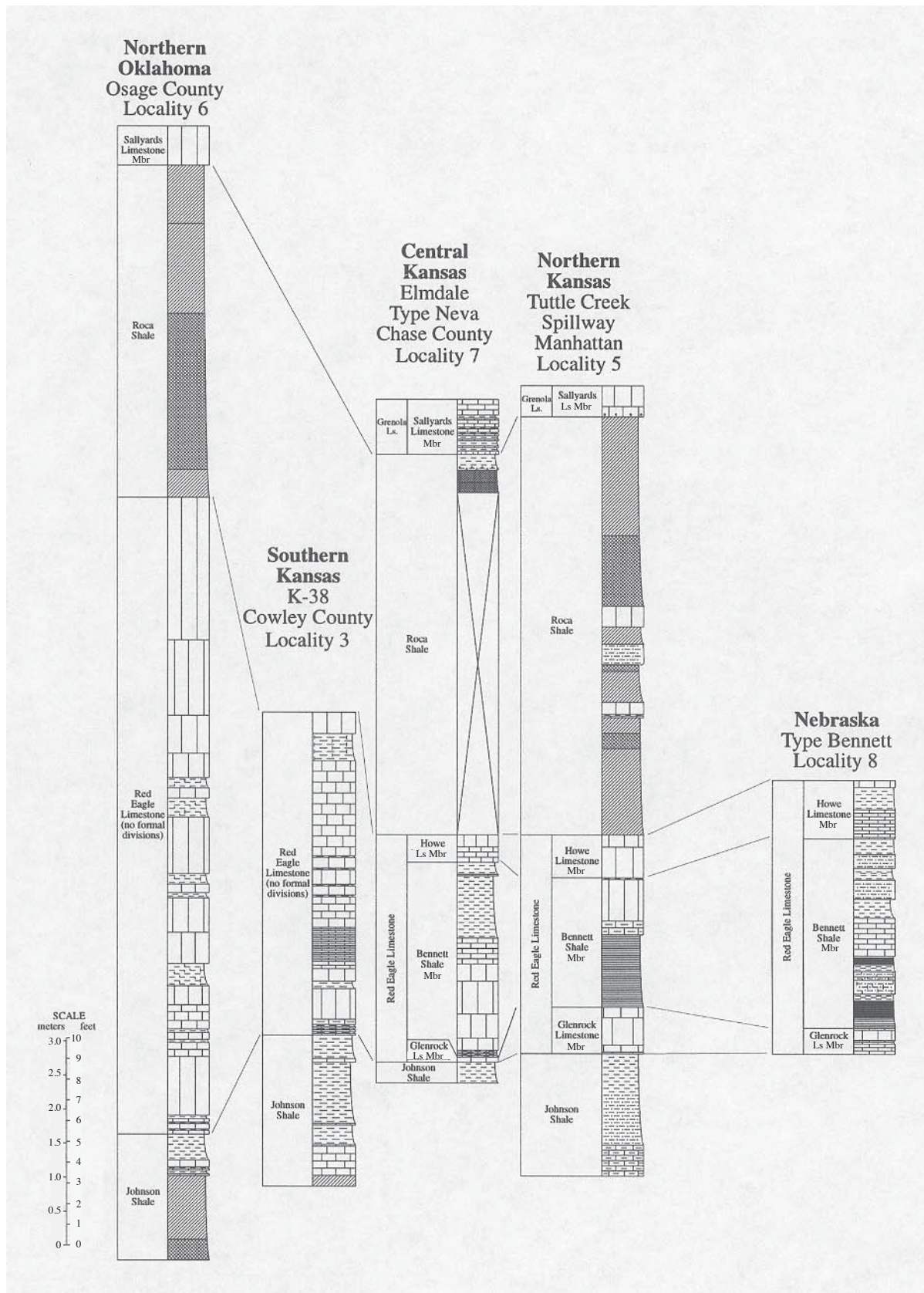
FIGURE 36—Lithostratigraphy of outcrop stratigraphic sections utilized to characterize the Red Eagle Composite Fourth-Order Sequence; localities A4, 4, A23, 6, and A3. Some stratigraphic data for this cross section were provided by Keairns (1995).

Streptognathodus isolatus (Chernykh et al., 1997). The Red Eagle Sequence consists of seven regionally correlative fifth-order depositional sequences. The transgressive surface of the Red Eagle Sequence occurs in the upper part of the Johnson Shale and is represented typically by a thin intraclastic packstone developed as a transgressive lag and ravinement. The lowermost Red Eagle Sequence is developed entirely within the top of the Johnson Shale and contains abundant ostracodes and rare conodonts of a mixed *Adetognathus–Streptognathus* assemblage, along with locally abundant mollusks and brachiopods including *Juresania, Linoproductus*, and *Derbyia*. This fifth-order sequence is terminated by silty dark mudstones and shales locally exhibiting silty rhythmites indicative of tidally influenced deposition. The next two fifth-order sequences (Red Eagle Fifth-Order Sequence B *and* C) both contain marine-condensed sections at maximum-marine flooding. Maximum-marine flooding of Red Eagle Fifth-Order Sequence B occurs at the base of the Bennett Shale Member and is represented by abundant *Streptognathodus* conodonts, orbiculoid brachiopods, ammonoids, and fish debris. In northern Kansas through Nebraska, this condensed section occurs in the base of black fissile shale of the Bennett Shale Member contrasted to central Kansas to Oklahoma where this condensed section occurs as a highly fossiliferous, shaly, glauconitic, phosphatic wackestone. This cycle is terminated by poorly fossiliferous siltstone within the Bennett Shale Member in Nebraska, upper black-shale facies with no evidence of condensation of the Bennett in northern Kansas, and a phylloid-algal-brachiopod-rich wackestone in central Kansas to northern Oklahoma. The maximum-marine flooding condensed section Red Eagle Fifth-Order Sequence C is represented by a black fissile shale above the poorly fossiliferous siltstone in Nebraska, by a calcite-cemented, black mudstone with horizontal boxworks of *Thalassinoides*, orbiculoid brachiopods, and abundant fish debris in the upper Bennett Shale Member in northern Kansas, and by either a highly fossiliferous, shaly, glauconitic, phosphatic wackestone or a thin, gray, highly fossiliferous phosphatic-shale parting (< 3 cm) in central Kansas to northern Oklahoma. In all regions *Streptognathodus* conodonts from 500 to 1,000 platforms/kilogram are noted from this condensed section. In northern Oklahoma and southern Kansas, the top three fifth-order sequences of the Red Eagle Sequence demonstrate a progressive shallowing of lithofacies and corresponding biofacies developed at maximum transgression. The top fifth-order sequence is capped by paleosols of the Roca Shale. In central Kansas through Nebraska, only Fifth-Order Sequence D is well developed in what is mapped as the Red Eagle Limestone. However, in those regions the Roca Shale is considerably thicker and contains two well-developed marine-flooding surfaces within the lower part of the shale (Miller and West, 1993). We interpret these additional marine-flooding surfaces that are not present in southern Kansas or northern Oklahoma to represent maximum-marine flooding of Fifth-Order Sequences E and F. This implies that northern Kansas and southern Nebraska were topographically higher on the shelf during deposition of the Red Eagle Sequence. According to this interpretation, while silty nearshore-marine shales and carbonates were being deposited in southern Kansas and northern Oklahoma during terminations of the Fifth-Order Sequences D and E, paleosols were forming in northern Kansas and Nebraska.

Marine flooding associated with Fifth-Order Sequences E and F then resulted in thin marine carbonates being deposited within the paleosol intervals.

The transgressive-systems tract of the Red Eagle Fourth-Order Depositional Sequence includes the interval from the transgressive lag in the upper Johnson Shale to the maximum-marine flooding surface condensed section in the upper Bennett (Red Eagle Fifth-Order Depositional Sequence C). The forced-regressive-systems tract includes the interval from the upper condensed section to the base of the Sallyards Limestone Member that marks the base of the Lower Grenola Fourth-Order Depositional Sequence.

The Red Eagle Sequence is characterized by *Streptogna-thodus isolatus* Chernykh, Ritter, and Wardlaw, *S. minacutus* Barskov and Reimers, *S. invaginatus* Reshetkova and Chernykh, *S. fuchengensis* Zhao, *S. nodulinearis* Reshetkova and Chernykh, S. *binodosus* Wardlaw, Boardman, and Nestell, new species, and *S. elongatus* Gunnell, along with the appearance of *Sweetognathus expansus* (Perlmutter). This occurrence is based on a single specimen from southern Kansas.

Lower Grenola (Burr) Composite Fourth-Order Depositional Sequence

The Sallyards Limestone, Legion Shale, Burr Limestone, and the Salem Point Shale Members in ascending order (figs. 3, 9, 37) comprise the Lower Grenola Sequence. The Lower Grenola Sequence is composed of four fifth-order depositional sequences. A transgressive lag (ravinement surface) marks the base of the Grenola Sequence. This lag generally coincides with the basal bed of the Sallyards Limestone Member except in central Kansas where it occurs in the top of the Roca Shale. The Sallyards (Fifth-Order Sequence A) includes the Sallyards Limestone and the Legion Shale Members. Maximum flooding occurs at the top of the Sallyards Limestone Member and is characterized by abundant pectinid and myalinid clams that are locally abundant at the top of the unit. No conodonts have been recovered from this fifth-order sequence. The lower part of the Legion Shale Member is typically gray to black silty mudstone with an abundant low-diversity ostracode assemblage. This unit is interpreted as being deposited in a shallow, perhaps lagoonal, marginal-marine environment. The abrupt contact between the maximum-flooding surface at the top of the Sallyards Limestone Member and the base of the Legion Shale Member with no transitional lithofacies or biofacies suggests a basinward shift of facies associated with rapidly falling sea level. In northern Kansas a thin conglomeratic ostracode-bearing carbonate is present near the top of the Legion Shale Member that represents the transgressive surface of the lower Burr Fifth-Order Sequence (Fifth-Order Sequence B). In other regions including northern Oklahoma, southern Kansas, central Kansas, and Nebraska, the base of the Burr Limestone Member contains the transgressive surface of the lower Burr Fifth-Order Sequence. Throughout the outcrop belt, the top of the lower limestone of the Burr Limestone Member is locally developed as a hard ground with abundant brachiopods (*Juresania*, *Composita,* and *Linoproductus*) along with a variety of mollusks, crinoids, and abundant phosphatic skeletal debris including fish and conodonts. This unit is
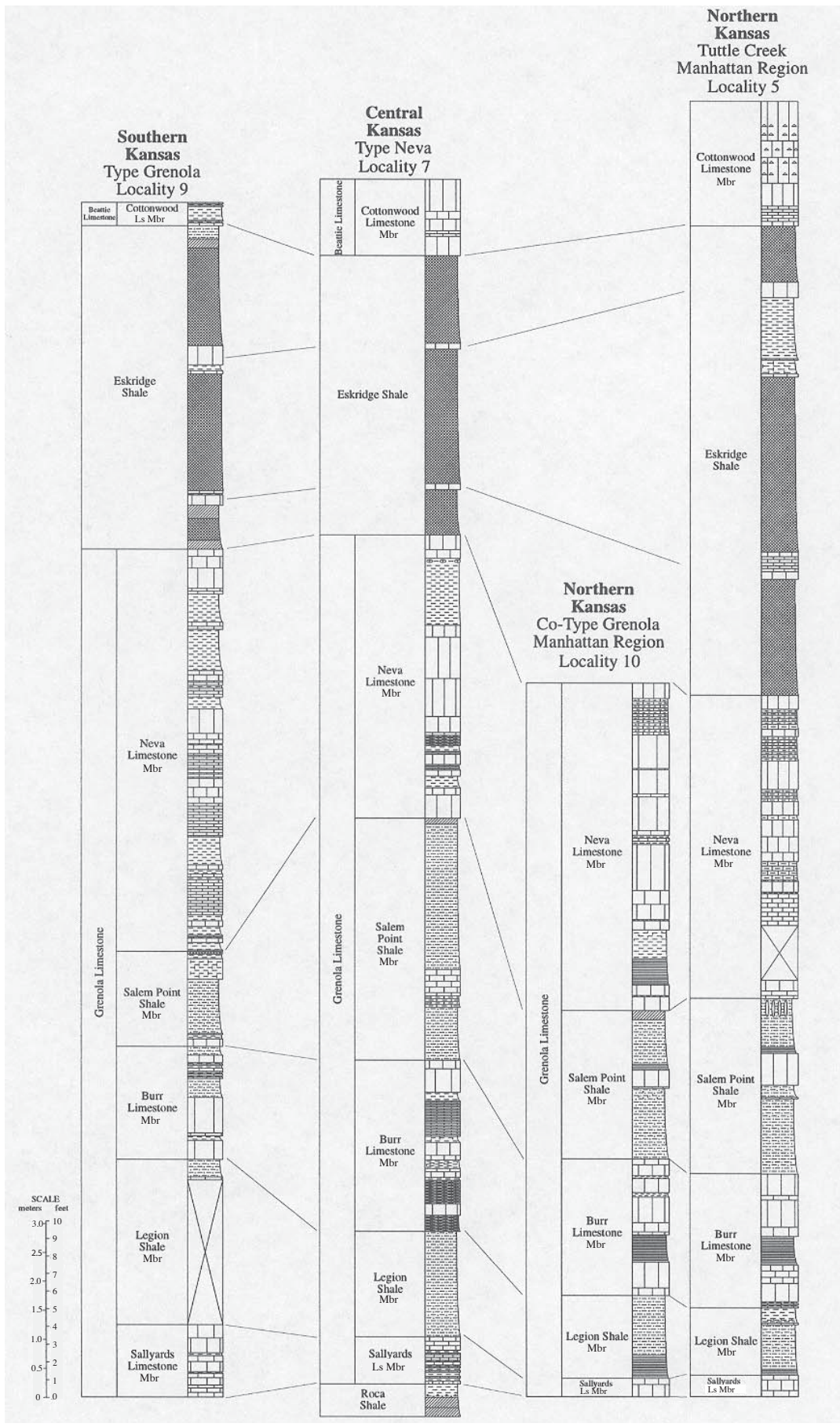
FIGURE 37—Lithostratigraphy of outcrop stratigraphic sections utilized to characterize the Lower Grenola and Upper Grenola Composite Fourth-Order sequences; localities 9, A23, 8, and 6.

interpreted to represent relatively minor condensation and maximum flooding. In northern Kansas, the top of the lower limestone of the Burr is immediately overlain by a gray to black silty, locally gypsiferous mudstone and shale that is characterized by a very sparse fauna of *Promytilus* clams and rare ostracodes. It is interpreted to represent a marginal-marine possibly hypersaline environment. The abrupt contact between diversely fossiliferous wackestone that marks the maximum-flooding surface and the overlying poorly fossiliferous black mudstone is indicative of a basinward shift in facies and forced regression. In central Kansas this interval is represented by thin-bedded poorly fossiliferous ostracode-bearing mudstone to wackestone, whereas poorly fossiliferous silty mudstones are present in southern Kansas and northern Oklahoma.

The base of the upper limestone of the Burr, present across the entire study area, is characterized by a transgressive lag with locally abundant skeletal-fish debris. It is interpreted to represent the transgressive surface of the upper Burr Fifth-Order Sequence (Lower Grenola Fifth-Order Sequence C). The upper part of the Burr Limestone Member contains abundant clams and locally abundant evaporite molds and is interpreted to represent a sabkha environment. The lower part of the overlying Salem Point Shale Member from Nebraska to southern Kansas consists of poorly fossiliferous, silty, blocky mudstones. Within the middle part of the Salem Point Shale Member, a thin pectinid- and myalinid-bearing carbonate is present from southern Nebraska to northern Oklahoma. This bed is interpreted to represent the base of Salem Point Fifth-Order Sequence (Lower Grenola Fifth-Order Sequence D). It is overlain by gray to black silty mudstones and shales with a low-diversity ostracode assemblage. The upper part of the Salem Point Shale Member across the outcrop belt consists of green to red blocky mudstones with locally developed columnar peds, blocky peds, slickensides, and other indications of paleosol development. This paleosol is well developed throughout the outcrop region.

The transgressive-systems tract of the Lower Grenola Fourth-Order Sequence includes the interval from the base of the Sallyards Limestone Member to the maximum-marine flooding surface at the top of the lower limestone of the Burr Limestone Member. The forced-regressive-systems tract includes the interval from the maximum-marine flooding surface to the Neva Limestone Member that marks the base of the Upper Grenola Fourth-Order Sequence.

The Burr Fifth-Order Sequence of the Grenola Sequence is characterized by a significant turnover in species of *Streptognathodus* including the appearances of *Streptognathodus postelongatus* Wardlaw, Boardman, and Nestell, *S. lineatus* Wardlaw, Boardman, and Nestell, *S. translinearis* Wardlaw, Boardman, and Nestell, and *S. nevaensis* Wardlaw, Boardman, and Nestell, along with the continued presence of *S. invaginatus* Reshetkova and Chernykh. Additionally, *Sweetognathus expansus* (Perlmutter) is a rare component of the conodont fauna.

Upper Grenola (Neva) Composite Fourth-Order Depositional Sequence

The Upper Grenola (Neva) Sequence includes the Neva Limestone Member and Eskridge Shale in ascending order (figs.

3, 9, 37). The Upper Grenola (Neva) Sequence is composed of five regionally correlative fifth-order sequences, the basal two of which have maximum-marine flooding condensed sections. The base of the Upper Grenola (Neva) Sequence is characterized by a regional transgressive lag that marks the base of the Neva Limestone Member and represents initial marine flooding. Maximum-marine flooding of the Lower Neva Fifth-Order Sequence A occurs in a tan, dark-gray, or black mudstone with ubiquitous skeletal phosphate composed of conodonts, orbiculoid brachiopods, and fish debris. It is present above the basal limestone of the Neva Limestone Member in Nebraska, throughout Kansas, and northern Oklahoma. This condensed section contains between 100–1,000 *Streptognathodus* platforms per kilogram throughout the outcrop belt. This fifth-order sequence is terminated by a phylloid-algal-rich wackestone to packstone throughout the outcrop belt. The unit is sharply overlain by a thin transgressive interval below a regionally developed maximum-flooding marine-condensed section of the Upper Neva Fifth-Order Sequence B that contains between 100–300 *Streptognathodus* platforms per kilogram. This fifth-order sequence is also terminated by a phylloid-algal-rich wackestone to packstone. The top three fifth-order sequences are exposure cycles as they are capped by subaerial-exposure surfaces developed as red to green blocky mudstone paleosols.

The Upper Grenola Sequence is significant in that it contains the last well-developed maximum-marine flooding condensed section and offshore black-shale facies in the Council Grove Group. Although maximum-marine flooding condensed sections are present in the lower Chase Group (Threemile, Schroyer, and basal Florence), no offshore black shales are present.

The maximum-marine flooding surface of the Upper Grenola (Neva) Fourth-Order Sequence occurs coincident with the Lower Neva Fifth-Order Sequence marine-condensed section. Therefore, the transgressive-systems tract includes the interval from the transgressive lag at the base of the Neva Limestone Member to the marine-condensed section. The forced-regressive-systems tract includes the interval from the condensed section to the base of the Cottonwood Limestone Member that marks the base of the Beattie Fourth-Order Depositional Sequence.

The Lower Neva Fifth-Order Sequence of the Grenola Sequence is characterized by *Streptognathodus lineatus* Wardlaw, Boardman, and Nestell, new species; *S. postelongatus* Wardlaw, Boardman, and Nestell, new species; *S. invaginatus* Reshetkova and Chernykh; *S. minacutus*; *S. isolatus* Chernykh, Ritter, and Wardlaw; *S. nodulinearis* Reshetkova and Chernykh; and *S. fuchengensis* Zhao, and the common occurrence of *Sweetognathus expansus* (Perlmutter).

The Upper Neva Fifth-Order Sequence is characterized by *Streptognathodus nevaensis* Wardlaw, Boardman, and Nestell, *S. fuchengensis* Zhao, and *S. postelongatus* Wardlaw, Boardman, and Nestell, and the common occurrence of *Sweetognathus expansus* (Perlmutter).

Beattie Composite Fourth-Order Depositional Sequence

The Cottonwood Limestone Member, Florena Shale Member, Morrill Limestone Member, and the lower Stearns Shale in ascending order (figs. 3, 10, 38) comprise the Beattie

Sequence. The Beattie Sequence is composed of two fifth-order depositional sequences. The base of the Cottonwood Limestone Member consists of a well-developed transgressive-lag deposit with abundant ostracodes in Nebraska through central Kansas. In southern Kansas, the lower Cottonwood Limestone Member changes facies from a massive, cherty, highly fossiliferous wackestone to packstone into highly fossiliferous shales and interbedded shaly wackestones, and the transgressive surface occurs as a transgressive lag in the first fossiliferous thin carbonate bed, which has previously been mapped with the Eskridge Shale. Maximum-marine flooding of the Cottonwood Beattie Fifth-Order Sequence A occurs near the center of the Cottonwood Limestone Member in Nebraska through central Kansas and is associated with fusulinaceans, a diverse brachiopod assemblage, corals, and some *Streptognathodus* platforms (10–30 platforms per kilogram). In southern Kansas, the Cottonwood Limestone Member and Florena Shale Member have a gradational contact and maximum-marine flooding occurs in a highly fossiliferous glauconitic wackestone about 0.5 m below the top of the limestone that has been mapped as the top of the Cottonwood Limestone Member in that region. In southern Kansas, maximum flooding contains a rich brachiopod assemblage of *Juresania, Reticulatia, Meekella, Neochonetes, Composita, Punctospirifer, Beecheria, Wellerella, Hustedia, Orbiculoidea*, and *Petrocrania* along with bryozoans, corals, trilobites, a rich and diverse foraminifer and ostracode assemblage, and a moderate abundance of *Streptognathodus*. This fifth-order sequence is terminated by poorly fossiliferous silty, locally dolomitic, shale and mudstones of the upper part of the Florena Shale Member. The Morrill Beattie Fifth-Order Sequence B is marked by a flooding surface at the base of the Morrill Limestone Member throughout the outcrop belt. Maximum-marine flooding occurs in a *Derbyia*-rich brachiopod interval in northern exposures and fusulinacean-rich fossiliferous shaly wackestone in central and southern exposures. This fifth-order sequence is terminated by a regionally correlative paleosol in the lower part of the Stearns Shale. This paleosol is represented for the most part by green to red blocky caliche-bearing mudstones and silty mudstones, and marks the sequence boundary between the Beattie Fourth-Order Sequence and the Eiss Fourth-Order Sequence.

The Beattie Sequence is characterized by *Streptognathodus fusus* Chernykh and Reshetkova, *S. longissimus* Chernykh and Reshetkova, *S. constrictus* Reshetkova and Chernykh, *S. nevaensis* Wardlaw, Boardman, and Nestell, and *Sweetognathus expansus* (Perlmutter).

Eiss Composite Fourth-Order Depositional Sequence

The Eiss (Lower Bader) Sequence is composed of the upper part of the Stearns Shale, Eiss Limestone Member, and the lower part of the Hooser Shale Member in ascending order (figs. 3, 11, 39). This sequence is characterized by three fifth-order sequences, one of which is developed in the upper part of the Stearns Shale and the other two in the Eiss Limestone Member. The transgressive surface of the Eiss (Lower Bader) Sequence occurs in slightly fossiliferous silty mudstones that overlie the paleosol interval. Maximum flooding of the Stearns Fifth-Order Sequence

occurs in gray shale above a thin fossiliferous wackestone in northern Kansas, and in a thin fossiliferous carbonate in central and southern Kansas. This shale contains an abundant fauna of ostracodes, foraminifers, and a low-diversity brachiopod and molluscan fauna. No evidence of condensed sedimentation or the presence of conodonts is noted in this fifth-order sequence. The Stearns Fifth-Order Sequence is terminated by poorly fossiliferous silty shales and mudstones of the uppermost Stearns Shale. In southern and central Kansas, the base of the Eiss Limestone Member marks the base of the Lower Eiss Fifth-Order Sequence and consists of a lower algal-rich carbonate with *Aviculopinna* clams and *Meekella* brachiopods that represents the initial marine flooding, whereas in northern Kansas a slightly fossiliferous silty shale denotes initial transgression of the sequence. Maximum flooding throughout the outcrop area occurs in an abundantly and diversely fossiliferous shale or shaly wackestone with moderately abundant *Streptognathodus* and containing trilobites, crinoids, bryozoans, and brachiopods including *Composita, Meekella, Juresania, Neochonetes*, and *Reticulatia*. This cycle is regionally terminated by poorly fossiliferous marginal-marine silty mudstones. The Upper Eiss Fifth-Order Sequence is characterized regionally by locally abundant gastropods and bivalves along with *Sweetognathus* conodonts. The top of the upper limestone of the Eiss shows direct evidence of subaerial exposure with regolith and red internal sediment infilling a massive vug network along with brecciated regolith developed at the top of the unit. Regionally, the basal Hooser Shale Member is a red to variegated blocky mudstone with numerous paleosol features. The maximum-marine flooding surface for the Eiss (Lower Bader) Fourth-Order Sequence is coincident with maximum flooding of the Lower Eiss Fifth-Order Sequence. The transgressive-systems tract includes strata from the transgressive surface in the Stearns Shale to the maximum-marine flooding surface, and the forced-regressive-systems tract includes strata from the maximum-flooding surface to the next transgressive surface in the Hooser Shale Member.

Dubois et al. (2003) interpret fourth-order sequences in the Council Grove Group as beginning at an exposed carbonate surface followed by primarily windblown silts, very fine sands, and clay-rich silt with paleosols. Though there is evidence for exposure for some carbonates, it is not true for all and this model does not allow for the cyclicity observed in the largely nonmarine section where several distinct fourth-order sequences exist. In the case of the Eiss Limestone Member where there is significant evidence of exposure of the upper limestone of the Eiss, that is the beginning of what we term the sequence-boundary zone that ends at the top of the paleosol developed in the lower part of the Hooser Shale Member. Dubois et al. (2003) would draw the fourth-order master depositional-sequence boundary on the top of the carbonate; we would draw it on top of the paleosol.

The Eiss sequence is characterized by *Streptognathodus barskovi* Kozur and *Streptognathodus constrictus* Reshetkova and Chernykh along with the appearance of *Sweetognathus merrilli*.

Middleburg Composite Fourth-Order Depositional Sequence

The Middleburg Sequence is composed of the Middleburg Limestone Member and the Easly Creek Shale in ascending
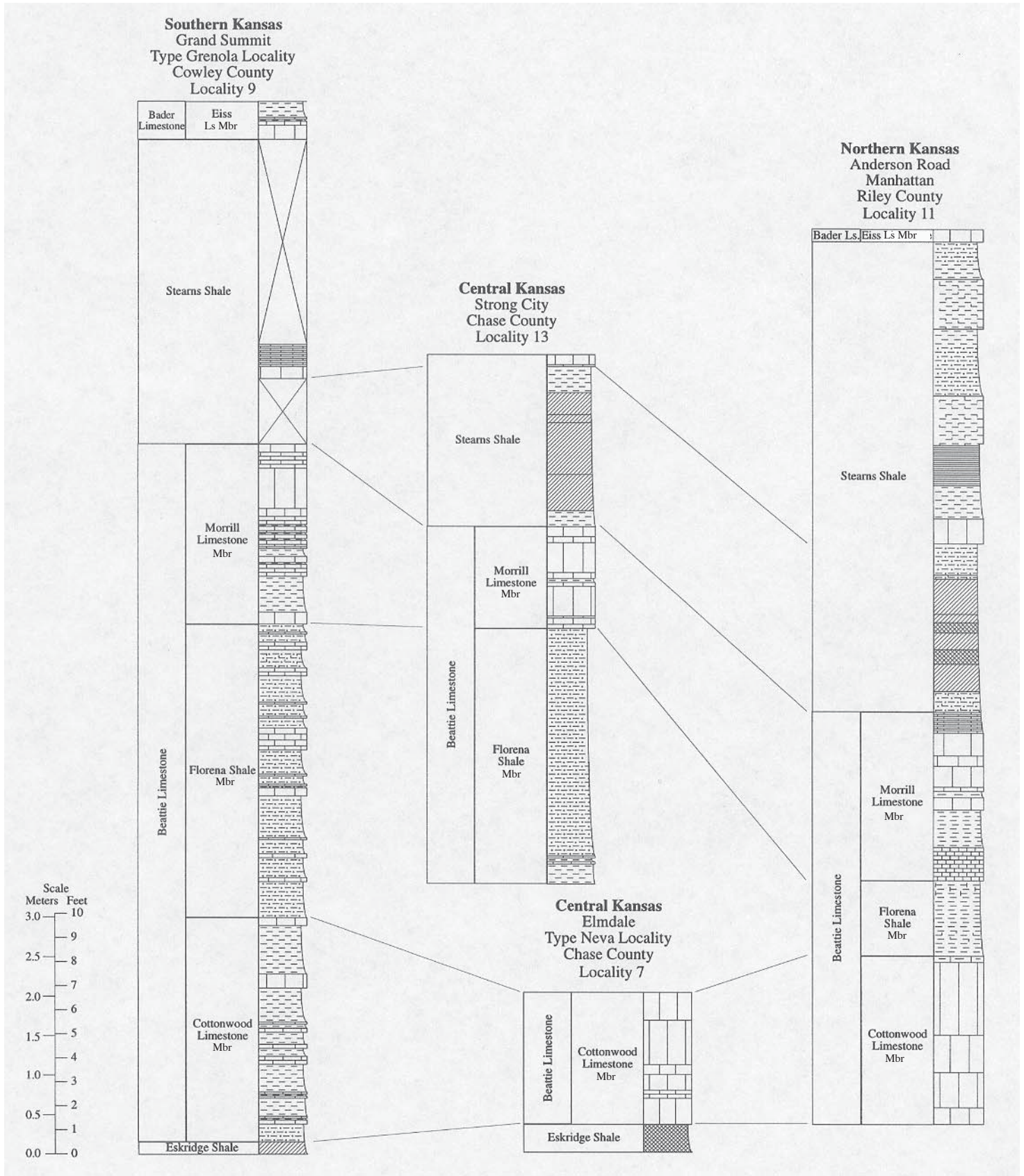
FIGURE 38—Lithostratigraphy of outcrop stratigraphic sections utilized to characterize the Beattie Composite Fourth-Order Sequence; localities 9, 21, A23, and 11.
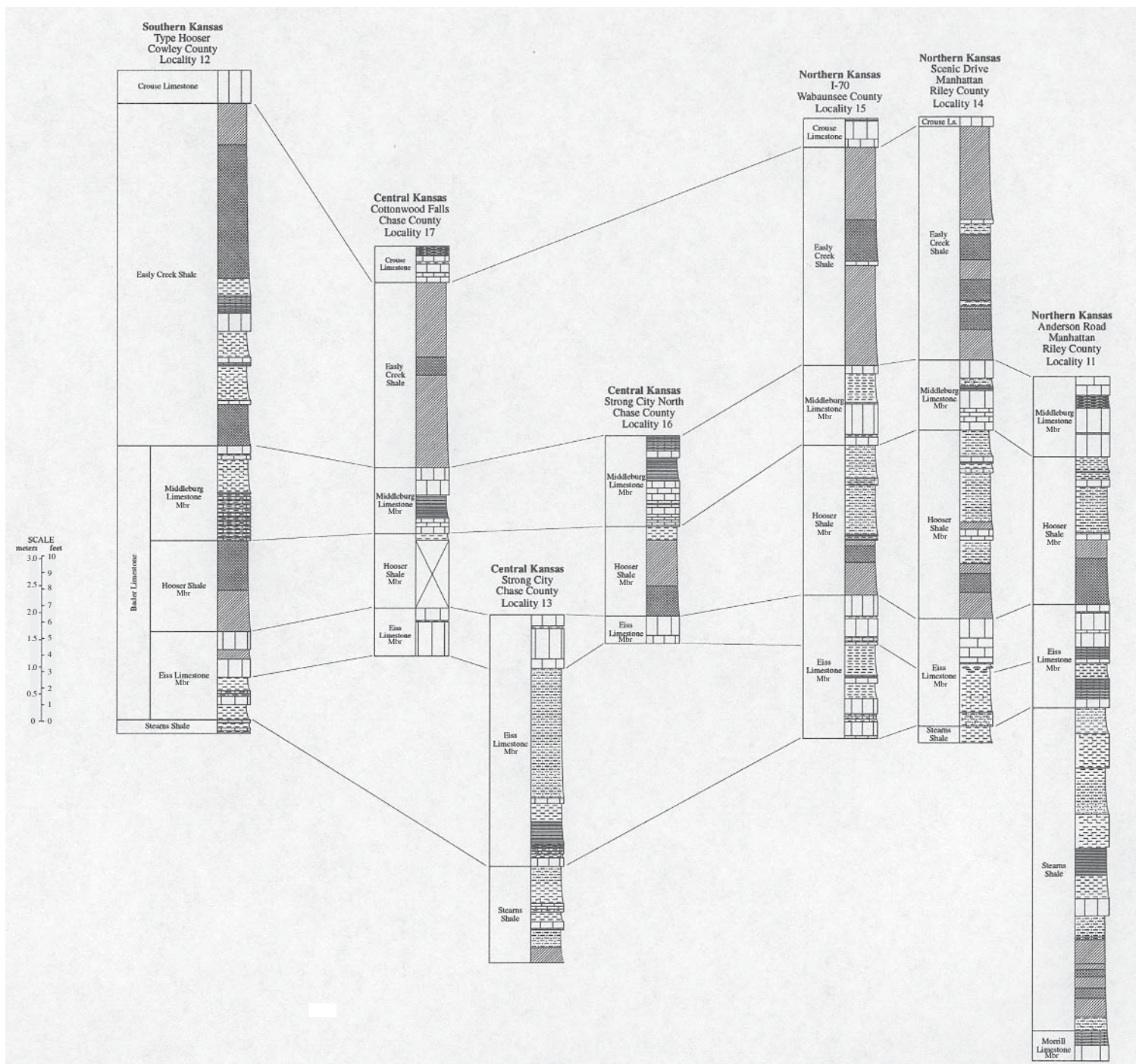
FIGURE 39—Lithostratigraphy of outcrop stratigraphic sections utilized to characterize the Eiss and Middleburg Composite Fourth-Order sequences; localities 12, 17, 13, 16, 15, 14, and 11. Some stratigraphic data for this cross section were provided by Yang (1996).

order (figs. 1, 11, 39). Two fifth-order sequences comprise the Middleburg Fourth-Order Sequence. The base of the Middleburg Fourth-Order Sequence is highly complex. In northern Kansas, the transgressive surface is coincident with a limestone in the middle part of the Hooser Shale Member. In central Kansas, the transgressive surface occurs in shale near the top of the Hooser Shale Member, whereas in southern Kansas, it occurs at the base of the Middleburg Limestone Member. Apparently, the middle and upper Hooser of the northern outcrop belt are stratigraphic equivalents of the basal Middleburg of southern Kansas. The Lower Middleburg Fifth-Order Sequence includes strata from

the transgressive surface to the base of the upper Middleburg ledge, and the Upper Middleburg Fifth-Order Sequence includes strata from the upper Middleburg ledge to the base of the Crouse Limestone. In northern Kansas, the Middleburg Limestone Member contains abundant gastropods near the base and sparse brachiopods and crinoids near the center of the unit with *Sweetognathus* and sparse *Streptognathodus* conodonts. In central and southern Kansas, the lower part of the lower Middleburg Limestone Member ledge contains abundant pectinid bivalves, local phylloid algae, and gastropods. The upper part of the lower Middleburg ledge contains an abundant and diverse open-marine

fauna including corals, bryozoans, brachiopods, crinoids, and trilobites, with some *Streptognathodus*. The brachiopod interval is interpreted as the maximum-marine flooding of the Lower Middleburg Fifth-Order Sequence. Immediately overlying this interval is a thin-bedded, shaly, dark-gray, poorly fossiliferous mudstone to wackestone in northern Kansas; a black fissile, somewhat silty, poorly fossiliferous shale in central Kansas; and a poorly fossiliferous, calcareous and silty shale in southern Kansas. This interval represents rapid shallowing and a basinward shift in facies and forced regression. The interval is sharply overlain by a fossiliferous wackestone to packstone with gastropods, encrusting foraminifers, and algal-coated grains that marks the base of the second Middleburg Fifth-Order Sequence. The base of the limestone also marks maximum flooding of the upper Middleburg Fifth-Order Sequence. This fifth-order sequence is apparently devoid of conodonts. The unit is capped by green and red blocky silty mudstones interpreted to represent paleosols within the Easly Creek Shale.

Maximum-marine flooding of the Middleburg Fourth-Order Sequence is coincident with the brachiopod facies near the top of the lower Middleburg ledge. In northern Kansas, the transgressive-systems tract includes strata from the base of the limestone in the middle part of the Hooser Shale Member to the top of the lower Middleburg. In central Kansas, the transgressive-systems tract includes strata from the uppermost Hooser Shale Member to the top of the lower Middleburg, and in southern Kansas it includes strata from the base of the Middleburg Limestone Member to the top of the lower Middleburg ledge. The forced-regressive-systems tract includes strata from the top of the lower Middleburg to the base of the Crouse Limestone.

The Middleburg (Upper Bader) Sequence is characterized by *Streptognathodus constrictus* and *Sweetognathus expansus*.

Crouse Composite Fourth-Order Depositional Sequence

The Crouse Limestone and the Blue Rapids Shale in ascending order (figs. 3, 12, 40) comprise the Crouse Sequence. Four fifth-order sequences comprise the Crouse Sequence, three of which are developed within the Crouse Limestone and one developed in the Blue Rapids Shale. The base of the Crouse Limestone throughout the outcrop area constitutes the transgressive surface of the sequence and locally exhibits a well-developed transgressive lag. The Lower Crouse Fifth-Order Sequence contains a moderately diverse fauna of brachiopods, bryozoans, and crinoids throughout the outcrop area and includes abundant *Ottonosia* algal colonies in central and southern Kansas. Commonly, the *Ottonosia* colonies contain silicified specimens of *Composita* in the nucleus of the algal masses. Maximum-marine flooding in northern and central Kansas occurs at the top of the lower Crouse Limestone ledge in a fossiliferous shaly wackestone with bryozoans, crinoids, and *Neochonetes* brachiopods. In southern Kansas, only one limestone ledge is present in the Crouse and maximum flooding occurs in a fossiliferous wackestone above the *Ottonosia*-bearing interval. Sparse numbers of *Streptognathodus* mark the maximum-marine flooding, but they are more abundant in central and southern Kansas. In central and northern Kansas, the Lower Crouse Fifth-Order Sequence is terminated by black, poorly fossiliferous

shales, which are overlain by increasing amounts of silt upwards in the section. In southern Kansas, the cycle is capped by poorly fossiliferous packstones. The base of the Middle Crouse Fifth-Order Sequence occurs at the base of the middle limestone ledge of the Crouse Limestone in northern Kansas. Maximum-marine flooding of that cycle occurs near the top of the middle ledge in that region represented by ostracodes and bivalves with moderate numbers of the conodont *Sweetognathus*. The base of the Middle Crouse Fifth-Order Sequence occurs at the base of the upper Crouse ledge in central Kansas as well. Likewise, in that region, *Sweetognathus*, pectinid bivalves, and ostracodes dominate the fauna. In southern Kansas, the Middle Crouse Fifth-Order Sequence occurs above a small shale break above the packstone that terminates the Lower Crouse Fifth-Order Sequence. It has a more open-marine fauna including brachiopods, bryozoans, and bivalves along with rare specimens of *Sweetognathus* and *Streptognathodus*. The Top Crouse Fifth-Order Sequence along with the lower Blue Rapids Shale Fifth-Order Sequence both are exposure cycles, which contain an assemblage of shallow-water ostracodes and encrusting foraminifers throughout the outcrop belt.

Maximum-marine flooding of the Crouse Fourth-Order Sequence occurs coincident with the maximum-flooding surface of the Lower Crouse Fifth-Order Sequence. The transgressive-systems tract includes strata from the base of the Crouse to the maximum-marine flooding surface. The forced-regressive-systems tract includes strata from the maximum-flooding surface to the sequence boundary in the upper Blue Rapids Shale.

The Crouse Sequence is characterized by *Streptognathodus postconstrictus* Wardlaw, Boardman, and Nestell, *Streptognathodus translinearis* Wardlaw, Boardman, and Nestell, and *Streptognathodus constrictus* Reshetkova and Chernykh.

Funston Composite Fourth-Order Depositional Sequence

The upper part of the Blue Rapids Shale, Funston Limestone, and the majority of the Speiser Shale in ascending order (figs. 3, 13, 41) comprise the Funston Sequence. Four fifth-order sequences comprise the Funston Sequence, one of which is developed in the top of the Blue Rapids Shale and three of which are developed in the Funston Limestone. The transgressive surface of the Funston Sequence occurs at the base of a regionally correlative limestone in the upper Blue Rapids Shale. This limestone marks the base of the Upper Blue Rapids Fifth-Order Sequence and is best developed in southern Kansas. It then gradually thins into central and northern Kansas. In southern and central Kansas, this carbonate contains algae, bivalves, and encrusting foraminifers at its base that are also interpreted to represent maximum-marine flooding. In northern Kansas it contains mainly ostracodes and encrusting foraminifera. Conodonts in this fifth-order sequence are restricted to southern Kansas where they include only rare specimens of *Sweetognathus*. This cycle is terminated by silty, poorly fossiliferous mudstones in central and northern Kansas and by poorly fossiliferous dark-gray shales in southern Kansas. The base of the Lower Funston Fifth-Order Sequence coincides with the base of the Funston in all areas except along Kansas Highway K–38 where it occurs a few centimeters below the base
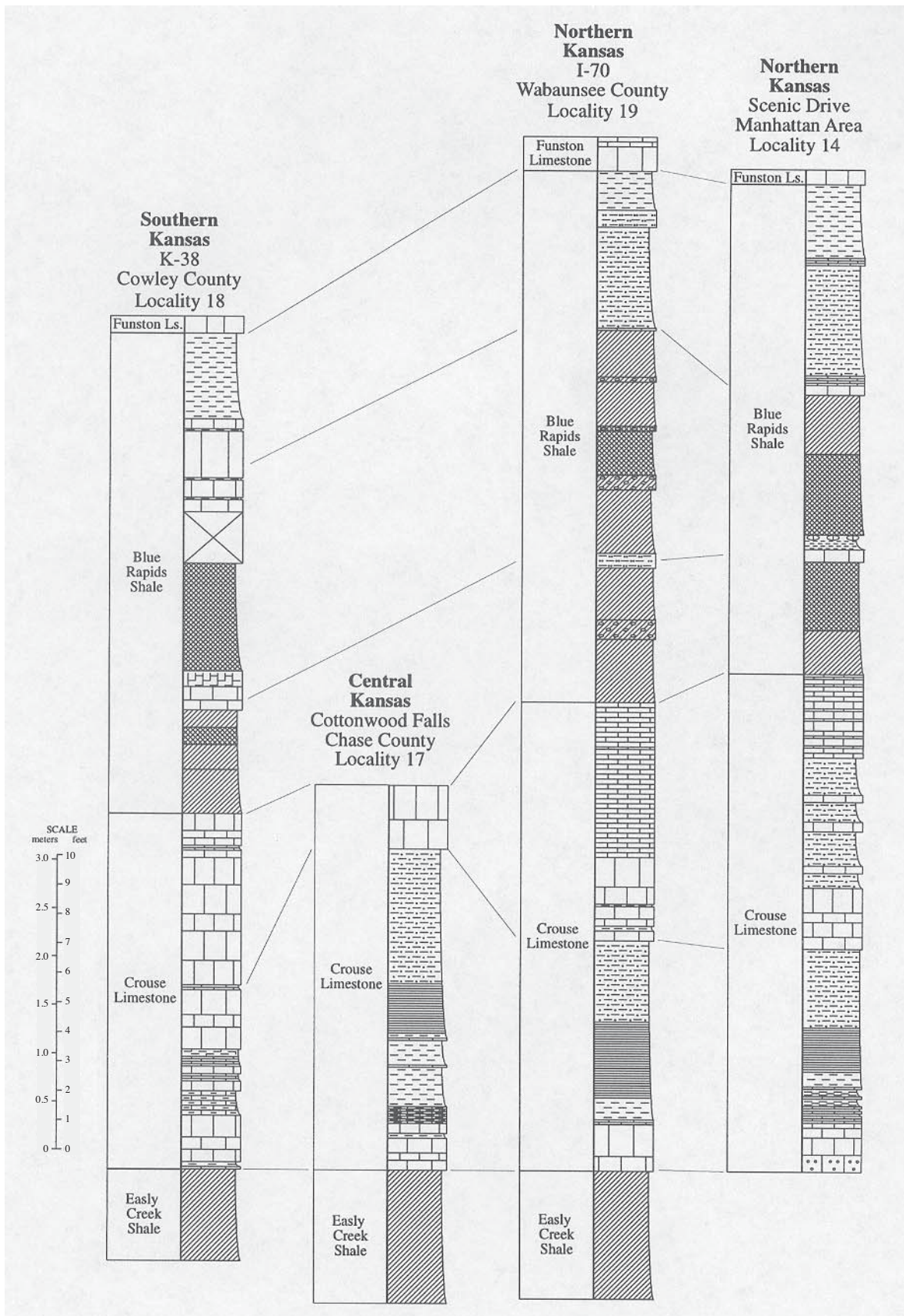
FIGURE 40—Lithostratigraphy of outcrop stratigraphic sections utilized to characterize the Crouse Composite Fourth-Order Sequence; localities 18, 17, 19, and 14. Some stratigraphic data for this cross section were provided by Yang (1996).
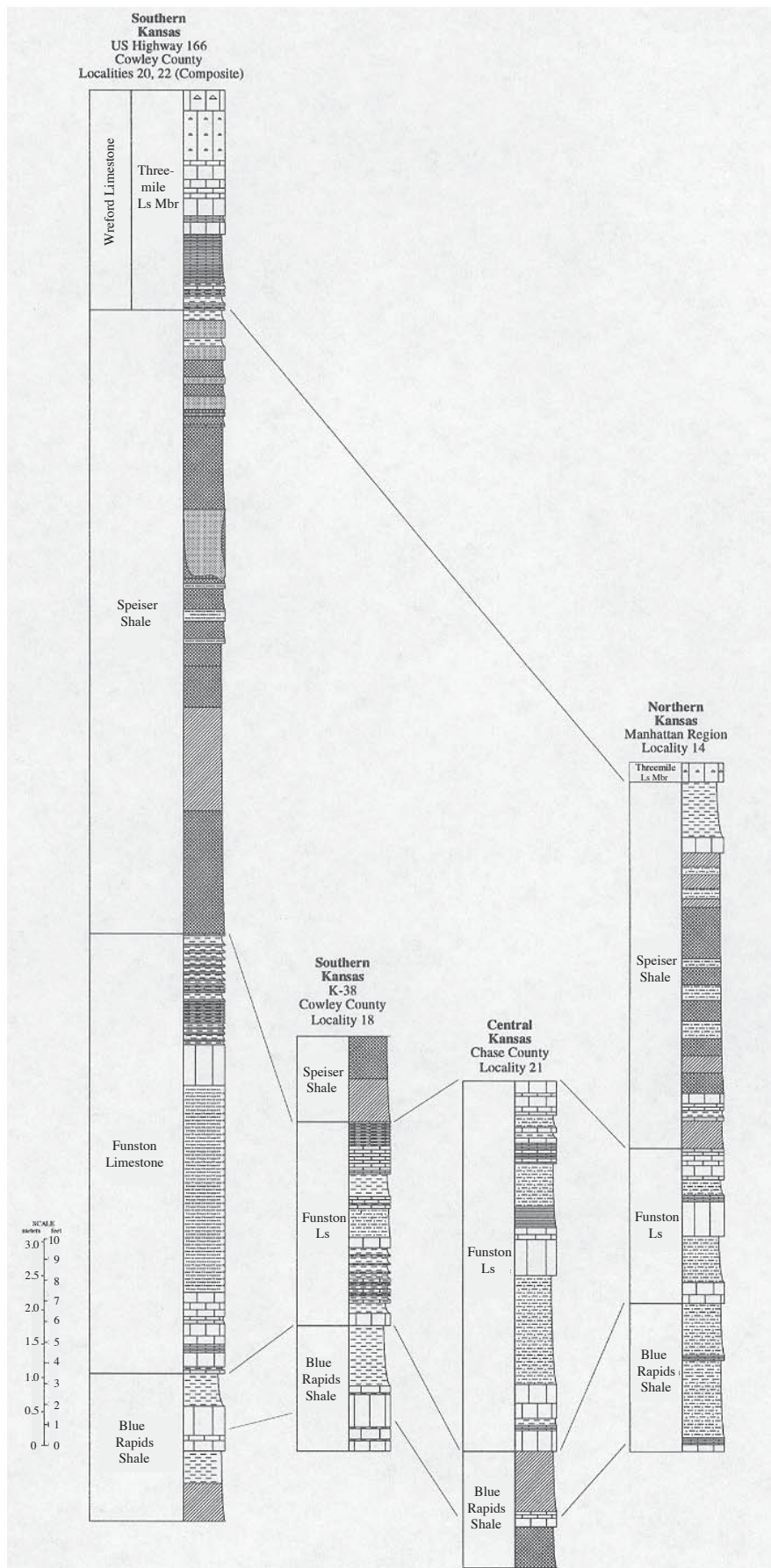
FIGURE 41—Lithostratigraphy of outcrop stratigraphic sections utilized to characterize the Funston Composite Fourth-Order Sequence; localities 20–22 (composite), 18, 21, and 14. Some stratigraphic data for this cross section were provided by Yang (1996).
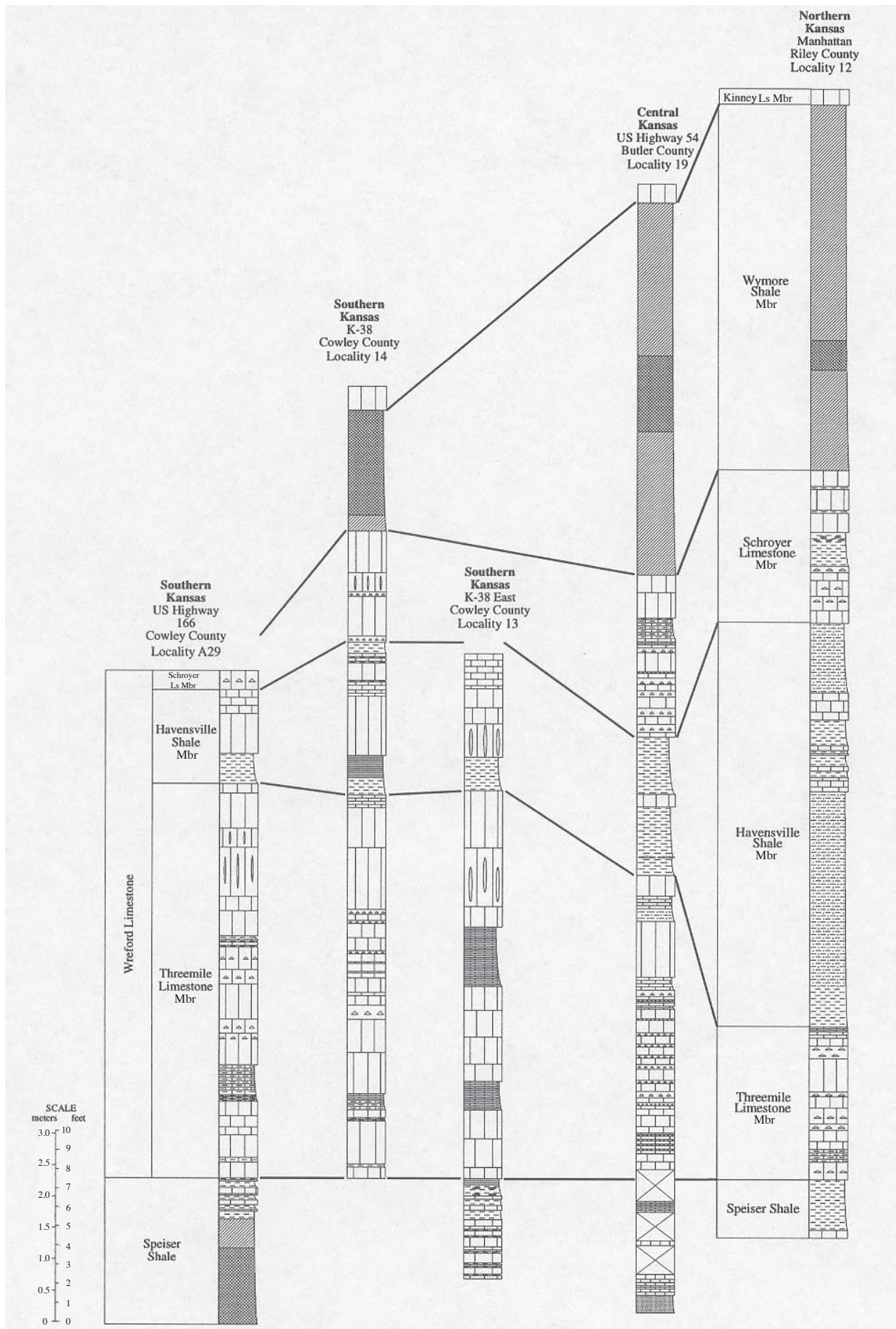
FIGURE 42—Lithostratigraphy of outcrop stratigraphic sections utilized to characterize the Wreford Composite Fourth-Order Sequence; localities A29, 14, 13, 19, and 12.

of the Funston. Maximum-marine flooding occurs at the base of the cycle where a moderately diverse assemblage of crinoids, bryozoans, bivalves, and brachiopods include *Juresania* and *Derbyia*. Low numbers of *Streptognathodus* and *Sweetognathu*s typify this horizon. This cycle is terminated by silty, poorly fossiliferous shales in all outcrop regions except southernmost Kansas, where it is denoted by a shaly, poorly fossiliferous carbonate. In central Kansas northward to I–70 in northern Kansas, a poorly fossiliferous, black shale sharply overlies the lower Funston Limestone and terminates the Lower Funston Fifth-Order Sequence. The top two fifth-order sequences contain a low-diversity bivalve and gastropod assemblage and contain rare specimens of *Sweetognathus*. The top fifth-order sequence is an exposure cycle overlain by red and green silty mudstones of the Speiser Shale.

Maximum-marine flooding of the Funston Fourth-Order Sequence corresponds to the top of the Lower Funston Fifth-Order Sequence maximum-marine flooding surface. The transgressive-systems tract includes strata from the transgressive surface in the upper Blue Rapids Shale to the maximum-marine flooding surface, and the forced-regressive-systems tract includes strata from the maximum-flooding surface to the transgressive surface near the top of the Speiser Shale that marks the base of the Wreford Fourth-Order Sequence. Along US–166 in southern Kansas, sandstones are common in the Speiser Shale and one bed is channeliform, indicating a return of fluvial deposition, which has been rare in the Council Grove Group in Kansas.

The Funston Sequence is characterized by *Streptognathodus translinearis* Wardlaw, Boardman, and Nestell, and *Sweetognathus expansus*.

Chase Sequences

Wreford Composite Fourth-Order Depositional Sequence

The Wreford Sequence is composed of the upper part of the Speiser Shale, Wreford Limestone, and the Wymore Shale Member in ascending order (figs. 3, 14, 42). Three fifth-order sequences comprise the Wreford Sequence. The uppermost part of the Speiser Shale, Threemile Limestone Member, and lower Havensville Shale Member constitute the basal fifth-order sequence (Wreford Fifth-Order Sequence A). The second fifth-order sequence is developed within the upper part of the Havensville Shale Member (Wreford Fifth-Order Sequence B), and the third sequence is composed of the Schroyer Limestone and Wymore Shale Members (Wreford Fifth-Order Sequence C).

The transgressive surface of the Wreford Sequence occurs throughout the outcrop belt as a fossiliferous wackestone-packstone in the upper 1–5 m of the Speiser Shale. Maximum flooding of the Wreford Fifth-Order Sequence A occurs in a highly fossiliferous, shaly, slightly glauconitic, and siliceous wackestone that occurs near the base of the Threemile Limestone Member. This interval contains abundant silicified brachiopods, bryozoans, and corals, along with a moderately abundant conodont fauna dominated by *Streptognathodus* with minor *Sweetognathus*. This fifth-order sequence is terminated by poorly fossiliferous silty shales and blocky mudstones of the middle part of the Havensville Shale Member.

The transgressive surface of the Wreford Fifth-Order Sequence B occurs at the base of a fossiliferous wackestone-packstone that occurs in the upper part of the Havensville Shale Member in all regions of the outcrop belt. Maximum-marine flooding occurs a short stratigraphic distance above the transgressive surface and is characterized by a low-diversity brachiopod assemblage with *Composita* along with abundant echinoids and a moderate abundance of *Sweetognathus*. This sequence is terminated by poorly fossiliferous silty shales of the topmost part of the Havensville Shale Member.

The transgressive surface of the Wreford Fifth-Order Sequence C occurs either immediately beneath the Schroyer Limestone Member or coincident with the base of the Schroyer Limestone Member. Maximum flooding occurs in a highly fossiliferous wackestone in southern Kansas and a highly fossiliferous calcareous shale with abundant brachiopods, bryozoans, and a moderately abundant *Streptognathodus* fauna in central and northern Kansas. This fifth-order sequence is capped by a foraminiferal grainstone at the top of the Schroyer Limestone Member that has well-developed subaerially exposed features including brecciated regolith and red-internal sediment in solution vugs and root cavities. This is overlain by red and green blocky mudstones with numerous paleosol features.

Maximum-marine flooding of the Wreford Fourth-Order Depositional Sequence is placed provisionally at the maximum-marine-flooding level within the Threemile Limestone Member. Therefore, the transgressive-systems tract includes the top part of the Speiser Shale and the basal part of the Threemile Limestone Member. The forced-regressive-systems tract includes the interval from the maximum-marine flooding level in the Threemile Limestone Member to the top of the Wymore Shale Member, which includes paleosols in its uppermost part.

The Wreford Sequence is characterized by *Streptognathodus trimilus* Wardlaw, Boardman, and Nestell, *S. postconstrictus* Wardlaw, Boardman and Nestell, *S. robustus* Wardlaw, Boardman, and Nestell, and *Sweetognathus merrilli* Kozur.

Kinney Composite Fourth-Order Depositional Sequence

The Kinney Sequence is composed of the Kinney Limestone Member and the Blue Springs Shale Member in ascending order (figs. 3, 15, 43). Three fifth-order sequences comprise the Kinney Sequence. The lower Kinney limestone ledge and unnamed shale separating the two Kinney limestone ledges comprise the lower fifth-order sequence (Kinney Fifth-Order Sequence A). The upper Kinney Limestone Member ledge and basal Blue Springs Shale Member constitute the second fifth-order sequence (Kinney Fifth-Order Sequence B), and the Bruno limestone bed and upper part of the Blue Springs Shale Member comprise the top fifth-order sequence (Kinney Fifth-Order Sequence C).

Maximum-marine flooding of the lower Kinney Sequence A is characterized by fossiliferous wackestones and packstones characterized by an abundant brachiopod fauna with *Composita, Derbyia*, and *Juresania* along with a mixed *Streptognathodus–Sweetognathus* conodont biofacies with moderate abundance. This sequence is terminated by poorly fossiliferous silty mudstones.
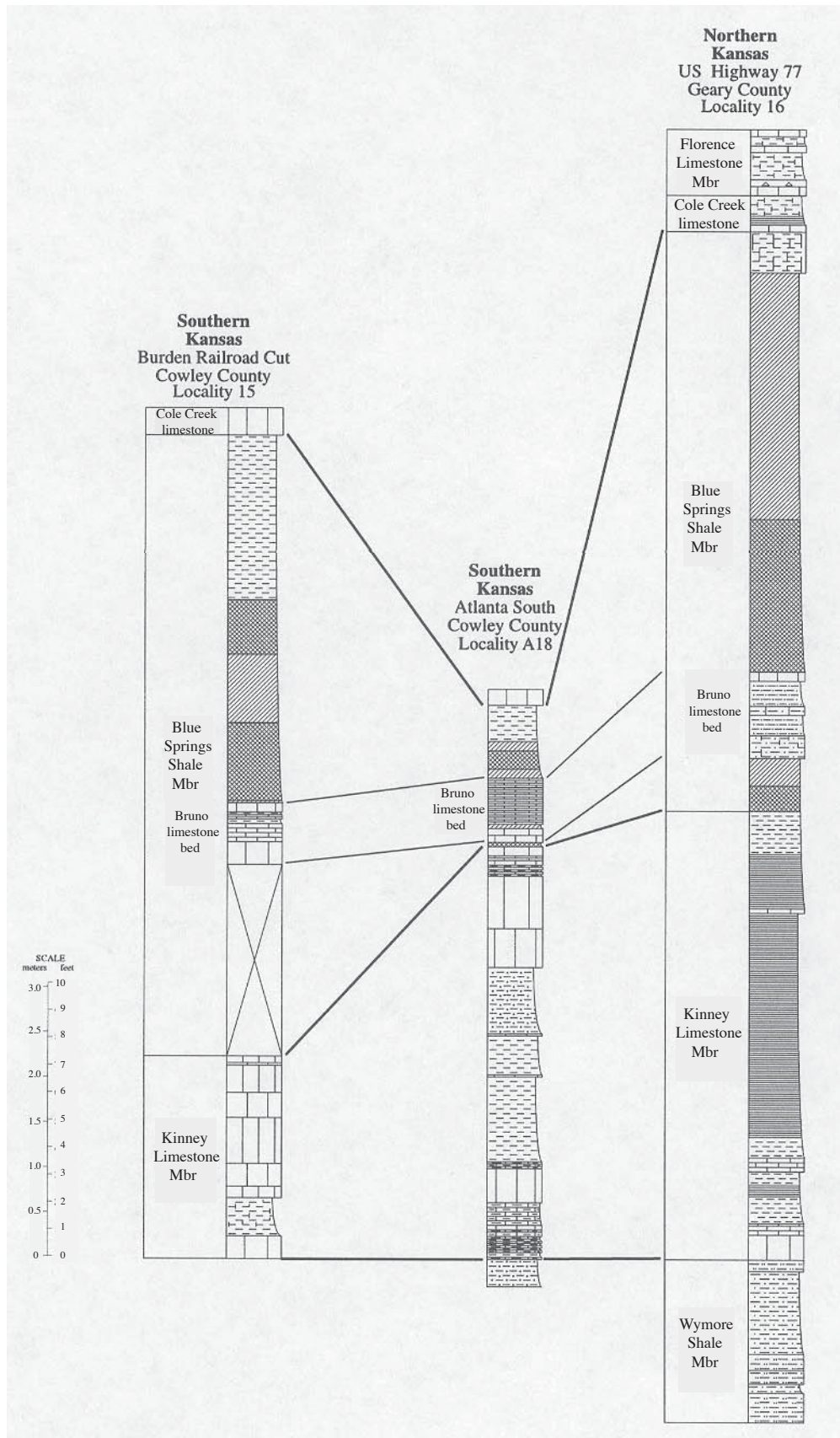
FIGURE 43—Lithostratigraphy of outcrop stratigraphic sections utilized to characterize the Kinney Composite Fourth-Order Sequence; localities 15, A18, and 16.
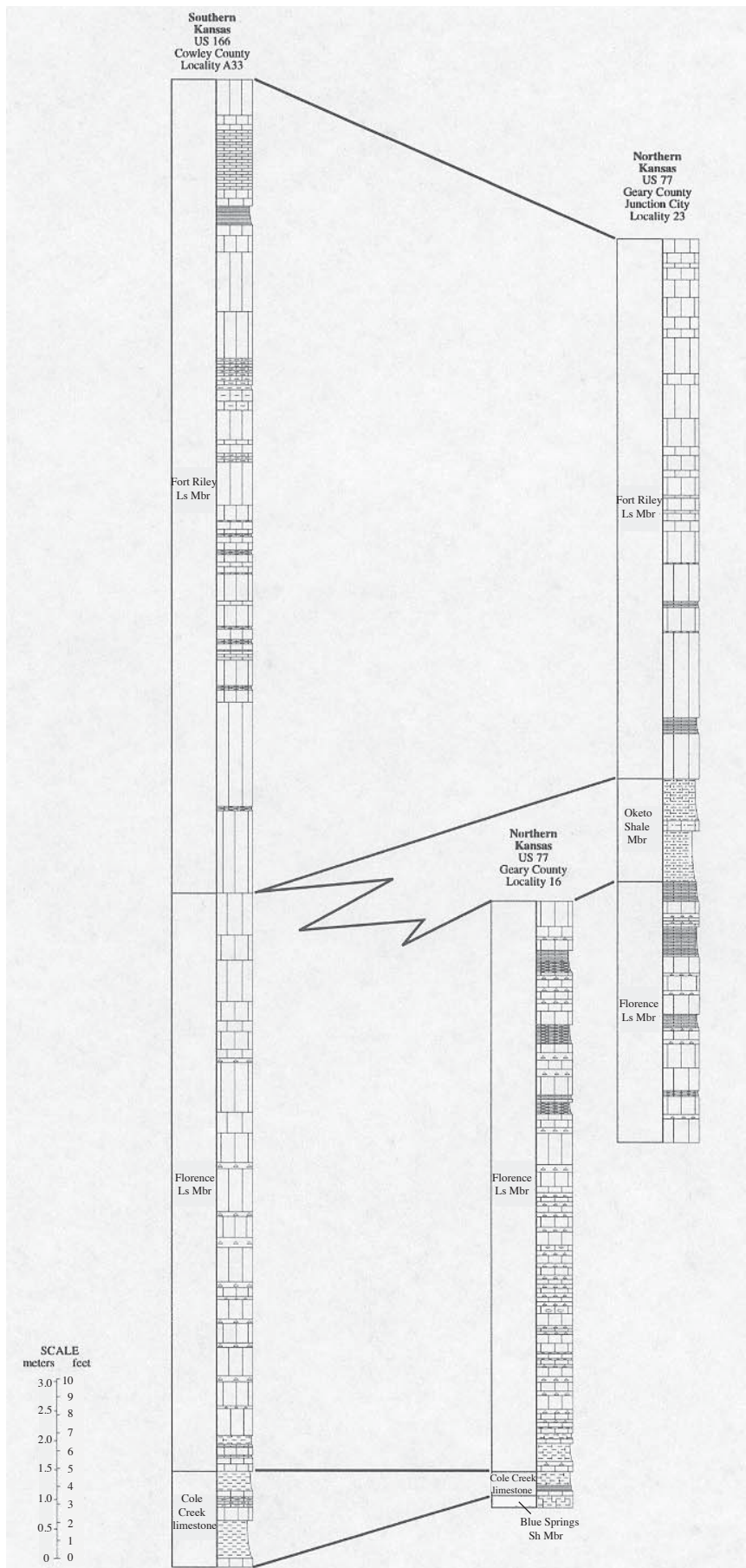
FIGURE 44—Lithostratigraphy of outcrop stratigraphic sections utilized to characterize the Barneston Composite Fourth-Order Sequence, localities A33, 16, and 23.

Maximum-marine flooding of the upper Kinney (Sequence B) is characterized by fossiliferous packstones with *Composita, Derbyia*, crinoids, and echinoids along with reduced numbers of *Sweetognathus* in southern outcrops and by thin, shaly wackestones bearing *Composita* in northern outcrops. Conodonts have been recovered only from southern outcrops in Kansas. In northern Kansas this sequence is capped by red and green mudstones with paleosol textures. In southern exposures the Kinney shows direct evidence of subaerial exposure as evidenced by brecciated regolith and red and green internal sediment in solution vugs and root traces.

The Bruno limestone marks the base of the Kinney Fifth-Order Sequence C. This unit typically consists of a foraminiferal grainstone with few macrofossils and an absence of conodonts. The unit is terminated by well-developed paleosols of the upper part of the Blue Springs Shale Member. Commonly, post-Bruno erosion has locally removed this thin marine bed, resulting in a sporadic distribution across the outcrop belt.

The Kinney Sequence is characterized by *Sweetognathus merrilli* Kozur and *Streptognathodus postconstrictus* Wardlaw, Boardman, and Nestell.

Barneston Composite Fourth-Order Depositional Sequence

The Barneston Limestone, Holmesville Shale Member, Towanda Limestone Member, and the Gage Shale Member in ascending order (figs. 3, 16, 44) comprise the Barneston Sequence. The Barneston Sequence is composed of three fifth-order sequences. The fossiliferous beds in the upper part of the Blue Springs Shale, the Florence Limestone, and Oketo Shale Members comprise the Barneston Fifth-Order Sequence A. The Fort Riley Limestone Member and Holmesville Shale Member constitute the Barneston Fifth-Order Sequence B, and the Towanda Limestone Member and lower part of the Gage Shale Member constitute the Barneston Sequence C. Only the lower two fifth-order depositional sequences are included in this study. However, we have sampled the upper fifth-order sequence, and it is barren of conodonts.

The transgressive surface of the Barneston Sequence occurs in fossiliferous wackestones and mudstones of the uppermost Blue Springs Shale Member. These deposits contain locally abundant bivalves along with a low-diversity brachiopod fauna. Maximum flooding occurs in a highly fossiliferous, shaly, glauconitic wackestone or calcareous shale near the base of the Florence Limestone Member. This interval is dominated by a high abundance of conodonts dominated by *Streptognathodus* with minor numbers of *Sweetognathus*. This marine-condensed section also contains a diverse assemblage of silicified brachiopods along with bryozoans, crinoids, and sponges, thereby showing significant evidence of condensed sedimentation. Immediately above this interval is dominated by fusulinaceans, including the unique occurrence of *Pseudoschwagerina* in the midcontinent. This fifth-order sequence is terminated by the Oketo Shale Member in northern outcrops or by grainstones and packstones with an abundance of algal-coated grains in central and southern Kansas and Oklahoma.

The base of the Barneston Fifth-Order Sequence B is marked by the base of the Fort Riley Limestone Member. Maximum flooding occurs at the base of the second limestone ledge above the base and is denoted by an open-marine fauna of brachiopods, bryozoans, and crinoids along with small numbers of *Streptognathodus* and *Sweetognathus*. The Barneston Fifth-Order Sequence B is terminated by a green blocky mudstone paleosol.

The base of the Barneston Fifth-Order Sequence C (not figured) is marked by the Towanda Limestone Member. Maximum-marine flooding occurs near the base of the Towanda Limestone Member and is denoted by gastropods and bivalves. No conodonts have been recovered from this interval. This sequence is terminated by red and green blocky mudstone paleosols in the lower Gage Shale Member.

Mazzullo et al. (1997) named the fossiliferous shaly glauconitic wackestone of the lower part of the Florence, the Cole Creek limestone, and implied that because of its abundance of bryozoans it represented a cooler-water fauna compared to those that are brachiopod-dominated. We see no significant change in the conodont faunal make-up to suggest a significant water-mass change.

The Barneston Sequence is characterized by *Streptognathodus florensis* Wardlaw, Boardman, and Nestell and *Sweetognathus whitei* (Rhodes).

Discussion and Conclusions

Sequence stratigraphic analysis of uppermost Carboniferous and Lower Permian Admire, Council Grove, and Chase Groups strata that crop out in the North American midcontinent strongly suggest a distinctive hierarchy of stratigraphic forcing (fig. 3). Fourth-order depositional sequences from the Admire Group represent the latest highstand sequence sets of a composite third-order sequence (1–10 m.y.) that includes the majority of Gzhelian (Virgilian) sequences. These fourth-order depositional sequences are composed of between two and three fifth-order depositional sequences (0.01–0.1 m.y.) each.

The Council Grove Group is composed of one composite third-order depositional sequence (1–10 m.y.) and is divisible into nine fourth-order depositional sequences (0.1–1 m.y.). Each fourth-order depositional sequence contains between two to eight high-frequency fifth-order depositional cycles (0.01–0.1 m.y.) that form the parasequences that stack into the retrogradational transgressive-systems tract, and the aggradational to progradational highstand/forced-regressive-systems tracts. In total, 38 widely correlatable fifth-order depositional sequences are present in the Council Grove Group.

The Chase Group is composed of one composite third-order depositional sequence (1–10 m.y.) and is divisible into five fourth-order depositional sequences (0.1–1 m.y.). Each fourth-order depositional sequence contains between two to three high-frequency fifth-order depositional cycles (0.01–0.1 m.y.) that form the parasequences that stack into the retrogradational transgressive-systems tract, and the aggradational to progradational highstand/forced-regressive-systems tracts. Only the lower three of the fourth-order depositional sequences are included in this study.

Several significant trends are noted in this study. Maximum-marine flooding condensed sections within the upper Wabaunsee through the Admire depositional sequences are represented by glauconitic fossiliferous wackestones contrasted to black fissile phosphatic shales, which typify maximum-marine flooding in the transgressive- and early-highstand sequence sets of the earlier parts of the Gzhelian (Virgilian) third-order composite sequence. This change is likely due to a progressive lowering of the magnitude of successive sea-level rises in the late-highstand part of the composite depositional sequence. Additionally, the Anadarko basin underwent a progressive infilling coupled with a lowered rate of basin subsidence.

Maximum-marine flooding condensed sections of the lower Council Grove are represented by either black shales with abundant skeletal phosphate including high abundances of conodonts or highly fossiliferous shaly, glauconitic carbonates with the same high conodont abundance. Maximum-marine flooding surfaces within the upper Council Grove Group sequences show much less evidence of condensation and demonstrate deposition in significantly shallower water regimes based on their contained lithofacies and biofacies. Sequences that contain the maximum-marine flooding condensed sections also demonstrate the greatest faunal diversity and a greater number of high-frequency fifth-order sequences, have a greater stratigraphic thickness, and extend further paleo-landward into Oklahoma. In contrast, the upper Council Grove depositional sequences that have maximum-marine flooding surfaces with little evidence of significant condensation contain fewer higher-frequency fifth-order sequences, are stratigraphically thinner, and pinch out into terrestrial facies only slightly south of the Oklahoma border.

This pattern is also seen in depositional sequences of the Chase Group. The lower Chase Group depositional sequences (Wreford and Barneston) contain maximum-marine flooding condensed sections and have a greater faunal diversity, are stratigraphically thicker, and extend further paleo-landward into Oklahoma.

Two independent tools for interbasinal and perhaps global correlation are provided by this study. The sea-level fluctuation curve derived from this study (fig. 3) and the biostratigraphic data obtained through the course of investigation provide working hypotheses for correlation of these sequences.

Previous Work and Discussion of *Streptognathodus* Species Illustrated from the Carboniferous–Permian Boundary Beds of the North American Midcontinent

Gunnell (1933), Ellison (1941), Perlmutter (1975), Larson and Clark (1979), Movschovitsch et al. (1979), Ritter (1994, 1995), and Chernykh et al. (1997) have either described or illustrated species of *Streptognathodus* from Carboniferous–Permian boundary strata from the North American midcontinent. Gunnell (1933) illustrated and described seven species of *Streptognathodus (S. elongatus, S. simplex, S. wabaunsensis, S. flangulatus, S. walteri, S. acuminatus*, and *S. farmeri)* from the Americus Limestone Member. Ellison (1941) recognized

only two of Gunnell's species as being valid, *Streptognathodus wabaunsensis* and *S. elongatus*. Additionally, Ellison (1941) broadened the species concept of *S. wabaunsensis* to include specimens from Missourian and Virgilian strata, thereby extending the stratigraphic range of the species. Perlmutter (1975) presented a comprehensive study of Carboniferous–Permian boundary conodonts of the North American midcontinent. Unfortunately, he presented no precise locality information and illustrated only highly generalized measured sections. He recognized only three species of *Streptognathodus* (as *Idiognathodus*) in strata from the Brownville Limestone Member through the Speiser Shale and only illustrated specimens from the "Five Point Limestone" and the Red Eagle Limestone. Perlmutter (1975) redefined *S. wabaunsensis* to include only broad platformed *Streptognathodus* with five or more nodes, thereby excluding the holotype of the species that possesses only one node. He did not recognize *S. elongatus* or *S. simplex* and instead placed most other species of *Streptognathodus* into *S. elegantulus*. A number of other workers (e.g., von Bitter and Merrill, 1990) have re-analyzed Perlmutter's data and have presented their own range charts based on his data set. Larson and Clark (1979) re-illustrated the holotype of *S. wabaunsensis*. Movschovitsch et al. (1979) illustrated a *Streptognathodus* that they identified as *S. barskovi* from the Neva Limestone Member as well as *S. elongatus* from the Americus Limestone Member. Ritter (1994) described *Streptognathodus brownvillensis* from the Brownville Limestone Member.

Ritter (1995) presented a comprehensive survey of Virgilian through Asselian conodonts from the midcontinent and proposed a broad *Streptognathodus*-based zonation for Virgilian (Gzhelian) through lower Asselian strata. He illustrated a number of specimens of *Streptognathodus* including *S. brownvillensis* from the Brownville Limestone Member; *S. simplex* from the Americus Limestone Member; *S. acuminatus* from the Americus Limestone Member; *S. wabaunsensis* from the Americus Limestone Member, Hughes Creek Shale Member, and Red Eagle Limestone; *S. flangulatus* from the Red Eagle Limestone; and *S. aff. S. barskovi*, *S.* sp. E., and *S. cf. S. longissimus* from the Neva Limestone Member. He proposed three zones to cover the stratigraphic interval from the Brownville through the Morrill Limestone Member and provided detailed summary correlations with supposed coeval succession in the Ural Mountains. Ritter (1995) defined the *Streptognathodus brownvillensis* Zone to range from the Brownville Limestone Member to the Falls City Limestone, followed by the *S. wabaunsensis s.l.* Zone that ranges from the Falls City Limestone to the Burr Limestone Member and finally by the *S. aff. S. barskovi* Zone that ranges from the Burr Limestone Member to the Morrill Limestone Member. Ritter's zonation (1995) was based on preliminary identifications of *Streptognathodus* species. Recently, Chernykh and Ritter (1997) improved the zonation for the southern Urals and, at least partially, correlated to the midcontinent. Certainly, his *Streptognathodus wabaunsensis s.l.* includes several of the nodular clade as does his *S. aff. S. barskovi,* which includes several species of the robust clade. Our refined zonation (see conodont biostratigraphy) provides a much more detailed zonation based on species ranges of well-defined species concepts (see conodont systematics).

Discussion of Stratigraphic Provenance of Previously Published *Streptognathodus* Species Illustrated from the Carboniferous–Permian Boundary Beds of the North American Midcontinent

Close examination of previously published locality and stratigraphic range data reveals that the stratigraphic provenance of a number of *Streptognathodus* species reported from the North American midcontinent is in serious doubt. To adequately evaluate the actual ranges of *Streptognathodus* species, we have attempted to resolve these questions along with presenting our own data base.

a) Gunnell's 1933 ?Americus Limestone Fauna

Gunnell (1933) illustrated and described seven species of *Streptognathodus (S. elongatus, S. simplex, S. wabaunsensis, S. flangulatus, S. walteri, S. acuminatus,* and *S. farmeri)* from the ?Americus Limestone. His Locality 7 is 3 mi (4.83 km) west of Belvue, Kansas. Ellison (1941) in his revision of Carboniferous and Permian conodonts gave a more specific locality stating that Gunnell's locality was 3 mi (4.83 km) west of Belvue, Kansas, in a roadcut in sec. 6, T. 10 S., R. 11 E. This more precise locality corresponded exactly to Gunnell's more general locality information. Our attempts to locate this section have not been successful. The authors did locate limestone boulders at this locality, but none appeared to have been in place. Apparently, these limestone boulders were brought in to stabilize the riverbanks. These boulders contain *Streptognathodus* species identical to those from the Brownville Limestone Member. Strata exposed at Gunnell's locality are mapped as Quaternary terrace alluvium according to the *Geologic Map of Pottawatomie County* (Scott et al., 1959). It is our opinion that Gunnell's locality was incorrectly located geographically. Other plausible localities for Gunnell's section include Mudge and Yochelson's (1963) measured section 257 (a roadcut in the NW SW sec. 21, T. 9 S., R. 11 E.), and a roadcut located in the SE sec. 36, T. 9 S., R. 11 E. Both localities have exposed Americus Limestone Member and the first locality is 3 mi (4.83 km) northwest of Belvue, whereas the second is 3 mi east (4.83 km) of Belvue, Kansas. We have duplicated the morphotypic species of *Streptognathodus* illustrated by Gunnell from the Americus Limestone Member from numerous other localities along the outcrop belt in Pottawatomie County, Kansas. Despite the inability to relocate this important type locality with absolute assurance, we have concluded that Gunnell's specimens probably did come from shale associated with the Americus Limestone Member. Our sampling of shale associated with the Americus Limestone Member in Pottawatomie County, Kansas, reveals that the shale immediately above the Americus Limestone Member is probably the precise stratigraphic interval that yielded Gunnell's species. In Pottawatomie County, the shale immediately above the uppermost ledge of the Americus Limestone Member has yielded numerous specimens of *Streptognathodus,* whereas the shale within and below the Americus Limestone Member yielded only *Adetognathus*.

b) Stratigraphic integrity of Perlmutter's (1971, 1975) species of *Streptognathodus* from the Admire–Council Grove Groups

Despite the vast stratigraphic scope covered by Perlmutter's (1971, 1975) reports on Carboniferous–Permian boundary conodonts, significant problems exist with the stratigraphic integrity of a significant number of his samples.

1) The stratigraphic range of the biostratigraphically significant species *Streptognathodus wabaunsensis* Gunnell is unresolved because Perlmutter (1975, p. 103) states that *S. wabaunsensis* makes its first appearance in the Falls City Limestone, whereas in the same publication Perlmutter (1975, p. 100) reports the first appearance in the Five Point Limestone Member. The locality data for Perlmutter's (1975) sampling localities was obtained from Perlmutter's (1971) unpublished Ph.D. dissertation. Perlmutter's Falls City Limestone (Locality 3, Perlmutter, 1975; Locality A8, this report) and his Five Point Limestone Member (Locality 4, Perlmutter, 1975; Locality A9, this report) localities are located on I–70 in Wabaunsee County, Kansas. We did the following in order to resolve the dilemma as to the actual first appearance of *S. wabaunsensis*: a) resampled each of Perlmutter's localities in considerable detail, b) sampled long stratigraphic sections that had continuous exposures from the Brownville Limestone Member through the Americus Limestone Member in three different regions (Locality 2, type locality for the Foraker Limestone, Osage County, Oklahoma; Localities 3, 4, K–38 roadcuts in Cowley County, Kansas; Locality 1, type locality for the Janesville Shale in Greenwood County, Kansas; c) sampled short sections in the I–70 regions with definitive Falls City Limestone (localities A12, A15, A26) and Five Point Limestone Member (Localities A15, A16, A19, A25, A26), d) compared the localities described in Perlmutter (1971) with previously measured and described sections, and e) compared the stratigraphic calls by Perlmutter (1975) with those presented on the *Geologic Map of Wabaunsee County* presented by Mudge and Burton (1959).

As a result of our analysis, we conclude that Perlmutter's (1975) Falls City Limestone as well as his Five Point Limestone Member have been seriously miscorrelated. Perlmutter's locality for the "Falls City Limestone" (Locality 3, Perlmutter, 1975; Locality A8, this report) exposes a complete section of the Foraker Limestone (Americus Limestone Member through the Long Creek Limestone Member). The most likely stratigraphic position for his sample of the "Falls City Limestone" is the Americus Limestone Member. A complete and detailed measured section for this locality from Little (1965, Locality 11) is presented herein along with our measured section. Additionally, the *Geologic Map of Wabaunsee County* presented by Mudge and Burton (1959) clearly shows that this locality corresponds to the Foraker Limestone. The "Five Point Limestone" exposed at Perlmutter's (1975) Locality 4 is actually a limestone in the Foraker Limestone. This locality, documented by Mudge and Burton (1959, Locality 42) and Little (1965, Locality 10) is presented in this report (Locality A9). Based on our analysis of the conodonts recovered from this locality, our best estimate is that the conodonts were recovered from the Hughes Creek Shale Member. Because Perlmutter (1975) miscorrelated the Five Point Limestone Member, the other stratigraphic units exposed at the same locality are also miscorrelated. His Hamlin Shale Member is equivalent to the uppermost Hughes Creek Shale Member,

his Americus Limestone Member equates to the Long Creek Limestone Member, his Hughes Creek Shale Member is the Johnson Shale, and his Long Creek Limestone Member is the Red Eagle Limestone.

Based on sampling, *Streptognathodus wabaunsensis* first appears in the Americus Limestone Member. We have documented it at numerous localities along the outcrop belt. In our opinion, Perlmutter (1975) did not sample the true Falls City nor the Five Point limestones, both of which contain distinctive conodont assemblages that are easily recognizable.

2) Perlmutter's (1971, 1975) Locality 5 that purportedly exposed the Grenola Formation (Sallyards Limestone, Legion Shale, Burr Limestone, Salem Point Shale, and Neva Limestone Members), Eskridge Shale, and the Beattie Limestone (Cottonwood Limestone, Florena Shale, and Morrill Limestone Members) also was apparently miscorrelated. He reported conodonts at a number of levels within his Sallyards Limestone Member that he claimed was 1.6 m (5.3 ft) thick (contrasted with its actual thickness in the area of 0.3 m (1 ft). He also reported that the Neva was unfossiliferous, and was only 1.5 m (5 ft) thick instead of its usual thickness of 4.9 m (16 ft) in the area. Perlmutter's Locality 5 is the same locality as Mudge and Burton's (1959) Locality 33. By directly comparing Mudge and Burton's measured section with that of Perlmutter (1971), it is concluded that Perlmutter misidentified all the units of the Grenola Formation. Perlmutter's Sallyards Limestone Member corresponds to the upper part of the Neva Limestone Member whereas his Legion Shale, Burr Limestone, Salem Point Shale, and Neva Limestone Members correlate to beds within the Eskridge Shale. His Cottonwood Limestone Member is accurately identified in the section.

Stratigraphic Provenance of *Sweetognathus* Species Illustrated from the Carboniferous–Permian Boundary Beds of the North American Midcontinent

Sweetognathus has been previously reported from Lower Permian Council Grove strata of the North American midcontinent including the Neva Limestone Member (Grenola Formation), Eiss Limestone Member (Bader Formation), and the Funston Limestone. *Sweetognathus* has been reported from the Chase Group including the Threemile Limestone and Schroyer Limestone Members of the Wreford Formation, and the Florence Limestone and Fort Riley Limestone Members of the Barneston Limestone. Specifically, *Sweetognathus expansus* is reported from the Neva Limestone Member (Ritter, 1995) and the Funston Limestone (Perlmutter, 1975; von Bitter and Merrill, 1990). *Sweetognathus merrilli* is reported from the Eiss Limestone Member (Merrill, 1973; Kozur, 1975). *Sweetognathus adenticulatus* is reported to range from the Funston Limestone through the Wreford Limestone (Ritter, 1986). *Sweetognathus inornatus* is reported to range from the Funston Limestone through the Fort Riley Limestone Member of the Barneston Limestone (Ritter, 1986). *Sweetognathus whitei* is reported in the Florence Limestone and Fort Riley Limestone Members of the

Barneston Limestone, and *Sw. windi* is reported in the Fort Riley Limestone Member (Ritter, 1986).

In this report, we document *Sweetognathus* in the Red Eagle Limestone, Burr Limestone Member, Cottonwood Limestone Member, Eiss Limestone Member, Middleburg Limestone Member, Crouse Limestone, Funston Limestone, Threemile Limestone Member, Havensville Shale Member, Schroyer Limestone Member, Kinney Limestone Member, Florence Limestone Member, and Fort Riley Limestone Member. Our analysis also reveals some problems concerning the stratigraphic provenance of previously reported species of *Sweetognathus*.

Of particular concern is the stratigraphic provenance of the type locality of *Sweetognathus expansus*. Perlmutter's (1975) type locality (Section 9) for *Ozarkodina expansa* (*Sweetognathus expansus*) is reported to occur in the Funston Limestone exposed in a roadcut on I–70, 2.3 mi (3.7 km) west of K–99 overpass in the SW SW sec. 29, T. 11 S., R. 10 W., of Wabaunsee County, Kansas. The detailed measured section for Section 9 appears in Perlmutter's (1971, p. 35–37) unpublished Ph.D. dissertation. The precise stratigraphic level that yielded the holotype is sample 53, which was 53.4–54.4 ft (16.3–16.6 m) above the base of the section. The Funston Limestone at this locality is 8.2 ft (2.5 m) thick, consisting of a lower 3.0 ft (0.9 m) of massive gray limestone overlain by a 5.2-ft (1.6-m) gray fine-grained flaggy limestone according to Perlmutter (1971).

The authors have two localities (A6, A7) near Perlmutter's Section 9. Locality A6 corresponds exactly to Perlmutter's Locality 9 (3.7 km [2.3 mi] west of the intersection of K–99 and I–70), whereas the other (Locality A7) is 4.35–4.67 km (2.7–2.9 mi) west of the intersection of K–99 and I–70. The stratigraphic interval from the top of the Crouse Limestone to the top of the Funston Limestone is exposed at Locality A6, whereas the base of the Eiss Limestone Member to the top of the Crouse Limestone is exposed at Locality A7.

Our data reveal that the true Funston, which is exposed at Locality A6 (fig. 113), consists of a basal 0.36-m (14-inch) limestone ledge, a 0.53-m (21-inch) black-shale bed, a 0.53-m (21-inch) gray-shale bed, a 0.15-m (6-inch) thin-bedded limestone, a 1.83-m (6-ft) covered interval, probably shale, and is capped by a 0.97-m (38-inch) massively bedded limestone. The entire stratigraphic thickness exposed from the top of the Crouse to the Funston at this locality is 10.67 m (35 ft). Both the descriptions of the Funston as well as the total thickness exposed at Locality A6 are incompatible with that given by Perlmutter (1971). However, the stratigraphic succession and thicknesses are identical with that of Locality A7. We recovered no platform conodonts from the true Funston Limestone exposed at Locality A6, but recovered abundant representatives of *Sweetognathus expansus* from the Crouse Limestone exposed at Locality A7 at a level that corresponds well to the description given in Perlmutter (1971). We therefore conclude that the holotype of *Sweetognathus expansus* probably is from the Crouse Limestone and not the Funston Limestone. We have recovered additional specimens of *Sw. expansus* from the Crouse Limestone on Scenic Drive (Locality 12), but have not recovered them from the Funston Limestone at that same locality. We have recovered specimens of *Sw. expansus* from the Funston Limestone of southern and central Kansas (Locality 13, Locality A33), but not from northern Kansas.

Ulsolka Conodont Ranges

Species labels (Figure 45): S. aff. elongatus, S. flexuosus, S. sp. nov. a, S. wabaunsensis, S. minacutus, S. isolatus, S. nodulinearis, S. invaginatus, S. cristellaris, S. glenisteri, S. sigmoidalis, S. longissimus, S. tulkassensis, S. latus, S. constrictus, S. fusus, S. nevaensis/barskovi
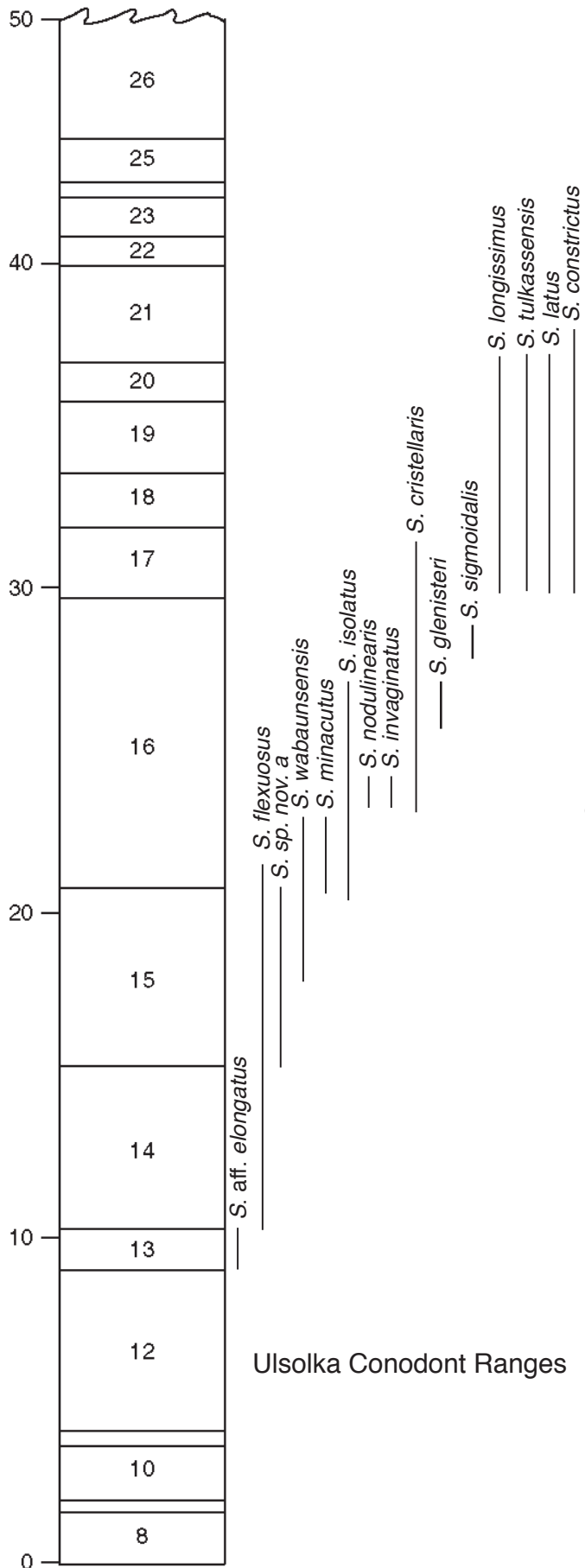
FIGURE 45—Range chart Usolka (derived from Chuvashov et al., 1991, and Chernykh and Ritter, 1997).

Species labels (Figure 46): Sweetognathus merrilli, barskovi, postconstrictus, fusus, fuchengensis, minacutus, isolatus, cristellaris, glenisteri, conjunctus, binodosus, "acuminatus", flexuosus, bellus, alius
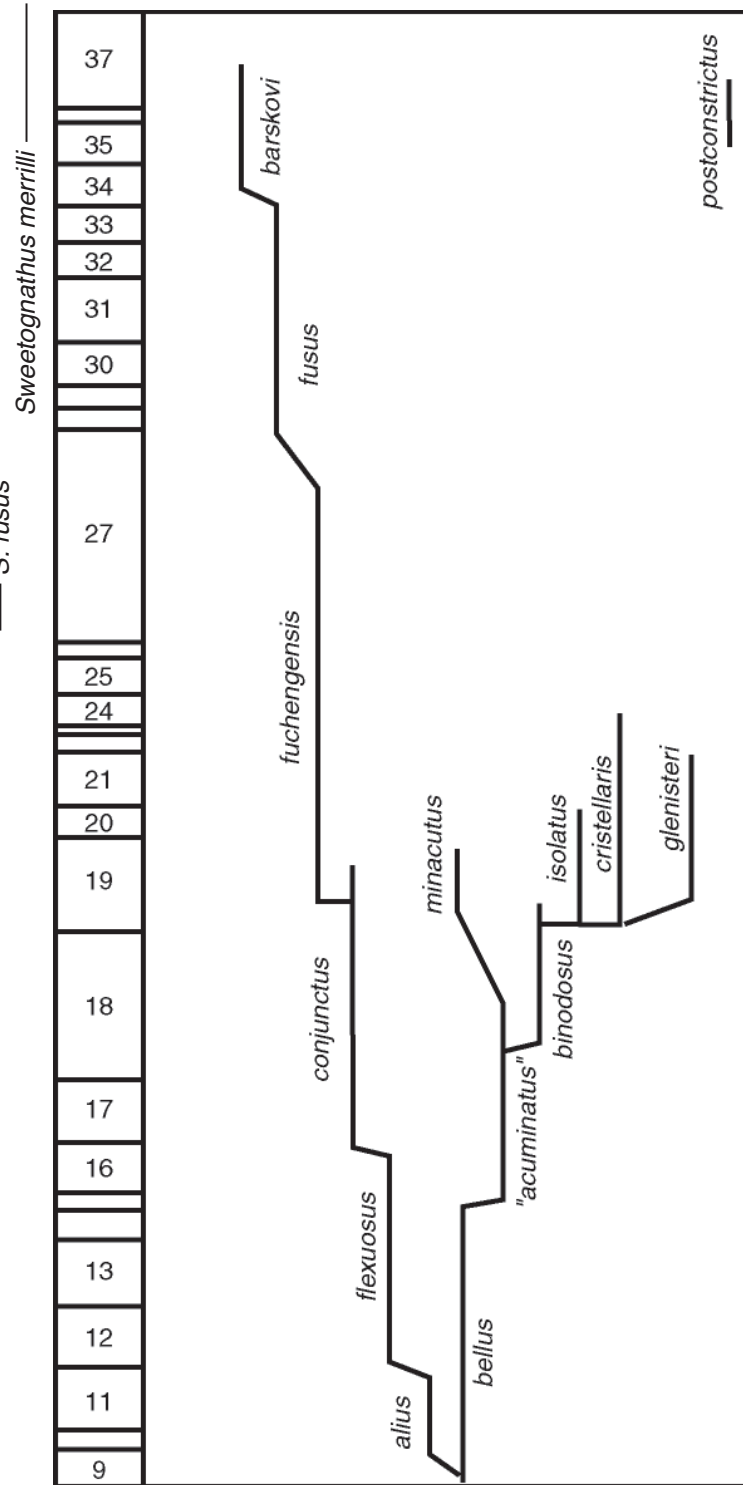
FIGURE 46—Range chart Aidaralash Creek (derived from Davydov et al., 1993, and Chernykh and Ritter, 1997).

Conodont Biostratigraphy

The succession of conodonts is represented by 13 minor and major faunal introductions (fig. 3). Four major and nine minor changeovers in *Streptognathodus* species are marked in stratigraphic succession by the introduction of **1)** *S. brownvillensis* (Ritter, 1994) in the Brownville Limestone Member of the Wood Siding Formation (minor), **2)** *S. alius* in the Falls City Limestone (minor), **3)** *S. flexuosus* in the Five Point Limestone Member of the Janesville Shale (minor), **4)** *S. elongatus, S. farmeri,* and *S. wabaunsensis* in the upper bed of the Americus Limestone Member of the Foraker Limestone (major), **5)** *S. conjunctus* in the lower part of the Hughes Creek Shale Member of the Foraker Limestone (minor), **6)** *S. binodosus* in the upper part of the Hughes Creek Shale Member of the Foraker Limestone (minor), **7)** *S. fuchengensis, S. invaginatus, S. nodulinearis, S. minacutus,* and *S. isolatus* in the Bennett Shale Member of the Red Eagle Limestone (major), **8)** *S. lineatus, S. nevaensis, S. postelongatus,* and *S. translinearis* in the Burr Limestone Member of the Grenola Limestone (major), **9)** *S. constrictus, S. fusus,* and *S. longissimus* in the Cottonwood Limestone Member of the Beattie Limestone (major), **10)** *S. barskovi* in the Eiss Limestone Member of the Bader Limestone (minor), **11)** *S. postconstrictus* in the Crouse Limestone (minor), **12)** *S. trimilus* and *S. robustus* in the Threemile Limestone Member of the Wreford Limestone (minor), and **13)** *S. florensis* in the Blue Springs Shale Member of the Matfield Shale (minor). This succession is very similar to that in the Usolka section in the southern Urals, Russia (Chuvashov et al., 1991), and ties the faunal introduction **4** in Kansas to bed 16/1 at Usolka, **7** to bed 16/3, **8** to bed 16/5, and **9** to bed 17/2. The first appearance of our *Streptognathodus isolatus* is the same as the isolated nodular morphotype of Chernykh and Ritter (1994) and *S. isolatus* of Chernykh et al. (1997). Although conodont taxonomy through this interval is difficult and many names are not agreed upon, the evolutionary clines displayed at the basinal section at Usolka can be replicated in the shallow-water shelf sequence in Kansas, showing their importance for worldwide correlation. The Kansas succession due to the cyclic nature of marine transgressions and regressions in a shallow shelf environment is very step-like (fig. 17) and matches the step-like pattern known from the Usolka section in Russia in a basinal sequence due to coarse sampling (Chuvashov et al., 1991; see fig. 45). This pattern is also seen in the Aidaralash Creek Section (see fig. 46). The conodont introductions represent glimpses of the evolution of four clades of the genus *Streptognathodus*. Those clades are recognized as a succession of minor variations on four basic plans of the platform (Pa) element. The other elements (non-Pa) of the apparatuses are very similar, especially within a clade, and are only subtly different between clades. The clades, or succession of species with similar architectural plans, are recognized because the species are stratigraphically useful and can be recognized worldwide. The clades are 1) Virgilian holdovers characterized by a long and wide groove, typically with a median nodose

posterior extension of the carina (fig. 47); 2) elongate forms typified by and beginning with *S. elongatus* (fig. 48); 3) nodose forms (containing common accessory denticles), which can be subdivided into a root stock that has a slit-like furrow typified by *S. wabaunsensis* (fig. 49) and the common stock that defines the Carboniferous–Permian boundary, which has a trough-like furrow anteriorly typified by *S. farmeri* (fig. 49); and 4) robust forms typified by *S. barskovi* (fig. 50).

Our *Streptognathodus isolatus* is the same as the isolated nodular morphotype proposed by Chernykh and Ritter (1994) as defining the Carboniferous–Permian boundary in the Aidaralash section in the southern Urals, northern Kazakhstan. This suggests that the relatively moderate species radiation in the nodose species clade found in the base of the Bennett Shale Member marks the same horizon and the Carboniferous–Permian boundary.

Species of *Sweetognathus* have been used to define the bases of the Sakmarian and Artinskian. We find the species very variable, but we can see three distinct species in our material: *Sweetognathus expansus, S. merrilli,* and *S. whitei* (fig. 51). *S. expansus* first occurs in the Bennett Shale Member of the Red Eagle Limestone with the species of *Streptognathodus* that we define the base of the Permian. *S. merrilli* first occurs in the Eiss Limestone Member of the Bader Limestone. It co-occurs with the first appearance of *Streptognathodus barskovi* in Kansas. In the Urals of Russia, *S. barskovi* characterizes the uppermost conodont zone of the Asselian. *Sweetognathus merrilli* typically identifies the base of the Sakmarian Stage. Unfortunately, the conodonts of the Sakmarian in its type area along the Sakmara River on Nos Mountain are poorly documented. A single occurrence of *Sweetognathus merrilli* is reported from the Karamurunian beds (Chuvashov et al., 1991). No *S. postfusus* (= *S. barskovi*) is reported from the section, though *S. constrictus* and *S. fusus* occur in bed 12 (Chuvashov et al., 1991), supposedly reworked and above the first and only occurrence of *S. merrilli* in bed 11. Wardlaw et al. (1999) and Chuvashov et al. (2002a) have clarified the situation a little. Wardlaw et al. (1999) report *S. barskovi* from bed 9; Chuvashov et al. (2002a) show a transitional morphotype to and *Sweetognathus merrilli* within bed 11. So, it appears that in the Urals, *S. barskovi* occurs below and overlaps the FAD of *Sweetognathus merrilli* in the Sakmarian type area (see composite range chart, fig. 52). *Sweetognathus whitei* first occurs in the Florence Limestone Member of the Barneston Limestone, close to the first occurrence of *Streptognathodus florensis*. The first occurrence of *Sweetognathus whitei* typically is used to define the base of the Artinskian Stage (see Chuvashov et al., 2002b). We would prefer defining the base on a lineage in *Streptognathodus* (in this case on the first appearance of *S. florensis*), but both seem to indicate that the Florence Limestone Member can be adequately correlated to the base of the Artinskian.
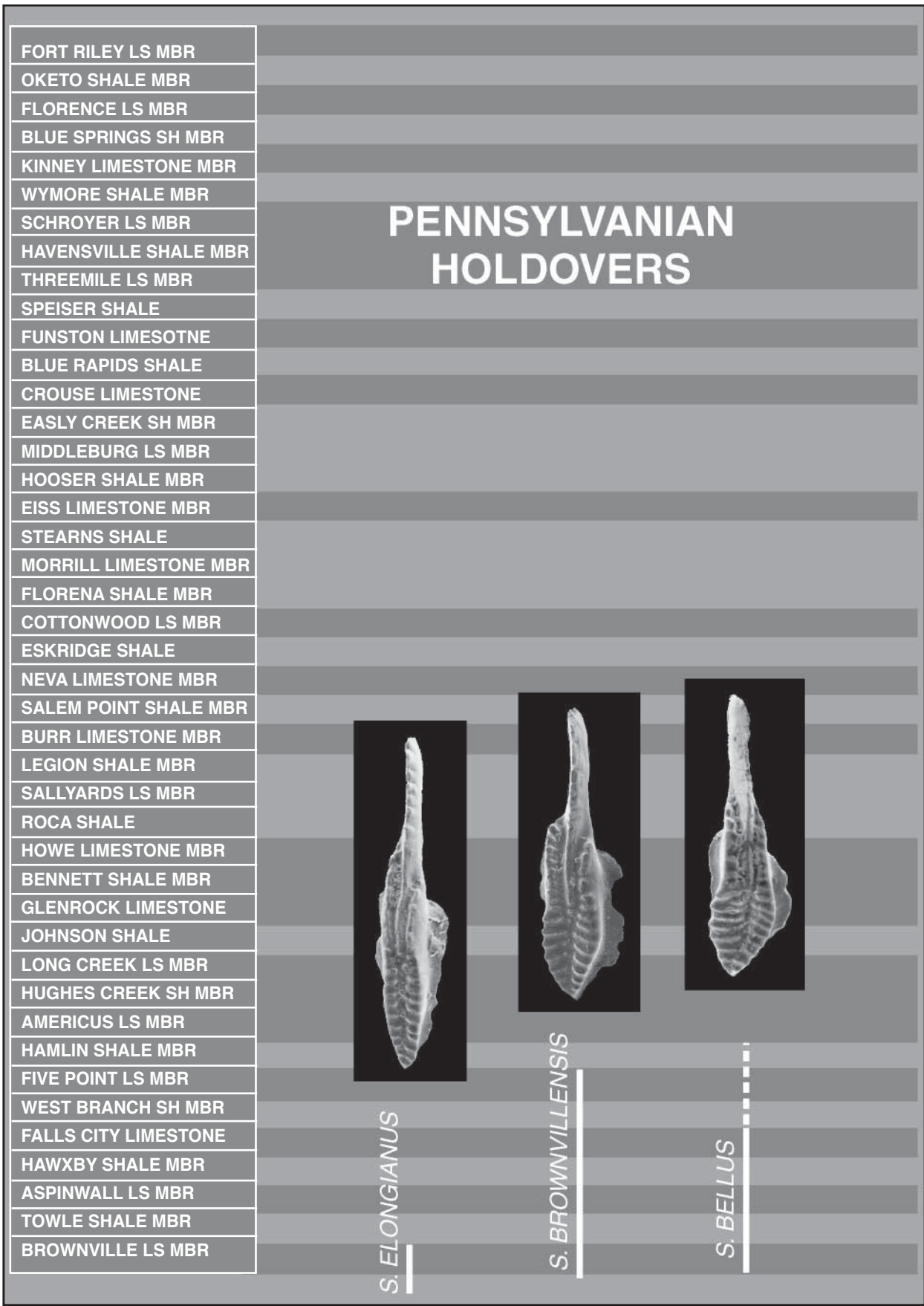
FIGURE 47—Pennsylvanian holdovers—*Streptognathodus*.
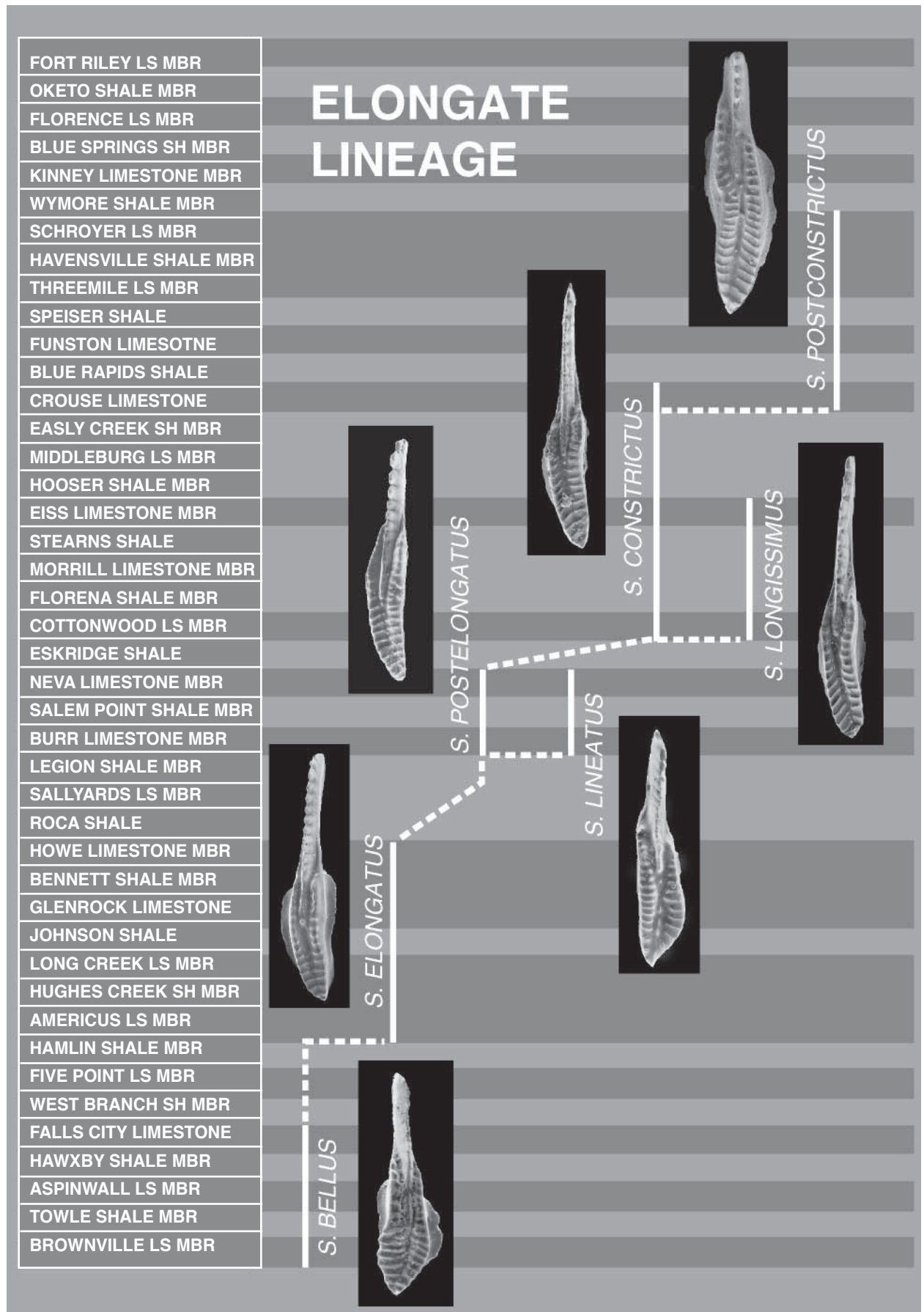
FIGURE 48—Elongate *Streptognathodus*—phylogeny.
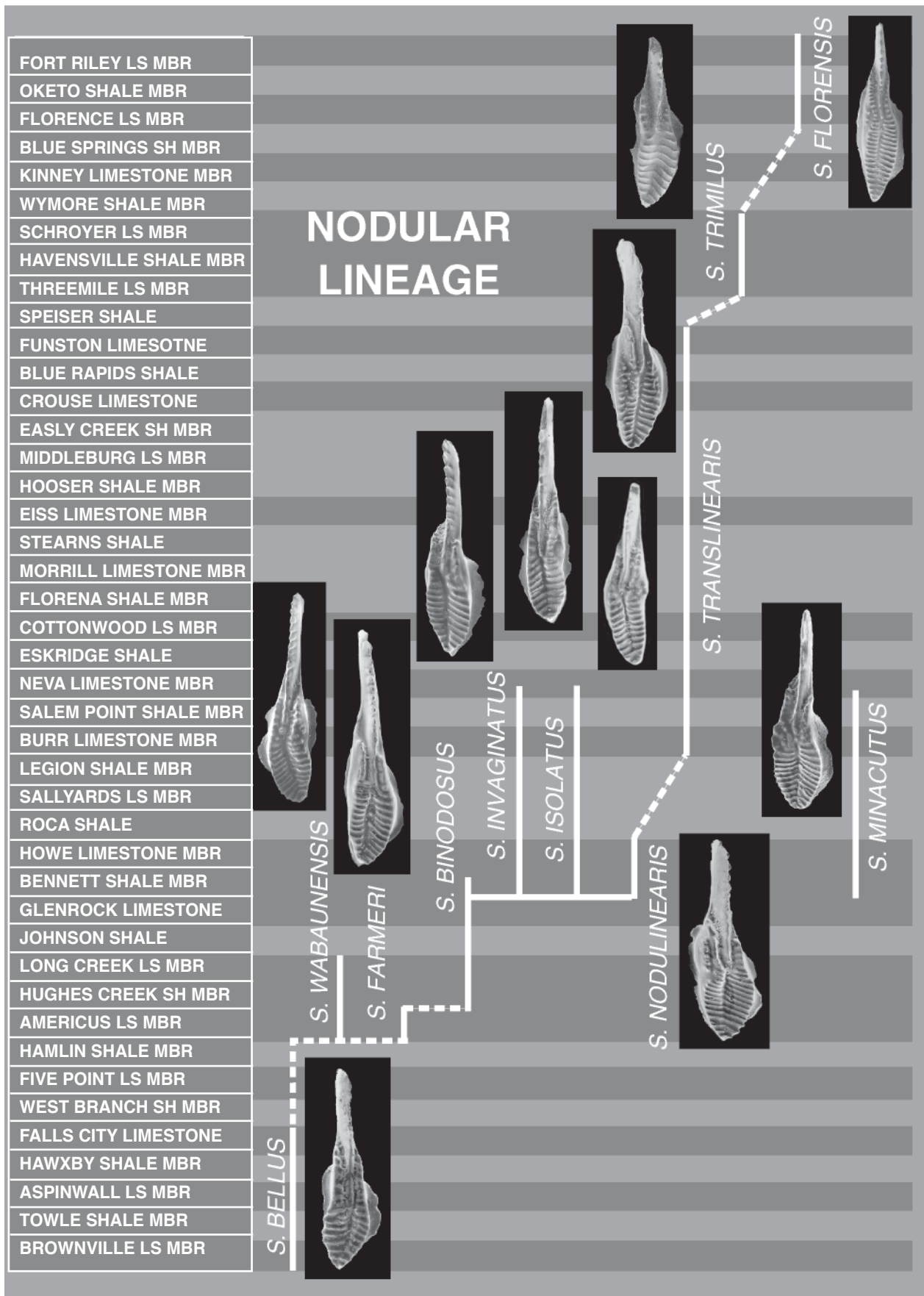
FIGURE 49—Nodular *Streptognathodus*—phylogeny.
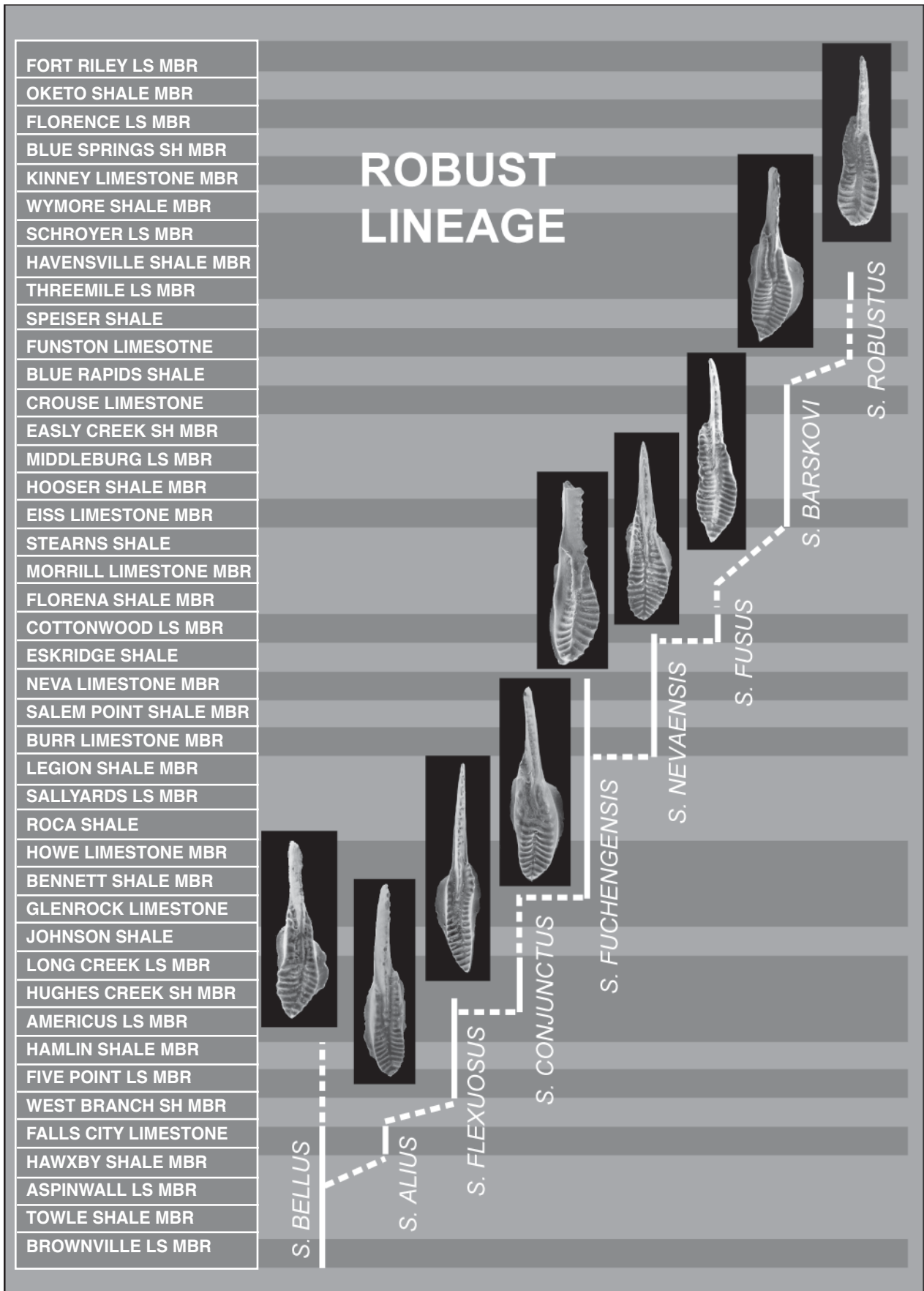
FIGURE 50—Robust *Streptognathodus*—phylogeny.

FORT RILEY LS MBR			
OKETO SHALE MBR			
FLORENCE LS MBR			
BLUE SPRINGS SH MBR			
KINNEY LIMESTONE MBR			
WYMORE SHALE MBR			
SCHROYER LS MBR			
HAVENSVILLE SHALE MBR			
THREEMILE LS MBR			
SPEISER SHALE			
FUNSTON LIMESOTNE			
BLUE RAPIDS SHALE			
CROUSE LIMESTONE			
EASLY CREEK SH MBR			
MIDDLEBURG LS MBR			
HOOSER SHALE MBR			
EISS LIMESTONE MBR			
STEARNS SHALE			
MORRILL LIMESTONE MBR			
FLORENA SHALE MBR			
COTTONWOOD LS MBR			
ESKRIDGE SHALE			
NEVA LIMESTONE MBR			
SALEM POINT SHALE MBR			
BURR LIMESTONE MBR			
LEGION SHALE MBR			
SALLYARDS LS MBR			
ROCA SHALE			
HOWE LIMESTONE MBR			
BENNETT SHALE MBR			
GLENROCK LIMESTONE			
JOHNSON SHALE			
LONG CREEK LS MBR			
HUGHES CREEK SH MBR			
AMERICUS LS MBR			
HAMLIN SHALE MBR			
FIVE POINT LS MBR			
WEST BRANCH SH MBR			
FALLS CITY LIMESTONE			
HAWXBY SHALE MBR			
ASPINWALL LS MBR			
TOWLE SHALE MBR			
BROWNVILLE LS MBR			

SWEETOGNATHUS EXPANSUS

SWEETOGNATHUS MERRILLI

SWEETOGNATHUS WHITEI

SWEETOGNATHUS LINEAGE

FIGURE 51—*Sweetognathus*—phylogeny.
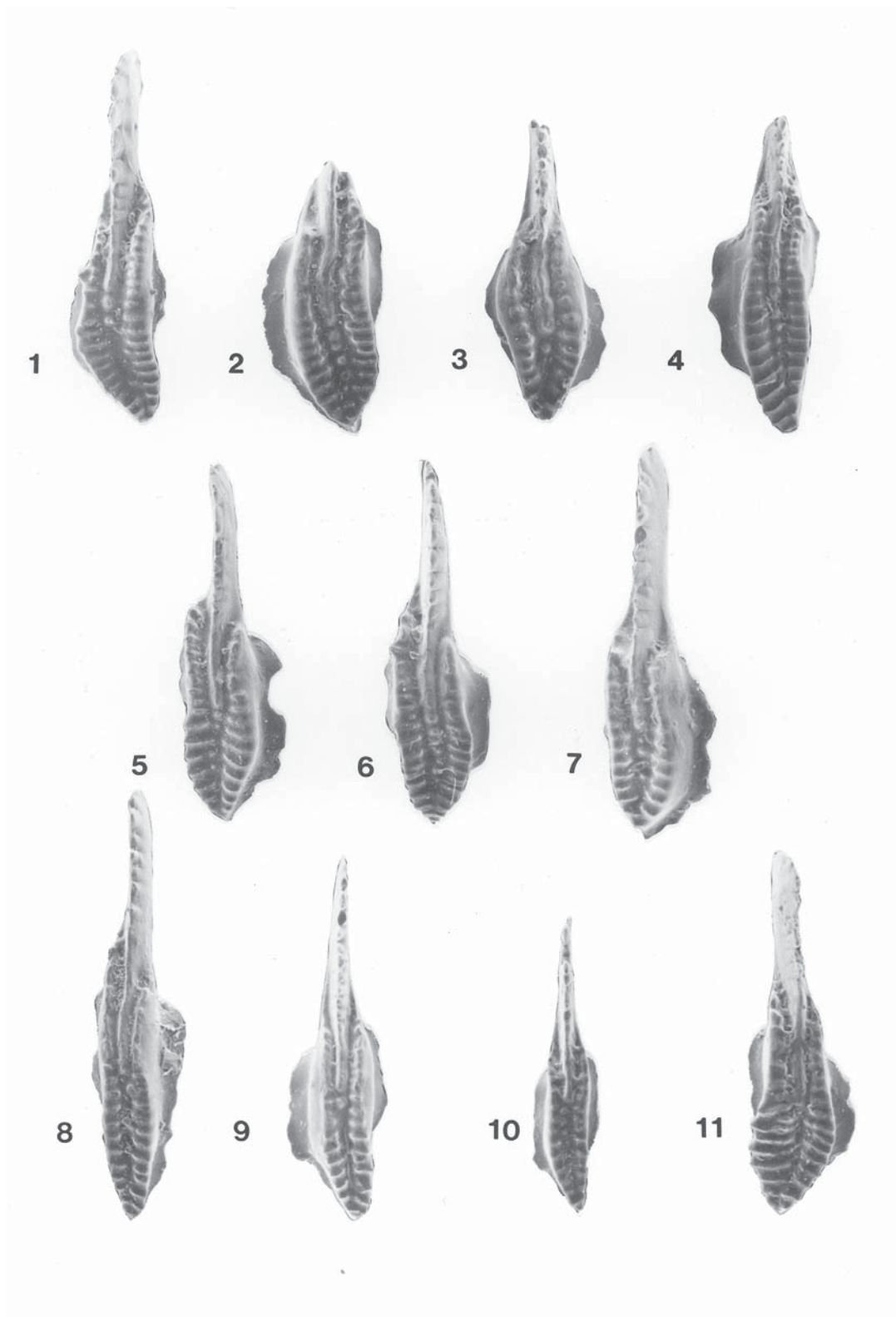
PLATE 2—Conodonts from the Brownville Limestone Member of the Wood Siding Formation, all upper views of Pa elements, x 72. (1, 11) *Streptognathodus bellus* Chernykh and Ritter, USNM 483972–483973. (2–7, 10) *Streptognathodus brownvillensis* Ritter, USNM 483974–483980. (8–9) *Streptognathodus elongianus* Wardlaw, Boardman, and Nestell, new species, 8, holotype, USNM 483981–483982. 1, 2, 10 from top Brownville Limestone Member, type Foraker Limestone (Locality 2); 3, 4, 8 from base Brownville Limestone Member, K–38 roadcut (Locality 3); 5, 7, 9, base of Brownville Limestone Member, type Janesville (Locality 1); 11, top Brownville Limestone Member, K–38 roadcut (Locality 3).
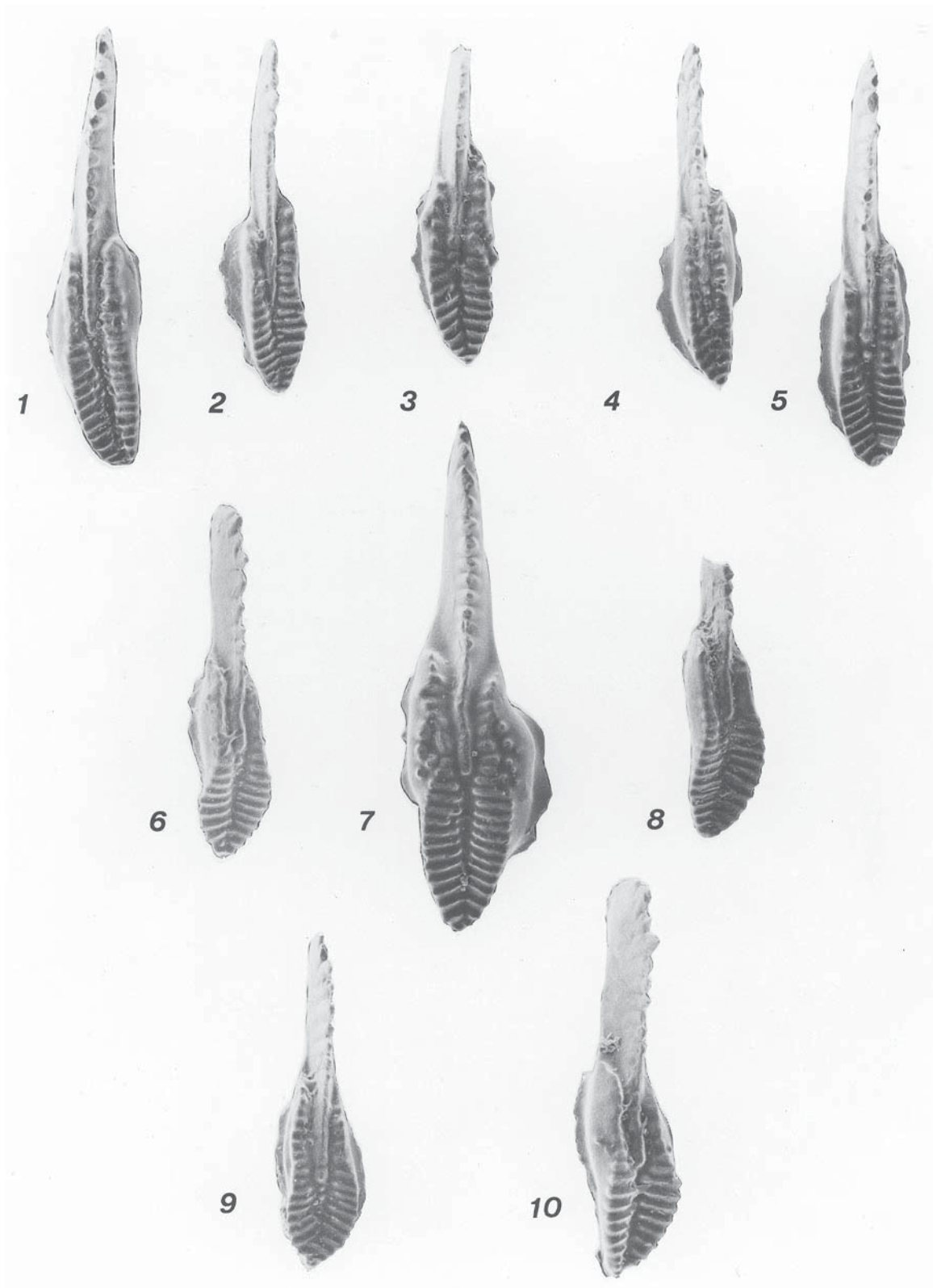
PLATE 3—Conodonts from the Falls City Limestone, all upper views of Pa elements, x 72. (1–8, 10) *Streptognathodus alius* Aktmetshina, USNM 483983–483991. (9) *Streptognathodus bellus* Chernykh and Ritter, USNM 483992. 1, 9, from base of Falls City Limestone, type Foraker Limestone (Locality 2); 2, 4, 6–7, 10 from base Falls City Limestone, K–38 roadcut (Locality 3); 3, 5, 8, base Falls City Limestone, type Janesville (Locality 1).
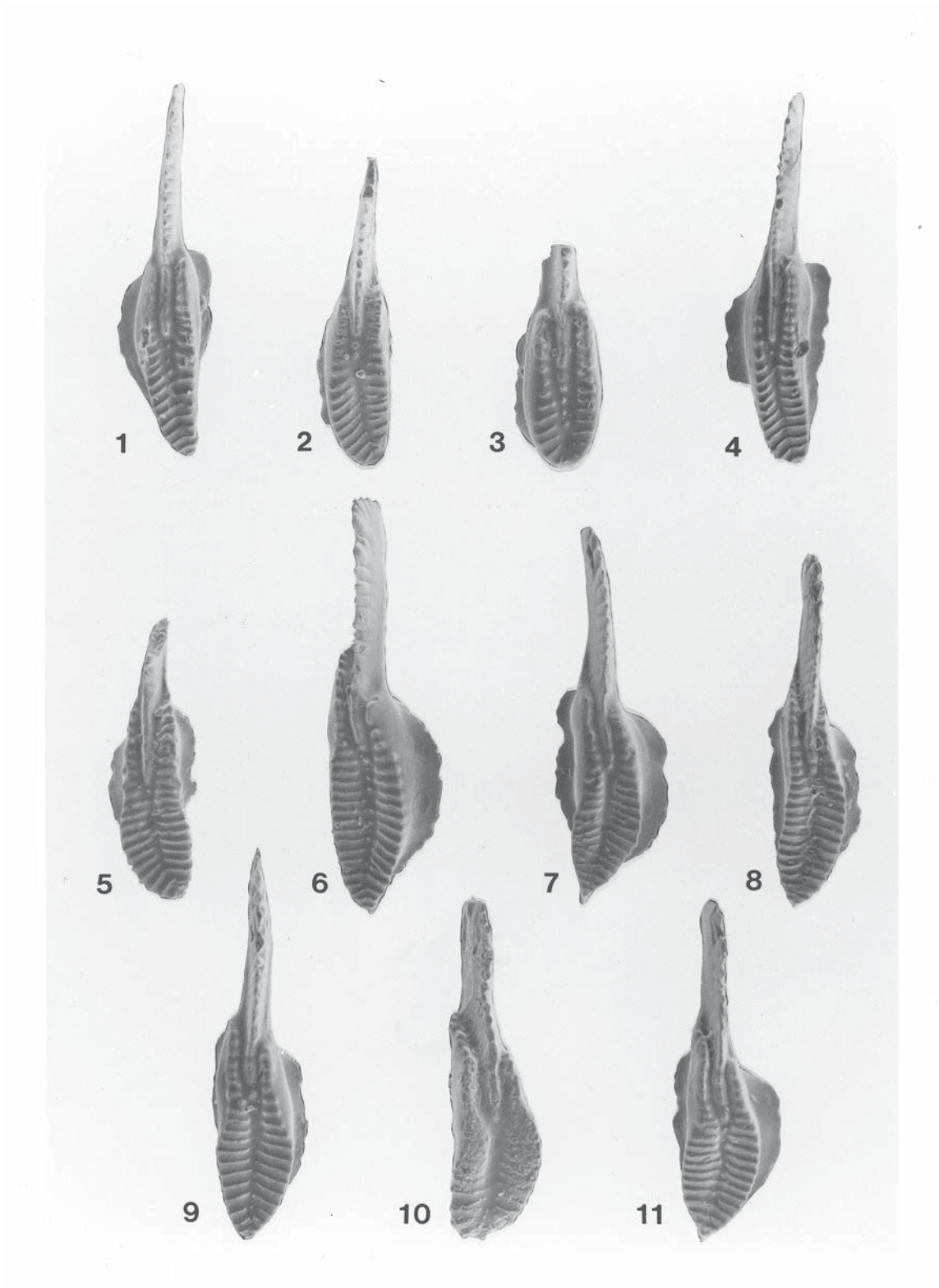
PLATE 4—Conodonts from the Five Point Limestone Member of the Janesville Shale, all upper views of Pa elements, x 72. (1–2, 4–11) *Streptognathodus flexuosus* Chernykh and Ritter, USN 483993–484003. (3) *Streptognathodus brownvillensis* Ritter, USNM 484004. 1–7, 9–11 from base Five Point Limestone Member, type Janesville (Locality 1); 8 from base Five Point Limestone Member, K–38 (Locality 4).
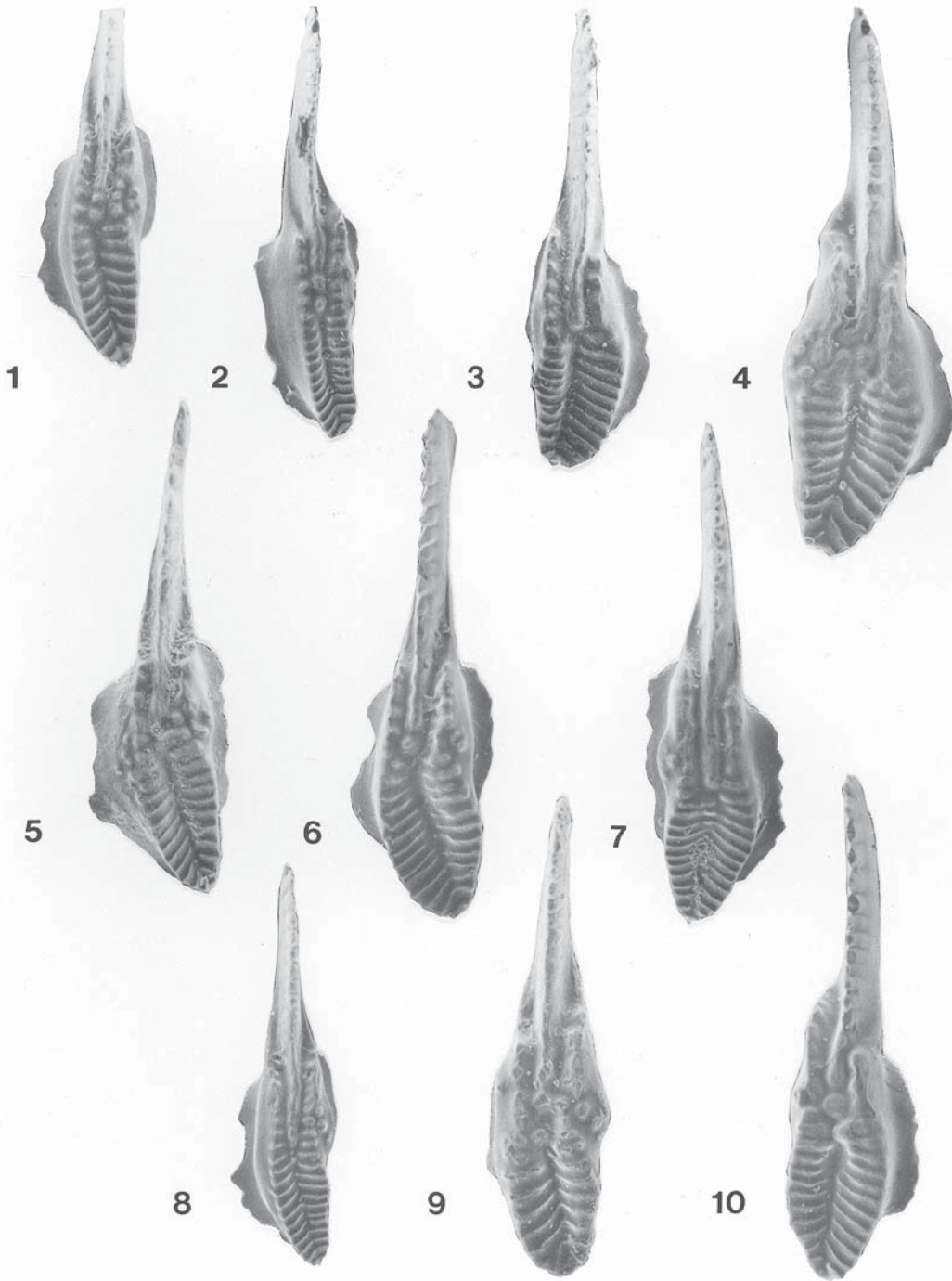
PLATE 5—Conodonts from the Americus Limestone Member of the Foraker Limestone, all upper views of Pa elements, x 72. (1–7, 9–10) *Streptognathodus wabaunsensis* Gunnell, USNM 484005–484013. (8) *Streptognathodus elongatus* Gunnell, USNM 484014. 1, 3, from top lower ledge of Americus Limestone Member, type Foraker (Locality 2); 2, 4, 6–10, from top lower ledge of Americus Limestone Member, type Janesville (Locality 1); 5, from top lower ledge of Americus Limestone Member, K–38 roadcut (Locality 4).
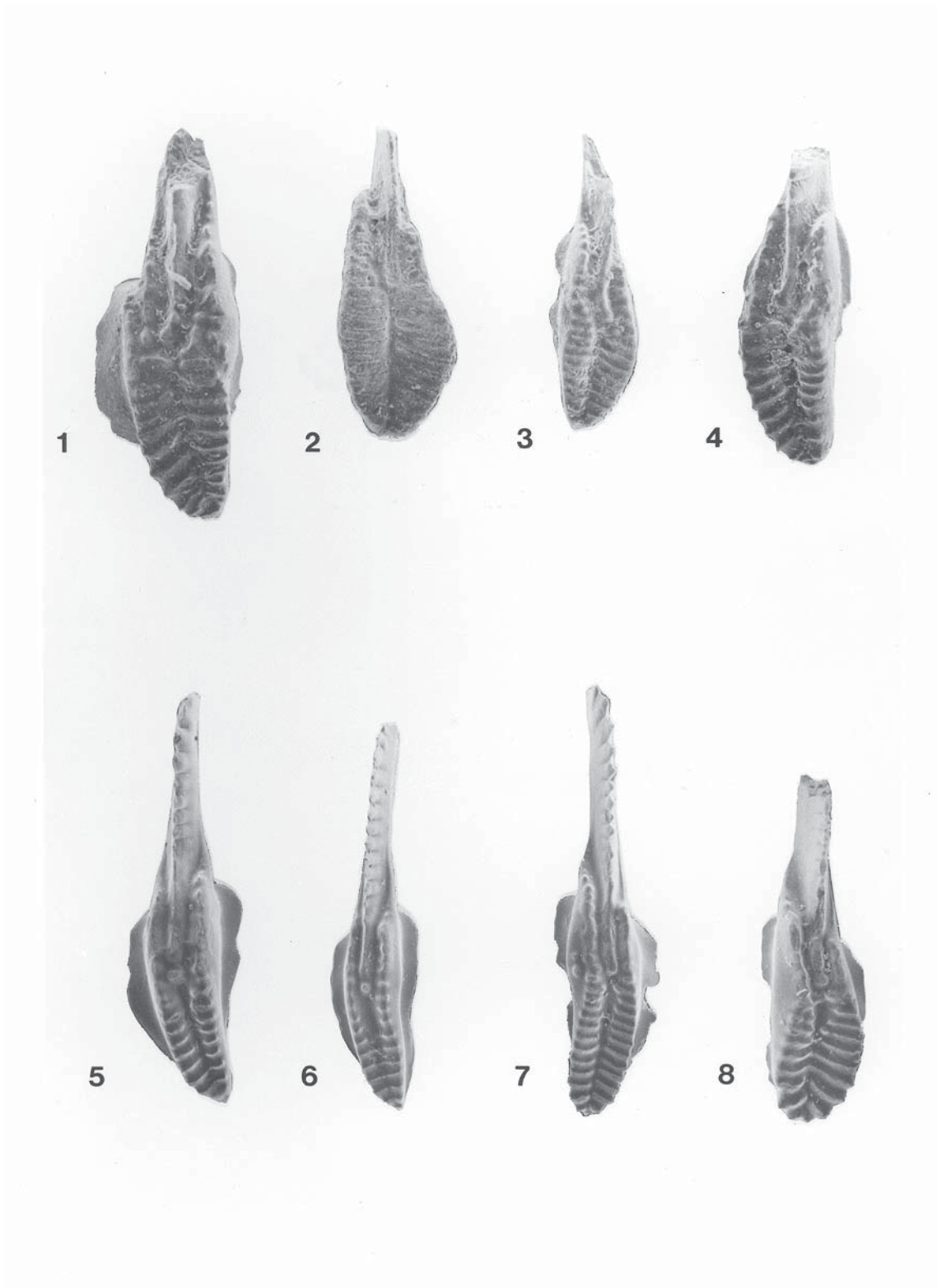
PLATE 6—Conodonts from the Americus Limestone Member of the Foraker Limestone, all upper views of Pa elements, x 72. (1, 3–4) *Streptognathodus farmeri* Gunnell, USNM 484015–484017. (2, 8) *Streptognathodus flexuosus* Chernykh and Ritter, USNM 484018–484019. (5–7) *Streptognathodus elongatus* Gunnell, USNM 484020–484022. 1–4 from shale parting, Americus Limestone Member, K–38 roadcut (Locality 4); 5–7 from base upper ledge of Americus Limestone Member, type Janesville, (Locality 1); 8 from base upper ledge of Americus Limestone Member, type Foraker (Locality 2).
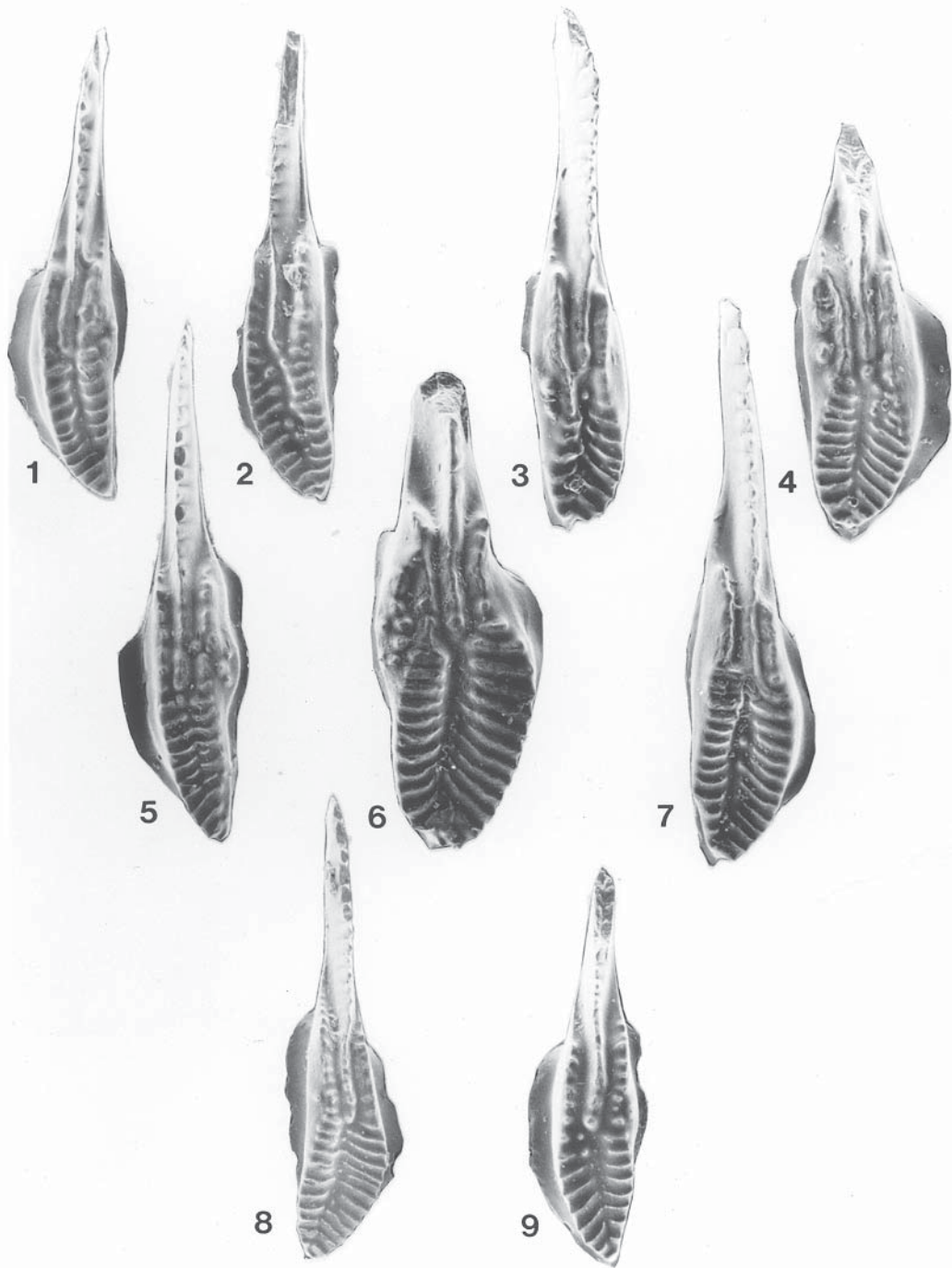
PLATE 7—Conodonts from the Americus Limestone Member of the Foraker Limestone, all upper views of Pa elements, x 75. (1–2, 5, 8–9) *Streptognathodus wabaunsensis* Gunnell, USNM 484023–484027. (3–4, 6–7) *Streptognathodus farmeri* Gunnell, USNM 484028–484031. 1–5, 7–9 from base of upper Americus Limestone Member, I–70 roadcut (Locality 5); 6 from shale above upper Americus Limestone Member, I–70 roadcut (Locality 5).

PLATE 8—Conodonts from the Hughes Creek Shale Member of the Foraker Limestone, all upper views of Pa elements, x 75. (1) *Streptognathodus flexuosus* Chernykh and Ritter, USNM 484032. (2–4, 8–11) *Streptognathodus conjunctus* Barskov, Isakova, and Shchastlivceva, USNM 484033–484039. (5–7) *Streptognathodus wabaunsensis* Gunnell, USNM 484040–484042. 1–5, 7, 9–10 from sample 5, lower Hughes Creek Shale Member, Tuttle Creek (Locality 6); 6, 8, 11 from sample 3, lower Hughes Creek Shale Member, Tuttle Creek (Locality 6).
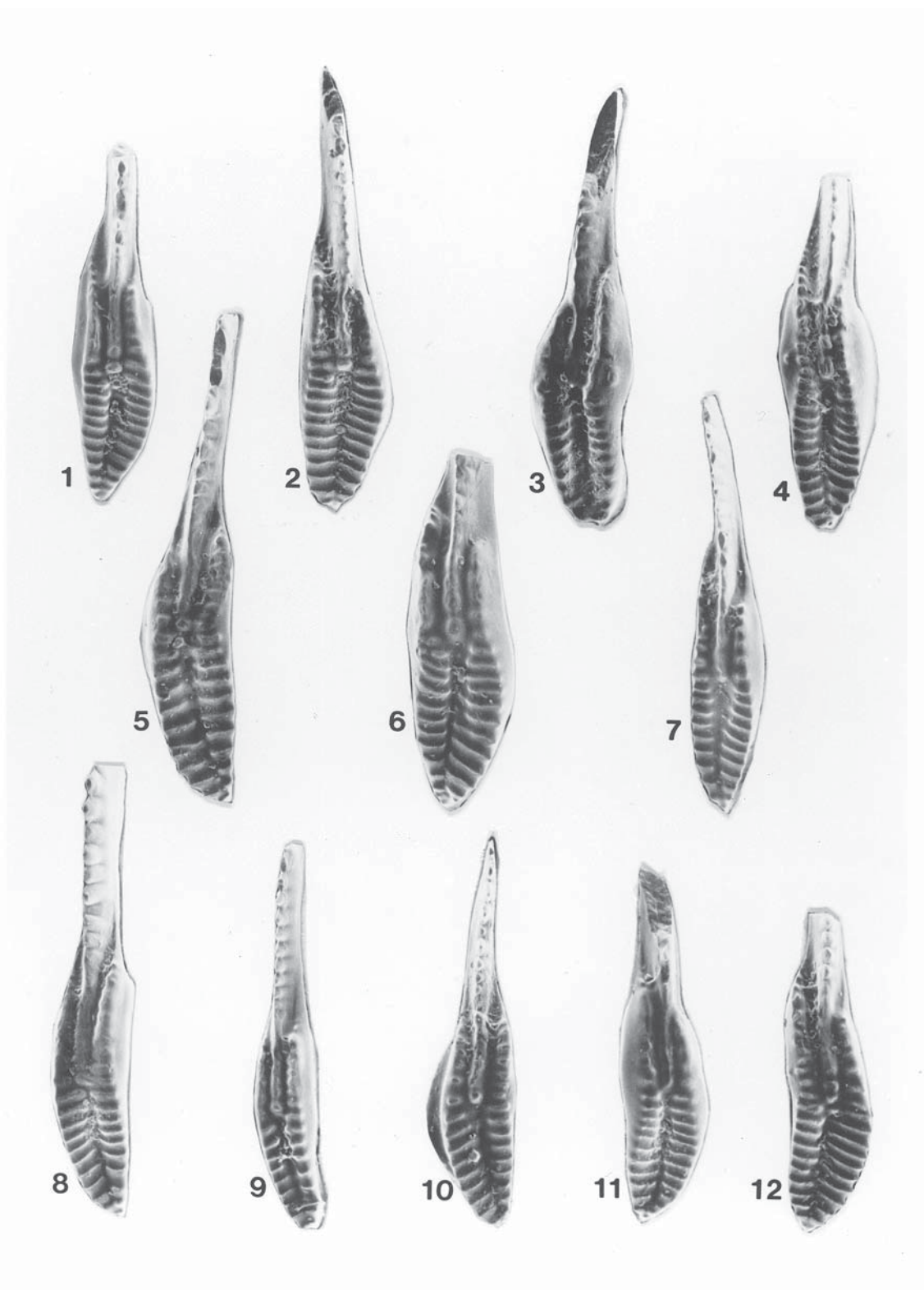
PLATE 9—Conodonts from the Hughes Creek Shale Member of the Foraker Limestone, all upper views of Pa elements, x 75. (1–2, 6, 8, 11–12) *Streptognathodus conjunctus* Barskov, Isakova, and Shchastlivceva, USNM 484043–484048. (3) *Streptognathodus farmeri* Gunnell, USNM 484049. (5, 7, 9–10) *Streptognathodus elongatus* Gunnell, USNM 484050–484053. (4) *Streptognathodus wabaunsensis* Gunnell, USNM 484054. 1–2, 5–6, 12, sample 3, lower Hughes Creek Shale Member, Tuttle Creek (Locality 6); 3–4, sample 6, lower Hughes Creek Shale Member, Tuttle Creek (Locality 6); 7–11, from sample 5, lower Hughes Creek Shale Member, Tuttle Creek (Locality 6).

PLATE 10—Conodonts from the Hughes Creek Shale Member of the Foraker Limestone, all upper views of Pa elements, ✕ 75. (1, 7) *Streptognathodus conjunctus* Barskov, Isakova, and Shchastlivceva, USNM 484055–484056. (2–6, 8–11) *Streptognathodus binodosus* Wardlaw, Boardman, and Nestell, new species, 6, holotype, USNM 484057–484065. 1, 7 from sample 23, upper Hughes Creek Shale Member, Tuttle Creek (Locality 6); 2, 8–10, from sample 22, upper Hughes Creek Shale Member, Tuttle Creek (Locality 6); 3–6, 11, from sample 21, upper Hughes Creek Shale Member, Tuttle Creek (Locality 6).
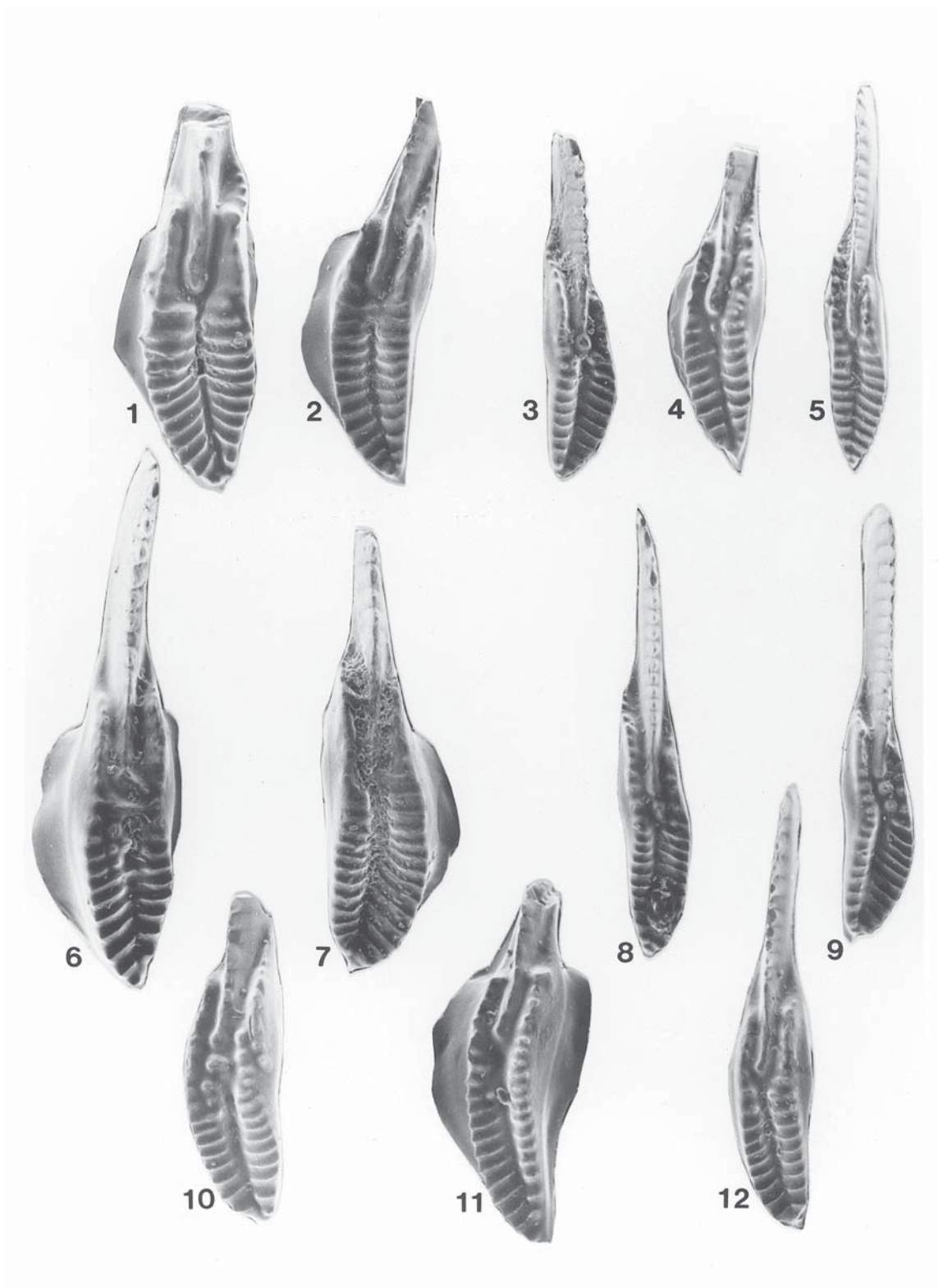
PLATE 11—Conodonts from the Hughes Creek Shale Member of the Foraker Limestone, all upper views of Pa elements, x 75. (1, 3–5, 7, 10, 12) *Streptognathodus binodosus* Wardlaw, Boardman, and Nestell, 10, transitional to *nodulinearis-minacutus*, USNM 484066–484072. (2, 6) *Streptognathodus conjunctus* Barskov, Isakova, and Shchastlivceva, USNM 484073–484074. (8–9, 11) *Streptognathodus elongatus* Gunnell, USNM 484075–484077. 1–2, 4–6, 8, 10–11 from sample 21, upper Hughes Creek Shale Member, Tuttle Creek (Locality 6); 3, 7, 12 from sample 22, upper Hughes Creek Shale Member, Tuttle Creek (Locality 6); 9 from sample 23, upper Hughes Creek Shale Member, Tuttle Creek (Locality 6).
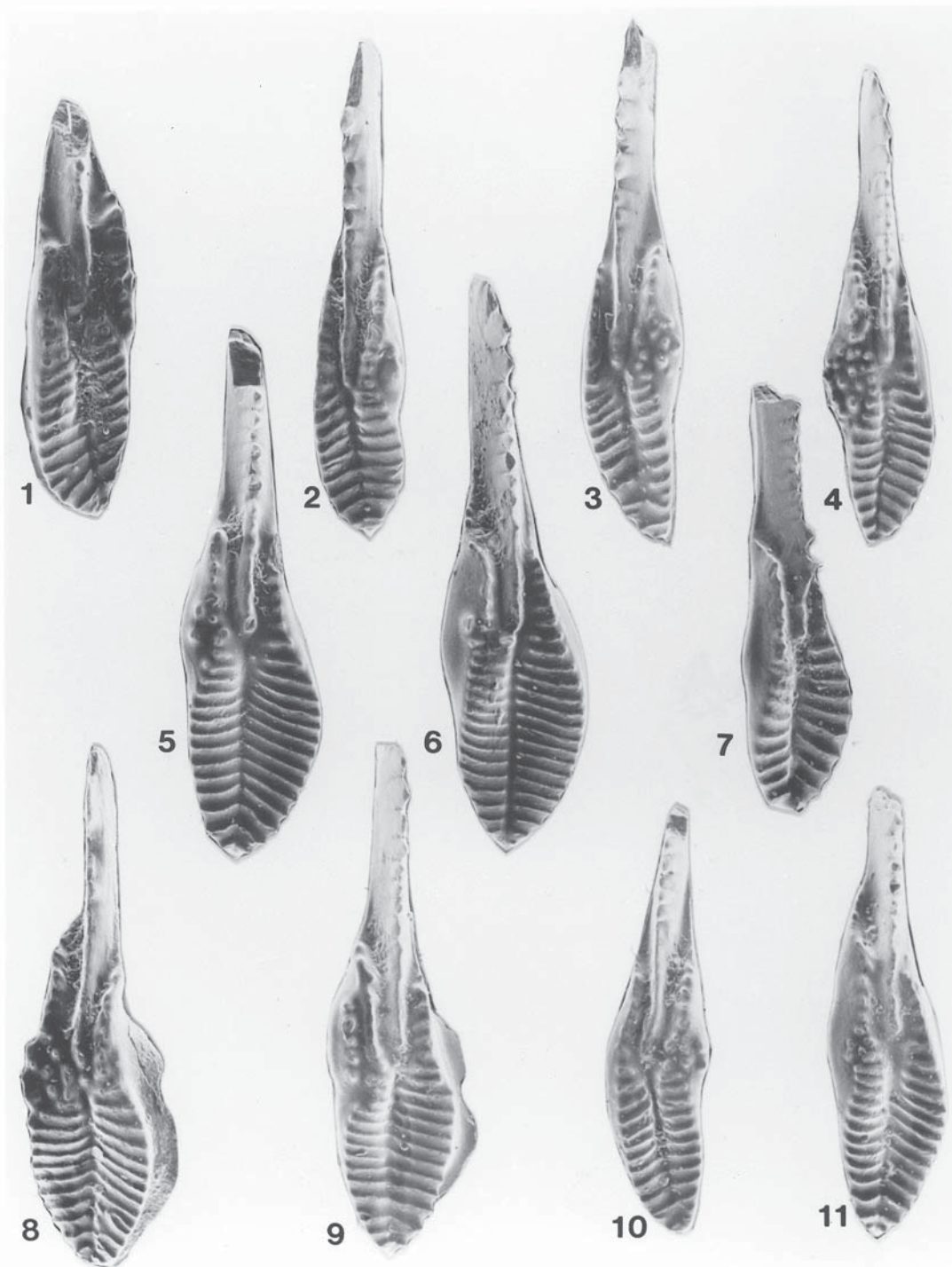
PLATE 12—Conodonts from the Bennett Shale and Howe Limestone Members of the Red Eagle Limestone, all upper views of Pa elements, x 75. (1, 8) *Streptognathodus minacutus* Barskov and Reimers, USNM 484078–484079. (3–4, 10) *Streptognathodus isolatus* Chernykh, Ritter, and Wardlaw, USNM 484080–484082. (2) *Streptognathodus invaginatus* Reshetkova and Chernykh, USNM 484083. (5–7) *Streptognathodus fuchengensis* Zhao, USNM 484084–484086. (9, 11) *Streptognathodus nodulinearis* Reshetkova and Chernykh, USNM 484087–484088. 1–9 from sample 8, Bennett Shale Member, Tuttle Creek (Locality 6); 10–11 from sample 3, Howe Limestone Member, Tuttle Creek (Locality 6).

PLATE 13—Conodonts from the Bennett Shale and Howe Limestone Members of the Red Eagle Limestone, all upper views of Pa elements, x 75. (1, 8, 10–12) *Streptognathodus isolatus* Chernykh, Ritter, and Wardlaw, USNM 484089–484093. (2) *Streptognathodus minacutus* Barskov and Reimers, USNM 484094. (3) *Streptognathodus binodosus* Wardlaw, Boardman, and Nestell, USNM 484095. (4–5) *Streptognathodus invaginatus* Reshetkova and Chernykh, USNM 484096–484097. (6) *Streptognathodus fuchengensis* Zhao, USNM 484098. (7) *Streptognathodus elongatus* Gunnell, USNM 484099. (9) *Streptognathodus nodulinearis* Reshetkova and Chernykh, USNM 484100. 1, 3, 5–8, 10, 12 from sample 8, Bennett Shale Member, Tuttle Creek (Locality 6); 2, 4, 9, 11 from sample 3, Howe Limestone Member, Tuttle Creek (Locality 6).
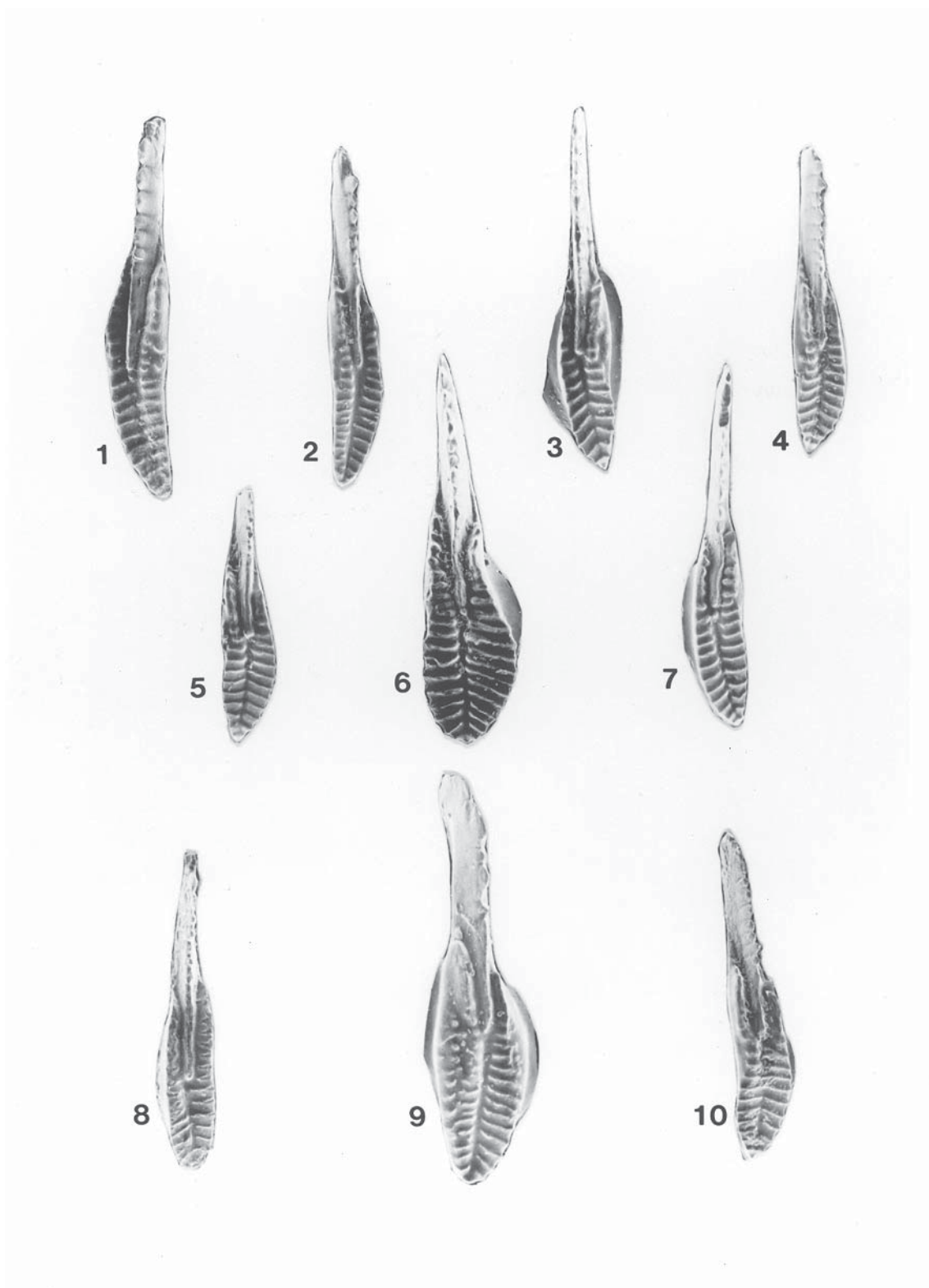
PLATE 14—Conodonts from the Burr Limestone Member of the Grenola Formation, all upper views of Pa elements, **x** 75. (1–2, 8) *Streptognathodus postelongatus* Wardlaw, Boardman, and Nestell, new species, 1, holotype, USNM 484101–484102. (3–5, 9) *Streptognathodus translinearis* Wardlaw, Boardman, and Nestell, new species, 9, holotype, USNM 484103–484107. (6, 7) *Streptognathodus nevaensis* Wardlaw, Boardman, and Nestell, USNM 484108–484109. (10) *Streptognathodus invaginatus* Reshetkova and Chernykh, USNM 484110. 1–5, 7–10 from top of the lower Burr Limestone Member, Tuttle Creek (Locality 6); 6 from top of the lower Burr Limestone Member, Fort Riley Boulevard (Locality 8).

PLATE 15—Conodonts from the Neva Limestone Member of the Grenola Formation, all upper views of Pa elements, x 75. (1, 14) *Streptognathodus lineatus* Wardlaw, Boardman, and Nestell new species, 14, holotype, USNM 484111–484112. (2–5, 10, 13, 15–17) *Streptognathodus postelongatus* Wardlaw, Boardman, and Nestell, USNM 484113–484121. (6) *Streptognathodus invaginatus* Reshetkova and Chernykh, 484122. (7–9) *Streptognathodus isolatus* Chernykh, Ritter, and Wardlaw, USNM 484123–484125. (11) *Streptognathodus nodulinearis* Reshetkova and Chernykh, USNM 484126. (12) *Streptognathodus fuchengensis* Zhao, USNM 484127. 1, 3–4, 7, 10, 12, 14–16 from basal phosphatic lag in lower Neva Limestone Member, Fort Riley Boulevard (Locality 8); 2, 5–6, 8–9, 11, 13, 17 from top of gray shale in lower Neva Limestone Member, Fort Riley Boulevard (Locality 8).
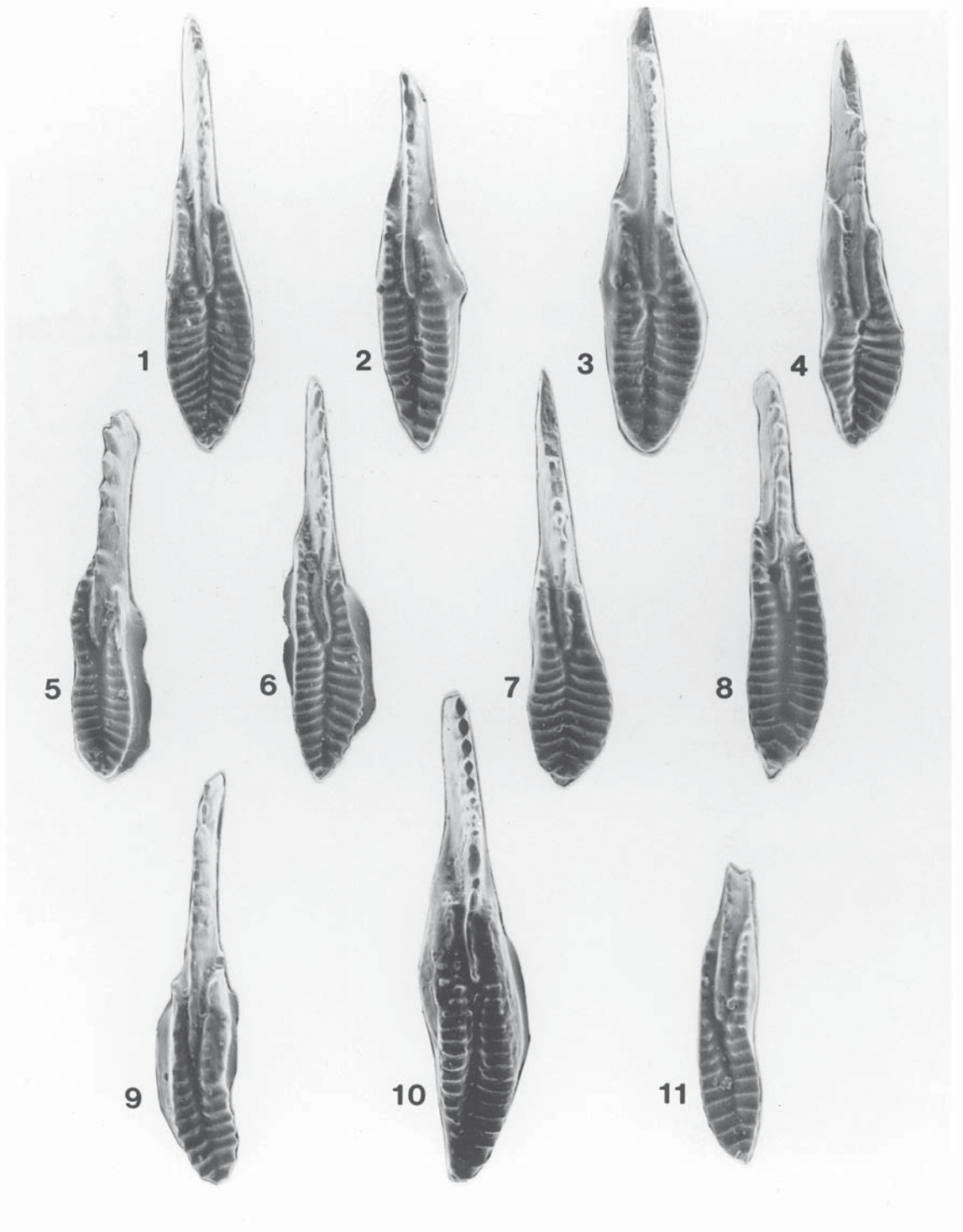
PLATE 16—Conodonts from the Neva Limestone Member of the Grenola Formation, all upper view of Pa elements, x 75. (1–3, 5–8, 11) *Streptognathodus nevaensis* Wardlaw, Boardman, and Nestell, new species, 7, holotype, USNM 484128–484135. (4) *Streptognathodus fuchengensis* Zhao, USNM 484136. (9–10) *Streptognathodus postelongatus* Wardlaw, Boardman, and Nestell, USNM 484137–484138. 1–11 from upper phosphatic lag, upper Neva Limestone Member, Fort Riley Boulevard (Locality 8).
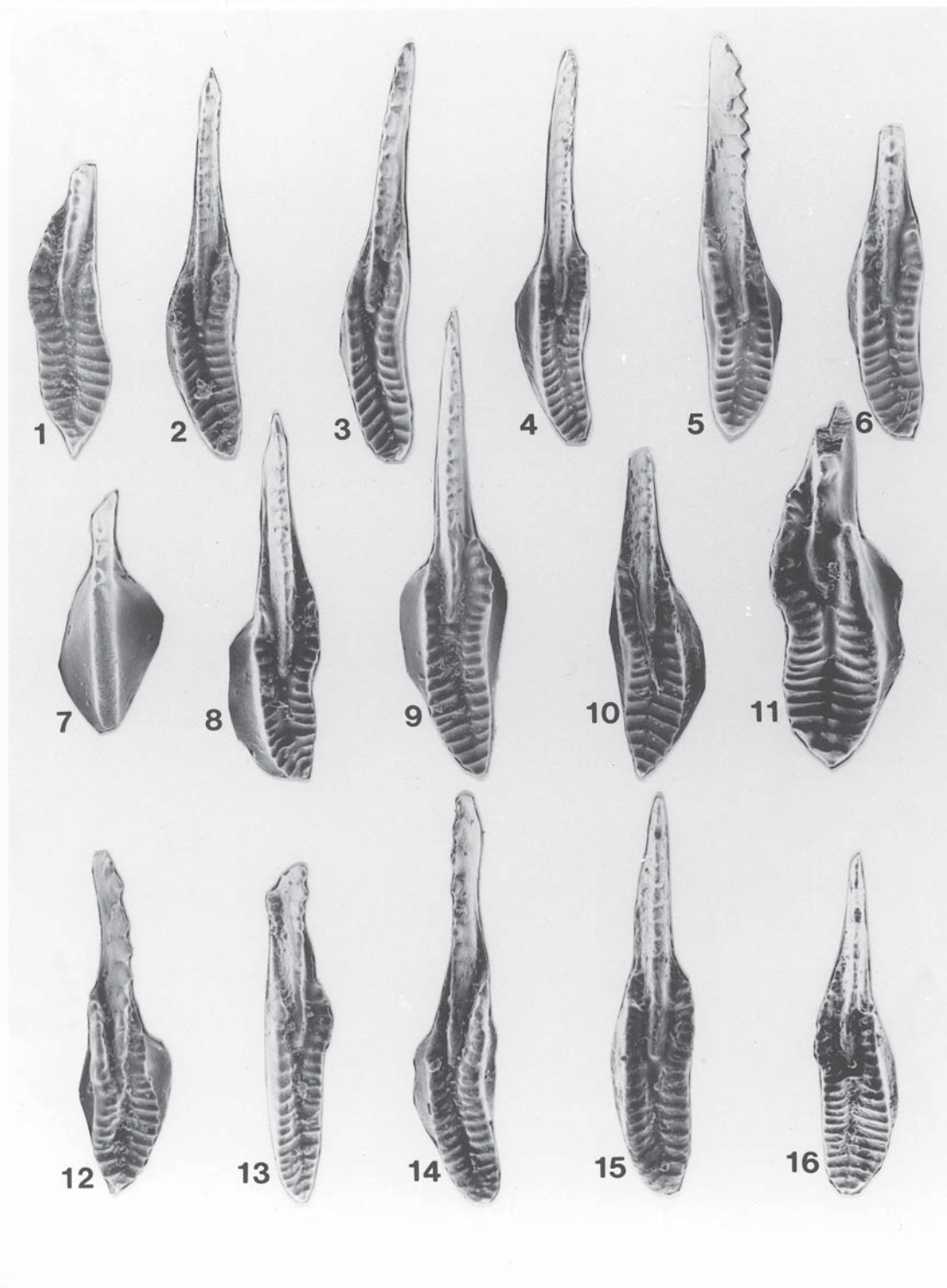
PLATE 17—Conodonts from the Cottonwood Limestone Member of the Beattie Limestone, all upper view of Pa elements, x 75. (1, 4, 6, 8–9, 11, 13, 15–16) *Streptognathodus fusus* Chernykh and Reshetkova, USNM 484139–484147. (3, 5, 14) *Streptognathodus longissimus* Chernykh and Reshetkova, USNM 484148–484150. (2, 10) *Streptognathodus constrictus* Reshetkova and Chernykh, USNM 484151–484152. (12) *Streptognathodus nevaensis* Wardlaw, Boardman, and Nestell, USNM 484153. (7) *Sweetognathus expansus* (Perlmutter), USNM 484154. 1–7, 9–10, 12–13, 15 from sample 3, Cottonwood Limestone Member (Locality 11); 8, 14 from sample 3, Cottonwood Limestone Member, Tuttle Creek (Locality 6); 11, 16 from sample 4, Cottonwood Limestone Member, Tuttle Creek (Locality 6).
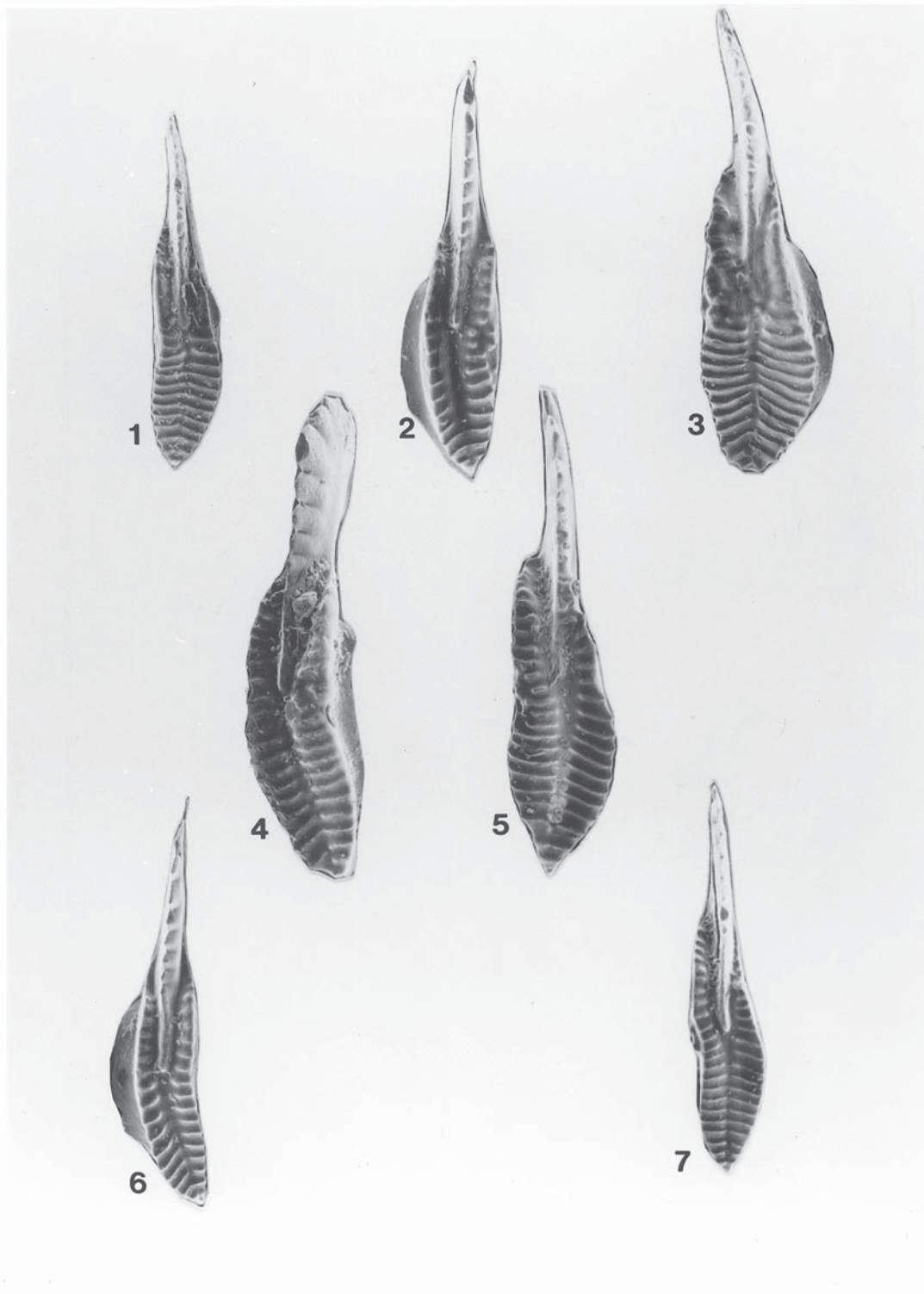
PLATE 18—Conodonts from the Eiss Limestone Member of the Bader Limestone, all upper view of Pa elements, x 75. (1–5, 7) *Streptognathodus barskovi* (Kozur), USNM 484155–484160. (6) *Streptognathodus constrictus* Reshetkova and Chernykh, USNM 484161. 1–3, 6 from sample 4, Eiss Limestone Member, type Hooser (Locality 10); 4–5, 7 from upper rubbly Eiss, Eiss Limestone Member (Locality 11).
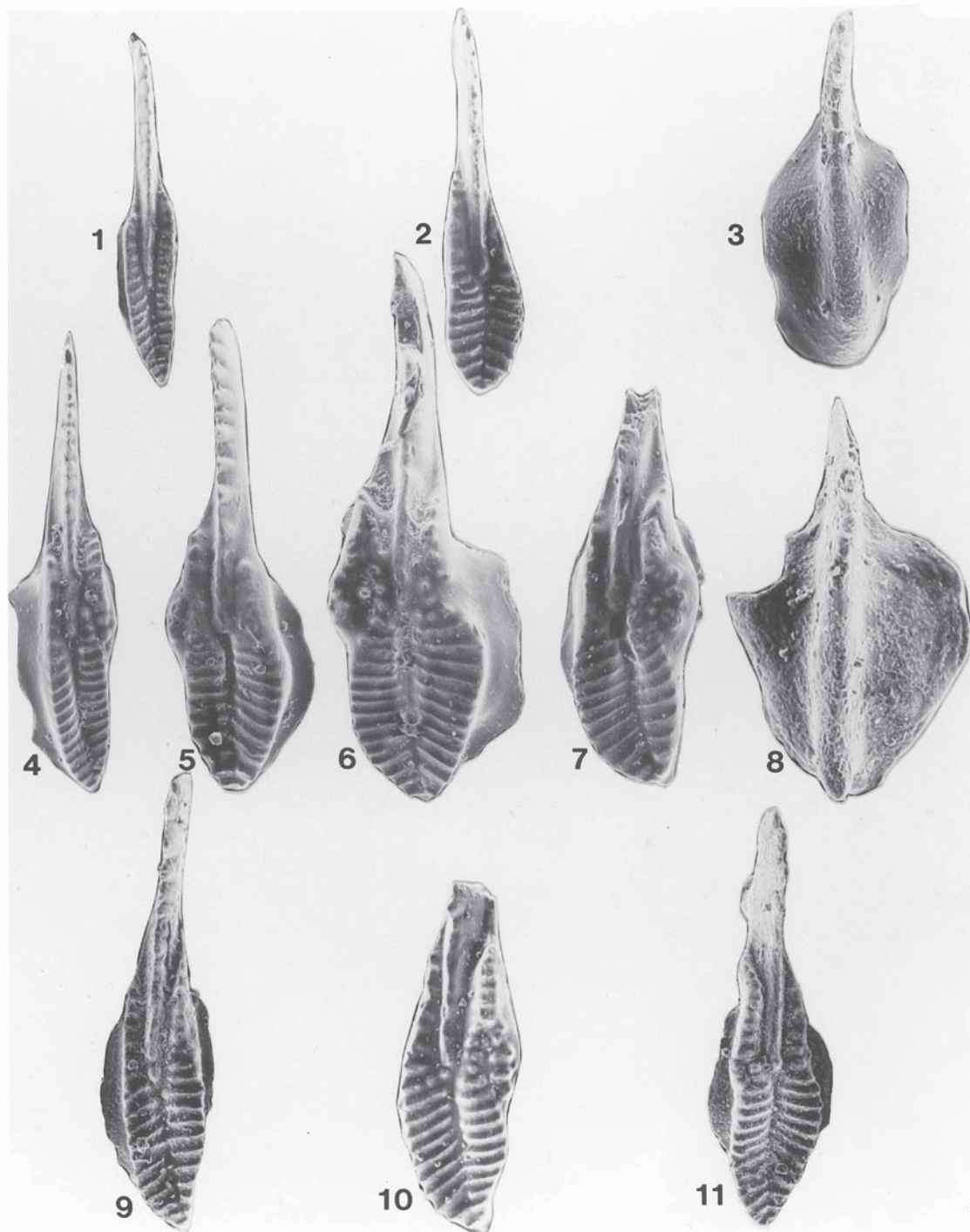
PLATE 19—Conodonts from the Grenola Limestone, Red Eagle Limestone, and Foraker Limestone, all upper view of Pa elements, x 75. (1) *Streptognathodus lineatus* Wardlaw, Boardman, and Nestell, USNM 484162. (2) *Streptognathodus nevaensis* Wardlaw, Boardman, and Nestell, USNM 484163. (3, 8) *Sweetognathus expansus* (Perlmutter), USNM 484164–484165. (4–6) *Streptognathodus minacutus* Barskov and Reimers, USNM 484166–484168. (7) *Streptognathodus isolatus* Chernykh, Ritter, and Wardlaw, USNM 484169. (9, 11) *Streptognathodus binodosus* Wardlaw, Boardman, and Nestell, USNM 484170–484171. (10) *Streptognathodus wabaunsensis* Gunnell, USNM 484172. 1–3 from base of lower Burr Limestone Member, Grenola Formation, K–38 roadcut (Locality 7); 4–8 from sample 6, Bennett Shale Member, Red Eagle Limestone, K–38 roadcut (Locality 4); 9–11 from limestone 5 at base of upper Hughes Creek Shale Member, Foraker Limestone, K–38 roadcut (Locality 4).
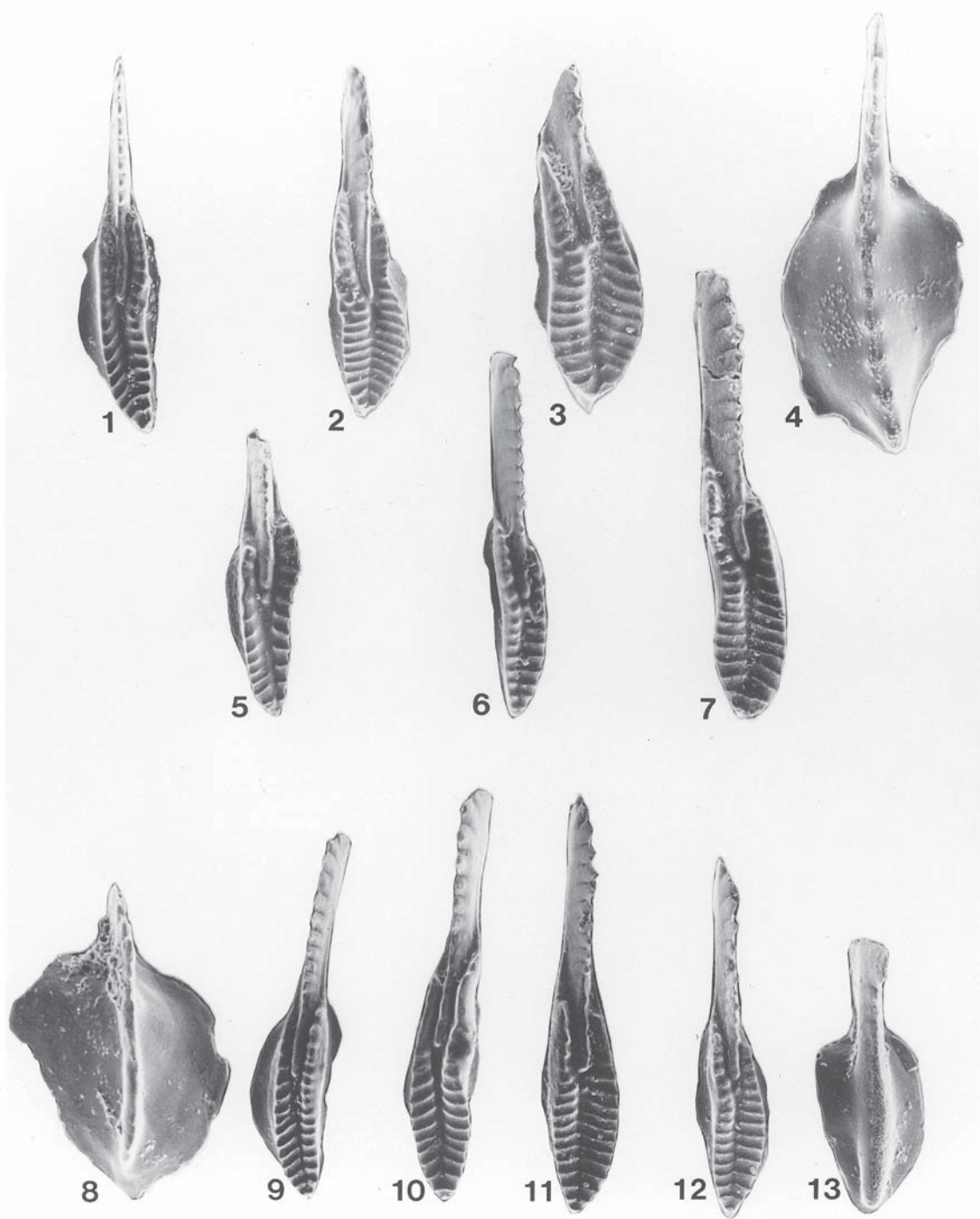
PLATE 20—Conodonts from the Bader Limestone, Beattie Limestone, and Grenola Limestone, all upper view of Pa elements, x 75. (1) *Streptognathodus longissimus* Chernykh and Reshetkova, USNM 484173. (2–3) *Streptognathodus barskovi* (Kozur), USNM 484174–484175. (4) *Sweetognathus merrilli* Kozur, USNM 484176. (5, 7) *Streptognathodus fusus* Chernykh and Reshetkova, USNM 484177–484178. (6) *Streptognathodus constrictus* Reshetkova and Chernykh, USNM 484179. (8) *Diplognathodus* sp., USNM 484180. (9, 11–12) *Streptognathodus postelongatus* Wardlaw, Boardman, and Nestell, USNM 484181–484183. (10) *Streptognathodus invaginatus* Reshetkova and Chernykh, USNM 484184. (13) *Sweetognathus expansus* (Perlmutter), USNM 484185. 1–4 from sample 4, Eiss Limestone Member, Bader Limestone, type Hooser (Locality 10); 5–7, from top of limestone, Cottonwood Limestone Member, Beattie Limestone, type Hooser (Locality 10); 8, 11–13 from 20 cm below lower ledge, Neva Limestone Member, Grenola Limestone, type Grenola, (Locality 9); 9–10 from lower Neva ledge, Neva Limestone Member, Grenola Limestone, type Grenola (Locality 9).
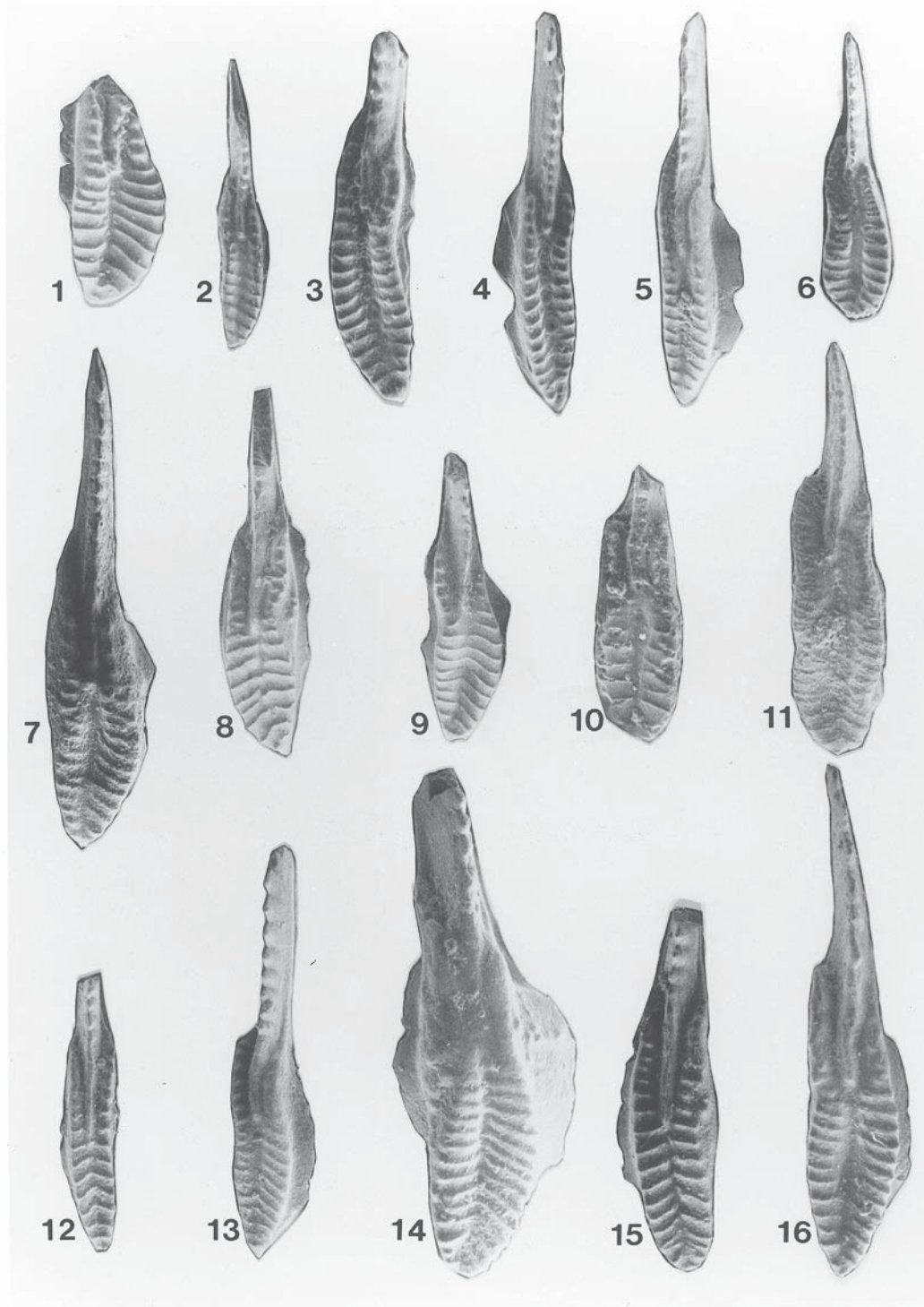
PLATE 21—Conodonts from the Crouse Limestone, Funston Limestone, and Threemile Limestone Member of the Wreford Limestone. All upper views of Pa elements, ✕ 75. (1, 8–9) *Streptognathodus trimilus* Wardlaw, Boardman, and Nestell, new species (fig. 9, holotype), USNM 487489–487491. (2–5, 13) *Streptognathodus postconstrictus* Wardlaw, Boardman, and Nestell, USNM 487492–487496. (6, 10–11) *Streptognathodus robustus* Wardlaw, Boardman, and Nestell, new species (fig. 6, holotype). USNM 487497–497499. (7, 14, 16) *Streptognathodus translinearis* Wardlaw, Boardman, and Nestell, USNM 497500–487502. 12, 15, *Streptognathodus constrictus* Reshetkova and Chernykh, USNM 487503–487504. 1, 5, 10, from the Threemile Limestone Member, Wreford Limestone, base of ledge 2, Scenic Drive roadcut (Locality 12); 2, 6, from the Threemile Limestone Member, Wreford Limestone, base of ledge 3, Scenic Drive roadcut (Locality 12); 3, 4, 11, from the Threemile Limestone Member, Wreford Limestone, top of massive burrowed bed, K–38 locality (Locality 14); 8–9, from the Threemile Limestone Member, Wreford Limestone, base shaly limestone, Scenic Drive roadcut (Locality 12), from the Funston Limestone, top cycle 2, Scenic Drive roadcut (Locality 12); 12–16, Crouse Limestone, bed 1 mm above oncoliths, K–38 roadcut (Locality 13).
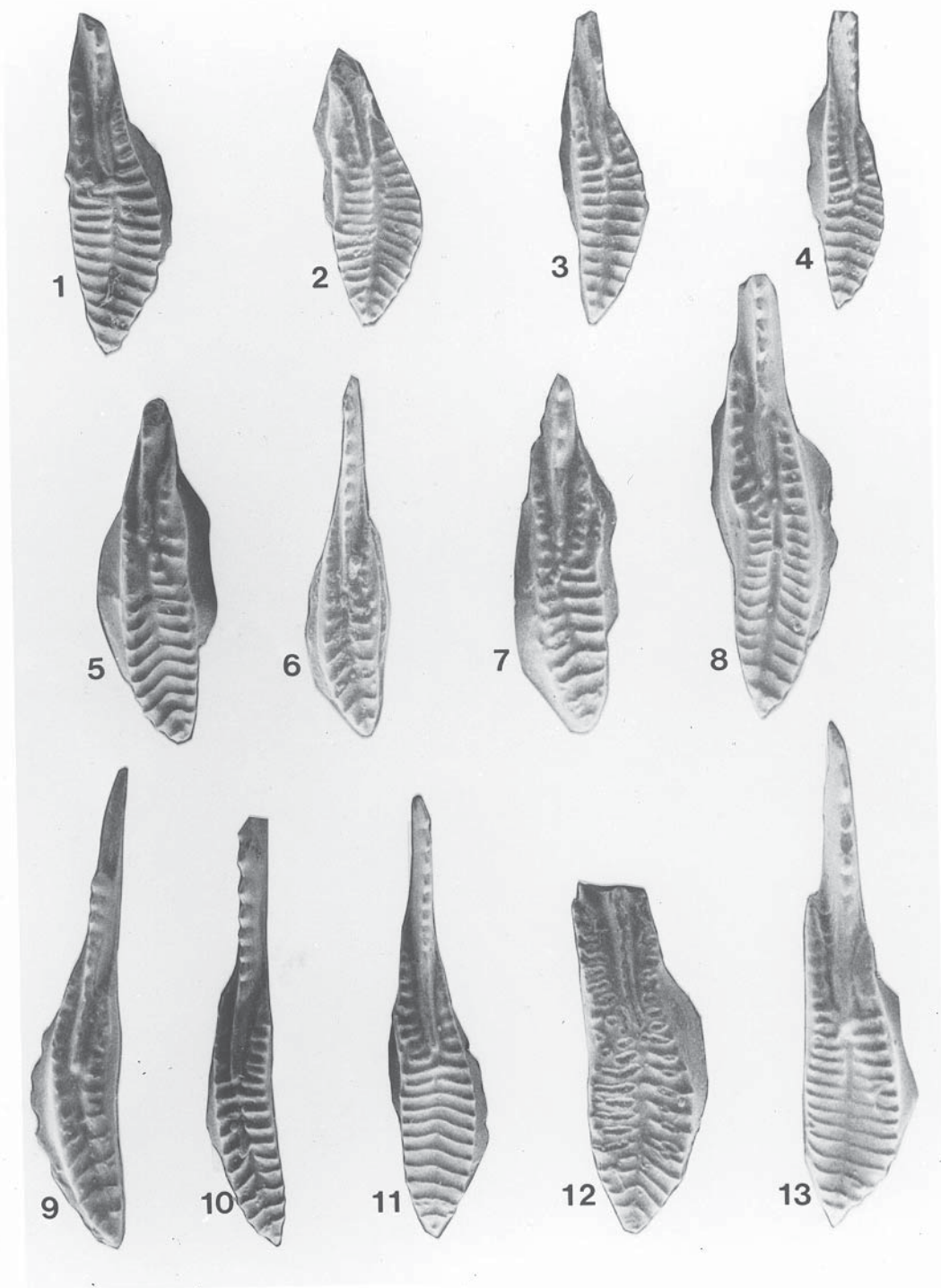
PLATE 22—Conodonts from the Schroyer Limestone Member of the Wreford Limestone. All upper views of Pa elements, x 75. (1–7, 9–13) *Streptognathodus trimilus* Wardlaw, Boardman, and Nestell, USNM 487505–487516. (8) *Streptognathodus postconstrictus* Wardlaw, Boardman, and Nestell, new species (holotype), USNM 487517. 1, 5, 10, 11, from top of Schroyer Limestone Member, Wreford Limestone, K–38 roadcut (Locality 14); 3, 4, 8, 9, 12, Schroyer Limestone Member, Wreford Limestone, base 3, Scenic Drive roadcut (Locality 12); 6, base of Schroyer Limestone Member, Wreford Limestone, K–38 roadcut (Locality 14); 7, 13, Schroyer Limestone Member, Wreford Limestone, top ledge 2, Scenic Drive roadcut (Locality 12).

PLATE 23—Conodont from the Florence Limestone Member of the Barneston Limestone. All upper views of Pa elements, x 75. (1–12) *Streptognathodus florensis* Wardlaw, Boardman, and Nestell, new species (fig. 10, holotype), USNM 487518–487529. 1–7, 9–12, from the Florence Limestone Member, Barneston Limestone, bed 1, K–38 roadcut (Locality 17); 8, from the Florence Limestone Member, Barneston Limestone, bed 3, K–38 roadcut (Locality 17).
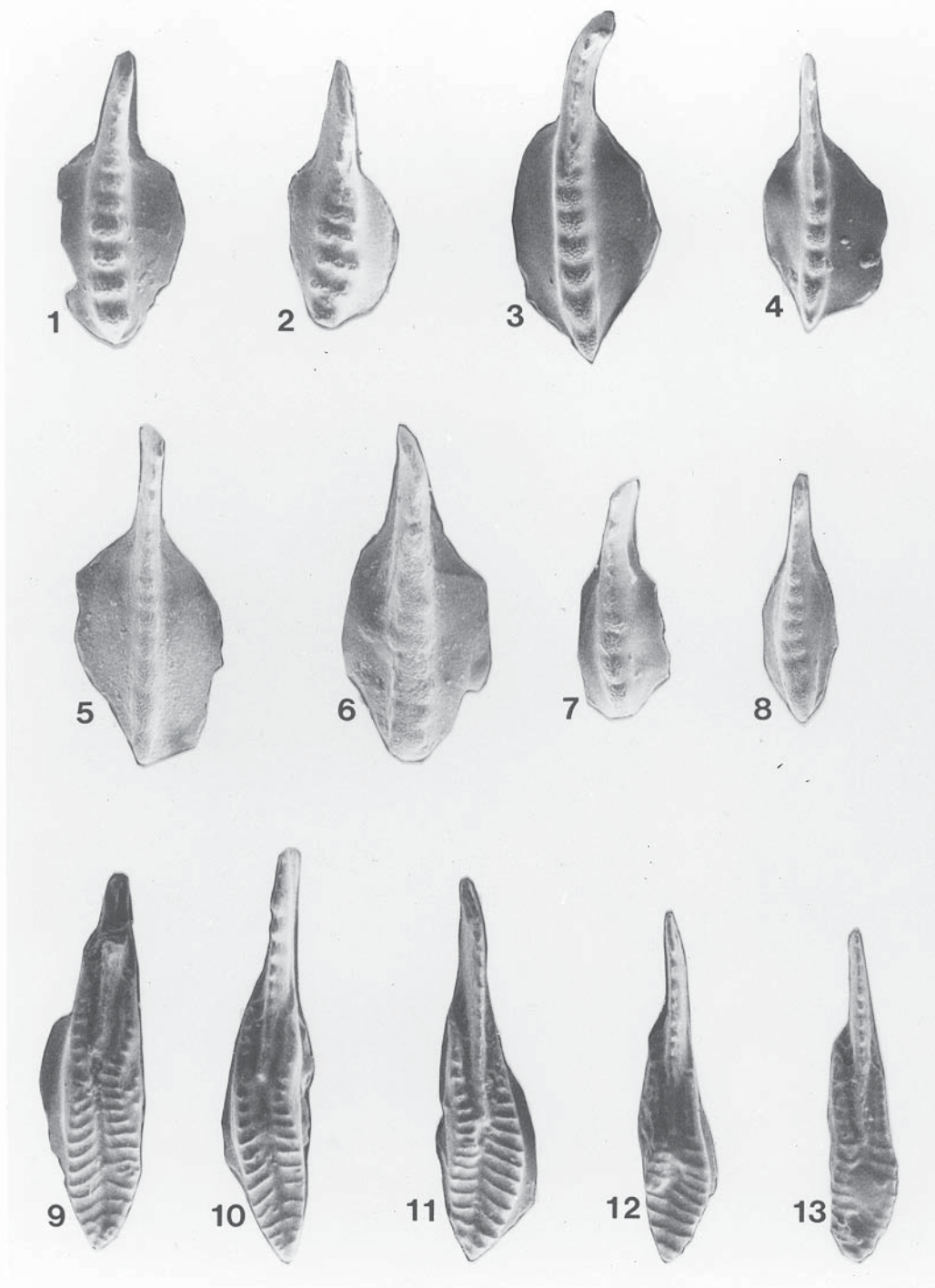
PLATE 24—Conodonts from the Florence Limestone Member of the Barneston Limestone, "pre-" Florence limestone beds in the Blue Spring Shale Member of the Matfield Shale, and Schroyer Limestone and Threemile Limestone Members of the Wreford Limestone. All upper views of Pa elements, x 75. (1) *Sweetognathus merrilli* Kozur, transitional to *S. whitei*, USNM 487530. (2) *Sweetognathus whitei* (Rhodes), USNM 487531. (3–4, 7–8) *Sweetognathus merrilli* Kozur, USNM 487532–487535. (5–6) *Sweetognathus expansus* (Perlmutter), USNM 487536–487537. (9–13) *Streptognathodus florensis* Wardlaw, Boardman, and Nestell, USNM 487538–487542. 1, 2, from the Florence Limestone Member, Barneston Limestone, bed 1, K–38 roadcut (Locality 17); 3–4, from top of the Schroyer Limestone Member, Wreford Limestone, K–38 roadcut (Locality 14) locality; 5–6, from Threemile Limestone Member, Wreford Limestone, top massive burrowed bed, K–38 roadcut (Locality 14); 7, from top lower Schroyer Limestone Member, Wreford Limestone, Scenic Drive roadcut (Locality 12); 8, from Schroyer Limestone Member, Wreford Limestone, base, Scenic Drive roadcut (Locality 12); 9–13, from "pre-" Florence limestone beds in the upper part of the Blue Spring Shale Member, Matfield Shale, K–38 roadcut (Locality 17).
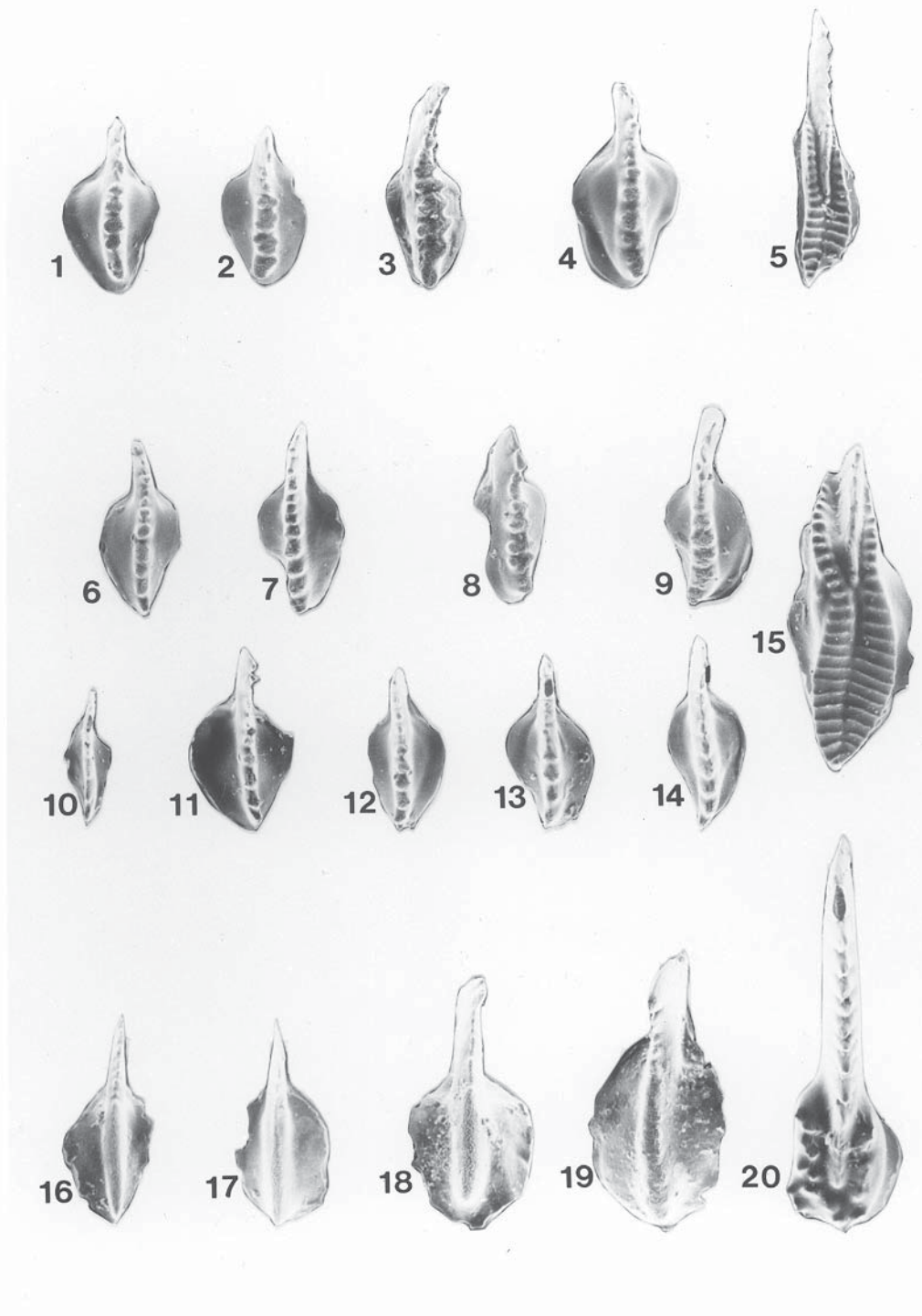
PLATE 25—Conodonts from the Neva Limestone Member of the Grenola Limestone and the Eiss Limestone Member of the Bader Limestone. All upper views of Pa elements, ✕ 75. (1–4, 6–14) *Sweetognathus merrilli* Kozur, USNM 487543–487555. (5, 15) *Streptognathodus barskovi* (Kozur), USNM 487556–487557. (16–19) *Sweetognathus expansus* (Perlmutter), USNM 487558–487561. (20) *Streptognathodus denticulatus* Wardlaw, Boardman, and Nestell, new species (holotype), USNM 487562. 1, 3, 7, 14, from upper Eiss Limestone Member, Bader Limestone, Strong City, US–50 (Locality 20) (topotypes of *merrilli*); 2, 8, 9, from upper Eiss Limestone Member, Bader Limestone, Strong City, US–50 (Locality 20); 4, 6, 12, 13, from upper Eiss Limestone Member, Bader Limestone, Strong City, US–77 (Locality 21); 5, 15, from Eiss Limestone Member, Bader Limestone, sample 8, Strong City, US–77 (Locality 21); 10–11, upper Eiss Limestone Member, Bader Limestone, sample 11, I–70 roadcut (Locality A7); 16–19, from upper Neva Limestone Member, Grenola Limestone, sample 5, intersection of US–60 and OK–18 roadcut, Locality 22; 20, from upper Neva Limestone Member, Grenola Limestone, sample 6, intersection of US–60 and OK–18 roadcut, Locality 22.
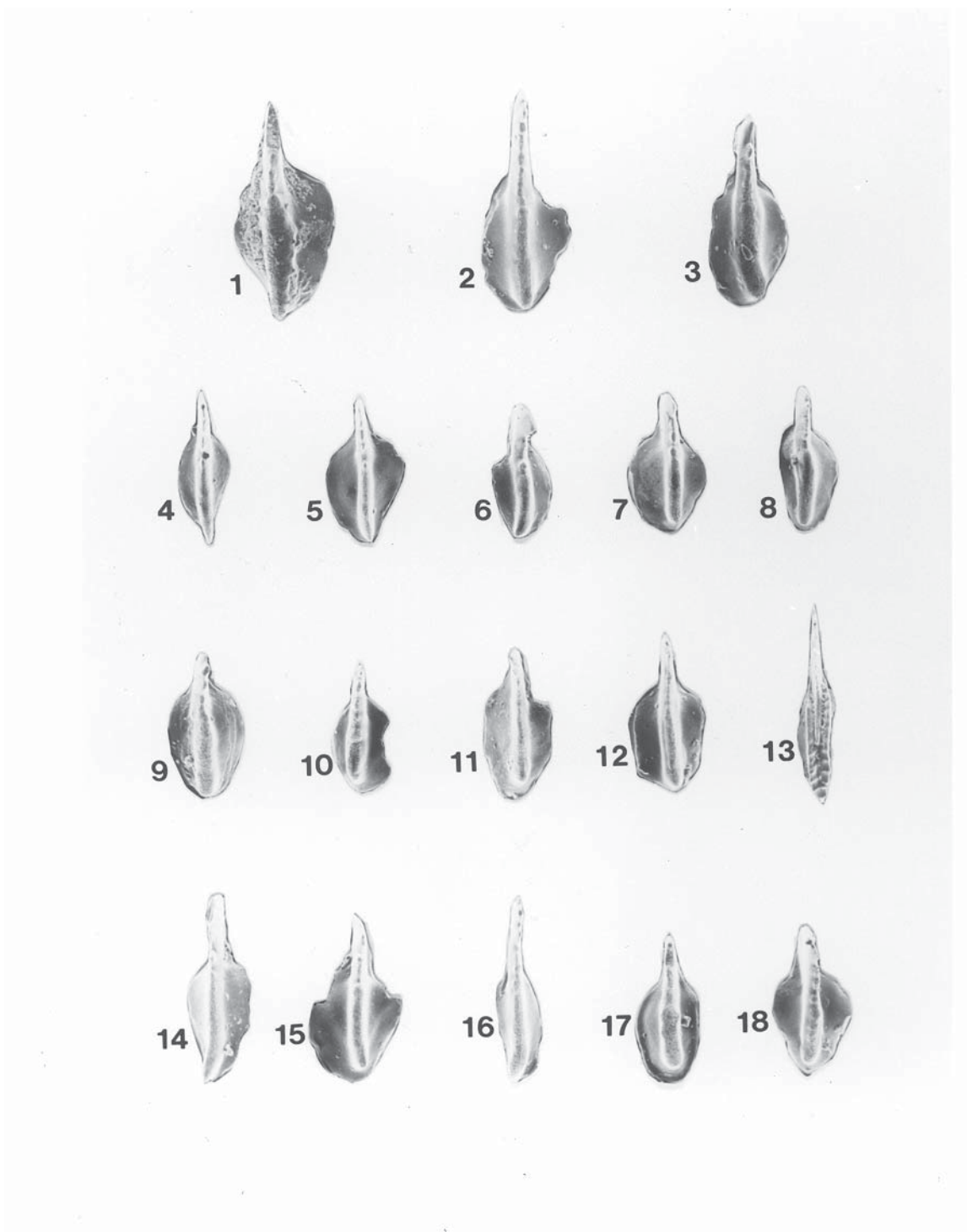
PLATE 26—Conodonts from the Crouse and Funston Limestones. All upper views of Pa elements, x 75. (1–12, 14–18) *Sweetognathus expansus* (Perlmutter), USNM 487563–487579. (13) *Streptognathodus constrictus* Reshetkova and Chernykh, USNM 487580. 1–3, from base of middle Funston Limestone, K–38 roadcut (Locality 13); 4, 8, 9, 11, 12, 17, from Crouse Limestone, sample 5, Scenic Drive roadcut (Locality 12); 5, 6, 7, 10, 15, 18, from upper Crouse Limestone, sample 4, Perlmutter section 9 (Locality A7 of this report), topotypes of *expansus*; 13–14, 16, from Crouse Limestone, base of lower ledge, K–38 roadcut (Locality 13).
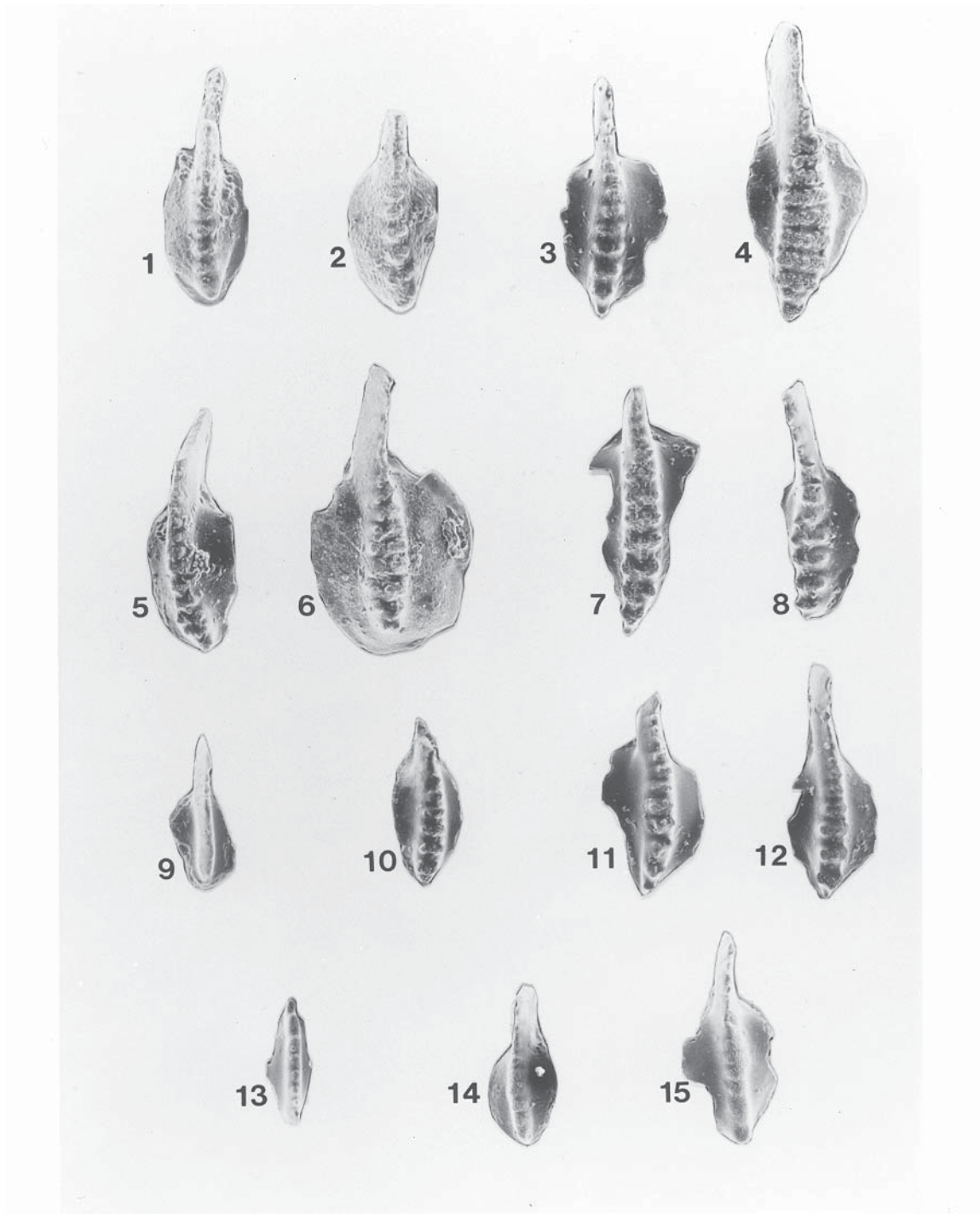
PLATE 27—Conodonts from the Havensville Shale Member of the Wreford Limestone and the Florence Limestone Member of the Barneston Limestone. All upper views of Pa element, x 75. (1–8, 10–12) *Sweetognathus whitei* (Rhodes), USNM 487581–487591. (9, 13–14) *Sweetognathus expansus* (Perlmutter), USNM 487592–487595. 1–2, from Florence Limestone Member, Barneston Limestone, base of parasequence 5, US–77 roadcut (Locality 16); 3, from Florence Limestone Member, Barneston Limestone, top of parasequence 7, US–77 roadcut (Locality 16); 4, from Florence Limestone Member, Barneston Limestone, base of parasequence 9, US–77 roadcut (Locality 16); 5–6, Florence Limestone Member, Barneston Limestone, top of parasequence 4, US–77 roadcut (Locality 16); 7–12, from Florence Limestone Member, Barneston Limestone, base of unit from 12 in condensed section, US–77 roadcut (Locality 16); 13–15, from top of limestone in Havensville Shale Member, Wreford Limestone, limestone 3, Scenic Drive roadcut (Locality 12).
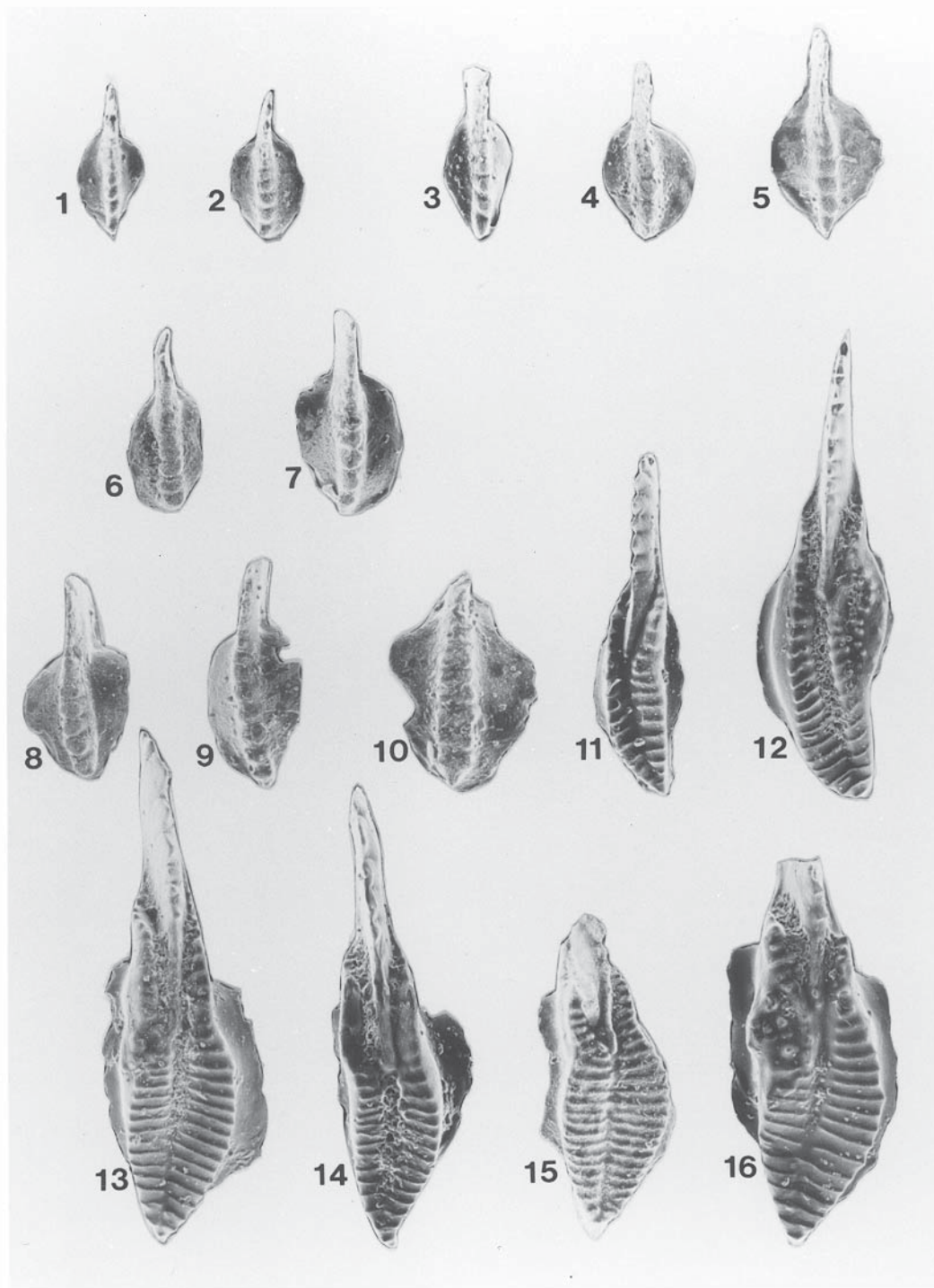
PLATE 28—Conodonts from the Fort Riley Limestone Member and the Florence Limestone Member of the Barneston Limestone. All upper views of Pa element, x 75. (1–9) *Sweetognathus merrilli* Kozur, USNM 487596–487604. (10) *Sweetognathus whitei* (Rhodes), USNM 487605. (11–16) *Streptognathodus florensis* Wardlaw, Boardman, and Nestell, USNM487606–487611. 1–2, 6–7, from base Fort Riley Limestone Member, Barneston Limestone, sample 1, US–77 roadcut (Locality 18); 3, from Fort Riley Limestone Member, Barneston Limestone, sample 9, US–77 roadcut (Locality 23); 4, from Fort Riley Limestone Member, Barneston Limestone, sample 9, US–77 roadcut (Locality 23); 5, 8–10, from Fort Riley Limestone Member, Barneston Limestone, sample 2, US–77 roadcut (Locality 23); 11, from Florence Limestone Member, Barneston Limestone, top of parasequence 7, US–77 roadcut (Locality 16); 12–14, 16, from Florence Limestone Member, Barneston Limestone, base of unit from 12 in condensed section, US–77 roadcut (Locality 16); 15, from Florence Limestone Member, Barneston Limestone, top of parasequence 3, US–77 roadcut (Locality 16).
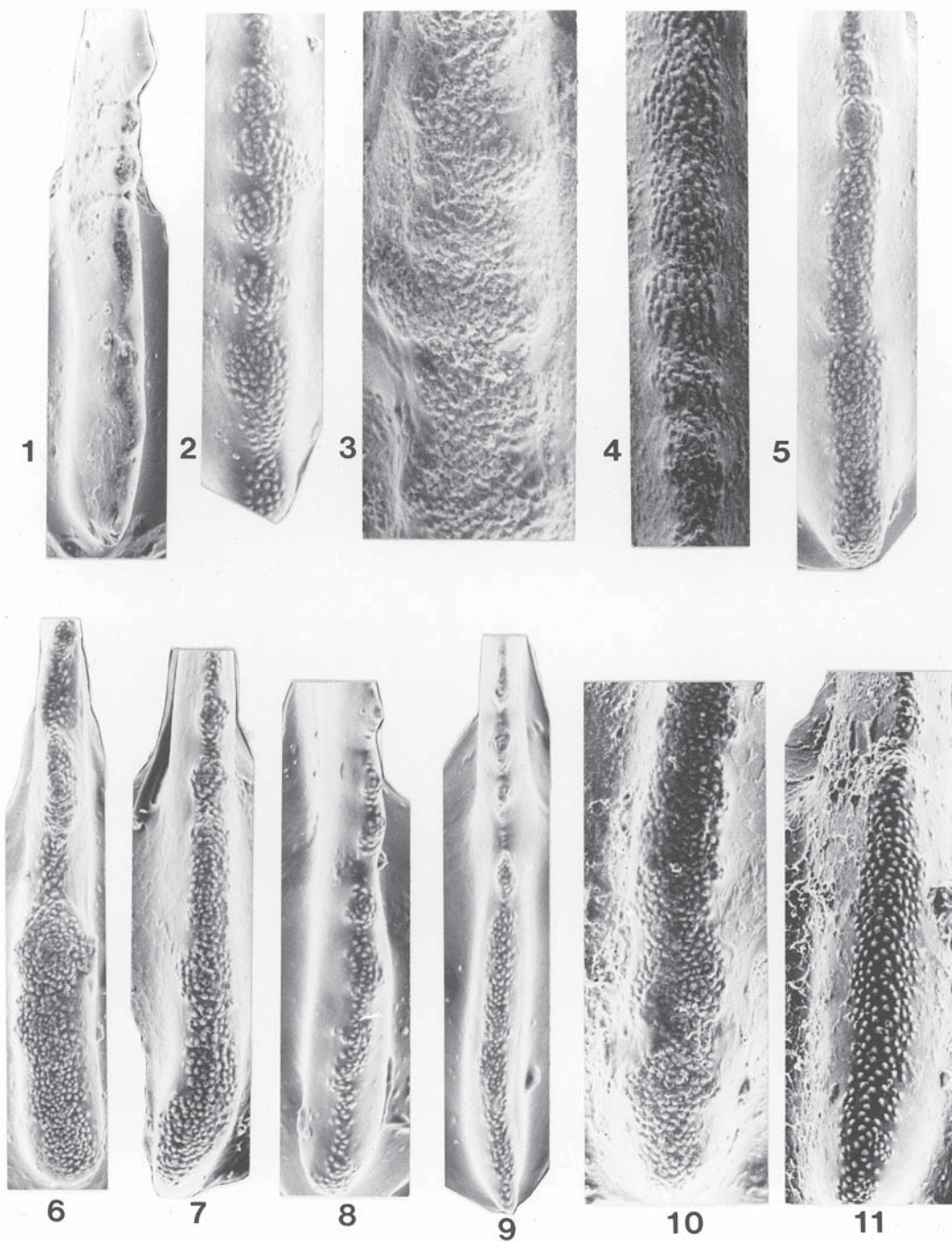
PLATE 29—Conodonts from the Neva Limestone Member of the Grenola Limestone, Crouse Limestone, Funston Limestone, Threemile Limestone Member and Havensville Shale Member of the Wreford Limestone, and Florence Limestone Member of the Barneston Limestone. All upper views of Pa element, x 300. (1–11) *Sweetognathus expansus* (Perlmutter). 1, from Florence Limestone Member, Barneston Limestone, base of unit from 12 in condensed section, US–77 roadcut (Locality 16), enlargement of pl. 26, fig. 9, USNM 487592; 2, from Havensville Shale Member, Wreford Limestone, top of limestone 3, Scenic Drive roadcut (Locality 12), enlargement of pl. 26, fig. 15, USNM 487595; 3–4, from Threemile Limestone Member, Wreford Limestone, top massive burrowed bed, K–38 roadcut (Locality 14), enlargements of pl. 23, fig. 6, and pl. 23, fig. 5, USNM 487586 and 487585, respectively; 5, from Funston Limestone, base of middle, enlargement of pl. 25, fig. 2, USNM 487564; 6, from Crouse Limestone, sample 5, Scenic Drive roadcut (Locality 12), enlargement of pl. 25, fig. 17, USNM 487578; 7, from Crouse Limestone, base of lower ledge, K–38 roadcut (Locality 13), enlargement of pl. 25, fig. 16, USNM 487577; 8–9, from upper Crouse Limestone, sample 4, Perlmutter section 9 (topotypes) (Locality A7 this report), enlargements of pl. 25, fig. 18 and pl. 25, fig. 5, USNM 487579 and 487567, respectively; 10–11, from the lower Neva Limestone Member, Grenola Limestone, sample 5, intersection of US–60 and OK–18 roadcut, Locality 22, enlargements of pl. 24, fig. 19 and pl. 24, fig. 18, USNM 487561 and 487560, respectively.
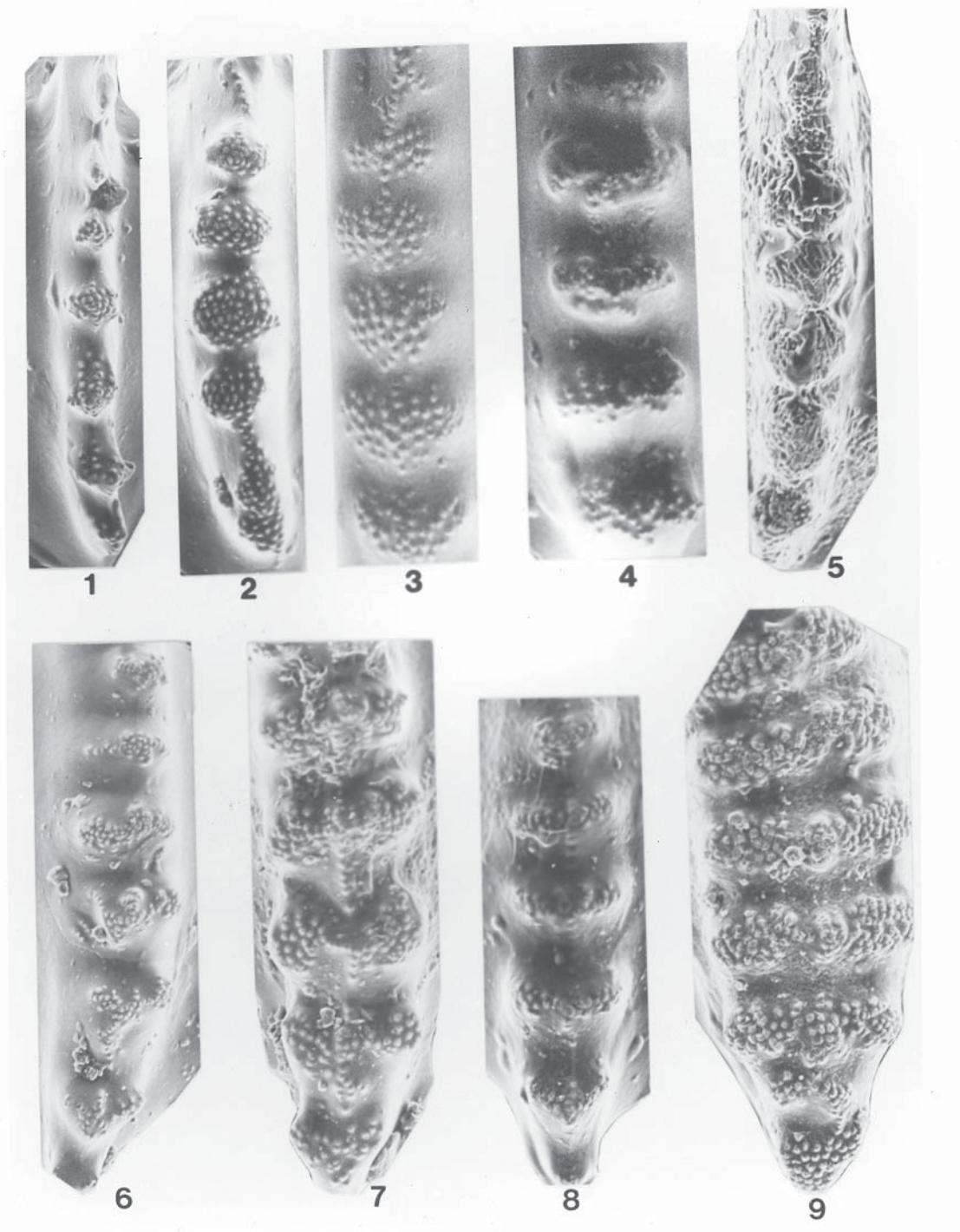
PLATE 30—Conodonts from the Eiss Limestone Member of the Bader Limestone, Schroyer Limestone Member of the Wreford Limestone, and Florence Limestone and Fort Riley Limestone Members of the Barneston Limestone. All upper views of Pa element, x 300. (1–5) *Sweetognathus merrilli* Kozur. (6–9) *Sweetognathus whitei* (Rhodes). 1, from upper Eiss Limestone Member, Bader Limestone, sample 11, I–70 roadcut (Locality A7), enlargement of pl. 24, fig. 11, USNM 487552; 2, from upper Eiss Limestone Member, Bader Limestone, Strong City, US–50 roadcut (Locality 20, topotype), enlargement of pl. 24, fig. 1, USNM 487543; 3, from top Schroyer Limestone Member, Wreford Limestone, K–38 roadcut (Locality 13), enlargement of pl. 23, fig. 3, USNM 487532; 4, from Florence Limestone Member, Barneston Limestone, sample 1, K–38 roadcut (Locality 17), enlargement of pl. 23, fig. 1, USNM 487530, transitional to *whitei*; 5, from base Fort Riley Limestone Member, Barneston Limestone, sample 1, Highway 77 roadcut (Locality 18), enlargement of pl. 27, fig. 7, USNM 487602; 6–7, from base Florence Limestone Member, Barneston Limestone, base of unit from 12 in condensed section, US–77 roadcut (Locality 16), enlargements of pl. 26, fig. 11 and pl. 26, fig. 7, USNM 487590 and 487587, respectively; 8, from Florence Limestone Member, Barneston Limestone, top parasequence 7, US–77 roadcut (Locality 16) enlargement of pl. 26, fig. 3, USNM 487583; 9, from Florence Limestone Member, Barneston Limestone, base of parasequence 9, US–77 roadcut (Locality 16), enlargement of pl. 26, fig. 4, USNM 487584.
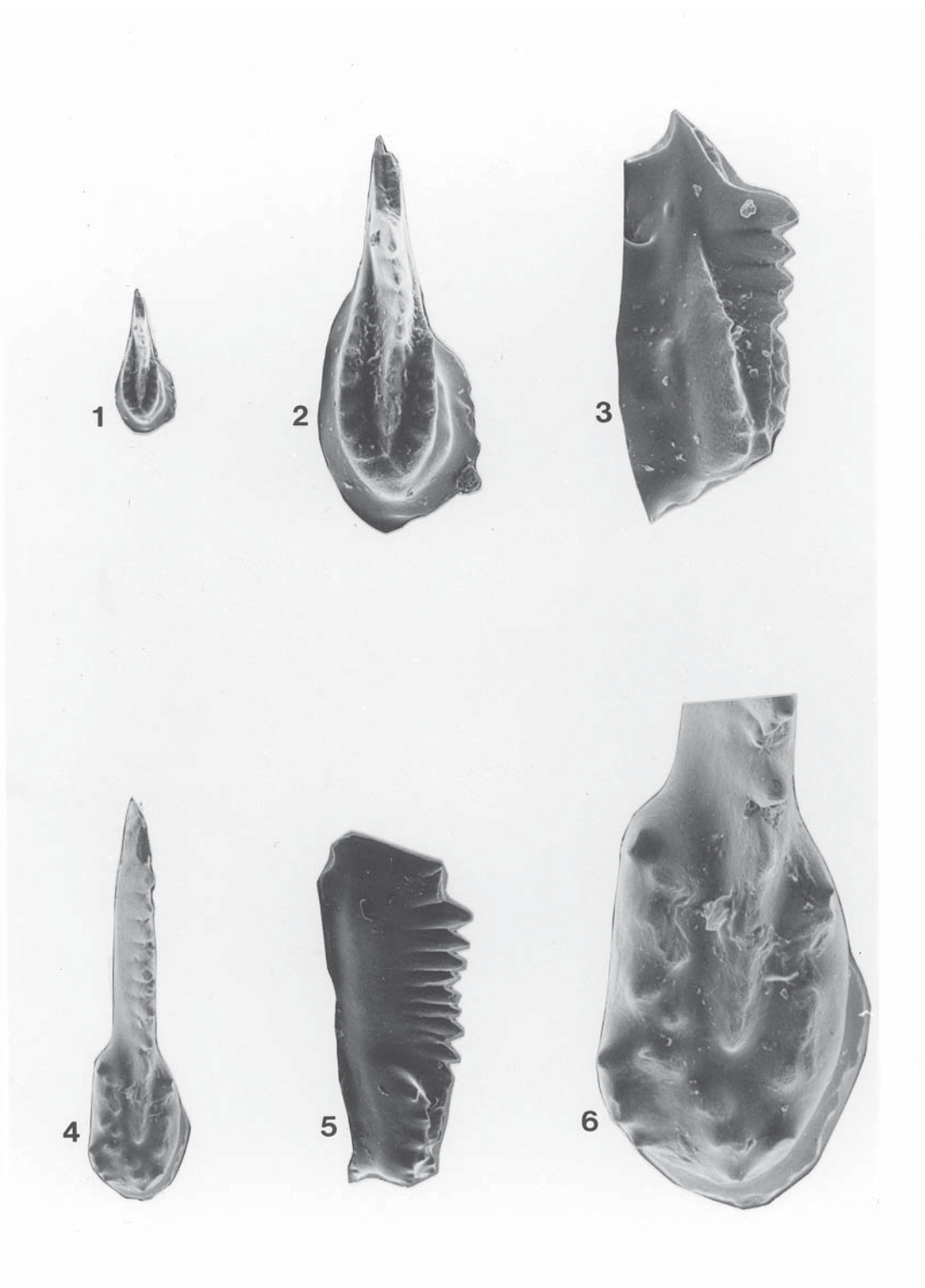
PLATE 31—Conodonts from the Neva Limestone Member of the Grenola Limestone. All views of Pa elements. (1–6) *Streptognathodus denticulatus* Wardlaw, Boardman, and Nestell. 1, upper view, x 75, 2, upper view, x 200, 3, lateral view, x 200, USNM 487612, 4, upper view, x 75, lateral view, x 75, upper view, x 200, USNM 487562, holotype. 1–3, from Neva Limestone Member, Grenola Limestone, sample 6, intersection of US–60 and OK–18 roadcut (Locality 22); 4–6, from Neva Limestone Member, Grenola Limestone, sample 6, intersection of US–60 and OK–18 roadcut (Locality 22).
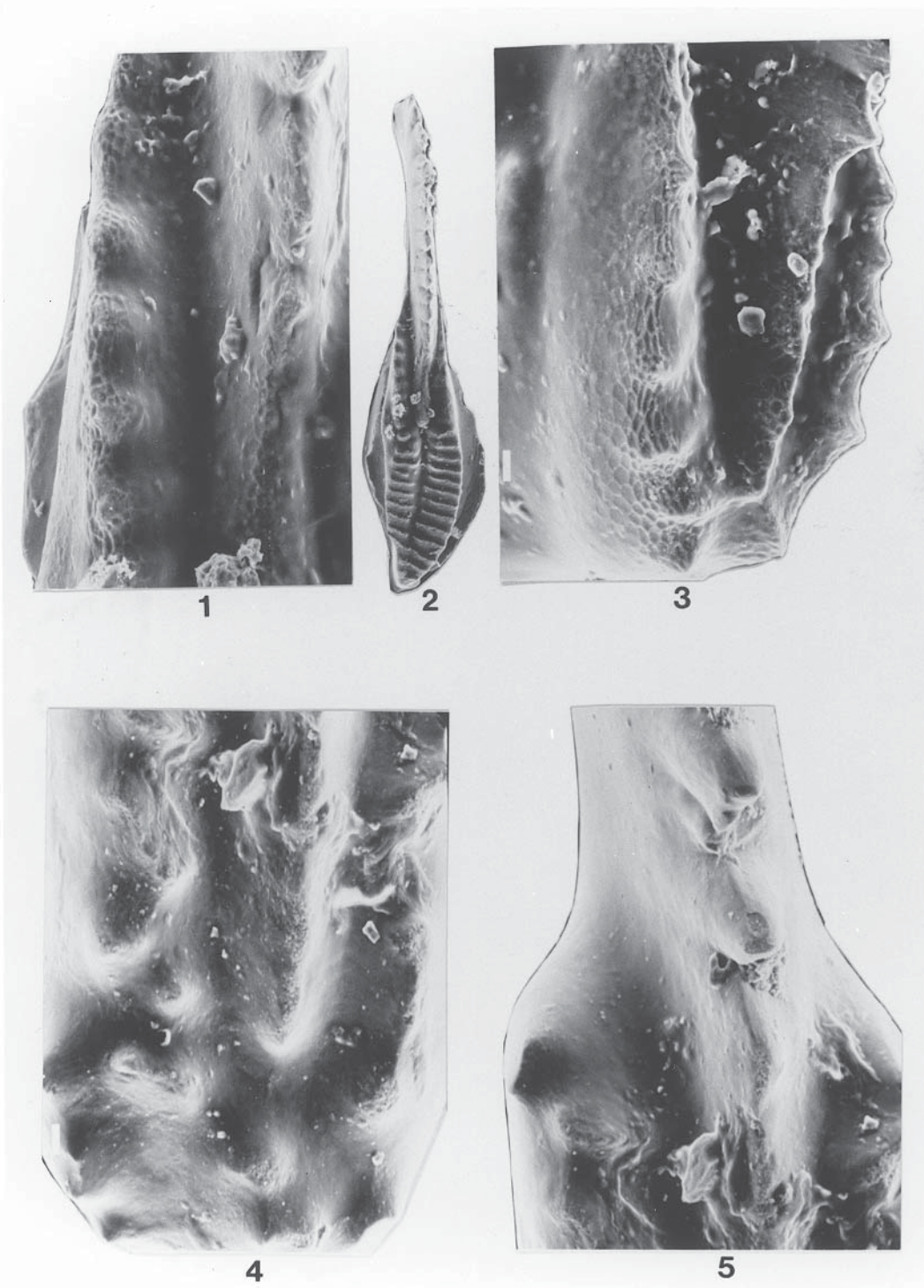
PLATE 32—Conodonts from the Neva Limestone Member of the Grenola Limestone. All views of Pa elements. (1–2) *Streptognathodus nevaensis* Wardlaw, Boardman, and Nestell. 1, upper view, ✕ 470 of inner adcarinal parapet and declination showing micro-reticulation; 2, upper view, ✕ 75 of specimen enlarged in 1, USNM 487613. (3–5) *Streptognathodus denticulatus* Wardlaw, Boardman, and Nestell. 3, oblique lateral view, ✕ 600, showing micro-reticulation on parapet and carina, partly overgrown, of small specimen, USNM 487612. 4–5, upper views, ✕ 600 of posterior part of platform (4) and anterior part of platform (5) showing faint relict micro-reticulation along sides of outside denticles and micro-pustulose ornament of tops of most denticles and carina, USNM 487562. 1–2, from Neva Limestone Member, Grenola Limestone, intersection of US–60 and OK–18 roadcut (Locality 22, A); 3, same specimen as pl. 30, figs. 1–3; 4–5, same specimen as pl. 30, figs. 4–6.

Systematics

This section will deal with the Pa elements of the stratigraphically important species of *Streptognathodus,* briefly review the apparent unreliable species of *Sweetognathus*, and illustrate a rare Pa element of *Diplognathodus*.

Genus *Streptognathodus*

Type Species: *Streptognathodus excelsus* Stauffer and Plummer

Streptognathodus has a fairly typical compliment of gnathodid ramiform elements in a septimembrate (15-element) apparatus. However, we believe from our abundant material, that Wardlaw et al. (1991) were correct in pointing out that the Pa element typically occurs as an asymmetric pair. Commonly, both dextral and sinistral elements have been identified specifically. We avoid this practice and consistently find that there are dextral and sinistral forms, the dextral being slightly more robust and the sinistral being slightly more elongate (more slender), that have the same stratigraphic range, which is our major concern in identifying morphospecies. The posterior carinal termination, the median furrow, and the style of denticulation are similar in both dextral and sinistral forms. The more robust form generally has a few more accessory denticles or develops them slightly earlier in growth (if size is a good proxy for growth) than the slender form. In forms that do not commonly develop accessory nodes, one or two may be present on gerontic examples of the robust form. The ramiform elements of the apparatus are very similar between species. This is not to say they are the same or to support the concept of vicariously shared elements. The elements do differ subtly between species.

Gunnell (1933) described seven species of *Streptognathodus* from the Americus Limestone Member of the Foraker Limestone. Review of the type specimens and analysis of our abundant material from the Americus indicate that there are three species in Gunnell's material from the Americus: an elongate form, a nodose form with a slit-like furrow, and a nodose form with a trough-like furrow anteriorly. The elongate form includes the species *Streptognathodus elongatus* and *S. simplex* of Gunnell (1933), and *S. elongatus* is the senior synonym by page priority and by principle of first reviser (Ellison, 1941). The nodose form with a slit-like furrow includes the species *Streptognathodus walteri*, *S. wabaunsensis*, and *S. acuminatus* of Gunnell (1933) of which *S. walteri* is the senior synonym by page priority, but by principle of first reviser (Ellison, 1941) and for stabilization and universality of usage, *S. wabaunsensis* is the accepted name. The nodose form with a trough-like furrow anteriorly includes the species *Streptognathodus farmeri* and *S. flangulatus,* of which *S. farmeri* is the senior synonym by page priority and so established herein as first re-revisers [Ellison, 1941, placed all nodose forms into *S. wabaunsensis*].

In addition to the three morphotypes discussed above recovered from the Americus Limestone Member, we have also recovered good examples of what we identify as *S. flexuosus*. So, in the Americus Limestone Member the three major lineages of *Streptognathodus* that dominate the latest Carboniferous and earliest Permian are present. These are a lineage of very closely related robust forms that are characterized by no to few accessory nodes (denticles) exemplified by *S. barskovi*, a lineage of moderate to robust forms that are characterized by common accessory nodes (denticles) and lobes exemplified by *S. wabaunsensis* and *S. farmeri*, and a lineage of elongate forms that are characterized by few accessory nodes (denticles) exemplified by *S. elongatus*. All three lineages appear to derive from *Streptognathodus bellus* (figs. 48, 49, 50). The marine record represented by the Kansas section is very interrupted, so reconstructing true clines is difficult. However, we see successive features that strongly imply close affiliation or lineages. Continuous basinal-marine sections like that at Usolka River in the southern Urals, Russia, when better sampled, will better demonstrate true clines. But not to be dismayed, we envision the following species successions to make up the three major lineages in the uppermost Carboniferous and lowermost Permian of Kansas:

1) *S. bellus* → *S. alius* → *S. flexuosus* → *S. conjunctus* → *S. fuchengensis* → *S. nevaensis* → *S. fusus* → *S. barskovi* → *S. robustus*.

2) *S. bellus* → *S. wabaunsensis* and *S. farmeri*, then *S. farmeri* → *S. binodosus* and *S. wabaunsensis* (of Chernykh and Ritter, 1997), then *S. binodosus* → *S. nodulinearis*, *S. invaginatus*, and *S. isolatus,* and *S. wabaunsensis* (of Chernykh and Ritter, 1997) → *S. minacutus*, then *S. nodulinearis* → *S. translinearis* → *S. trimilus* → *S. florensis*.

3) *S. bellus* → *S. elongatus* → *S. postelongatus* and *S. lineatus,* then *S. postelongatus* → *S. constrictus* and *S. longissimus,* and then *S. constrictus* → *S. postconstrictus*.

The forms described from Russia, *Streptognathodus cristellaris, S. latus, S. glenisteri, S. sigmoidalis,* and *S. tulkassensis* are not present in our material. These forms appear very local and possibly endemic to the Uralian region. Chernykh and Reshetkova (1987) established the *Streptognathodus cristellaris* Zone of which the nominal species is not appropriate for international correlation because it is not well known outside the Uralian region. The form identified here as *S. wabaunsensis* (of Chernykh and Ritter, 1997) is clearly the predecessor of *S. minacutus* but does not occur in our material from Kansas; however, it occurs in our material from the Urals and seems also to be an endemic form (see discussion of *S. minacutus* for placement of these forms). A summary diagram of the possible relationships of several of the species, including a few of the endemic Uralian forms is shown in fig. 52. In the previous lineage diagrams (figs. 47–51), marine-dominated units (carbonate hemicycles) are represented by a darkened interval vs. nonmarine-dominated units (siliciclastic hemicycles, generally no *Streptognathodus* species) to show the reader the lack of constraint on the ranges. In one particular case the range of a species is significantly different than that shown in the midcontinent. *Streptognathodus barskovi* clearly appears below the first appearance of *Sweetognathus merrilli* in the Urals (Wardlaw et al., 1999; Chuvashov et al., 2002a, bed 9 vs. bed 11, Kondurovsky Section) and its range is extended down to reflect this (fig. 52).
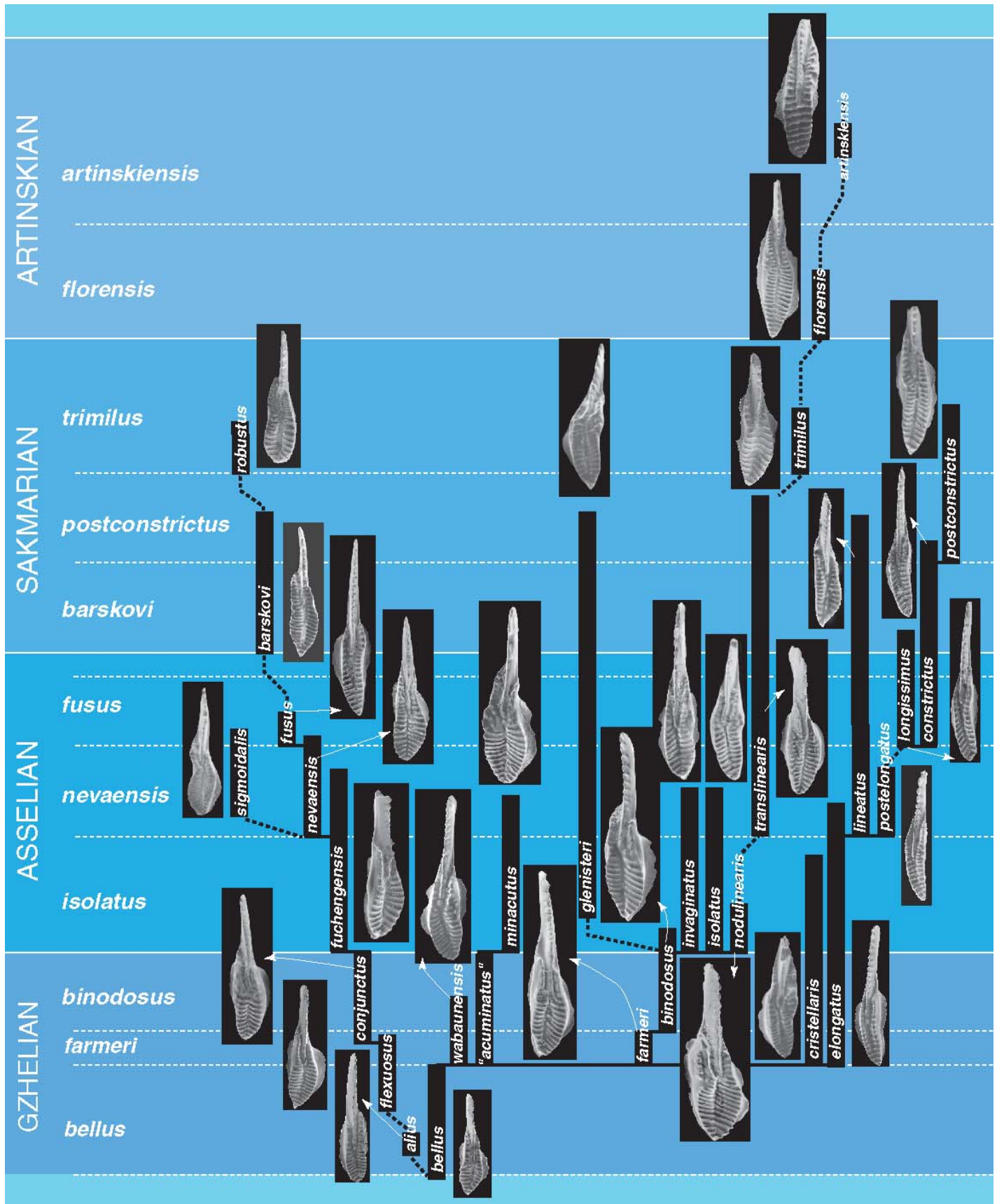
FIGURE 52—Composite range chart for *Streptognathodus* species, southern Urals and midcontinent, upper Gzhelian through lower Artinskian. Ranges in Kansas shown as thick bar; *Streptognathodus cristellaris*, *S.* "*acuminatus*", *S. glenisteri*, and *S. sigmoidalis* have not been recovered in our Kansas material.

The terms for the morphology of *Streptognathodus* are not very standardized. We illustrate (fig. 19) an example of an elongate form, a nodular form, and a robust form with the major features we use pointed out. Other terms that should be discussed include: adcarinal ridge = a completely fused adcarinal parapet; adcarinal groove = smooth groove between carina and parapet, which is basically similar in all our species of *Streptognathodus* and not used here as a identifying character; constriction = any narrowing or pinching of the platform observed from the top side of the element; furrow and groove = longitudinal depressions, furrow for wide depressions (but smaller than a sulcus), groove for narrow depressions; and lobe = any lateral expansion of the platform supported by a lateral process or expansion of the basal cavity, which is common in species of *Idiognathodus* but is not present in any of our species of *Streptognathodus* that do not show an expansion in the basal cavity. Node and denticle have been used interchangeably in the literature and by us, though we prefer denticle.

Streptognathodus alius Akhmetshina

Plate 3, figs. 1–8, 10.
Streptognathodus alius Akhmetshina, 1990, p. 86–87, pl. 1, figs. 9, 10.
Streptognathodus tenuialveus Chernykh and Ritter, 1997 (part), p. 471, fig. 4.13, 4.15, 4.16, 4.18.
Streptognathodus costaeflabellus Chernykh and Ritter, 1997, p. 466, fig. 5.1–5.6.
Streptognathodus longilatus Chernykh and Ritter, 1997 (part), p. 469, fig. 5.15–5.17

Original Diagnosis [abstracted from the original description and comparison]: A species of *Streptognathodus* distinguished by a Pa element with a broad, robust platform similar to *S. barskovi* lacking accessory lobes, but with one to two accessory inner nodes in large specimens, and short anterior parapets.

Amended Diagnosis: A species of *Streptognathodus* characterized by an asymmetric pair of Pa elements, the dextral element robust with a long inner adcarinal parapet that is fused to partly fused, a sinistral element with a nearly straight inner adcarinal parapet ornamented by transverse denticles, one or two accessory denticles on either side (typically more on the inner side in most moderate to large specimens, very large specimens with many accessory denticles), generally wide groove anteriorly that narrows posteriorly, and typically one carinal denticle posterior to the fused carina.

Description—Pa element moderate in length, bowed, widest in posterior platform in dextral elements in most specimens, widest along carina in sinistral elements and very large dextral elements, free blade one-fourth to one-third of the element, denticles on blade partly fused, compressed, posterior denticles of about equal size or in pattern of alternating slightly larger and slightly smaller size for about half the blade length (typically the attached portion, but not always), then increasing in size anteriorly except the anteriormost two, which decrease in size, as blade joins platform becomes fused nodose ridge, generally the denticles decrease in size posteriorly, but variable, except the posteriormost on carina which is larger and less fused, rarely nearly discrete, 0–2 carinal denticles posterior to and well spaced from fused carina in median groove decreasing in size posteriorly,

posterior termination of platform subrounded, commonly as a single transverse denticle, parapets ornamented by transverse ridges posteriorly becoming transverse denticles anteriorly, transverse ridges form a broad oblique angle with each other, angle becoming lesser anteriorly so that opposing transverse ridges nearly form a straight line, ridges become transverse denticles at or near the posterior termination of the fused carinal ridge, inner parapet extends further to the anterior than outer parapet, dextral element with a long inner adcarinal parapet that is fused to partly fused, sinistral element with a nearly straight inner adcarinal parapet ornamented by transverse denticles, outer adcarinal parapet variously fused, denticles generally decreasing in size anteriorly, outer parapet termination sharply declines down fixed blade with one or two denticles (decreasing in size) before becoming a short, narrow, smooth rib along lower side of blade, inner parapet termination declines less sharply than outer and generally bears more denticles on each specimen, one to three, decreasing in size anteriorly, one or two accessory denticles on either side (typically more on the inner side in most moderate to large specimens, very large specimens with many accessory denticles, generally wide groove anteriorly that narrows posteriorly, and typically one carinal denticle posterior to the fused carina, basal cavity moderately flared.

Dextral and sinistral elements differ in that dextral forms are more robust, have a long inner adcarinal parapet that is, at least, partly fused, and sinistral forms have a nearly straight inner adcarinal parapet.

Remarks—*S. alius* is most like its successor, *S. flexuosus,* which it differs from by having a lower inner adcarinal parapet, a subrounded posterior platform termination as opposed to a pointed termination in *S. flexuosus*, and less disparity in the anterior declination of the parapets, the inner extending well beyond the outer in *S. flexuosus*.

Streptognathodus barskovi (Kozur)

Plate 18, figs. 1–5, 7; plate 20, figs 2–3.
Gnathodus barskovi Kozur, 1976, p. 6–7, pl. 3, figs. 2, 4, 6.
Streptognathodus postfusus Chernykh and Reshetkova, 1987, p. 72–73, pl. II, fig. 11–13.
Streptognathodus barskovi (Kozur), Chernykh and Ritter, 1997, p. 463–464, fig. 8.1–8.9.
Streptognathodus constrictus Chernykh and Reshetkova, Chernykh and Ritter, 1997 (part), fig. 8.17.

Original Diagnosis: Carina short; it stops considerably prior to middle [of platform] and consists in its posterior part of smooth rib. Towards direction of free blade, small denticles occur which on free blade become longer and broader towards anterior. Frontmost denticle again shorter. Platform broad and only weakly depressed. It possesses very long narrow ribs partly fused in middle.

Original Diagnosis (*postfusus*): Platform high, from above flattened, elongated, constricted at level of end of median carina, with almost symmetrically located axial groove. Axial carina takes up less than one-fourth of length of platform.

Amended Diagnosis: A species of *Streptognathodus* characterized by an asymmetric platform pair with flared adcarinal parapets and several crude and irregular accessory denticles on the inner side, especially in large specimens.

Description—Pa element moderate in length, bowed, dextral elements (which are robust) widest in middle of posterior platform, sinistral elements widest just posterior to termination of carina, free blade approximately one-third of the length of the element, denticles on blade partly fused, compressed, increasing in size anteriorly except for anteriormost two, which decrease in size, as blade joins platform becomes fused ridge with denticles barely noticeable, carina thinnest and lowest near parapet declination, posteriorly forming a ridge of subequal size, carina extends posteriorly beyond ridge as one small discrete denticle, commonly minute to obscure, posterior termination pointed to rounded, parapets ornamented posteriorly by transverse ridges, anteriorly by denticles, transverse ridges at slight obtuse angle to each other slightly curved anteriorly at median end, outer parapet changing from transverse ridges to transverse denticles over a short space along the posterior termination of the carina, adcarinal parapet variously fused, denticles roughly subequal in size, high, with one or two larger denticles in middle, giving the slight flare to the parapet, anterior declination of the parapet gradual with zero to four denticles on declining parapet before becoming a smooth rib anteriorly, inner parapet changes abruptly from transverse ridges to a double set of align denticles (denticle doublet) or transverse denticles with accessory denticles roughly placed on the lateral side of the platform adjacent to denticle, parapet disrupted at this point and it is not clear that the inner anterior parapet joins either accessory denticle or inner denticle, anterior adcarinal parapet well developed in most specimens except very large ones where several seemingly random denticles are overgrown giving a very hectic pattern, generally two to three doublets or triplets of crudely transversely aligned denticles disrupt the posterior and anterior parapet just posterior or at the posterior termination of the carina, generally anterior adcarinal parapet denticles are partly fused to fused, anterior inner parapet high, slightly flared with one or two larger denticles, or of subequal size, one or two additional accessory denticles may develop on the lateral wall of the platform posterior to the disruptive doublets/triplets, anterior declination of the parapet commonly gradual bearing one to four mostly discrete small denticles decreasing in size anteriorly, groove narrow to moderate variable in length, from extending to the posterior end to short, disrupted by most transverse ridges merging across the platform, generally medianly placed, basal cavity moderately flared.

Dextral and sinistral elements differ in that the dextral elements are robust and the sinistral elements are not, other features are relatively the same except that in very large dextral specimens a very hectic denticulation pattern develops due to overgrowths, which is not common in the sinistral specimens.

Remarks—*S. barskovi* differs from *S. fusus* by having a longer carina, high but less flared inner adcarinal parapet, one to many denticle doublets that disrupt the inner parapet, and the parapet declinations are more unequal, the inner extending further anteriorly than the outer, especially in dextral elements.

The original paradigm for *S. barskovi* was poorly established and illustrated; one of the figured specimens was from Bed 12 of the Ajdaralasi (Aidaralash) section, occurring well below the Permian, where the type is from ammonoid matrix from the Tabantal River, well above the base of the Permian. Hence, almost every morphologic form we are identifying as part of

the robust lineage has been placed in *S. barskovi*, typically in range charts and not illustrated, which confuses the true range of the morphospecies. Recently, Kozur rephotographed the type specimen (personal communication, 1997) and Chernykh and Ritter (1997) illustrated several topotypes clarifying the true nature of *S. barskovi* showing it to be the same as *S. postfusus*, sending that species into synonymy.

Streptognathodus bellus Chernykh and Ritter

Plate 2, figs. 1, 11; plate 3, fig. 9.
Streptognathodus bellus Chernykh and Ritter, 1997 (part), p. 464, fig. 4.1–4.8, 4.10; *non* fig. 4.9 (=*S. binodosus*).
Streptognathodus tenuialveus Chernykh and Ritter, 1997 (part), p. 471, fig. 4.11, 4.14.

Original Diagnosis: Pa element slightly asymmetrical with shallow V-shaped trough and relatively long transverse ridges.

Amended Diagnosis: A species of *Streptognathodus* characterized by a relatively robust Pa element with prominent transverse ridges for most of the length of the platform, extending nearly to anterior end of parapet, transverse ridges at angle to each other from each side with at least one pair forming a crisscross pattern, especially posteriorly, generally a laterally placed groove, and a carina that extends posteriorly as one to three discrete denticles.

Description—Pa element of moderate length, relatively robust (wide), widest just posterior to carina termination, in posterior one-fourth of the platform, platform straight anteriorly with marked inward bend in posterior third of element, free blade one-fourth to one-third of element, denticles on blade partly fused, compressed, increasing in size anteriorly except anteriormost one or two, as blade joins platform becomes fused ridge, with denticles partially expressed as undulations in ridge and as fused denticles, carina becomes one to three discrete denticles posteriorly, extends two-thirds to three-quarters of the platform length when measured against the inner (longer) parapet, posterior termination of platform pointed to slightly rounded, parapets ornamented by transverse ridges, becoming denticles only for the anteriormost few on either parapet, transverse ridges at angle to each other from each side, slight for anterior part of parapet and becoming pronounced posteriorly, with at least one pair of transverse ridges forming a crisscross pattern, especially posteriorly, apparently truncating the end of an opposing ridge, inner parapet extends further to the anterior than outer parapet, both parapets terminate by declining gradually down the fixed blade, the declining portion of the parapet ornamented by denticles as opposed to transverse ridges elsewhere along the parapet, median groove generally latterly placed, toward outer side, generally shallow, moderate to narrow in size just posterior to posterior termination of carina but becoming slightly to very disrupted by crisscrossing or truncating ridges posteriorly, extends for a variable length posteriorly, from the posterior termination to several ridges anterior to the termination, basal cavity flared. One or more accessory denticles occur on some large specimens on either the outer or inner margin at or near the posterior termination of the fused carina.

Dextral and sinistral elements are similar, sinistral elements tend to have a better developed and more centrally placed groove, and a tendency to have an accessory denticle on the outer margin

whereas dextral elements tend to have an accessory denticle on the inner margin on large specimens.

Remarks—This species appears to be the root stock for most of the *Streptognathodus* species of the Carboniferous–Permian boundary. It is easily distinguished from the less robust species *S. elongianus* and *S. brownvillensis* by its transverse ridges extending for most of the platform and crisscrossing. It appears transitional between the two mentioned species in the character of the posterior carina, extending further on to the platform than *S. elongianus* but not as far as *S. brownvillensis*.

Streptognathodus binodosus Wardlaw, Boardman, and Nestell

Plate 10, figs. 2–6, 8–11; plate 11, figs. 1, 3–5, 7, 10, 12; plate 13, fig. 3; plate 19, figs. 9, 11.
Streptognathodus binodosus Wardlaw, Boardman and Nestell, *this volume*, Part A, pl. 1, fig. 1.
Streptognathodus bellus Chernykh and Ritter, 1997 (part), p. 464, fig. 4.9.

Diagnosis: A species of *Streptognathodus* characterized by a Pa element that has at least one pair of denticles in a transverse row on the inner side immediately posterior to the posterior termination of the carina.

Description—Pa element moderate to long, widest in posterior one-fourth of element, near middle of platform, somewhat elongate, platform bowed, free blade makes up one-third to nearly one-half of the element, denticles on blade partly fused, compressed, increasing in size anteriorly except anteriormost one or two, as blade joins platform denticles become fused, typically as fused nodose carina, rarely anterior part of carina completely fused, posteriormost denticle on fused carina more discrete, no or one denticle in groove posterior to fused carina, posterior termination slightly curved toward outer side in dextral forms and inner side in sinistral forms nearly aligning with a pair of denticles or transverse ridge to form a 'J', posterior termination of platform pointed, but not acutely, typically termination with a single denticle, parapets ornamented by transverse ridges posteriorly becoming denticles anteriorly in back of posterior termination of carina, transverse ridges forming a broad oblique angle with each other near posterior end, angle becoming lesser anteriorly so that opposing transverse ridges nearly form a straight line, high parapets terminate at about the same point anteriorly where inner parapet sharply declines as denticulate rib, the outer parapet declines more sharply or terminates and is smooth, median groove generally deep anteriorly becoming well-expressed narrow groove posteriorly, rarely do one or two transverse ridges merge and cross the groove, groove is laterally placed toward inner side generally extends to posteriormost denticle, but not always, basal cavity flared.

Dextral and sinistral elements differ in that the 'J' pattern of the carinal extension to the parapet is on the outer side in dextral forms and on the inner side in sinistral forms.

Holotype: USNM 484061, pl. 10, fig. 6.

Remarks—The specimen illustrated (pl. 10, fig. 10) is transitional to *S. nodulinearis* from the upper Hughes Creek Shale Member, strongly suggesting that *S. binodosus* gave rise to *S. nodulinearis* and that this may occur slightly before level 7 as

it may also occur in the Urals of Russia. The deep anterior groove and 'J' pattern of the carinal extension to the parapet suggest that *S. binodosus* derived from *S. farmeri* but differs in aligned accessory nodes forming denticle pairs.

Streptognathodus brownvillensis Ritter

Plate 2, figs. 2–7; plate 4, fig. 3.
Streptognathodus brownvillensis Ritter, 1994, p. 873, fig. 3.1–3.17.

Original Diagnosis: The Pa element possesses a long carina that grades from an adenticulate ridge anteriorly to a row of discrete nodes posteriorly, and numerous transverse ridges that correspond in position to the carinal nodes.

Amended Diagnosis: A species of *Streptognathodus* characterized by a Pa element that is slightly sigmoidal in outline especially expressed by the carina, carina extends for most of the platform, anteriorly as a fused ridge, posteriorly as discrete denticles decreasing in size posteriorly, inner parapet flares slightly anteriorly with one to three denticles of increased size, inner parapet extends anteriorly slightly further than outer parapet.

Description—Pa element short to moderate in length, upper platform surface widest near or just posterior to fused carina termination, slightly sigmoidal in outline, especially shown by subtle inflections or curves in the carina, free blade approximately one-third of element, denticles on blade partly fused, compressed, increasing in size anteriorly except anteriormost one or two, as blade joins platform becomes fused ridge, with denticles barely expressed, variable, generally one nearly discrete denticle at posterior end of ridge, carina becoming a series of well-spaced denticles decreasing in size posteriorly, fused carina approximately half the platform length when measured against the inner (longer) parapet, denticles extending nearly to posterior end of platform, disappearing for last two to three lateral ridges or merging with inner ridges, rarely remaining partially discrete, posterior termination of platform slightly rounded to pointed, parapets ornamented by transverse ridges posteriorly, becoming denticles anteriorly near posterior termination of fused carina, transverse ridges at slightly greater than 90° angle to median line forming a broad oblique angle with each other toward the posterior near posterior end, angle becoming greater anteriorly so that opposing transverse ridges nearly form a straight line, inner parapet extends further to the anterior than outer parapet, typically with one to three denticles of increased size near anterior termination, forming a slight lateral flare in the inner parapet, outer parapet anterior termination gradually declining down fixed blade, denticles partially fused (more so than inner denticles), inner parapet termination abruptly declining down fixed blade, median groove of moderate width, roughly centrally placed, generally extends to the last one or two posterior denticles, basal cavity greatly flared.

Dextral and sinistral elements are very similar, sinistral elements with more rounded posterior termination, slightly less wide, and more equal inner and outer parapet anterior terminations than dextral elements.

Remarks—Ritter (1994) did not compare *S. brownvillensis* with the species it is most like *S. ruzhencevi* or *S. firmus*, both have long posterior carinal extensions. *S. brownvillensis* differs

in its sigmoidal outline and its flared inner parapet; it differs from *S. ruzhencevi* in that its carinal denticles do not merge with the parapet denticles or ridges. Ritter (1994) pointed out that in *S. brownvillensis* the carinal denticles are aligned with the parapet ridges and stressed this as a diagnostic feature. We find this to be the case with all forms with long carinal extensions and not particularly diagnostic.

Streptognathodus conjunctus Barskov, Isakova, and Shchastlivceva

Plate 8, figs. 2–4, 8–11; plate 9, figs. 1–2, 8, 11–12; plate 10, figs. 1, 7; plate 11, figs. 2, 6.
Streptognathodus conjunctus Barskov, Isakova, and Shchastliv-ceva, 1981, p. 86–87, pl. II, figs. 1–5.
Streptognathodus tenuialveus Chernykh and Ritter, 1997 (part), p. 471, fig. 4.12, 4.17.

Original Diagnosis: Platform with asymmetrically located axial groove of 'V'-shaped cross section. Axial carina takes up less than one-third of length of platform and ends usually with large node, which joins with transverse ribs of one or both parapets, and in this way forms continuous transverse rib over whole platform. Posterior part of axial groove flattens out, and in this part has one to three transverse ribs which pass through groove uninterrupted. Accessory lobes absent.

Amended Diagnosis: A species of *Streptognathodus* characterized by a Pa element that has reduced and partly fused denticles on the parapet adjacent to the carina and a variably disrupted groove posterior to the posterior termination of the carina commonly disrupted by a transverse ridge extending into or merging across the groove.

Description—Pa element moderate in length, widest near middle of platform, about two-thirds the length of the element from anterior, platform slightly bowed to nearly straight, free blade approximately one-third of the element, denticles on blade partly fused, compressed, roughly increasing in size anteriorly with one or two small denticles on posterior part of the blade breaking the succession, as blade joins platform becomes a fused nodose ridge, posteriormost node on fused carina more discrete, generally one or two discrete denticles posterior to end of fused carina, the posterior termination of the platform is rounded to slightly pointed, generally with a single denticle, parapet ornamented by transverse ridges gradually becoming denticles anteriorly along carina by shortening of the ridges, the ridges/denticles adjacent to the carina are reduced (low) and partly fused appearing smoothed compared to those to the anterior and posterior, typically with one to six accessory denticles on the inner side, partly fused and commonly partly merging with denticles of the parapet forming irregular patterns, rarely one denticle may form on the inner side of the element, the transverse ridges form a nearly straight line anteriorly, just posterior to the carina and form a slight oblique angle near the posterior, many of the transverse ridges merge across or extend into the groove commonly as small denticles, inner parapet extends slightly further anteriorly than outer parapet, the outer parapet declines sharply down the attached blade whereas the inner declines a little less sharply, both have denticles variously developed along the anterior declinations, the outer parapet with fewer, typically smaller denticles, and may even be smooth, the inner parapet

with common denticles, generally decreasing is size anteriorly and the anteriormost part may be smooth, median groove roughly centrally placed but irregular and commonly disrupted, generally shallow and narrow, the basal cavity is only slightly flared.

Dextral and sinistral elements are very similar.

Remarks—This species is very variable but in that variability is its distinctiveness. It appears to be a distinct member of the robust "*barskovi*" morphocline, but is the least robust of that lineage. It differs from *Idiognathodus*, which it mimics, by its irregular groove that is present for most of the platform in some specimens.

Streptognathodus constrictus Reshetkova and Chernykh

Plate 17, figs. 2, 10; plate 18, fig. 6; plate 20, fig. 6; plate 21, figs. 12, 15.
Streptognathodus constrictus Reshetkova and Chernykh, 1986, p. 111, pl. 1, figs. И, К, Л, М, Н, О, П, Р.

Original Diagnosis [abstracted from original description and comparison]: A species of *Streptognathodus* distinguished by a Pa element with a distinct constriction in the middle part of the platform, deep flaps formed by the anterior parapets, and a symmetric position of the axial furrow.

Amended Diagnosis: A species of *Streptognathodus* characterized by a Pa element with a narrow elongate platform that is bowed, with a marked inflection on the inner side of the platform opposite the posterior end of the carina and a slightly flared anterior inner parapet so that the inflection and flared parapet form a "constriction" in the platform.

Description—Pa element moderate in length, elongate, narrow, upper surface widest on posterior one-fourth, platform bowed with a marked inflection on the inner side of the platform positioned opposite the posterior end of the carina, free blade one-half to one-fourth the length of the element, denticles on blade partly fused increasing in size anteriorly, except for anteriormost which is smaller, as blade joins platform becomes a fused ridge, with denticles barely expressed, carina continuing posteriorly beyond fused ridge as one or two very small discrete denticles, posterior platform termination pointed as a single transverse denticle, parapet ornamented by transverse ridges at a slightly obtuse angle, nearly straight in dextral elements, transverse ridges gradually becoming denticles anteriorly along the carina, inner parapet extends slightly further anteriorly, both parapets slightly flared along carina, higher and more flared in dextral elements, inner parapet with a sharp partial anterior declination that may bear a few denticles decreasing in size anteriorly then becoming a smooth rib that declines gradually along the attached blade, outer anterior declination relatively sharp, generally smooth or bearing one denticle, extending anteriorly as a short smooth rib, median groove narrow and extends nearly to posterior end with one to four of the posterior ridges merging across the platform closing off the groove from the posterior end, basal cavity moderately flared.

The dextral and sinistral elements vary as mentioned above in that the dextral element has a more flared and higher adcarinal parapet than the sinistral element and the transverse ridges are nearly straight in alignment.

Remarks—*S. constrictus* is most like *S. longissimus* but differs in its shorter platform, flared inner adcarinal parapet, and aligned transverse ridges.

Streptognathodus denticulatus **Wardlaw, Boardman, and Nestell**

Plate 25, fig. 20; plate 31, figs. 1–6; plate 32, figs. 3–5.
Streptognathodus denticulatus Wardlaw, Boardman, and Nestell, *this volume*, Part A, pl. 1, fig. 2.

Diagnosis: A species of *Streptognathodus* characterized by a Pa element with a short posterior platform ornamented by numerous denticles and a long free blade with the largest denticle the anteriormost.

Description—Pa element long, widest in middle of posterior platform, platform short, free blade makes up two-thirds of the element, denticles on blade with three compressed, smaller denticles in middle of blade breaking pattern of decreasing size posteriorly, anteriormost denticle is the largest, as blade joins platform becomes nodose fused ridge, nodes and carina decreasing in size posteriorly, in large specimens carina extends for two-thirds length of short platform, posterior carinal termination is abrupt, posterior platform termination is very rounded, in small specimens two lateral parapets are ornamented by partly fused transverse denticles partially ornamented by reticulate micro-ornamentation, partially overgrown, large specimens are completely overgrown with little reticulate micro-ornamentation remaining, only traces on the sides of outside denticles, larger specimens develop a micro-pustulose ornament on top of each denticle and along the crest of the carina, anterior declination of the parapets abrupt, declining a short distance and narrowing rapidly over a short distance to disappear anteriorly, secondary denticles added in a haphazard fashion all around the posterior platform outside the initial denticles on the lateral parapets, adcarinal grooves become infilled and parapets become overgrown to become indistinct with growth, a short groove or furrow in small specimens divides the lateral parapets as a short gap in back of the carina, becomes overgrown and filled in with secondary denticles in larger specimens so that no median groove is present, moderately flared basal cavity with consistent posterior flare forming a lip at the bottom of the element throughout growth.

Dextral and sinistral elements appear to be very similar.

Holotype: USNM 487562, pl. 25, fig. 20, pl. 31, figs. 4–6, pl. 32, figs. 4–5.

Remarks—This species represents a rare morphotype that we can demonstrate a growth sequence for so we feel qualifies it for specific identification. It is only known from the Neva Limestone Member in our material. It shows reticulate micro-ornament in small specimens and relict reticulate micro-ornament in large specimens. Reticulate micro-ornament is common to well-preserved specimens of *Streptognathodus* (see plate 31, figs. 1–2, *Streptognathodus nevaensis*, for an example) and not known in *Sweetognathus,* confirming that this rare morphotype belongs to *Streptognathodus*. The presence of a long blade is also common to *Streptognathodus* and not known in *Sweetognathus*. No species in our Kansas material is similar to this short platformed denticulate form.

Streptognathodus elongatus **Gunnell**

Plate 5, fig. 8; plate 6, figs. 5–7; plate 9, figs. 5, 7, 9–10; plate 11, figs. 8–9, 11; plate 13, fig. 7.
Streptognathodus elongatus Gunnell, 1933, p. 283–284, pl. 33, fig. 30.
Streptognathodus simplex Gunnell, 1933, p. 285e–286, pl. 33, fig. 40.

Original Diagnosis [*S. elongatus*]: Plate gently curving toward left side [a sinistral element]. Length to width ratio of plate oral surface 4 to 1. Median groove on oral surface increasing gradually in strength from anterior [posterior] extremity to posterior [anterior] end of plate on either side of which occur nodes or transverse ridges, and in which occur few small nodes in anterior [posterior] half with nodose carinal ridge occurring in posterior [anterior] one-third of groove total length. Oral surface to left, lobate portion of plate bearing few nodes. Sides of plate bearing flanges on basal portion. Anterior [posterior] end blunt.

[*S. simplex*]: Oral surface 'V'-shape in cross section. Sides on longitudinal groove on oral surface anterior to carinal ridge bearing transverse ridges. Oral margins opposite sides of carinal ridge bearing nodes of which front nodes on left side almost form ridges. Carinal ridge on posterior five-elevenths of plate total length. Sides of plate vertical with flanges on basal portion.

The absence of nodes in the median groove of the oral surface distinguishes this species from *S. elongatus*.

Amended Diagnosis: A species of *Streptognathodus* characterized by an elongate platform with a short carina with one or two posterior denticles less fused or discrete and larger than those on the carina, a relatively large anterior denticle on the parapet, a well-developed narrow groove that is deep anteriorly, and strong asymmetry in the anteriormost parapets.

Description—Pa element short to moderate in length, narrow, elongate, and inwardly bowed, free blade approximately one-fourth of the element, fixed blade relatively long, denticles on blade partly fused, compressed, increasing is size anteriorly except anteriormost one, as blade joins platform becomes fused ridge, with denticles barely expressed, fused carina rising posteriorly with last fused denticle slightly less fused and the largest on the carina, generally followed posteriorly by one discrete denticle nearly as large, rarely carina continuing as one or two discrete denticles rapidly decreasing in size, posterior termination of platform generally bluntly pointed, parapets ornamented by transverse ridges becoming denticles anteriorly at the posterior termination of the fused carinal ridge, transverse ridges nearly in straight alignment anteriorly corresponding to bowing of the element, forming a slight oblique angle to each other near posterior, denticles along fused carina decrease and then increase in size, most pronounced on the inner side which is less fused, anterior parapet terminations close to each other on sinistral elements, inner parapet extending anteriorly further in dextral elements, inner parapet on sinistral elements declines down sides of fixed blade sharply with one or two denticles, decreasing in size anteriorly, becoming a smooth rib anteriorly, outer parapet on sinistral element declines less sharply and rarely bears denticles, being a smooth rib to its anterior termination, inner parapet on dextral forms declines anteriorly along fixed

blade less sharply than sinistral elements and bears several denticles decreasing in size anteriorly, becoming a smooth rib only for its most anterior part, outer parapet anteriorly declines sharply typically bearing one denticle, becoming a smooth rib for most of its anterior part, groove well developed, anteriorly narrow and deep, extending posteriorly, generally to the posteriormost two transverse ridges which roughly merge, rarely up to five posteriormost ridges roughly merge, the groove commonly slightly to the inward side of the median, one or two accessory denticles occur on large specimens situated well on the slope of the lateral side of the element, basal cavity moderately flared.

Dextral and sinistral elements are dissimilar in the anterior parapet declination and terminations mentioned above.

Remarks—Elongate forms throughout the uppermost Carboniferous and Lower Permian have been ascribed to *S. elongatus* and its junior synonym *S. simplex*, but all differ in denticulation and adcarinal parapets. *S. elongatus* has few accessory denticles and low adcarinal parapets, *S. postelongatus* has several denticle doublets as does *S. lineatus* which has a long carina extension among other features, *S. constrictus* and *S. postconstrictus* have flared inner adcarinal parapets, and *S. longissimus* is very long with short adcarinal parapets.

Streptognathodus elongianus Wardlaw, Boardman, and Nestell

Plate 2, figs. 8–9.
Streptognathodus elongianus Wardlaw, Boardman, and Nestell, this volume, Part A, pl. 1, fig. 3.

Diagnosis: A species of *Streptognathodus* characterized by an elongate Pa element with relatively high fused to partially fused parapets and carina in the middle of the element, irregular transverse ridges, an irregular median furrow, and the carina extends for less than half of the platform with generally only one discrete posterior denticle.

Description—Pa element moderate to long, narrow and elongate, upper surface slightly wider just posterior to carinal termination, platform is relatively straight with a slight curve inward toward posterior end and a slight constriction in width at the posterior end of the fused carina and parapets, free blade approximately one-fourth of element, denticles on blade compressed and partly fused, increasing in size anteriorly except anteriormost one or two, as blade joins platform becomes fused ridge, with denticles barely expressed, carina has one isolated denticle posterior to fused ridge, generally situated close to outer transverse ridge and nearly merging with it, carina extends for about one-half of the platform length when measured against the inner (longer) parapet, posterior termination of platform pointed, parapets ornamented by transverse ridges posteriorly, forming a partially nodose fused ridge in middle portion of element adjacent to fused carina with two or more relatively more discrete nodules anterior to highly fused portion, inner transverse ridges nearly perpendicular to median line of element, except for posteriormost one or two, outer transverse ridges at slight oblique angle to median line, one or two transverse ridges on either side of platform generally at angle to general plan or spaced closer to neighboring ridge and even partially merging with it to form diagnostic irregular ridge ornament, transverse ridges of

irregular size, varying in length and size adding to the irregular ornamentation, inner parapet extends further to the anterior than outer parapet, both parapets gradually decline down fixed blade, median groove narrow, deep, roughly centrally placed, and very irregular, partially disrupted by irregular transverse ridges, generally still expressed as a narrow slit between the posterior-most few transverse ridges, ends at terminal posterior transverse denticle, basal cavity flared.

Dextral and sinistral elements are very similar; sinistral elements with more equal inner and outer anterior parapet terminations than dextral elements.

Holotype—USNM 483981, pl. 2, fig. 8.

Remarks—This species is easily recognizable from other forms that occur with it in the Brownville Limestone Member by its narrow, elongate shape, fused parapets, relatively deep and irregular groove, and lack of many posterior carinal denticles.

Streptognathodus farmeri Gunnell

Plate 6, figs. 1, 3–4; plate 7, figs. 3–4, 6–7; plate 9, fig. 3.
Streptognathodus farmeri Gunnell, 1933, p. 285c, pl. 33, fig. 34
Streptognathodus flangulatus Gunnell, 1933, p. 285d, p. 33, fig. 35.

Original Diagnosis [*S. farmeri*]: Length to width ratio plate 13 to 5. Median groove on oral surface biconvex in outline anterior [posterior] to anterior [posterior] extremity of carinal ridge. Carinal ridge occupying posterior [anterior] one-third of total length of median groove. About nine transverse ridges on oral surface of plate each side of biconvex portion of median groove. To right of carinal ridge occur single row of nodes and ridge; nodes on left postero-lateral [anterolateral] area of oral surface. Flange largest on right basal side of plate.

[*S. flangulatus*]: Oral surface of plate with row of 10 transverse ridges on right side, and eight transverse ridges on left side of narrow, deep, median groove anterior [posterior] to anterior [posterior] extremity of nodose carinal ridge; opposite each side of carinal ridge occurs longitudinal ridge posterior [anterior] to small nodose areas. Right postero-lateral [antero-] side of plate bearing large basal flange; upper margin with three nodes. Outline of oral surface serrate.

The larger basal flange on the right side of the plate distinguishes this species from *S. farmeri* [a feature of growth within the same species].

Amended Diagnosis: A species of *Streptognathodus* characterized by a Pa element with common accessory nodes, a deep groove anteriorly, and the carina posteriorly aligning or merging with an outer transverse ridge or line of nodes.

Description—Pa element moderate to long, widest near the posterior carinal termination, free blade one-third of the element, denticles on the blade partly fused, compressed, increasing in size anteriorly except anteriormost, as blade joins platform becomes a fused ridge, with denticles barely expressed especially on the posteriormost part of the fixed blade and the anteriormost part of the carina, denticles becoming progressively (though slightly) more discrete posteriorly, typically largest denticle on the carina is near the posterior end of the fused ridge and is the denticle anterior to the marked carinal inflection and joining with the outer parapet ornamentation, posterior termination of platform rounded, parapets ornamented by transverse ridges

posteriorly, becoming denticles near posterior carinal termination, transverse ridges generally at a large obtuse angle to each other, especially posteriorly, generally the transverse ridges break up into at least one double set of denticles on one or both sides near the carinal termination, denticles on parapets partly fused to fused adjacent to the carina, generally forming a nodose to smooth ridge for some portion of the length of the carina, roughly adcarinal denticles or ridge decreasing in size anteriorly except anteriormost before parapet declination which is larger, both parapets decline sharply, at about the same point, the inner high parapet extending slightly to noticeable anterior to the outer parapet before declination, inner parapet extends further anteriorly then outer parapet and bears more denticles before becoming an anteriorly smooth rib, number of denticles anterior to declination variable, from one to five on the inner side, zero to four on outer side, one to several accessory denticles developed on inner side along adcarinal parapet and just posterior to carinal termination, number of accessory denticles generally increases with size of specimen, one or two small accessory denticles develop on large specimens on outer side, well down the side of the element, median groove deep, narrow, and 'U'-shaped anteriorly becoming obscure posteriorly, slightly laterally placed to the inner side, extends a variable length to the posterior, irregular, generally at least one to several transverse ridges extend into the groove or break up to form one or two isolated denticles in the groove or merge with an opposing ridge across the groove, more common in posteriormost part of the platform, basal cavity greatly flared to outer side [the right side of sinistral elements (types) if the anterior is taken as the posterior as Gunnell (1933) did].

Dextral and sinistral elements are very similar.

Remarks—This species is very discernable by the carina merging with the lateral parapet ornamentation. No immediately previous species show this feature. Most immediately following species do show a variation of this feature clearly indicating that *S. farmeri* **not** *S. wabaunsensis* gave rise to most of the rapid radiation of late Carboniferous–Early Permian morphotypes.

Streptognathodus flexuosus Chernykh and Ritter
Plate 4, figs. 1, 2, 4–11; plate 6, figs. 2, 8; plate 8, fig. 1.
Streptognathodus flexuosus Chernykh and Ritter, 1997, p. 466, fig. 5.7–5.12.
Streptognathodus longilatus Chernykh and Ritter, 1997 (part), p. 469, fig. 5.13, 5.14, 5.18.
Streptognathodus n. sp. A Chernykh and Ritter, 1997, p. 473, fig. 7.1, 7.2.

Original Diagnosis (*S. flexuosus*): Pa element with short carina and distinct inward and downward flexure of the posterior part of the platform. Symmetrical trough deep and narrow anteriorly, but shallow and more open posteriorly. Margins of equal height in anterior one-fourth of post-carinal platform, but in posterior one-fourth, outer margin is distinctly higher than inner margin.

(*S. longilatus)*: Unornamented streptognathodid with long adcarinal ridges and relatively broad platform bearing distinct constriction in anterior one-third.

Amended Diagnosis: A species of *Streptognathodus* characterized by an asymmetrical pair of Pa elements with the

dextral element robust and the sinistral element elongate to robust, both with a short fused carina, and a platform posteriorly ornamented by nearly aligned transverse ridges, the dextral element has a long and high inner adcarinal parapet, extending anteriorly further than the outer parapet, a posterior platform termination that is pointed, and the sinistral element has inner and outer adcarinal parapets of nearly equal length, but the inner parapet is higher than the outer, and a posterior platform termination that is rounded to pointed.

Description—Pa element moderate in length, in asymmetrical pairs with a robust dextral element and an elongate to robust sinistral element, dextral element widest near middle of posterior platform, sinistral element widest in middle of posterior platform (for robust forms) and near fused carina posterior termination in elongate forms, dextral forms subtly sigmoidal with carina having a slight inflection and curving to the outside while platform is bowed, curving to the inside, sinistral forms are just bowed, free blade approximately one-third of the element, denticles on the blade increasing in size anteriorly, except anteriormost one to six denticles, which are smaller on the sharply declining anterior end of the blade, partly fused, compressed, becoming less fused anteriorly, as blade joins platform becomes fused, nodose ridge, fused carina short, generally with one small fused denticle near the anterior declination of the outer parapet, increasing in size posteriorly to middle of fused carina, then decreasing in size posteriorly, typically one well-developed, discrete denticle is present posterior to the fused carina, though in rare forms it is partly fused to the fused carina, a variable amount of small denticles continue posteriorly, 0–8, posterior termination of platform sharply pointed in dextral forms, rounded in sinistral forms, parapets ornamented by transverse ridges posteriorly, becoming transverse denticles at the posterior termination of the fused carina, transverse ridges at slightly greater than 90° to the median line forming a broad oblique angle with each other near the posterior end, angle becoming less anteriorly so that opposing transverse ridges nearly form a straight line, one to many irregular interridge ridges in many large specimens, rarely many (see pl. 3, fig. 7), posteriormost one to three ridges merging across median, one or two additional ridges merging across median, variously placed on platform, outer high parapet short, declining sharply down blade at or just anterior to inflection in carina on dextral forms, at or near the anterior end of the carina in sinistral forms, generally ornamented by three to four transverse denticles decreasing in size anteriorly, rarely (pl. 3, fig. 7) transition from ridge to denticle may show up as a split ridge into two denticles, denticle variously fused, one to two small denticles on declining parapet before becoming a smooth short rib along lower part of the blade, inner parapet generally extends further anteriorly than the fused carina, just anterior to fused carina on sinistral forms and further on the blade on dextral forms, the high portion of the inner parapet typically remains nearly as high as the carina, declines sharply toward anterior down the blade, but is more gradual than outer declination and bears more denticles, decreasing in size anteriorly, denticles on high carina, generally decrease in size anteriorly, less fused than outer parapet denticles and more numerous, generally about seven denticles before anterior declination, rarely a small denticle toward median just

posterior to posterior well-developed discrete denticle of the carina (see pl. 3, figs. 7, 9) and first transverse denticle anterior to it may be split into two denticles (pl. 3, fig. 7), anterior declination of the inner parapet relatively sharp generally bearing one to four denticles before becoming a smooth rib along lower part of blade, extending a short distance to the anterior, accessory denticles develop along the lateral walls of the element on some large specimens, one to two on either side, near the posterior termination of the fused carina, median groove typically well developed anteriorly for a variable distance becoming a narrow slit posteriorly, extending to last three to four posterior ridges which merge and terminate the groove, moderately flared basal cavity to the outer side.

Dextral and sinistral elements differ in that dextral elements are more robust, posteriorly pointed, have more disparity in lengths between the inner and outer parapets, and appear sigmoidal in shape because of an inflection in the carina where sinistral forms appear just bowed.

Remarks—Essentially, Chernykh and Ritter (1997) described sinistral (*flexuosus*) and dextral elements (*longilatus*) as separate species. Chernykh and Ritter (1997) further confused two separate dextral morphotypes, those to *S. alius* and *S. flexuosus*, in their paradigm for *longilatus*. They also confused the locality for the holotype listing it as bed 15–1 at Usolka in the description but list it as bed 16–1 in the figure caption. Our notes from reviewing material from Usolka in 1991 suggest that this species first appears in bed 15–1, and that that is the probable type stratum. The holotype of *longilatus* is the dextral morphotype of *flexuosus*. *S. flexuosus* is the senior synonym by principle of page priority and first reviser. The differences between *S. alius* and *S. flexuosus* are discussed in the remarks of *S. alius*. Two specimens illustrated by Chernykh and Ritter (1997, figs. 5.9 and 5.12) are transitional morphotypes between *S. flexuosus* and *S. conjunctus*.

Streptognathodus florensis Wardlaw, Boardman, and Nestell

Plate 23, figs. 1–12; plate 24, figs. 9–13.
Streptognathodus florensis Wardlaw, Boardman, and Nestell, *this volume*, Part A, pl. 1, fig. 4.

Diagnosis: A species of *Streptognathodus* characterized by asymmetric paired Pa elements with commonly two to three accessory denticles on the inner side, a dextral element with an anteriorly deep but narrow groove, a posterior carinal termination that aligns with an outer parapet transverse ridge, a flared inner adcarinal parapet, a sinistral element that is narrower, with a wider groove and an abrupt posterior carinal termination, transverse ridges at least for some portion of the posterior platform appear shingled.

Description—Pa element of moderate length, widest in middle of posterior platform in dextral forms, but of only modest width, widest at the posterior carinal termination in sinistral forms, but sinistral forms narrow and of nearly equal width, bowed, free blade one-fourth to one-third length of element, denticles on blade partly fused, compressed increasing in size anteriorly except for anteriormost two which decrease, as blade joins platform becomes fused ridge, with denticles barely expressed, generally decreasing in size posteriorly but with one or two gaps (larger space between denticles and one

or two denticles typically just anterior to gap that are slightly larger and posteriormost denticle on carina which is also slightly larger, fused carina ends abruptly posteriorly, in dextral forms carina slightly curves to outer edge and aligns with a transverse ridge forming a vague backward 'J', in sinistral forms carina terminates posteriorly in middle of platform showing no curving or alignment, posterior termination of platform pointed except in very large forms which may be rounded, parapets ornamented by transverse ridges posteriorly becoming transverse denticles along adcarinal parapets, transverse ridges at a very slight angle to one another forming a nearly straight line from side to side, on both dextral and sinistral forms at least some ridges appear shingled with a sloping posterior and sharp ledge-like anterior in succession, dextral forms show almost all ridges to be shingled, the outer adcarinal parapet gradually declines along carina from posterior carinal termination, in sinistral forms vaguely denticulate, with partly fused denticles before becoming a short smooth rib along lower side of blade, in dextral forms denticulated for almost entire length, inner adcarinal parapet on dextral forms slightly raised and flared posteriorly before gradually declining, denticulate for almost entire length, anteriorly ending as a short smooth rib along lower side of blade, inner adcarinal parapet on sinistral forms gradually declining anteriorly but with an abrupt drop downwards at or about the carina-blade transition then continuing a short distance anteriorly as a generally smooth rib along lower side of blade, rarely vaguely denticulate in large forms (pl. 22, fig. 9), one to three accessory denticles common on inner side at or near the posterior carinal termination situated in the inner curve of the bowed element, less well developed in dextral forms, median groove in dextral forms narrow but deep, placed toward inner side, becoming variously disrupted by transverse ridges posteriorly, commonly with one or two ridges merging across the groove, extends to near the posterior end. Groove in sinistral forms narrow, generally deep anteriorly, wider than in dextral forms, placed toward inner side, rarely disrupted by a ridge near posterior termination of carina, commonly disrupted by transverse ridges posteriorly, though rarely merging across the groove except for posteriormost one or two, basal cavity moderately to greatly flared.

Dextral and sinistral elements are very different as described above with sinistral elements narrower with a wider groove, less shingled transverse ridges, better developed and typically larger (per size) accessory denticles, and less clearly denticulate adcarinal parapets.

Holotype—USNM 487527, pl. 23, fig. 10.

Remarks—*S. florensis* is the youngest *Streptognathodus* in our collections from Kansas. The section above the Florence Limestone Member appears to be deposited in an inhospitable environment for *Streptognathodus* species with only *Sweetognathus* and *Rabeignathus* present. The immediate predecessor to *S. florensis*, *S. trimilus* is most similar to it and the differences are discussed under that species. *S. florensis* appears to start (at least in dextral forms) the long gradually declining denticulate adcarinal and anterior parapets that are continued and better developed in *S. artinskiensis* but differs in having a much shorter carina and well-developed groove.

Streptognathodus fuchengensis Zhao

Plate 12, figs. 5–7; plate 13, fig. 6; plate 15, fig. 12; plate 16, fig. 4.

Streptognathodus fuchengensis Zhao, 1982, p. 107, pl. 3, figs. 1, 2.

Streptognathodus retangularis Chernykh and Ritter, 1997, p. 469–470, fig. 7.3–7.6.

Streptognathodus isolatus Chernykh, Ritter, and Wardlaw, Chernykh and Ritter, 1997 (part), p. 469, fig. 6.18.

Original Diagnosis: The species is most similar to *Streptognathodus wabaunsensis* in the features of transverse ridges, in the depth and width of the median trough, and differs from the latter in no accessory lobe. Because of the narrow and shallow median trough of the new species, it is different from *Streptognathodus elongatus* which are of the deep median trough and of the 'V'-shape in the transverse section of the platform, and from *Streptognathodus elegantulus* which are of the wider median trough and of the 'U'-shape in the transverse section of the platform, too.

Only right forms of this species were found at present.

Amended Diagnosis: A species of *Streptognathodus* characterized by a robust Pa element with a narrow median groove, a short to moderate fused carina, relatively straight transverse ridges, and one to four accessory denticles on the inner side.

Description—Pa element that is moderate to long, widest generally in middle of posterior platform, but in forms with large accessory denticles developed as wide or slightly wider near posterior carina termination, free blade greater than one-fourth but less than one-third length of the element, denticles on blade partly fused, compressed, generally increasing in size anteriorly, except anteriormost which is smaller, second anterior denticle is very large, one or two denticles between carina and fixed blade at or immediately anterior to the anterior declination of the parapet are also large, much larger than those on the carina or those immediately preceding on the blade which are very small starting the anteriorly increasing in size pattern, as blade joins platform becomes a short fused nodular ridge, nodules on the fused carina are irregular in size with one or two in middle being slightly larger and terminal posterior node is also slightly larger, the carina ends at the posterior node of the fused ridge, no carinal denticles continue posteriorly down the median groove, posterior termination sharply rounded to bluntly pointed, parapets ornamented by transverse ridges that are nearly straight, aligning with each other and forming only a slight oblique angle in the posteriormost part of the platform, in large forms one or two transverse ridge extend into the groove and break up to form a small denticle on the edge of the groove, transverse ridges gradually shorten along outer adcarinal parapet to become transverse denticles, inner parapet sharply changes from transverse ridges to denticles at or just posterior to posterior carinal termination, in moderate to large specimens one to two of the anteriormost ridges break up partially into denticles, inner adcarinal parapet variously fused, forming a roughly parallel ridge to carina, denticles of varying sizes, subequal with some slightly larger and some slightly smaller, typically the posteriormost and anteriormost at the anterior declination of the parapet are of the slightly larger type, one to four accessory

denticles develop with progressive size on inner side near the posterior carinal termination, inner parapet declines sharply down the attached blade, ornamented by one to four irregularly placed and sized denticles (though small) before becoming smooth rib, inner high parapet appears to extend anteriorly further than outer parapet because outer parapet has a much more gradual declination down the attached blade, bears one or two small denticles before becoming a smooth rib anteriorly, median groove narrow, sharply defined, extending nearly to or to the posterior end, roughly in a straight line placed laterally to the inner side.

Dextral and sinistral elements are similar, but for the same length elements dextral elements are more robust (wider) and less bowed than sinistral elements.

Remarks—*S. fuchengensis* differs from *S. conjunctus* and *S. flexuosus* by having an undisrupted groove, shorter carina, and more equally placed parapet declinations.

Streptognathodus fusus Chernykh and Reshetkova

Plate 17, figs., 1, 4, 6, 8–9, 11, 13, 15–16; plate 20, figs. 5, 7.

Streptognathodus fusus Chernykh and Reshetkova, 1987, p. 70, pl. I, figs. 12–14.

Streptognathodus constrictus Chernykh and Reshetkova, Chernykh and Ritter, 1997 (part), p. 464, fig. 8.14, 8.15.

Original Diagnosis: Platform elongate, noticeably constricted at level of end of middle carina, with asymmetrically arranged axial groove. Axial carina occupies less than half of length of platform. Anterior part of platform asymmetrically constructed; more developed inner parapet isolated from free blade [fixed blade] by deep scoop-shaped trough, narrow outer parapet by slit-shaped trough. Regular ribbing of parapets broken in area of narrowing of platform.

Amended Diagnosis: A species of *Streptognathodus* characterized by asymmetrically paired Pa elements with a robust dextral element and an elongate sinistral element, both distinguished by a high flared inner adcarinal parapet, few to no accessory denticles, short carina, and ornamented by one to several short transverse inter-ridge ridges.

Description—Pa element moderate to long, widest in dextral forms in middle of posterior platform, widest in sinistral forms in middle of adcarinal flared parapet, free blade approximately one-third or more of element length, denticles on blade increasing in size anteriorly, except for distal one to three which decrease, and first posterior denticle on attached blade which may be larger than adjacent denticles, typically there is a slight gap in denticulation between the carina and the fixed blade, carina as a short fused ridge, rarely extending posteriorly as discrete one or two denticles, generally as discrete one or two denticles, only in small specimens, carina as ridge to nodular ridge with typically only the posteriormost denticle of the ridge larger and less fused, so, discernable; posterior platform termination pointed to bluntly pointed, parapets posteriorly ornamented by transverse ridges, transverse ridges nearly straightly aligned in dextral forms with only a slight obtuse angle to each other and at a slightly larger angle in sinistral forms, most moderate to large specimens exhibit short inter-ridge ridges scattered between the transverse ridges on either side of the element, ridges grade to transverse denticles anteriorly on outer side which are variously fused along the adcarinal parapet, decreasing in size anteriorly, except for

anteriormost on the high parapet which is larger and may be high, outer parapet declines sharply down the side of the carina, zero to two small denticles on declining parapet before it becomes a smooth rib, posterior transverse ridges grade anteriorly on inner side to high transverse denticles near the posterior end of the fused carina, adcarinal parapet flares out laterally from carina, typically one or two very large denticles in middle of adcarinal parapet, denticles decreasing in size both posteriorly and anteriorly, high inner parapet ends anteriorly at about the anterior end of the carina and gap in denticulation, declines down attached blade gradually with one to two denticles on declining parapet before it becomes a smooth rib, accessory denticles have not been observed on this species, median groove variable, generally moderately wide just at the posterior termination of the carina becoming shortly a narrow irregular groove, commonly disrupted by uneven transverse ridge extensions, extends to the posterior one to three transverse ridges which merge across platform, groove placed just to inner side in dextral elements, laterally placed to inner side in sinistral element, basal cavity moderately flared to outer side.

Dextral and sinistral elements are very asymmetric with dextral forms being more robust, with straight transverse ridge ornamentation and less laterally displaced median groove.

Remarks—This species continues the trend set by its predecessor, *S. nevaensis*, of very asymmetric paired Pa elements. It differs from *S. nevaensis* by its flared inner adcarinal parapet.

Streptognathodus invaginatus Reshetkova and Chernykh

Plate 12, fig. 2; plate 13, figs. 4–5; plate 14, fig. 10; plate 20, fig. 10.
Streptognathodus invaginatus Reshetkova and Chernykh, 1986, p. 111–112, pl. 1, figs. C, T, У, Ф.
Streptognathodus isolatus Chernykh, Ritter, and Wardlaw, 1997 (part), p. 162–162, fig. 1.1.

Original Diagnosis [abstracted from the original description and comparison]: A species of *Streptognathodus* distinguished by a Pa element with a wide rounded platform with a nearly symmetrically located axial furrow, a distinct sinus on the inner lateral side, behind an inner lobe ornamented by two to five closely spaced nodes lateral to the parapet.

Amended Diagnosis: A species of *Streptognathodus* characterized by a Pa element with a marked inflection or invagination in the inner parapet near the posterior termination of the carina that is filled with one to three accessory denticles, of which at least one is large.

Description—Pa element is short to moderate in length, widest in middle of posterior platform, free blade greater than one-third the element length, denticles on blade increasing in size anteriorly except for anteriormost two which are smaller and commonly the second or third denticle posterior to the largest denticle which is smaller than adjacent denticles, as blade joins platform becomes fused ridge, with denticles poorly expressed, roughly decreasing in size posteriorly, carina extends beyond the end of the fused ridge in several specimens as one or two partially discrete to discrete denticles of decreasing size posteriorly, posterior termination of platform pointed, parapets ornamented by transverse ridges posteriorly becoming denticles

at or about the posterior carinal termination, transverse ridges at slight oblique angle to one another, outer parapet gradually grades anteriorly to denticles whereas the inner parapet changes sharply at the inward inflection (invagination) of the parapet, denticles at the inflection are smaller than ridges posterior and denticles anterior to them, outer adcarinal parapet denticles discrete to partly fused gradually decrease in size anteriorly, except for anteriormost on the high parapet which may be larger then adjacent denticles, outer parapet gradually declines down attached blade becoming a smooth rib anteriorly, with no to three indistinct denticles on declining part, inner adcarinal parapet denticles roughly increase than decrease in the middle and then increase again anteriorly to the end of the high parapet, the parapet gradually declines down the attached blade, but it is sharper in its declination than the outer parapet, with two to three denticles on declining parapet, of decreasing size anteriorly, becoming a smooth rib anteriorly, one to three accessory denticles develop in the invagination created by the inner parapet, in moderate to large specimens one to two of the accessory denticles are large, median groove narrow extending to posteriormost second or third transverse ridge which merge across the platform and close the groove, groove is variously disrupted by a few transverse ridges that merge across it along the posterior platform, medially placed to slightly placed to the inner side, basal cavity moderately flared.

Dextral and sinistral elements are very similar.

Remarks—*S. invaginatus* is unlike any other species with its marked invagination with one to three accessory denticles.

Streptognathodus isolatus Chernykh, Ritter, and Wardlaw

Plate 12, figs. 3, 4, 10; plate 13, figs. 1, 8, 10–12; plate 15, figs. 7–9; plate 19, fig. 7.
Streptognathodus isolatus Chernykh, Ritter, and Wardlaw, 1997 (part), p. 162–164, fig. 4, 5, 6?, 7–8, 11–13, 15; *non* fig. 1 (=*S. invaginatus*), figs. 2, 9 (=*S. minacutus*), figs. 10, 14 (=*S. nodulinearis*); Chernykh and Ritter, 1997 (part), p. 469, fig. 6.13–6.17; *non* fig. 6.7 (=*S. minacutus)*, fig. 6.18 (=*S. fuchengensis*).
Streptognathodus wabaunsensis Gunnell, Chernykh and Ritter, 1997 (part), p. 471, fig. 6.12.
Streptognathodus flangulatus Gunnell, Chuvashov, Chernykh, and Mizens, 1993, p. 14–15.

Original Diagnosis: Pa element with nodose inner accessory lobe separated from remainder of platform by a narrow, shallow trough. Inner parapet continuous, although it may be deflected inwardly at position of lobe.

Amended Diagnosis: A species of *Streptognathodus* characterized by a Pa element with common accessory denticles on the inner side of the element, a narrow groove, anteriorly fused to partially fused adcarinal parapet that aligns with the posterior platform parapet, largest denticle on adcarinal parapet near the anterior, and a flared anterior declination of the parapet.

Description—Pa element moderate to long, widest on anterior part of posterior platform, but nearly as wide across accessory denticle field near posterior termination of fused carina in many specimens, free blade one-third to one-half of the element, denticles on blade partly fused, compressed, increasing in size anteriorly except anteriormost one or two,

which are smaller and greatly pointed to the anterior, as blade joins platform becomes a very fused ridge, carina short, generally decreasing in size posteriorly, typically with one partially fused to discrete denticle posterior to carina, which may or may not increase in size, no additional posterior carinal denticles beyond the one, posterior termination of platform bluntly pointed, parapets ornamented by transverse ridges variable, curving to the posterior, at various angles to midline, becoming nearly aligned near posterior termination of the carina, but generally still with some curve, one or two interridge ridges or one or several ridges broken-up into short aligned ridges or transverse denticles, region near the posterior termination of the carina generally very broken up with parapets as discrete denticles, abundant accessory denticles, mostly on inner side and single denticle termination of the carina, anterior portion of the high adcarinal parapets generally fused to partly fused, rarely discrete (see pl. 14, fig. 7, inner side), fused to partially fused inner adcarinal parapet aligning with the posterior platform parapet "isolating" to the inner lateral side the field of accessory denticles, adcarinal parapets generally decrease in size from adjacent to the anteriormost part of high carina where it bears the largest denticle or is the widest, highest part of the parapet, but may have one denticle of larger size near posterior carinal termination, anterior declination of parapets generally fairly sharp, denticulate and slightly flared on inner side, vaguely denticulate on outer side, inner high parapet extends further anteriorly than outer parapet, both extending as a narrowing smooth rib on lower side of blade for a considerable distance, accessory denticles numerous, mostly discrete, mostly clustered in field on inner side opposite the posterior termination of the carina, rarely one or two denticles on outer wall of element below the platform or the anteriormost transverse ridge is broken-up into denticles on outer parapet of platform, median furrow deep and narrow near posterior termination of the carina becoming an inconsistent groove posteriorly, laterally place to the inner side that is variously disrupted by merging transverse ridges, basal cavity moderately flared.

Dextral and sinistral elements are similar, although for a given size sinistral elements tend to be slightly less robust, or slightly more elongate.

Remarks—Large specimens from samples that yield this species invariably contain specimens that dextral forms show the very fused anterior adcarinal parapet either more fused to the continuing parapet denticles (*S. isolatus*) or to the accessory denticles (*S. minacutus*). In smaller specimens, there may be a vague split in the parapet aligning with both some of the accessory denticles and the posterior part of the adcarinal parapet, which we were unable to differentiate. However, the sinistral forms of *S. isolatus* are similar, though typically more slender than the dextral forms, whereas the sinistral forms of *S. minacutus* show a gap between the adcarinal parapet and the posterior platform parapet throughout growth. That the dextral elements of both *S. isolatus* and *S. minacutus* are indistinguishable in small specimens and only subtly distinguishable in large specimens indicates to us that they are very closely related species. The dextral element of *S. minacutus* and both elements of *S. isolatus* are the most nodose in the nodular lineage and are easy to differentiate from other

species in large specimens. The only other very nodose form, *S. denticulatus,* is an aberrant rare form that is easily distinguished from more normal *Streptognathodus* species.

Streptognathodus lineatus Wardlaw, Boardman, and Nestell

Plate 15, figs. 1, 14; plate 19, fig. 1.
Streptognathodus lineatus Wardlaw, Boardman, and Nestell, *this volume*, Part A, pl. 1, fig. 5.

Diagnosis: A species of *Streptognathodus* characterized by a Pa element with a marked gap in the carina in the anterior part of the posterior platform and concomitant pinching of the groove, one to seven accessory denticles align in rows representing the break up of what are posteriorly transverse ridges.

Description—Pa element short to moderate in length, bowed, widest in middle of posterior platform, nearly as wide at or near the posterior end of the fused carina where most accessory denticles have developed, free blade short, approximately one-fourth the element length, longer in small specimens, denticles on blade partly fused, compressed, increasing in size anteriorly, except for anteriormost, which is smaller, as blade joins platform becomes a fused ridge, denticles barely discernable, generally denticles or ridge decrease in size (height and width) posteriorly except for posteriormost which is slightly larger, carina continues as one or two discrete denticles, then there is a gap with no denticles and a constriction of the groove before carina posteriorly continues as small discrete denticles in the middle of the groove, generally about five, posterior termination of platform pointed, parapets ornamented posteriorly by transverse ridges becoming denticles anteriorly, transverse ridges form a slight obtuse angle with one another, outer parapet continues ornamented by transverse ridges along fused carina gradually becoming transverse denticles decreasing in size anteriorly, rarely one transverse ridge breaks up into two aligned transverse denticles (pl. 14, fig. 1) at the anterior end of the narrowing of the groove and of the gap in denticulation of the carina, anterior part of high adcarinal parapet is fused, outer parapet declines abruptly down attached blade as a smooth rib, inner parapet declines at about the same point or slightly anterior to the outer parapet, inner parapet becomes ornamented by several rows of transverse denticles (the break-up of transverse ridges) just anterior to the narrowing of the groove, number of rows depends on size of specimens, in small specimens there is one (pl. 18, fig. 1, barely noticeable) to as many as four or five in large specimens (pl. 14, fig. 1), denticles on adcarinal parapet decline in size anteriorly and become partly fused just behind the anterior declination of the parapet, the inner parapet declination is sharp, but not as sharp as the outer parapet, the declining parapet bears two to four denticles, partly fused, rarely (as in the holotype) the anterior two are fused into a ridge, median groove wide with a marked narrowing or constriction in the anterior part of the posterior platform corresponding to the gap in the carina apparently caused by lengthening of lateral transverse ridges, groove widens posteriorly, bears several denticles, and extends nearly to the posterior end of the element, basal cavity moderately flared.

Dextral and sinistral elements are very similar.
Holotype—USNM 484112, pl. 14, fig. 14.

Remarks—The constriction of the groove and gap in carinal denticulation is only shown in this species in our material. The denticle doublets on the inner side near the posterior end of the fused carina are similar to those found in *S. postelongatus* suggesting that these two species developed from the same common stock, *S. elongatus*.

Streptognathodus longissimus Chernykh and Reshetkova

Plate 17, figs. 3, 5, 14; plate 20, fig. 1.
Streptognathodus longissimus Chernykh and Reshetkova, 1987, p. 72, pl. II, figs. 4–7.

Original Diagnosis: Strongly elongated platform, usually symmetric, with weak constriction in middle part. Anterior part of platform makes up about one-third of length, has well-developed furrows. Posterior part of platform bears uniform, clearly delineated ribs.

Amended Diagnosis: A species of *Streptognathodus* characterized by an elongate Pa element with a weak constriction in the platform posterior to the fused carina, a long, well-developed groove, and rare accessory denticles.

Description—Pa element is long and narrow (elongate), bowed, widest just anterior to posterior end, except in small specimens which may be wider along the carina, free blade makes up about one-third of the length of the element, but in this species it is difficult to differentiate the free from fixed blades, nevertheless the blade is long, about one-half of the element, denticles on blade partly fused and compressed increasing in size anteriorly except anteriormost three, anteriormost one is smaller, anterior second and third are still increasing in length but are lower in height than adjacent denticles posteriorly, as blade joins platform becomes a fused ridge with denticles barely recognizable, roughly decreasing in height and width posteriorly except for posterior termination of fused carinal ridge that is slightly more discrete denticle and slightly larger than adjacent denticles on carina, carina ends abruptly at this denticle, posterior termination of platform rounded, parapets ornamented by transverse ridges posteriorly becoming transverse denticles adjacent to the carina, transverse ridges form an oblique angle with each other, roughly decreasing in size anteriorly especially in anterior part of the posterior platform and anteriorly, except for one or two on both sides at the weak platform constriction, which are smaller, platform constricts just posterior to carinal termination, adcarinal parapets low, parapets decline gradually down attached blade bearing one to three denticles before becoming a long smooth rib, declination of both inner and outer parapets at about the same point, rarely a single small accessory denticle may develop on the side of the platform on the inner side below the constriction in the platform, median groove of moderate width, long, narrowing posteriorly, extending near to the posterior end of the platform, basal cavity moderately flared to the outer side.

Dextral and sinistral forms differ in that dextral elements are slightly more robust (wider), have a longer carina, and the transverse ridges are at a lesser angle and irregularly break up along posterior outer parapet forming aligned ridges and small denticles.

Remarks—This species differs from *S. constrictus* which it closely resembles by being longer, lacking a flared inner adcarinal parapet, lacking a posterior discrete denticle on the carina, and having the transverse ridges at a larger angle to one another.

Streptognathodus minacutus Barskov and Reimers

Plate 12, figs. 1, 8, plate 13, fig. 2, plate 19, figs. 4–6.
Streptognathodus minacutus Barskov and Reimers, 1996, p. 437, pl. 2, figs. 3, 5, 12.
Streptognathodus acuminatus Gunnell, Chernykh and Reshetkova, 1987, p. 34, pl. 7, fig. 5; Akhmetshina, 1990, pl. 1, figs. 5, 8; Barskov and Reimers, 1992, pl. 1, fig. 4; Chernykh and Ritter, 1997, p. 463, fig. 6.2.
Streptognathodus n. sp. B Chernykh and Ritter, 1997, p. 473, fig. 7.9–7.11.
Streptognathodus isolatus Chernykh, Ritter, and Wardlaw, Chernykh and Ritter, 1997 (part), p. 469, fig. 6.7.

Original Diagnosis (from the comparison): *Streptognathodus minacutus* is distinguished from all *Streptognathodus* species by a peculiar rupture of the parapet at the inner side of the platform.

Amended Diagnosis: A species of *Streptognathodus* characterized by very unsymmetrical pair of Pa elements with robust dextral element and a more slender sinistral element, sinistral element with distinct gap or "rupture" between the fused to partially fused adcarinal parapet and the posterior platform parapet, dextral form with common accessory denticles on the inner side, anteriorly fused to partially fused adcarinal parapet that aligns with accessory denticles and not with the posterior platform parapet, so that accessory denticles are interior to the fused to partially fused inner lateral margin wall formed by fused adcarinal parapet and more fused accessory denticles that are aligned with it.

Description—Pa element moderate to long, widest on anterior part of posterior platform, but nearly as wide across accessory denticle field near posterior termination of fused carina in many specimens, free blade one-third to one-half of the element, denticles on blade partly fused, compressed, increasing in size anteriorly except anteriormost one or two, which are smaller and greatly pointed to the anterior, as blade joins platform becomes a very fused ridge, carina short, generally decreasing in size posteriorly, typically with one partially fused to discrete denticle posterior to carina, which may or may not increase in size, no additional posterior carinal denticles beyond the one, posterior termination of platform bluntly pointed, parapets ornamented by transverse ridges variable, curving to the posterior, at various angles to midline, becoming nearly aligned near posterior termination of the carina, but generally still with some curve, one or two interridge ridges or one or several ridges broken-up into short aligned ridges or transverse denticles, region near the posterior termination of the carina generally very broken up with parapets as discrete denticles, abundant accessory denticles, mostly on inner side and single denticle termination of the carina, anterior portion of the high adcarinal parapets generally fused to partly fused, rarely discrete (see pl. 14, fig. 7, inner side), fused to partially fused inner adcarinal parapet commonly shows a subtle to vague bifurcation continuing posteriorly with discrete or more discrete denticles of the parapet and aligning with a few accessory denticles, in large specimens

becoming more fused showing anterior adcarinal parapet aligning with an inner lateral accessory ridge forming a lateral marginal wall or posterior extension of the adcarinal parapet, adcarinal parapets generally decrease in size from adjacent to the anteriormost part of high carina where it bears the largest denticle or is the widest, highest part of the parapet, but may have one denticle of larger size near posterior carinal termination, anterior declination of parapets generally fairly sharp, denticulate and slightly flared on inner side, vaguely denticulate on outer side, inner high parapet extends further anteriorly than outer parapet, both extending as a narrowing smooth rib on lower side of blade for a considerable distance, accessory denticles numerous, fused to discrete, mostly clustered on inner side opposite the posterior termination of the carina, rarely one or two denticles on outer wall of element below the platform or the anteriormost transverse ridge is broken-up into denticles on outer parapet of platform, median furrow deep and narrow near posterior termination of the carina becoming an inconsistent groove posteriorly, laterally place to the inner side that is variously disrupted by merging transverse ridges, basal cavity moderately flared.

Dextral and sinistral elements are very dissimilar forming a very unsymmetrical pair, sinistral element is slender with a distinct gap or "rupture" between the fused to partially fused adcarinal parapet and the posterior platform parapet and with few accessory denticles, dextral element is robust with common accessory denticle on the inner side of the element, anteriorly fused to partially fused adcarinal parapet that aligns with accessory denticles to form a inner lateral margin wall so that accessory denticles are interior to the fused to partially fused inner lateral margin wall.

Remarks—Barskov and Reimers (1996) clearly saw that this form is distinct from but commonly confused with *S. acuminatus* by simply changing the order of the syllables and dropping an "a" from *"a-cu-min-a-tus"* to *"min-a-cu-tus"*. *S. acuminatus* is a junior synonym of *S. wabaunsensis* Gunnell (see discussion of *wabaunsensis*) and does not range into the Permian. Both Barskov and Reimers (1996) and Chernykh and Ritter (1997) have difficulty in identifying dextral and sinistral elements. What we identify as sinistral and dextral forms occur in every sample together with the same stratigraphic range and are significantly alike in the adcarinal ridge not aligning with the posterior platform parapet and different from all other forms that we strongly feel they are the same species. The form illustrated as *Streptognathodus wabaunsensis* Gunnell, Chernykh and Ritter (1997, p. 471, fig. 6.10, 6.11) is clearly related to *S. minacutus* and is its probable ancestor. One author (BRW) will describe this form from his abundant material from the southern Urals and clarify the various forms assigned to "*acuminatus*" in a later paper. We have none of these morphotypes in our material from Kansas.

Diagnosis: A species of *Streptognathodus* characterized by asymmetrically paired Pa elements with robust dextral element, short fused carina, high inner adcarinal parapet, and one to two accessory denticles on the inner side.

Description—Pa element moderate to long, slightly bowed, widest in middle of posterior platform, free blade one-third or more of the element length, denticles on blade partly fused, compressed, increasing in size anteriorly except for anterior one or two, which may be smaller, as blade joins platform becomes fused ridge, carina pinches and swells in width indicating fused denticles of alternating size, typically with one small discrete denticle posterior to fused ridge showing a marked decrease in carina height and width at the posterior end, posterior platform termination bluntly pointed, parapets ornamented by transverse ridges that become transverse denticles anteriorly, transverse ridges at low to moderate obtuse angle to one another generally slightly curving anteriorward along median groove, outer parapet ornamentation gradually changes from shortening transverse ridges to transverse denticles, decreasing in size along carina, except anteriormost at declination of parapet which may be larger, outer parapet declines very sharply down the attached blade and is smooth or bears one or two denticles and is very short, inner parapet changes more abruptly to transverse denticles at or near the posterior carina termination, decrease in size anteriorly except anteriormost before declination of parapet which is larger, inner parapet gradually declines down attached blade bearing one to four denticles, rarely two or more may be fused to form small ridge before lowered parapet continues anteriorly for a short distance as a smooth rib, one or two accessory denticles develop in larger specimens on inner lateral side of platform at or near posterior carina termination, in larger specimens transverse ridges near the posterior carina termination may break-up into aligned transverse denticles appearing as additional accessory denticles, but on top of platform not on its side, median groove generally narrow, nearly straight, extends a variable distance posteriorly generally extending to near the posterior end with the posteriormost two to three transverse ridges merging across it, but in rare specimens several transverse ridges merge across groove (pl. 15, fig. 7), basal cavity moderately flared.

Dextral and sinistral elements are dissimilar in that dextral forms are robust and sinistral forms are elongate but all of the descriptive features are the same.

Holotype—USNM 484134, pl. 16, fig. 7.

Remarks—*S. nevaensis* is similar to *S. fuchengensis* but differs in having a higher, longer inner parapet, presaging the development of a flared parapet in *S. fusus*, has more aligned platform ornamentation, and is more asymmetrically paired, the sinistral element not having a good counterpart in *S. fuchengensis*.

Streptognathodus nevaensis Wardlaw, Boardman, and Nestell

Plate 14, figs. 6–7; plate 16, figs. 1–3, 5–8, 11; plate 17, fig. 12; plate 19, fig. 2; plate 32, figs. 1–2.
Streptognathodus nevaensis Wardlaw, Boardman, and Nestell, *this volume*, Part A, pl. 1, fig. 6.

Streptognathodus nodulinearis Reshetkova and Chernykh

Plate 12, fig. 9, 11; plate 13, fig. 9; plate 15, fig. 11.
Streptognathodus nodulinearis Reshetkova and Chernykh, 1986, p. 112, pl. 1, figs. Х, Ц, Ч, Ш, Щ.
Streptognathodus isolatus Chernykh, Ritter, and Wardlaw, 1997 (part), p. 162, fig. 1.10, 1.14.

Original Diagnosis [abstracted from the original description and comparison]: A species of *Streptognathodus* distinguished by a Pa element ornamented by a linear row of nodes, parallel to the axial groove, on the inner side accessory lobe, lateral to the parapet.

Amended Diagnosis: A species of *Streptognathodus* characterized by a Pa element ornamented by a linear row of accessory denticles on the inner side outside the parapet that is parallel to the carina and median groove.

Description—Pa element moderate in length, dextral element nearly straight, sinistral elements bowed, widest in middle of posterior platform, free blade approximately one-third the length of the element, denticles on blade partly fused and compressed, increasing in size anteriorly, except for anteriormost one, which is smaller, as blade joins platform becomes a fused ridge, denticles barely discernable, carina short and posteriorly ends with fused ridge that is slightly elevated indicating a slightly larger fused denticle at the posterior termination of the carina, posterior platform termination bluntly pointed, parapets ornamented posteriorly by transverse ridges anteriorly by denticles, transverse ridges are nearly straight forming a very low obtuse angle with one another, outer parapet abruptly changes from transverse ridges to denticles near posterior carina termination, anteriormost transverse ridge may break up into two aligned transverse denticles in some specimens, outer adcarinal parapet relatively high, generally partly fused, commonly portions very fused, fused portions irregularly distributed but generally higher than partly fused denticles, anterior declination of the outer parapet sharp, generally bearing one denticle before becoming a short smooth rib, inner parapet with one or two shorter transverse ridges that start near the groove but do not extend as far laterally as posterior ridges near anterior of posterior platform as an apparent invagination, accessory denticles start at or anterior to this invagination, transverse ridges abruptly change to denticles just posterior to posterior carina termination, inner adcarinal denticles discrete to partly fused posteriorly becoming partly fused to fused anteriorly, increasing in size anteriorly, declination of inner parapet sharp, generally bearing two to three partly fused denticles that are decreasing in size anteriorly from largest denticle, inner parapet continues anteriorly as a short smooth rib, typically declination of the parapets is about the same point with high outer parapet extending slightly more to the anterior as often as the high inner parapet does, accessory denticles develop in a linear row through growth, begin posteriorly at or just anterior to the invagination in the ridges on the inner side of the element, a row of five or more only in large specimens, typically most specimens have fewer; dextral elements, because they are straighter develop a straight row, sinistral elements because they are bowed, develop a curved row, and tend to have more accessory denticles for a given size, median groove narrow and short becoming more and more closed off posteriorly by more and more merging transverse ridges in specimens of increasing size, in large specimens just a shallow trough with almost all ridges merging across it (pl. 11, fig. 9), groove is roughly centrally placed, basal cavity moderately flared to the outside.

Dextral and sinistral elements are dissimilar in that dextral elements are more robust, straighter, and have fewer accessory denticles.

Remarks—*S. nodulinearis* is one of the rarer species we have identified. Large specimens with the well-developed line of accessory denticles are easy to differentiate. Small specimens with one or two accessory denticles developed are difficult to differentiate from small specimens of *S. invaginatus* and *S. minacutus* which differ in having well-developed grooves, *S. invaginatus* has a better developed invagination, generally filled by a single, large accessory denticle and *S. minacutus* has a inner adcarinal parapet that forms to the lateral side of the accessory denticles.

Streptognathodus postconstrictus Wardlaw, Boardman, and Nestell

Plate 21, figs. 2–5, 13; plate 22, fig. 8.
Streptognathodus constrictus Chernykh and Reshetkova, Chernykh and Ritter, 1997 (part), p. 464, fig. 8.10–8.13, 8.16.
Streptognathodus postconstrictus Wardlaw, Boardman, and Nestell, *this volume*, Part A, pl. 1, fig. 7.

Diagnosis: A species of *Streptognathodus* characterized by a Pa element that is elongate with a slight constriction posteriorly, becoming more pronounced with increasing size, a narrow but well developed and deep groove posteriorly, and commonly has one to three accessory denticles.

Description—Pa element elongate, widest near posterior and nearly as wide near posterior termination of the carina, slightly sigmoidal in outline, free blade approximately one-fourth or less of the element, denticles on blade partly fused, compressed, increasing in size anteriorly except anteriormost, as blade joins platform becomes nodose fused ridge, generally decreasing in size posteriorly, except posteriormost denticle which is more discrete and slightly larger than those anterior to it, fused carina short, carina continues posteriorly as a single discrete denticle, developing in larger specimens, posterior termination of the platform pointed generally as a single denticle, parapets ornamented by transverse ridges posteriorly becoming transverse denticles anteriorly, at slightly greater than 90° angle to median line, inner parapet on dextral forms extends much further to the anterior, outer parapet in sinistral forms extends slightly further to the anterior, inner parapet shows a slight to marked constriction just posterior to the posterior termination of the carina, one to three accessory denticles develop anterior to constriction on inner side align with transverse denticles to form "double" ridges or denticle doublet in larger forms, one to five transverse denticles on outer parapet along the carina or posterior to it also break up to form a "double" ridge or denticle doublet, inner parapet is slightly flared adjacent to the posterior part of the carina, outer parapet anterior termination generally abrupt with sharp decline down fixed blade, continuing anteriorly for a short distance as a thin rib near the lower margin of the blade, inner parapet declines slightly along anterior part of the carina, descends moderately sharply to gradually on the fixed blade and continues anteriorly as a rib along lower margin of the blade for much of the blade length, descending parapet and anterior rib generally smooth on both inner and outer sides, median groove narrow, well developed, and deep, extending most of the length of the posterior platform to the posteriormost or next posterior denticle or transverse ridge, basal cavity slightly to moderately flared.

Dextral and sinistral elements differ in anterior parapet termination (discussed above) but are similar in that both are narrow, elongate forms.

Holotype—USNM 487517, plate 22, fig. 8.

Remarks—*S. postconstrictus* differs from *S. constrictus* in that it commonly has accessory denticles forming doublets with parapet denticles and the inner parapet extends much further anteriorly.

Streptognathodus postelongatus Wardlaw, Boardman, and Nestell

Plate 14, figs. 1–2, 8; plate 15, figs. 2–5, 10, 13, 15–17; plate 16, figs. 9–10; plate 20, figs. 9, 11–12.
Streptognathodus postelongatus Wardlaw, Boardman, and Nestell, *this volume*, Part A, pl. 1, fig. 8.

Diagnosis: A species of *Streptognathodus* characterized by an elongate Pa element that has at least one double set of transversely aligned denticles.

Description—Pa element narrow, of moderate length (elongate), bowed, generally widest near posterior end of carina, rare specimens wider on anterior to middle of posterior platform, free blade variable in length from nearly one-half to almost one-fourth the length of the element, the carina/blade length to posterior platform length ratio is relatively constant but the length of the high adcarinal parapets is quite variable, the high posterior parapets apparently decline down the side of the carina/blade from the middle of the posterior fused portion (carina) to the partly fused denticulate blade in different specimens, the fused to denticulate portions of the carina/blade remain at a relatively constant ratio of 1:2, carina is fused ridge, rarely extends posteriorly as one small discrete denticle, commonly that small posteriormost denticle is partially fused to fused carinal ridge, posterior platform termination is pointed, parapets are posteriorly ornamented by transverse ridges becoming denticles anteriorly at or about the posterior carina termination, transverse ridges at slight to moderate obtuse angle to each other, typically a higher angle in more bowed specimens, outer parapet gradually changes anteriorly from transverse ridges to transverse denticles, rarely in large specimens a transverse double set of denticles develops form the break up of one transverse ridge just posterior to the posterior carina termination, denticles roughly decrease in size anteriorly, declination of the parapet is mildly sharp to gradual with no to three denticles before becoming a short smooth rib, inner parapet changes abruptly from ornamented by transverse ridges posteriorly to a transverse double set of denticles (denticle doublet) at or near the posterior carina termination, up to four double sets develop on the inner parapet, sets increasing with the size of the specimen, adcarinal parapet variously fused, generally in the anterior part from partly fused to overgrown, generally decreasing in size anteriorly in front of double sets of denticles except anteriormost before parapet declination which may be larger, double sets commonly of unequal size, anterior declination of parapet mildly sharp bearing one to three denticles, before becoming a short smooth rib, both parapets decline at about the same point, median groove narrow, long, generally extending nearly to posterior end, in rare specimens and very large specimens several transverse ridges at various points along

the posterior platform merge across the groove, basal cavity moderately flared.

Dextral and sinistral elements are very similar.

Holotype—USNM 484101, pl. 14, fig. 1.

Remarks—*S. postelongatus* differs from *S. elongatus* by possessing at least one denticle doublet in almost any sized specimen. Its descendants differ by *S. constrictus* developing a constriction and *S. longissimus* developing a long clear groove.

Streptognathodus robustus Wardlaw, Boardman, and Nestell

Plate 21, figs. 6, 10–11.
Streptognathodus robustus Wardlaw, Boardman, and Nestell, *this volume*, Part A, pl. 1, fig. 9.

Diagnosis: A species of *Streptognathodus* characterized by robust Pa element with a deep and wide furrow, rounded posterior platform termination, flared inner adcarinal parapet, no to few accessory denticles, and a short free blade.

Description—Pa element short to moderate in length widest near posterior end of platform, slightly sigmoidal in outline shown by subtle inflections or curves in the carina and a slight invagination of the inner side of the platform, free blade short, one-third to one-fourth of the length of the element, denticles on blade partly fused, compressed, increasing in size anteriorly except for anteriormost, as blade joins platform becomes nodose fused carina, typically at or just anterior to outer parapet anterior declination is one larger denticle on the blade/carina, carina inflects at this denticle, denticles decreasing in size posteriorly, becoming more discrete posteriorly generally one small discrete denticle posterior to posterior fused carinal termination, fused carina short, posterior termination of platform bluntly rounded, parapets ornamented by transverse ridges posteriorly becoming transverse denticles along carina, ridges and denticles at slightly greater than 90° angle to median line except posteriormost two to three which are at a much greater angle and merging or nearly merging across furrow to form broad inverted 'V's , inner adcarinal parapet with one or two larger and(or) more elevated denticles than adjacent ones giving a flare to the inner parapet, outer parapet declines abruptly from anteriormost very transverse denticle which is larger and more elevated than the few posterior to it which forms a slight invagination on the outer side, anterior continuation of parapet after the abrupt declination obscure or as a smooth or slightly denticulate rib for a short distance, inner parapet anterior declination sharp with a few denticles, decreasing in size anteriorly before becoming a short smooth rib, inner high parapet extends further anteriorly than outer high parapet, median furrow wide and deep, extending nearly to the posterior end of the platform where the posteriormost one to three transverse ridges may join, basal cavity only slightly flared.

Dextral and sinistral elements are similar.

Holotype—USNM 487497 pl. 21, fig. 6.

Remarks—This species appears to be the last robust morphotype in our material and differs from its predecessor, *S. barskovi* by its much wider furrow, rounded posterior platform termination, shorter free blade, sigmoidal outline, and carina with a larger denticle near where the blade joins the platform.

Streptognathodus translinearis Wardlaw, Boardman, and Nestell

Plate 14, figs. 3–5, 9; plate 21, figs. 7, 14, 16.

Streptognathodus translinearis Wardlaw, Boardman, and Nestell, *this volume*, Part A, pl. 1, fig. 10.

Diagnosis: A species of *Streptognathodus* characterized by a Pa element with a relatively straight fused to partially fused inner adcarinal parapet that parallels the carina or posteriorly slightly converges toward the carina, a sharp anterior declination of the inner parapet, and generally a few to several accessory denticles on the inner side.

Description—Pa element moderate to long, widest on anterior of posterior platform, generally just beyond posterior termination of the carina, free blade approximately one-third of the element, denticles on blade partly fused, compressed, generally increasing in size anteriorly, but with one distinctly smaller denticle three to four from the anteriormost and the anteriormost which decreases in size, as blade joins platform becomes short fused ridge, denticles barely expressed, generally decreasing in size posteriorly except for posteriormost which may be slightly larger than adjacent few denticles, no posterior extension of the fused carina with discrete denticles, posterior termination of the platform bluntly pointed, parapets ornamented by transverse ridges posteriorly, fused to partially fused denticles anteriorly, ridges at slightly greater than 90° angle to midline forming a broad oblique angle with each other except at posteriormost end in some specimens where marked inverted 'V' is formed, angle becoming lesser anteriorly so that opposing transverse ridges nearly form a straight line, ridges variable in large specimens, broken-up into several short ridges (typically on inner side), or short allowing for a large median sulcus to form, or several merging across median so that groove is obscure, adcarinal parapets fused, inner adcarinal parapet a little less fused, becoming less so posteriorly so that there is one discrete to partially fused denticle opposite the posterior carinal termination, inner adcarinal denticles of subequal size with one slightly larger denticle in middle of adcarinal ridge, outer adcarinal ridge generally decreasing in size anteriorly, inner high parapet extends further anteriorly than outer high parapet, inner adcarinal parapet anterior declination sharp, with zero to three small denticles, decreasing in size anteriorly, before becoming short smooth rib along lower side of blade, outer adcarinal parapet anterior declination sharp, but less so than inner declination, with zero to three small denticles before becoming short smooth rib along lower side of blade, median groove, furrow, or sulcus variously developed, generally in all but large specimens as a narrow, moderate-depth groove extending for most of the posterior platform, generally zero to three small accessory denticles developed on inner lateral wall of platform, opposite posterior termination of carina, in large specimens several accessory denticles on inner side with most in rough linear alignment, paralleling midline, and on outer lateral wall of platform, basal cavity moderately flared.

Dextral and sinistral elements are very similar.

Holotype—USNM 484106, pl. 14, fig. 9.

Remarks—This species suggests a close affinity to *S. nodulinearis* by its roughly aligned accessory denticles in larger specimens and the highly fused inner adcarinal parapet; it differs

in lacking the well-developed line of nodes developed in large specimens, in having the variable groove to sulcus, and in having the more or less discrete denticle at the posterior end of the inner fused adcarinal parapet.

Streptognathodus trimilus Wardlaw, Boardman, and Nestell

Plate 21, figs. 1, 8–9; plate 22, figs. 1–7, 9–13.

Streptognathodus elongatus Gunnell, Ritter, 1986 (part), p. 154, pl. 4, fig. 16.

Streptognathodus trimilus Wardlaw, Boardman, and Nestell, *this volume*, Part A, pl. 1, fig. 11.

Diagnosis: A species of *Streptognathodus* characterized by asymmetric paired Pa elements with a narrow median groove, one to many transverse ridges that merge across the middle of the platform, a posterior carinal termination that aligns with an inner parapet transverse ridge, a sinistral element that is narrower, with a wider groove, transverse ridges at least for some portion of the posterior platform appear shingled.

Description—Pa element moderate in length, widest near middle of platform in dextral forms, sinistral forms are elongate with platform of near equal width, generally widest just posterior to posterior carinal termination, free blade one-fourth to one-third length of element, denticles on blade partly fused, compressed, increasing in size anteriorly except anteriormost one, as blade joins platform becomes fused ridge, with denticles barely expressed, decreasing in size posteriorly except of posteriormost denticle which is partially discrete and larger than those anterior to it, carinas on dextral forms terminate at this partially discrete denticle, sinistral forms as often as not have one additional discrete carinal denticle, carinal termination aligns with and sometimes merges with curving transverse ridge generally to the inner side, but ridges from both sides curve to the carinal termination, posterior platform termination pointed, parapets ornamented by transverse ridges at slightly greater than 90° angle to greater angle to median line, generally curving, in dextral forms, several merge across the platform, in sinistral forms one to several merge across the platform, adcarinal parapets with transverse denticles, gradually lowering down side of carina anteriorly, anterior declination generally not pronounced, in rare large specimens (pl. 21, fig. 13) declination is mildly abrupt, in dextral forms inner parapet extends further anteriorly than outer parapet, in sinistral forms roughly of equal length, the inner parapet in dextral forms is denticulate for more of its length, denticles decreasing in size anteriorly, before becoming a smooth rib along side of the blade, in sinistral forms the opposite is true in that the outer parapet is more denticulate, zero to three accessory denticles occur on the inner side near the posterior carinal termination, more common on sinistral forms than on dextral forms, median groove more pronounced in sinistral forms and only partially disrupted by merging transverse ridges, disrupted to almost not present in dextral forms, basal cavity moderately flared.

Dextral and sinistral elements are very dissimilar with sinistral elements being elongate with a moderately developed median groove, common accessory denticles and subequal anterior parapet terminations and dextral elements of moderate

size with a disrupted median groove, rare accessory denticles, and inner parapet longer than the outer parapet.

Holotype—USNM 487491, pl. 21, fig. 9.

Remarks—This species is most like its daughter species, *S. florensis*, but is less asymmetrical. The sinistral elements are most alike between the two species but differ in that those of *S. florensis* have a wider groove and more accessory denticles generally for a given size. The dextral elements differ in that *S. trimilus* specimens have a much less developed groove, common transverse ridges merging across the middle of the platform, the inner adcarinal parapet that is not noticeably flared, a carina that aligns with an inner transverse ridge as opposed to an outer one in *S. florensis*, and typically it has fewer and less well developed accessory denticles. It differs from *S. translinearis* by the inner adcarinal parapet being less fused, more denticulated, not paralleling, or nearly so, the carina, and by having fewer broken-up and more curving transverse ridges.

Streptognathodus wabaunsensis Gunnell

Plate 5, figs. 1–7, 9–10; plate 7, figs. 1–2, 5, 8–9; plate 8, figs. 5–7; plate 9, fig. 4; plate 19, fig. 10.
Streptognathodus wabaunsensis Gunnell, 1933, p. 285a, pl. 33, fig. 32
Streptognathodus walteri Gunnell, 1933, p. 284, p. 33, fig. 31
Streptognathodus acuminatus Gunnell, 1933, p. 285b, pl. 33, fig. 33

Original Diagnosis [*S. wabaunsensis*]: Oral surface with nine transverse ridges anterior [posterior] to anterior [posterior] extremity of carinal ridge; posterior [anterior] eight being cut by small median groove. Greatest width of oral surface anterior [posterior] to mid-length of plate. Oral surface to right [left] of carinal ridge bearing nodes; left [right] postero-lateral [antero] area bearing nodose, longitudinal ridge. Anterior [posterior] end sharp.

The greater length to width ratio of *S. acuminatus* distinguishes it from this form [a growth feature].

[*S. walteri*]: Length to width ratio of plate oral surface 27 to 11. Median groove on oral surface biconvex in outline anterior [posterior] to anterior [posterior] extremity of carinal ridge. Carinal ridge nodose; occupying posterior [anterior] 10–27's total length of median groove. About 21 short transverse ridges occur on left [right] side, and 19 on right [left] side of oral surface with nodes on right [left], lobate portion. Large flange on basal portion of left [right] side of plate. Anterior [posterior] end blunt.

The greater length to width ratio of the plate oral surface distinguishes this species from *S. wabaunsensis* [a growth feature].

[*S. acuminatus*]: Length to width ratio of plate 23 to 7. Median groove on oral surface slightly biconvex in outline anterior [posterior] to anterior [posterior] extremity of nodose carinal ridge. Ten transverse ridges occur on each side of biconvex portion of median groove. Carinal ridge nodose, to right [left] of which occur nodes, and to left [right] of which occur single row of nodes. Left [right] side of plate with flange on basal portion. Anterior [posterior] end sharp.

The sharp anterior [posterior] end distinguishes this species from *S. walteri* [a growth feature].

Amended Diagnosis: A species of *Streptognathodus* characterized by a Pa element with accessory denticles, a narrow groove, adcarinal parapets that either one or both sides do not join the posterior parapet ornamentation smoothly.

Description—Pa element moderate to long, widest near posterior carinal termination or posterior to it, bowed, free blade one-third or more of element, denticles on blade partially fused, compressed, generally increasing in size anteriorly, but with one or two of smaller size in middle part of blade, and anteriormost two or three, which decrease in size, as blade joins platform becomes fused nodular ridge, posterior end of carina variable, typically posteriormost one or two denticles more discrete on ridge, posteriormost denticle being the largest or second-largest denticle on carina, carina extends only a short distance on posterior part of platform, posterior termination of platform rounded, parapets ornamented by transverse ridges posteriorly abruptly becoming denticles near posterior termination of the carina, transverse ridges at oblique angle to one another, angle decreasing anteriorly, adcarinal parapets ornamented by denticles, decrease in size anteriorly except anteriormost before anterior declination of the parapet which may be larger, but variable, one or two denticles on adcarinal parapet may be larger and disrupt decreasing size pattern, typically but not invariably, outer adcarinal parapet aligns with some accessory denticles rather than posterior platform parapets forming a marked disruption, anterior declination of the parapets along the fixed blade sharp at about the same position or inner high parapet extends further anteriorly, both parapets with one to four small denticles decreasing in size anteriorly anterior to the parapet declination, generally a few more denticles on the inner parapet, both parapets become smooth ribs anteriorly, accessory denticles present, variable, from one to several on inner side and from none to several on outer side, in large forms a few merge to make short irregular transverse or oblique ridges, median groove generally narrow and shallow, either placed on inner side or placed on outer side anteriorly and going to inner side posteriorly, generally extending to the posteriormost one or two transverse ridges, rarely extending to posterior termination, but variable, with none to many transverse ridges merging across groove in irregular pattern, basal cavity flared to outer side.

Dextral and sinistral elements are similar with dextral elements tending to be slightly more robust and sinistral elements more consistently displaying the adcarinal parapet aligning with accessory denticles.

Remarks—This species is probably the most variable in our collections which also explains why it is the most misidentified, typically applied to all forms with accessory denticles. It differs from *S. farmeri* by having a disrupted outer parapet, a narrow groove, and the posterior carinal termination not aligning with a transverse ridge.

Genus *Sweetognathus*

Type Species: *Sweetognathus whitei* (Rhodes)

The Lower Permian species of the genus *Sweetognathus* have been dealt with extensively by Ritter (1986). We find it to be a generally rare-occurring genus in our material, with occasional

exceptions where examples of the genus literally swamp a given sample. The species are very plastic, showing a lot of variability. We are not happy with the way they have been described or with the general proposed utility of the group. As discussed previously, we can see three distinct species in our material, *Sw. expansus, Sw. merrilli,* and *Sw. whitei.* In every sample that we have recovered abundant specimens of *Sweetognathus expansus*, we have two morphotypes: an adenticulate form and a subtly nodose form. The adenticulate form has been ascribed to the species *Sw. adenticulatus* and the subtly nodose form to the species *Sw inornatus* by Ritter (1986). We find that the adenticulate form tends to dominate in lower samples (the Bennett Shale, the Neva Limestone, the Threemile Limestone Members) and the subtly nodose form tends to dominate in upper samples (the Crouse Limestone, the Schroyer Limestone Member), but with lots of exceptions suggesting these forms are ecophenotypes of the same species. By our yardstick, they have the same range, they show complete intergradation, they are the same. Kozur (1994) implied that there are two separate lineages within *Sweetognathus* from separate origins. Kozur (1994) introduced this in an informational note suggesting a formal publication to follow. The adenticulate and subtly nodose forms which he ascribed a new genus, *Wardlawella*, and to the species *W. expansa* and *W. adenticulata* (both equal our *Sw. expansus*). The other lineage he identified as *Sweetognathus*, containing *Sw. merrilli* and *Sw. whitei* at its beginnings. In our material we see the development of more discrete nodes from the nodose form of *Sw. expansus* to *Sw. merrilli* as a natural and plausible progression. So, even though we applaud the name *Wardlawella*, we find it unnecessary.

Sweetognathus expansus Perlmutter

Plate 17, fig. 7; plate 20, fig. 13; plate 24, figs. 5–6; plate 25, figs. 16–19; plate 26, figs. 1–12, 14–18; plate 27, figs. 9, 13–14; plate 29, figs. 1–11.
Ozarkodina expansa Perlmutter, 1975, p. 98–99, pl. 3, figs. 1–27.
Sweetognathus expansus Perlmutter, von Bitter and Merrill, 1990, p. 107, pl. 3, A–O.
Sweetognathus adenticulatus Ritter, 1986, p. 149, pl. 4, figs. 18–19, 21.
Sweetognathus inornatus Ritter, 1986 (part), p. 150, pl. 3, figs. 1, 6, 13, 15; pl. 4, figs. 2, 9.

Original Diagnosis: Free blade consists of three or four denticles, which are subequal in height. There is a gap in denticulation between the free blade and carina in which germ denticles are present. The carina consists of fused denticles, distinctly lower than those of the free blade. Platform is broadly expanded and occupies the posterior two-thirds to four-fifths of the unit length. Basal cavity is deep and wide with a straight longitudinal groove.

Remarks—The holotype of *S. expansus* is a specimen from the Funston Limestone, which has at least a partially denticulate carina. Perlmutter listed the range of the species as Bennett Shale Member, Red Eagle Limestone, to Funston Limestone. Ritter (1986) illustrated *S. inornatus* from the Reipetown Formation in Utah, the Chase Group in Kansas, and the Tensleep Sandstone in Wyoming, many of which are clearly conspecific with *S. expansus*. Ritter (1986) illustrated the holotype of *S. adenticulatus* from the Threemile Limestone Member

and reported it to also occur in the Funston Limestone. His description, of an adenticulate, Type I carina, fits our specimens. The range shown in our material is from the Bennett Shale Member to the Florence Limestone Member of the Barneston Limestone.

Sweetognathus merrilli Kozur

Plate 20, fig. 4; plate 24, figs. 1, 3–4, 7–8; plate 25, figs. 1–4, 6–14; plate 28, figs. 1–9; plate 30, figs 1–5.
Sweetognathus merrilli Kozur, 1975, p. 3.
Sweetognathus whitei Rhodes, Merrill, 1973, p. 310, pl. 3, figs. 1–7.
Sweetognathus inornatus Ritter, 1986 (part), p. 150, pl. 3, figs. 7, 12, 14; pl. 4, figs. 13–14.

Original Diagnosis: The blade bears anterior three to five, rarely six, denticles which are fused up to the upper edge and of which the foremost is the biggest and often appears to be the main cusp. On the posterior there are four to six, rarely up to eight, laterally elongated, knotlike, well-formed denticles which are in part more or less heavily fused. The basal cavity is very large and wide, and occupies approximately two-thirds of the aboral side of the conodont.

Remarks—Kozur (1975) established this species on the illustrations of Merrill (1973) from the Eiss Limestone Member of the Bader Limestone in Kansas. Ritter (1986) illustrates some specimens that fit this description as *S. inornatus,* including the holotype of that species.

Sweetognathus whitei (Rhodes)

Plate 24, fig. 2; plate 27, figs. 1–8, 10–12; plate 28, fig. 10; plate 30, figs. 6–9.
Spathognathodus whitei Rhodes, 1963, p. 464–465, pl. 47, figs. 4, 9, 10, 25, 26.
Sweetognathus whitei (Rhodes), Behnken, 1975, p. 312, p. 1, fig. 26; Igo, 1981 (part), p. 44, pl. 6, figs. 17, 19–21, pl. 7, 1–7; Ritter, 1986, p. 151–152, pl. 3, figs. 2, 4, 8–11, 16–21; Mei, Henderson, and Wardlaw, 2002, p. 86–88, figs. 10.25, 13.2.

Original Diagnosis: [Pa element] bearing 13 to 15 denticles, anteriorly as a blade with up to seven laterally compressed, fused denticles, posterior with about eight denticles, nodelike, discrete, being separated from each other by an interval about equal to the anterior posterior length, the denticles are joined only by a low median bladelike ridge, whose oral surface lies well below that of the denticles and is the only thing filling the intervening depressions, the main feature of the posterior denticles is their lateral expansion, which is such that their width is two or three times greater than their anterior-posterior length, the denticles vary in shape from subcrescentic to suboval to dumbbell-shaped in top view.

Remarks—Though the shape of the denticles has been used in attempts to divide this species, we are quite comfortable with the original diagnosis, find all the variations in node-like denticles in most of our large samples from throughout the U.S., and feel that they adequately belong to one species. Mei et al. (2002) include all of *S. inornatus* (Ritter, 1986) in *S. whitei*, but we feel most of his specimens belong to *S. merrilli.* We also retain the species *Sweetognathus primus* and S. *behnkeni*, which Mei et al. (2002) place in synonymy with *S. whitei. S. primus* and *S. behnkeni* do not occur in our Kansas material.

Genus *Diplognathodus*

**Type Species: *Diplognathodus coloradoensis*
(Murray and Chronic)**

***Diplognathodus* sp.**
Plate 20, fig. 8.

Remarks—This one specimen is dissimilar to those illustrated by von Bitter and Merrill (1990) as *Diplognathodus* n. sp.? H from the Crouse Limestone and the Bennett Shale Member of the Red Eagle Limestone in that it does not have an abrupt posterior termination of the carina.

References

Adler, F. J., 1971, Future petroleum provinces of the midcontinent, region 7; *in*, Future Petroleum Provinces of the United States—Their Geology and Potential: American Association of Petroleum Geologists, Memoir 15, p. 985–1,120.

Akhmetshina, L. Z., 1990, Conodonts of Carboniferous–Permian boundary deposits of the eastern margin of the Caspian depression: Byulleten' Moskovskogo Obshchestva Ispytateley Prirody, Otdel Geologicheskiy, v. 65, no. 1, p. 80–88.

Akhmetshina, L. Z., Barskov, I. S., and Isakova, T. N., 1984, Conodonts of the Gzhelian, Asselian, and Sakmarian stages (Russian platform, the South Urals, the Prikaspiyskaya depression); *in*, The Upper Carboniferous of the USSR, V. V. Menner and A. D. Grigoreva, eds.: Ministry of Geology, Interdepartmental Stratigraphic Committee, Transactions, v. 13, p. 48–50 (in Russian).

Aldis, D. S., Grossman, E. L., Yancey, T. E., and McLerran, R. D., 1988, Isotope stratigraphy and paleodepth changes of Pennsylvanian sedimentary deposits: Palaios, v. 3, p. 487–506.

Amador, C., 2000, High-resolution correlation and type log development of the Council Grove Group in southern Kansas: M.S. thesis, Oklahoma State University, Stillwater, 166 p.

Archer, A. W., and Feldman, H. R., 1995, Incised valleys and estuarine facies of the Douglas Group (Virgilian)—Implications for similar Pennsylvanian sequences in the U.S. midcontinent; *in,* Sequence Stratigraphy of the Midcontinent, N. Hyne, ed.: Tulsa Geological Society, Special Publication No. 4, p. 119–140.

Barrick, J. E., and Boardman, D. R., II, 1989, Stratigraphic distribution of morphotypes of *Idiognathodus* and *Streptognathodus* in Missourian–lower Virgilian strata, north-central Texas; *in,* Late Pennsylvanian Chronostratigraphic Boundaries in North-Central Texas—Glacial-eustatic Events, Biostratigraphy, and Paleoecology, Part II: Contributed Papers, D. R. Boardman II, J. E. Barrick, J. M. Cocke, and N. Nestell, eds.: The Geological Society of America, South-Central Section, 23rd Annual Meeting, Arlington, Texas; Texas Tech University, Studies in Geology 2, p. 167–188.

Barskov, I. S., and Alekseev, A. S., 1975, New species of the genus *Idiognathodus* (conodonts) from the middle upper Carboniferous of Moscow region: Paleontologicheskiy Zhurnal, v. 10, p. 492–494.

Barskov, I. S., Alekseev, A. S., Kononova, L. I., and Migdisova, A. V., 1987, Atlas of Devonian and Carboniferous conodonts: Moscow University Press, Moscow USSR, 141 p. (in Russian).

Barskov, I. S., Isakova, T. N., and Schastlivtseva, N. P., 1981, Conodonts of the Gzhelian and Asselian boundary beds, southern Urals: Izvestiya Academii Nauk SSR, Seriya Geologicheskaya, v. 5, p. 78–87.

Barskov, I. S., and Reimers, A. N., 1996, Carboniferous–Permian boundary as indicated by conodonts: Stratigraphy and Geological Correlation, v. 4, no. 5, p. 428–439.

Barskov, I. S., and Reimers, A. N., 1992, Main features of the conodont historic development in the Early Permian: Vestnik Moskovsky Universitet, Series 4–Geology, no. 2, p. 44–53.

Behnken, F. H., 1975, Leonardian and Guadalupian (Permian) conodont biostratigraphy in western and southwestern United States: Journal of Paleontology, v. 49, p. 284–315.

Boardman, D. R., II, 1999, Virgilian and lowermost Permian sea-level curve and cyclothems; *in*, Guidebook for XIV–ICCP Field Trip No. 8, P. H. Heckel, ed.: Middle and Upper Pennsylvanian (Upper Carboniferous) Cyclothem Succession in Midcontinent Basin, USA, held in association with XIV International Congress on the Carboniferous–Permian, Calgary, Canada, sponsored by Kansas Geological Survey and the University of Kansas Energy Research Center; Kansas Geological Survey, Open-file Report 99–27, p. 103–118.

Boardman, D. R., II, and Heckel, P. H., 1989, Glacial-eustatic sea-level curve for early Late Pennsylvanian sequence in north-central Texas and biostratigraphic correlation with curve for midcontinent North America: Geology, v. 17, p. 802–805.

Boardman, D. R., II, and Nestell, M. K., 1993, Glacial-eustatic sea-level fluctuation curve for Carboniferous–Permian boundary strata based on outcrops in the North American midcontinent and north-central Texas; *in,* Transactions and Abstracts, R. Crick, ed.: Southwest Section, American Association of Petroleum Geologists, p. 15–25.

Boardman, D. R., II, Nestell, M. K., and Knox, L. W., 1995, Depth-related microfaunal biofacies model for late Carboniferous and Early Permian cyclothemic sedimentary sequences in midcontinent North America; *in*, Sequence Stratigraphy of the Midcontinent, N. Hyne, ed.: Tulsa Geological Society, Special Publication No. 4, p. 93–118.

Boardman, D. R., II, Mapes, R. H., Yancey, T. E., and Malinky, J. M., 1984, A new model for the depth-related allogenic community succession within North American Pennsylvanian cyclothems and implications on the black shale problem; *in,* Limestones of the Midcontinent, N. Hyne, ed.: Tulsa Geological Society, Special Publication No. 2, p. 141–182.

Boardman, D. R., II, Work, D. M., Mapes, R. H., and Barrick, J. E., 1994, Biostratigraphy of Middle and Late Pennsylvanian (Desmoinesian–Virgilian) ammonoids: Kansas Geological Survey, Bulletin 232, 121 p.

Boyd, M. W., 1999, High resolution sequence stratigraphic analysis of the upper Carboniferous (Virgilian, Wabaunsee Group) of the North American midcontinent: M.S. thesis, Oklahoma State University, Stillwater, 129 p.

Branson, C. C., 1964, Cyclicity in Oklahoma Paleozoic rocks; *in*, Symposium on Cyclic Sedimentation, D. F. Merriam, ed.: Kansas Geological Survey, Bulletin 169, v. 1, p. 57–62.

Broecker, W. S., and van Donk, J., 1970, Insolation changes, ice volumes and the O^{18} record in deep-sea cores: Reviews Geophysics Space Physics, v. 8, p. 169–188.

Busch, R. M., and West, R. R., 1987, Heirarchial genetic stratigraphy—a framework for paleoceanography: Paleooceanography, v. 2, p. 141–164.

Carter, R. M., Abbott, S. T., Fulthorpe, D. W., Haywick, D. W., and Henderson, R. A., 1991, Application of global sea-level and sequence-stratigraphic models in Southern Hemisphere Neogene strata from New Zealand; *in*, Sedimentation, Tectonics and Eustacy Sea-level Changes at Active Margins, D. I. M. Macdonald, ed.: Blackwell Scientific Publications, International Association of Sedimentologists, Special Publication No. 12, p. 41–68.

Carter, R. M., Carter, L., and Johnson, D. P., 1986, Submergent shorelines in the SW Pacific—evidence for an episodic post-glacial transgression: Sedimentology, v. 33, p. 629–649.

Chaplin, J. R., 1996, Ichnology of transgressive-regressive surfaces in mixed carbonate-siliciclastic sequences, Early Permian Chase Group, Oklahoma; in, Paleozoic Sequence Stratigraphy—Views from the North American Craton, B. J. Witzke, G. A. Ludvigson, and J. Day, eds.: Geological Society of America, Special Paper 306, p. 399–418.

Chernykh, V. V., and Chuvashov, B. I., 1986, Conodont complexes in boundary strata of the Carboniferous and Permian; in, Boundary Strata of the Carboniferous and Permian of the Urals, Preurals, and Central Asia (Biostratigraphy and Correlations), G. N. Papulov, ed.: Russian Academy of Sciences, Moscow, p. 63–67 (in Russian).

Chernykh, V. V., and Reshetkova, N. P., 1987, Biostratigraphy and conodonts of the Carboniferous and Permian boundary beds of the western slope of the southern and central Urals: Uralian Science Center, Academy of Science, U.S.S.R., p. 1–50.

Chernykh, V. V., and Ritter, S. M., 1994, Preliminary biostratigraphic assessment of conodonts from the proposed Carboniferous–Permian boundary stratotype, Aidaralash Creek, northern Kazakhstan: Permophiles, no. 25, p. 4–7.

Chernykh, V. V., and Ritter, S. M., 1997, *Streptognathodus* (Conodonta) succession at the proposed Carboniferous–Permian boundary stratotype section, Aidaralash Creek, northern Kazakhstan: Journal of Paleontology, v. 71, p. 459–474.

Chernykh, V. V., Ritter, S. M., and Wardlaw, B. W., 1997, *Streptognathodus isolatus* new species (Conodonta)—Proposed index for the Carboniferous–Permian boundary: Journal of Paleontology, v. 71, p. 162–164.

Chuvashov, B. I., Chernykh, V. V., Leven, E. Ya., Davydov, V. I., Bowring, S. A., Ramezani, J., Glenister, B. F., Henderson, C. M., Schiappa, T. A., Northrup, C. J., Synder, W. S., Spinosa, C., and Wardlaw, B. R., 2002a, Proposal for the base of the Sakmarian Stage—GSSP in the Kondurovsky Section, southern Urals, Russia: Permophiles, no. 41, p. 4–13.

Chuvashov, B. I., Chernykh, V. V., Leven, E. Ya., Davydov, V. I., Bowring, S. A., Ramezani, J., Glenister, B. F., Henderson, C. M., Schiappa, T. A., Northrup, C. J., Synder, W. S., Spinosa, C., and Wardlaw, B. R., 2002b, Progress report on the base of the Artinskian and base of the Kungurian by the Cisuralian Working Group: Permophiles, no. 41, p. 13–16.

Chuvashov, B. I., Chernykh, V. V., and Mizens, G. A., 1993, Zonal divisions of the boundary deposits of the Carboniferous and Permian in sections of different facies in the south Urals: Permophiles, no. 22, p. 10–16.

Chuvashov, B. I., Djupina, G. V., Mizens, G. A., and Chernykh, V. V., 1991, Krasnousolsk sections; in, International Congress on the Permian System of the world, Perm, USSR—1991, Guides to Geological Excursions, Excursion I—Southern Urals, B. I. Chuvashov and A. E. M. Nairn, eds.: Urals Branch USSR Academy of Sciences and Earth Sciences and Resources Institute; University of South Carolina, p. 2–33.

Collier, R. E. Ll., Leeder, M. R., and Maynard, J. R., 1990, Transgressions and regressions—a model for the influence of tectonic subsidence, deposition and eustacy, with application to Quaternary and Carboniferous examples: Geological Magazine v. 127, p. 117–128.

Connolly, W. M., and Stanton, R. J., 1992, Interbasinal cyclostratigraphic correlation of Milankovitch band transgressive-regressive cycles—Correlation of Desmoinesian–Missourian strata between southeastern Arizona and the midcontinent of North America: Geology, v. 20, p. 999–1,002.

Crowell, J. C., 1978, Gondwana glaciation, cyclothems, central positioning, and climatic change: American Journal of Science, v. 278, p. 1,345–1,372.

Crowell, J. C., and Frakes, L. A., 1975, The late Palaeozoic glaciation: International Gondwana Symposium No. 3, Gondwana Geology, p. 313–331.

Crowley, T. J., and Baum, S. K., 1991, Estimating Carboniferous sea-level fluctuations from Gondwana ice extent: Geology, v. 19, p. 975–977.

Davydov, V. I., Popov, A. V., Bogoslovskaya, M. F., Chernyk, V. V., Kozitskaya, R. I., and Akhmetshina, L. Z., 1993, Aidaralash Section, Part 2—Southern Urals–Permian System, Guides to Geological Excursions in the Uralian Type Localities: Published jointly by the Uralian Branch, Russian Academy of Sciences, Ekaterinburg, Russia and the Earth Sciences and Resources Institute, University of South Carolina, Columbia, South Carolina, Occasional Publications ESRI, New Series, Number 10, p. 131–146.

Denton, G. H., and Hughes, T. J., 1983, Milankovitch theory of ice ages—hypothesis of ice-sheet linkage between regional insolation and global climate: Quaternary Research, v. 20, p. 125–144.

Dubois, M. K., Byrnes, A. P., Bohling, G. C., Seales, S. C., and Doveton, J. H., 2003, Statistically based lithofacies predictions for 3-D reservoir modeling—an example from the Panoma (Council Grove) field, Hugoton embayment, southwest Kansas: Kansas Geological Survey, Open-file Report 2003–30, 3 panels.

Elias, M. K., 1937, Depth of deposition of the Big Blue (late Paleozoic) sediments in Kansas: Geological Society of America, Bulletin 48, p. 403–432.

Ellison, S. E., Jr., 1941, Revision of Pennsylvanian conodonts: Journal of Paleontology, v. 15, p. 244–252.

French, J. A., and Watney, W. L., 1993, Stratigraphy and depositional setting of the lower Missourian (Pennsylvanian) Bethany Falls and Mound Valley limestones, analogues for age-equivalent ooid-grainstone reservoirs, Kansas; in, Current Research on Kansas Geology: Kansas Geological Survey, Bulletin 235, p. 27–39.

Galloway, W. E., 1989a, Genetic stratigraphic sequences in basin analysis I—Architecture and genesis of flooding-surface bounded depositional units: American Association of Petroleum Geologists, Bulletin, v. 73, p. 125–142.

Galloway, W. E., 1989b, Genetic stratigraphic sequences in basin analysis II—Application to northwest Gulf of Mexico Cenozoic basin: American Association of Petroleum Geologists, Bulletin, v. 73, p. 143–154.

Goldhammer, R. K., Dunn, P. A., and Hardie, L. A., 1987, High frequency glacio-eustatic sea level oscillations with Milankovitch characteristics recorded in Middle Triassic platform carbonates in northern Italy: American Journal of Science, v. 287, p. 853–892.

Goldhammer, R. K., Dunn, P. A., and Hardie, L. A., 1990, Depositional cycles, composite sea level changes, cycle stacking patterns, and the hierarchy of stratigraphic forcing—examples from platform carbonates of the Alpine Triassic: Geological Society of America, Bulletin, v. 102, p. 535–562.

Goldhammer, R. K., Oswald, E. J., and Dunn, P. A., 1991, Hierarchy of stratigraphic forcing—example from Middle Pennsylvanian shelf carbonates of the Paradox basin; in, Sedimentary Modeling—Computer Simulations and Methods for Improved Parameter Definition, E. K. Franseen, W. L. Watney, C. G. St. C. Kendall, and W. Ross, eds.: Kansas Geological Survey, Bulletin 233, p. 415–430.

Gunnell, F., 1933, Conodonts and fish remains from the Cherokee, Kansas City, and Wabaunsee Groups of Missouri and Kansas: Journal of Paleontology, v. 7, p. 262–298.

Heckel, P. H., 1977, Origin of phosphatic black shale facies in Pennsylvanian cyclothems of midcontinent North America: American Association of Petroleum Geologists, Bulletin, v. 61, p. 1,045–1,068.

Heckel, P. H., 1986, Sea-level curve for Pennsylvanian eustatic marine transgressive-regressive depositional cycles along midcontinent belt, North America: Geology, v. 14, p. 330–335.

Heckel, P. H., and Weibel, C. P., 1991, Current status of conodont-based biostratigraphic correlation of Upper Pennsylvanian succession between Illinois and midcontinent; *in*, Sequence Stratigraphy in Mixed Clastic-Carbonate Strata, Upper Pennsylvanian, East-central Illinois, C. P. Weibel, ed.: Champaign, Great Lakes Section, Society of Economic Paleontologists and Mineralogists, 21st Annual Field Conference; Illinois State Geological Survey, p. 60–69.

Hunt, D., and Tucker, M. E., 1992, Stranded parasequences and the forced regressive wedge systems tract—deposition during base-level fall: Sedimentary Geology, v. 81, p. 1–9.

Hunt, D., and Tucker, M. E., 1995, Stranded parasequences and the forced regressive wedge systems tract—deposition during base-level fall–Reply: Sedimentary Geology, v. 95, p. 147–160.

Igo, Hisaharu, 1981, Permian conodont biostratigraphy of Japan: Palaeontological Society of Japan, Special Papers, no. 24, 51 p.

Imbrie, J., Hays, J. D., Martinson, D. G., McIntyre, A., Mix, A. C., Morley, J. J., Pisias, N. G., Prell, W. L., and Shackleton, N. J., 1984, The orbital theory of Pleistocene climate—support from a revised chronology of the marine $\delta^{18}O$ record; *in*, Milankovitch and Climate, Part I, A. L. Berger, J. Imbrie, J. Hays, G. Kukla, and B. Saltzman, eds.: Dordrecht, D. Reidel Publishing Co., NATO Advanced Workshop on Milankovitch and Climate, p. 269–305.

Isakova, T. N., 1986, Gzhelian–Asselian boundary in southern Urals, Fusulinina and Conodonta: Byulleten' Moskovskogo Obshchestva Ispytateley Priorody, Otdel Geologicheskiy, v. 61, p. 111–121 (in Russian).

Jervey, M. T., 1988, Quantitative geological modeling of siliciclastic rock sequences and their seismic expression; *in*, Sea-level Changes—An Integrated Approach, C. K. Wilgus, B. S. Hastings, C. G. St.C. Kendall, H. Posamentier, C. A. Ross, and J. van Wagoner, eds.: Society of Economic Paleontologists and Mineralogists, Special Publication No. 42, p. 47–70.

Joeckel, R. M., 1989, Geomorphology of a Pennsylvanian land surface—pedogenesis in the Rock Lake Shale Member, southeastern Nebraska: Journal of Sedimentary Petrology, v. 59, no. 3, p. 469–481.

Joeckel, R. M., 1991, Paleosol stratigraphy of the Eskridge Formation; Early Permian pedogenesis and climate in southeastern Nebraska: Journal of Sedimentary Petrology, v. 61, no. 2, p. 234–255.

Keairns, C. E., 1995, Sequence stratigraphy of Pennsylvanian–Permian boundary strata from the North American midcontinent: M.S. thesis, Oklahoma State University, Stillwater, 255 p.

Keairns, C. E., and Boardman, D. R., II, 1994, Sequence stratigraphy of Carboniferous–Permian boundary strata from the North American midcontinent: Geological Society of America, Abstracts with Programs, v. 26, no. 7, p. 432.

Kozur, H., 1975, Beiträge zur Conodontenfauna des Perm: Geologisch–Paläontologische Mitteilungen Innsbruck, v. 5, p. 1–44 (in German).

Kozur, H., 1976, *Gnathodus barskovi*; *in*, Neue Conodonten aus dem Jungpalaozoikum un der Trias, H. Kozur and H. Mostler, ed.: Geologische–Palaontologische Mitteiolungen Innsbruck, v. 5, p. 1–44.

Kozur, H., 1994, Permian pelagic and shallow-water conodont zonation: Permophiles, no. 24, p. 16–20.

Kozur, H., and Movschovitsch, E. V., 1979, *Gnathodus artinskiensis* Kozur and Movschovitsch sp. nov.; *in*, Conodonts of Urals and their Stratigraphic Significance, G. N. Papulov and V. N. Puchkov, eds.: Academy of Science, Ural Research Center, Trudy Institute of Geology and Geochemistry, p. 116 (in Russian).

Kozur, H., and Mostler, H., 1976, New conodonts from the late Paleozoic and the Triassic: Geologisch–Palaontologische Mitteilungen Innsbruck, v. 6, no. 3, 33 p. (in German).

Larson, J. A., and Clark, D. L., 1979, The Lower Permian (Sakmarian) portion of the Oquirrh Formation, Utah; *in*, Conodont Biostratigraphy of the Great Basin and Rocky Mountains, C. A. Sandberg and D. L. Clark, eds.: Brigham Young University, Geology Studies, v. 26, p. 135–142.

Little, J. M., 1965, Conodont faunas in the Hughes Creek shale and Bennett shale of Riley and Wabaunsee counties, Kansas: M. S. thesis, Kansas State University, Manhattan, 79 p.

Loutit, T. S., Hardenbol, J., Vail, P. R., and Baum, G. R., 1988, Condensed sections—the key to age determinations and correlation of continental margin sequences; *in*, Sea-Level Change—An Integrated Approach, C. K. Wilgus, B. S. Hastings, C. G. St. C. Kendall, H. Posamentier, C. A. Ross, and J. van Wagoner, eds.: Society of Economic Paleontologists and Mineralogists, Special Publication, no. 42, p. 183–213.

Mazzullo, S. J., Teal, C. S., and Burtnett, C. A., 1995, Facies and stratigraphic analysis of cyclothemic strata in the Chase Group (Permian, Wolfcampian), south-central Kansas; *in*, Sequence Stratigraphy of the Midcontinent, N. Hyne, ed.: Tulsa Geological Society, Special Publication No. 4, p. 217–248.

Mazzullo, S. J., Teal, C. S., and Burtnett, C. A., 1997, Outcrop stratigraphy and depositional facies of the Chase Group (Permian, Wolfcampian) in Kansas and southeastern Nebraska: Kansas Geological Survey, Technical Series 6, 210 p.

Mei, S. L., Henderson, C. M., and Wardlaw, B. R., 2002, Evolution and distribution of the conodonts *Sweetognathus* and *Iranognathus* and related genera during the Permian, and their implications for climate change: Palaeogeography, Palaeoclimatology, Palaeoecology, v. 180, p. 57–91.

Merrill, G. K., 1973, Pennsylvanian nonplatform conodont genera, 1—*Spathognathodus*: Journal of Paleontology, v. 47, p. 289–314.

Merrill, G. K., 1974, Pennsylvanian conodont localities in northeastern Ohio: Ohio Division of Geological Survey, Guidebook 3, 25 p.

Miller, K. B., 1994, Tuttle Creek Lake spillway exposure—cycle patterns and paleosol profiles: Kansas Geological Survey, Open-file Report 94–23, 26 p.

Miller, K. B., McCahon, T. J., and West, R. R., 1992, Introduction to Lower Permian (Wolfcampian) cycles of Kansas; *in*, Project Pangea Workshop Fieldtrip Guidebook—Global Sedimentary Geology Program: International Union of Geological Sciences, Lawrence, Kansas, p. I1–I47.

Miller, K. B., McCahon, T. J., and West, R. R., 1996, Lower Permian (Wolfcampian) paleosol-bearing cycles of the U.S. midcontinent—evidence of climatic cyclicity: Journal of Sedimentary Research, v. 66, p. 71–84.

Miller, K. B., and West, R. R., 1993, Reevaluation of Wolfcampian cyclothems in northeastern Kansas—significance of subaerial exposure and flooding surfaces; *in*, Current Research on Kansas Geology: Kansas Geological Survey, Bulletin 235, p. 1–26.

Mitchum, R. M., Jr., and van Wagoner, J. C., 1991, High-frequency sequences and their stacking patterns—sequence-stratigraphic evidence of high-frequency eustatic cycles: Sedimentary Geology, v. 70, p. 131–160.

Moore, R. C., 1964, Paleoecological aspects of Kansas Pennsylvanian and Permian cyclothems; *in*, Symposium on Cyclic Sedimentation, D. F. Merriam, ed.: Kansas Geological Survey, Bulletin 169, v. 1, p. 287–380.

Moore, T. C., Jr., Pisias, N. G., and Dunn, D. A., 1982, Carbonate time series of the Quaternary and late Miocene sediments in the Pacific Ocean—a spectral comparison: Marine Geology, v. 46, p. 217–233.

Movschovitsch, E. V., Kozur, H., Pavlov, A. M., Pnev, V. P., Polozova, A. N., Chuvashov, B. I., and Bogoslovskaya, M. F., 1979, Complexes of conodonts of Lower Permian of the Ural region and problems in correlation of Lower Permian deposits; *in*, Conodonts of Urals and their Stratigraphic Significance, G. N. Papulov and V. N. Puchkov, eds.: Academy of Science, Ural Research Center, Trudy Institute of Geology and Geochemistry, p. 94–125 (in Russian).

Mudge, R., and Burton, R. H., 1959, Geology of Wabaunsee County, Kansas: U. S. Geological Survey, Bulletin 1068, 210 p.

Mudge, R., and Yochelson, E. L., 1963, Stratigraphy and paleontology of the uppermost Pennsylvanian and lowermost Permian rocks in Kansas: U.S. Geological Survey, Professional Paper 323, 213 p.

Nummedal, D., 1992, The falling sea level systems tract in ramp settings in Mesozoic of the Western Interior: Society of Economic Paleontologists and Mineralogists, Theme Meeting, Ft. Collins, Colorado, p. 50.

Nummedal, D., and Molenaar, C. M., 1995, Sequence stratigraphy of ramp-setting strand plain successions—the Gallup Sandstone, New Mexico; *in*, Sequence Stratigraphy of Foreland Basin Deposits—Outcrop and Subsurface Examples from the Cretaceous of North America, J. C. van Wagoner and G. T. Bertram, eds.: American Association of Petroleum Geologists, Memoir 64, p. 277–310.

Olszewski, T. D., and Patzkowsky, M. E., 2003, From cyclothems to sequences—the record of eustasy and climate on icehouse epeiric platform (Pennsylvanian–Permian, North American midcontinent): Journal of Sedimentary Research, v. 73, p. 15–30.

Perlmutter, B., 1971, Conodonts from the uppermost Wabaunsee Group (Pennsylvanian) and the Admire and Council Grove Groups (Permian) Kansas: Ph.D. dissertation, University of Iowa, Iowa City, 121 p.

Perlmutter, B., 1975, Conodonts from the uppermost Wabaunsee Group (Pennsylvanian) and Admire and Council Grove (Permian) in Kansas: Geologica et Paleontologica, v. 9, p. 93–115.

Posamentier, H. W., Jervey, M. T., and Vail, P. R., 1988, Eustatic controls on clastic deposition. I.–Conceptual framework; *in*, Sea-level Changes—An Integrated Approach, C. K. Wilgus, B. S. Hastings, C. G. St. C. Kendall, H. Posamentier, C. A. Ross, and J. van Wagoner, eds.: Society of Economic Paleontologists and Mineralogists, Special Publication No. 42, p. 109–124.

Posamentier, H. W., Allen, G. P., and James, D. P., 1992, High resolution sequence stratigraphy—The East Coulee delta, Alberta: Journal of Sedimentary Petrology, v. 62, p. 310–317.

Posamentier, H. W., Allen, G. P., James, D. P., and Tesson, M., 1992, Forced regressions in a sequence stratigraphic framework—concepts, examples, and exploration significance: American Association of Petroleum Geologists, Bulletin, v. 76, p. 1,687–1,709.

Puckette, J., Boardman, D. R., II, and Al-Shaieb, Z., 1995, Evidence for sea-level fluctuation and stratigraphic sequences in the Council Grove Group (lower Permian), Hugoton embayment, southern midcontinent; *in*, Sequence Stratigraphy of the Midcontinent, N. Hyne, ed.: Tulsa Geological Society, Special Publication No. 4, p. 269–290.

Raatz, W. D., 1996, Sequencing stratigraphy of the Beeman Formation; interaction of eustacy, tectonics, and climate on a mixed terrigenous clastic/carbonate shelf and basin, Upper Pennsylvanian, Sacramento Mountains, New Mexico: Ph.D. dissertation, University of Wisconsin at Madison, 514 p.

Rascoe, B., 1962, Regional stratigraphic analysis of Pennsylvanian and Permian rocks in the western midcontinent (Colorado, Kansas, Oklahoma, Texas): American Association of Petroleum Geologists, Bulletin, v. 46, p. 1,345–1,370.

Rascoe, B., Jr., and Adler, F. J., 1983, Permo–Carboniferous hydrocarbon accumulations, midcontinent, U.S.A.: American Association of Petroleum Geologists, Bulletin, v. 67, no. 6, p. 979–1,001.

Reshetkova, N. P., and Chernykh, V. V., 1986, New species of Asselian conodonts from the western slopes of the Urals: Paleontologicheski i zhurnal, v. 4, p. 99–104 (in English), p. 108–113 (in Russian).

Rhodes, F. H. T., 1963, Conodonts from the topmost Tensleep Sandstone of the eastern Big Horn Mountains, Wyoming: Journal of Paleontology, v. 37, p. 401–408.

Ritter, S. M., 1986, Taxonomic revision and phylogeny of post-Early Permian crisis *bisselli-whitei* Zone conodonts with comments on late Paleozoic diversity: Geologica et Palaeontologica, v. 20, p. 139–165.

Ritter, S. M., 1994, New species and subspecies of *Streptognathodus* (Conodonta) from the Virgilian (late Carboniferous) of Kansas: Journal of Paleontology, v. 68, p. 870–878.

Ritter, S. M., 1995, Upper Missourian-lower Wolfcampian (upper Kasimovian-lower Asselian) conodont biostratigraphy of the midcontinent, U.S.A.: Journal of Paleontology, v. 69, p. 1,139–1,154.

Ross, C. A., 1979, Carboniferous; *in*, Treatise on Invertebrate Paleontology Part A, Introduction, Fossilization (Taphonomy), Biogeography, and Biostratigraphy, R. A. Robison and C. Teichert, eds.: Geological Society of America and the University of Kansas, p. A254–A291.

Ross, C. A., and Ross, J. R. P., 1985, Late Paleozoic depositional sequences are synchronous and worldwide: Geology, v. 13, p. 194–197.

Ross, C. A., and Ross, J. R. P., 1987, Late Paleozoic sea levels and depositional sequences; *in*, Timing and Depositional History of Eustatic Sequences—Constraints on Seismic Stratigraphy, C. A. Ross and D. Haman, eds.: Cushman Foundation for Foraminiferal Research, Special Publication 24, p. 137–149.

Ruzhencev, V. E., 1952, Biostratigraphy of the Sakmarian Stage in the Aktyubinsk region of the Kazakh SSR: Transactions of the Paleontological Institute, USSR Academy of Science, v. 42, 90 p.

Scotese, C., 1986, Atlas of Paleozoic base maps–paleoceanographic mapping project: University of Texas (Austin) Institute for Geophysics, Technical Report 66, 23 p.

Scott, G. R., Foster, F. W., and Crumpton, C. F., 1959, Geology and construction material resources of Pottawatomie County, Kansas: U.S. Geological Survey, Bulletin 1060–C, 178 p.

Schenk, P. E., 1967, Facies and phases of the Altamont Limestone and megacyclothem (Pennsylvanian), Iowa to Oklahoma: Geological Society of America, Bulletin, v. 78, p. 1,369–1,384.

Shaffer, B. L., 1990, The nature and significance of condensed sections in Gulf Coast Late Neogene sequence stratigraphy: Transactions, Gulf Coast Association of Geological Societies, v. XL, p. 767–776.

Soreghan, G. S., 1994, Stratigraphic responses to geologic processes—Late Pennsylvanian eustacy and tectonics in the Pedrogosa and Orogrande basins, Ancestral Rocky Mountains: Geological Society of America, Bulletin, v. 106, p. 1,195–1,211.

Stauffer, C. R., and Plummer, H. J., 1932, Texas Pennsylvanian conodonts and their stratigraphic relations: University of Texas, Bulletin 3201, p. 13–50.

Vail, P. R., Audemard, F., Bowman, S. A., Eisner, P. N., and Perez–Cruz, C., 1991, The stratigraphic signatures of tectonics, eustacy, and sedimentology—an overview; *in*, Cycles and Events in Stratigraphy, G. Einsele, W. Ricken, and A. Seilacher, eds.: New York, Springer Verlag, p. 617–659.

Vann, B. W., 1994, Condodont biofacies and eustatic events of the outcropping uppermost Wabaunsee Group through the basal Council Grove Group from northern Oklahoma to Greenwood County, Kansas: M.S. thesis, Oklahoma State University, Stillwater, 199 p.

van Wagoner, J. C., Posamentier, H. W., Mitchum, R. M., Jr., Vail, P. R., Sarg, J. F., Loutit, T. S., and Hardenbol, J., 1988, An overview of the fundamentals of sequence stratigraphy and key definitions; *in*, Sea-level Changes—An Integrated Approach, C. K. Wilgus, B. S. Hastings, C. G. St. C. Kendall, H. Posamentier, C. A. Ross, and J. van Wagoner, eds.: Society of Economic Paleontologists and Mineralogists, Special Publication No. 42, p. 39–46.

van Wagoner, J. C., 1990, Sequence boundaries in siliciclastic strata on the shelf; physical expression and recognition criteria (abs.): Abstracts, Distinguished Lecture Tours, American Association of Petroleum Geologists, Bulletin, v. 74, p. 1,774–1,775.

Veevers, J. J., and Powell, C. McA., 1987, Late Paleozoic glacial episodes in Gondwanaland reflected in transgressive-regressive depositional sequences in Euramerica: Geological Society of America, Bulletin v. 98, p. 475–487.

von Bitter, P. H., 1972, Environmental control of conodont distribution in the Shawnee Group (Upper Pennsylvanian) of eastern Kansas: University of Kansas, Paleontological Contributions, Article 59, 105 p.

von Bitter, P. H., and Merrill, G. K., 1990, Effects of variation on the speciation of phylogeny of *Diplognathodus*: Courier Forschungsinstitut Senckenberg, v. 118, p. 105–129.

Wang, Z. h., 1991, Conodonts from Carboniferous–Permian boundary strata in China with comments on the boundary: Acta Palaeontologica Sinica, v. 30, no. 1, p. 6–41 (in Chinese with English summary).

Wanless, H. R., and Shepard, F. P., 1936, Sea level and climatic changes related to late Paleozoic cycles: Geological Society of America, Bulletin, v. 47, p. 1,177–1,206.

Wardlaw, B. R., 1990, Conodonts and the definition of the Carboniferous–Permian boundary; *in*, Working Group on the Carboniferous–Permian Boundary, B. R. Wardlaw, ed.: Proceedings at the 28th International Geological Congress; U.S. Geological Survey, Open-file Report 90–233, p. 34–37.

Wardlaw, B. R., Ritter, S. M., and Nestell, M. K., 1991, Variability in *Streptognathodus* species populations in the uppermost Carboniferous and lowermost Permian of the USA: Program and Abstracts, International Congress on the Permian System of the World, Perm, USSR, p. A21.

Wardlaw, B. R., Leven, E. Ya., Davydov, V. I., Schiappa, T. A., and Snyder, W. S., 1999, The base of the Sakmarian Stage—Call for discussion (possible GSSP in the Kondurovsky Section, Southern Urals, Russia): Permophiles, no. 34, p. 19–20.

Watney, W. L., French, J. A., and Franseen, E. K., 1989, Sequence-stratigraphic interpretations and modeling of cyclothems: Guidebook, 41st Annual Field Trip, Kansas Geological Survey and Kansas Geological Society, 211 p.

Watney, W. L., French, J. A., Doveton, J. H., Youle, J. C., and Guy, W. J., 1995, Cycle heirarchy and genetic stratigraphy of Middle and Upper Pennsylvanian strata in the upper midcontinent; *in*, Sequence Stratigraphy of the Midcontinent, N. Hyne, ed.: Tulsa Geological Society, Special Publication No. 4, p. 141–192.

Yang, Wan, 1996, Cycle symmetry and its causes, Cisco Group (Virgilian and Wolfcampian), Texas: Journal of Sedimentary Research, v. 66, p. 1,102–1,121.

Youle, J. C., Watney, W. L., and Lambert, L. L., 1994, Stratal hierarchy and sequence stratigraphy—Middle Pennsylvanian, southwestern Kansas, U. S. A.: Geological Society of America, Special Paper 288, p. 267–285.

Zhao, S., 1982, Upper Carboniferous conodonts of the Qinshui basin, Shanxi: Bulletin of the Tianjin Institute of Geology and Mineral Resources, Chinese Academy of Geological Sciences, v. 4, p. 97–111.

Appendices I and II follow